Lagrangian Mechanics Modeling of Free Surface-Affected Marine Craft

Thomas Battista

Dissertation submitted to the Faculty of the
Virginia Polytechnic Institute and State University
in partial fulfillment of the requirements for the degree of

Doctor of Philosophy
in
Aerospace Engineering

Craig A. Woolsey, Chair
Francis Valentinis, Co-Chair
Stefano Brizzolara
Eric G. Paterson

March 13, 2018
Blacksburg, Virginia

Keywords: Lagrangian Mechanics, Potential Flow Hydrodynamics, Fluid-Body Interactions

Lagrangian Mechanics Modeling of Free Surface-Affected Marine Craft

Thomas Battista

(ABSTRACT)

This dissertation presents the first nonlinear unified maneuvering and seakeeping model for marine craft derived from first principles. Prior unified models are based on linearity assumptions. Linear models offer a concise representation of the system dynamics and perform reasonably well under the modeling assumptions, but they neglect nonlinear hydrodynamic forces and moments incurred from more aggressive vehicle maneuvers. These nonlinear effects are amplified in a natural seaway where the vehicle is subject to random, and sometimes significant, wave forcing.

Lagrangian mechanics modeling techniques are used in this dissertation to model the motion of marine craft which are affected by a free surface. To begin the modeling effort, the system Lagrangian is decomposed into a rigid body Lagrangian, a fluid body Lagrangian, and a free surface Lagrangian. Together, these Lagrangian functions characterize the energy of a closed system containing the vehicle, the ambient fluid, and the free surface. These Lagrangian functions are first used to construct a free surface-affected nonlinear maneuvering model which characterizes the hydrodynamic forces and moments due to arbitrary vehicle motions in a semi-infinite volume of perfect fluid. The effects due to incident waves are then incorporated using a fourth function, the disturbance Lagrangian. The disturbance Lagrangian accounts for the fluid energy due to externally generated fluid motions. Combining the four Lagrangian functions enables one to the derive equations of motion for a marine craft undergoing arbitrary maneuvers in a seaway.

The principal contribution of this modeling effort is that it yields ODE representations of the potential flow hydrodynamic effects for nonlinear vehicle motions. These nonlinear expressions alleviate the small-motion assumptions inherent to prior unified models, enabling higher model fidelity for a number of critical applications including rapid design optimization,

training simulator design, nonlinear control and observer design, and stability analysis.

This work was supported by the Office of Naval Research under grant numbers N00014-14-1-0651 and N00014-16-1-2749.

Lagrangian Mechanics Modeling of Free Surface-Affected Marine Craft

Thomas Battista

(GENERAL AUDIENCE ABSTRACT)

Although ships have been used for thousands of years, modeling the dynamics of marine craft has historically been restricted by the complex nature of the hydrodynamics. The principal challenge is that the vehicle motion is coupled to the ambient fluid motion, effectively requiring one to solve an infinite dimensional set of equations to predict the hydrodynamic forces and moments acting on a marine vehicle. Additional challenges arise in parametric modeling, where one approximates the fluid behavior using reduced-order ordinary differential equations. Parametric models are typically required for model-based state estimation and feedback control design, while also supporting other applications including vehicle design and submarine operator training.

In this dissertation, Lagrangian mechanics is used to derive nonlinear, parametric motion models for marine craft operating in the presence of a free surface. In Lagrangian mechanics, one constructs the equations of motion for a dynamic system using a system Lagrangian, a scalar energy-like function canonically defined as the system kinetic energy minus the system potential energies. The Lagrangian functions are identified under ideal flow assumptions and are used to derive two sets of equations. The first set of equations neglects hydrodynamic forces due to exogenous fluid motions and may be interpreted as a nonlinear calm water maneuvering model. The second set of equations incorporates effects due to exogenous fluid motion, and may be interpreted as a nonlinear, unified maneuvering and seakeeping model. Having identified the state- and time-dependent model parameters, one may use these models to rapidly simulate surface-affected marine craft maneuvers, enabling model-based control design and state estimation algorithms.

It may be worth while, however, to remark that the hydrodynamical systems afford extremely interesting and beautiful illustrations of the Principle of Least Action, the Reciprocal Theorems of Helmholtz, and other general dynamical theories.

- Sir Horace Lamb, *Hydrodynamics*

To my grandfather, Ralph.

Acknowledgements

I am incredibly thankful for my time in Blacksburg and all the wonderful people that made these eight years so memorable. I could not have completed my PhD if it wasn't for the camaraderie and support of a number of people. I would first like to thank my undergraduate friends who helped me to fall in love with Blacksburg, including my hall mates Brian Chase, Andrew Hemmen, and Dan Naiman, my roommates Kenny Maben, Dan Mead and Andrew Renner, and my senior design team David Black, Garrett Hehn, Caroline Kirk, Peter Marquis, Brian McCarthy, Khanh Ngo, Lindsay Wolff, and Will Woltman.

I also owe thanks to my graduate school friends for all the enlightening and entertaining conversations in both bars and classrooms. In particular, I have to thank Dr. David Allen, Dr. Matt Chan, Danielle Cristino, Javier Gonzalez-Rocha, Allie Guettler, Seyong Jung, Dr. Ben Lutz, Hunter McClelland, Dr. Shibabrat Naik, Gary Nave, Dr. Andrew Rogers, Klajdi Sinani, Dylan Thomas, and Will Tyson.

I must also thank several professors for helping me to realize my passion for mathematics, mechanics, and control theory, including Dr. Mazen Farhood, Dr. Serkan Gugercin, Dr. Shane Ross, Dr. Cornel Sultan and my former co-advisor Dr. Leigh McCue-Weil. I am also thankful for my conversations with Dr. Tristan Perez at Queensland University of Technology, whose expertise in ship dynamics helped to guide me throughout my graduate career.

None of this would be possible without the sponsorship of the Office of Naval Research. I am also thankful for all the assistance I received from the staff in the Kevin T. Crofton Department of Aerospace and Ocean Engineering at Virginia Tech.

My committee members played a tremendous role throughout the course of my PhD program. Dr. Eric Paterson's and Dr. Stefano Brizzolara's extensive knowledge of naval architecture and fluid mechanics helped me to keep my research grounded in the "real world". I am also thankful for the support of my co-advisor, Dr. Francis Valentinis, who often contributed valuable remarks all the way from Australia. I am also grateful for the year that

Dr. Valentinis spent with us at Virginia Tech. My constant exposure to such a passionate and knowledgable person had an invaluable impact on so many aspects my graduate studies. I am also indebted to my co-advisor Dr. Craig Woolsey, who recruited me straight from my undergraduate program at Virginia Tech. His consistent mentoring and dedication to my academic development helped me to grow as both a researcher and a person over these four years.

I am incredibly thankful for the Blacksburg Community Band and the Summer Musical Enterprise for giving me the opportunity to immerse myself in music on a regular basis. I cannot overstate my appreciation for the therapeutic relief that music has brought me over the years.

I must also thank the people in my hometown of Colts Neck for helping me grow into the person I am today, including my best friends Mike Aragones, Will Feng, Eric Gutierrez, Justin Geringer, Ryan McDonough, Andrew Oh, Nick Reardon, and Rob Romano. I would also like to thank Mr. Bryan Parks and Mr. Joe Santonacita for being great teachers who taught me how exciting and powerful education can be. Finally, I have to thank my high school band director, Jack Maniaci, for his character advice and for showing me that I would always have an outlet in music.

It should go without saying (but I'll say it anyway) that I would not be where I am today without the love and support of my family. My parents Joe and Michele were always there for me, despite being eight hours away, and for that I am sincerely grateful. I would also like to thank my grandfather, Ralph, who gave up his dream of pursuing a PhD to support his family, but who always hoped that one of his decedents would earn the title of "Doctor". He instilled his passion for knowledge in me at a young age and this played a major part in my choice to pursue a PhD. Finally, I would like to thank my loving girlfriend Liz for keeping me sane during my final year of grad school and for believing in me every step of the way.

Contents

List of Figures

List of Tables

Chapter 1

Introduction

1.1 Background and Motivation

The earliest recorded uses of seafaring vessels predate the rise of classical mechanics by several millennia. Without the intricate working knowledge of statics and dynamics that we take for granted today, the shipbuilders of old must have resorted to design methodologies based solely on experience. Contemporary mathematical physics, founded by visionaries like Newton and Euler, was instrumental in developing the analysis tools and design methods used today in marine applications.

In an environment as dynamic and uncertain as the ocean, reliable models are required to ensure the safe operation of marine craft. Model-based control design strategies generate feedback control laws from a set of ordinary differential equations (ODEs) which faithfully represent the vehicle dynamics [1, 2]. Feedback control laws can be used to improve vehicle performance and expand the safe operating envelope for marine craft. During the design process, one also leverages model predictions to make decisions within a design space. For instance, characterizing how changes to the hull form affects a ship's response to incident waves can be used to predict ride quality which influences crew functionality [3] and stability

margins for catastrophic events like capsize [4, 5].

Though ships have been used for thousands of years, modeling the dynamics of marine craft has historically been restricted by the complex nature of the hydrodynamics. The principle challenge is that the fluid behavior is governed by a set of partial differential equations, effectively requiring one to solve an infinite dimensional set of equations to predict the hydrodynamic forces and moments acting on a marine vehicle. One can circumvent the task of solving the fluid equations by running a series of physical experiments and using the resulting data to construct empirical models [6]. However, there are a number of issues associated with physical experiments. The cost and time required to manufacture a suitable model is sometimes impractical and generating the desired operating conditions in an experimental setting often demands highly specialized equipment.

With the increasing availability of modern high performance computing, numerical experiments have become more popular. Computational fluid dynamics (CFD) modeling is typically performed by discretizing a fluid volume into a mesh and solving the Navier-Stokes equations for each degree of freedom. High-fidelity CFD modeling can employ millions of degrees of freedom which require upwards of thousands of processor-hours to predict fluid behavior to generate only seconds or minutes of real-time operations [7]. While certain modeling applications require high fidelity to yield meaningful results, the extensive computation time precludes the use of high fidelity CFD for any iterated modeling procedures, like rapid design optimization or control-gain tuning. In these cases, one might employ a CFD approach which trades lower model fidelity for shorter computation times. Strip methods [8, 9] and panel methods [10, 11] are two low fidelity CFD approaches which are commonly used for hydrodynamic predictions. However, even the low fidelity approaches cannot be used for real-time hydrodynamic predictions.

Parametric ODE models offer a blend of versatility, model fidelity, and computational efficiency. As shown in Figure 1.1, data-driven modeling and physics-driven modeling are two approaches to constructing parametric models. Data-driven approaches fit empirical rela-

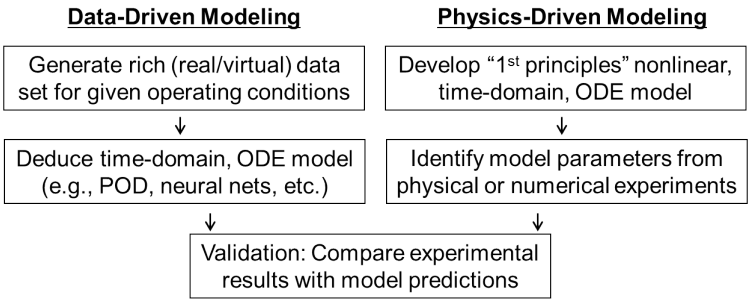

Figure 1.1: A comparison between data-driven and physics-driven modeling approaches.

tionships to experimental data, for instance from CFD. For simple cases where the data is easily visualized, one can often construct a model by selecting a series of parametric functions which well represents the data. This was done in [12], where the authors empirically constructed a two-parameter model to predict the hydrodynamic forces and moments acting on a submarine undergoing longitudinal motion in calm seas. For complex scenarios, one might desire a more algorithmic approach. Proper orthogonal decomposition (POD) [13], Koopman operator theory [14] and dynamic mode decomposition (DMD) [15] are mathematical techniques for extracting reduced-order approximations of the dominant fluid behaviors from either numerical or physical data. On the other hand, physics-driven modeling is rooted in first principles, for instance Newton's Laws or Hamilton's Principle [16, 17]. Rather than passing large data sets through an algorithm to extract a model, one uses a physical understanding of a complex system to decompose the modeling effort into manageable parts. Applying first principles to each part is often more fruitful, yielding partial models which are physically intuitive. One then attempts to combine these parts to approximate the full system behavior.

Even before considering more complex hydrodynamic phenomena, like boundary layer mechanics and shed vortex interaction, there are several idealized flow effects that should be present in a parametric model. These effects include added mass and wave resistance in steady maneuvering and wave excitation forces in the presence of ambient waves [8, 18, 1]. The simplifying assumptions which enable the parametric representation of these idealized

potential flow forces have traditionally divided the modeling effort into two categories: maneuvering and seakeeping. Maneuvering models predict the response of a vessel undergoing various maneuvers in otherwise calm seas. Seakeeping models instead predict the vessel response in a seaway (subject to ambient waves), though only for "small" amplitude vessel motions. The treatment of maneuvering and seakeeping models is presented from a hydrodynamic standpoint in [8], or from a guidance and navigation standpoint in [1] and [2].

For a marine craft maneuvering in a seaway, the assumptions for maneuvering and seakeeping models would both be violated, leading to poor model predictions. This shortcoming begs the development of a "unified" maneuvering and seakeeping model. To date, the most comprehensive unified model derives from the work of Cummins [19] and culminates with the work of Fossen [20] and Perez [2]. For surface ships, Cummins [19] used impulse response functions to derive a set of small-perturbation, integro-differential equations which capture the "memory effects", or the history dependent hydrodynamic forces and moments acting on the vessel. The resulting equations capture transient hydrodynamic effects due to maneuvering in a seaway. However, the memory effects are incorporated as convolution integrals which preclude the use of Cummins' equations for applications like control design and stability analysis. Building upon the work of Cummins, Bailey et al. [21] unified the maneuvering and seakeeping frameworks into a single, small-perturbation model that reduces to the standard maneuvering and seakeeping models under their respective assumptions. The model developed in [21] is unsuitable for control design, again because of the convolution integrals used to express the memory effects. To address this issue, Kristiansen et al. [22] constructed a linear filter to approximate the memory effects using a high-dimensional state space model. Kristiansen et al. [22] then used model reduction techniques, *e.g.* as outlined in [23], to reduce the number of states to a manageable number, enabling a low-order approximation of the memory effects. Building upon these results, Perez [2] and Fossen [20] constructed a control-oriented unified maneuvering and seakeeping model. Their model incorporates the standard maneuvering and seakeeping forces into a common framework, being careful not to double-count the overlapping forces which appear in both models. This model was employed

in [24] as the basis for a simulation environment for an unmanned surface vehicle. It is important to note, however, that the unified model [2, 20] and the work on which it was built [21, 22] directly derive from the work of Cummins [19]; the unified model is only valid when considering small perturbations from a nominal speed and heading.

Submerged craft models are often treated separately from surface craft since, in most scenarios, they operate at depths where surface effects can be safely ignored. Neglecting the free surface greatly simplifies the hydrodynamic modeling problem. This leads to Kirchhoff's equations for rigid body motion in an unbounded ideal fluid [25]. Though Kirchhoff's equations assume the fluid motion results only from the motion of the vehicle, Fossen [1] reasons that these equations may also be used to describe scenarios where the vehicle is moving through a uniform flow field. Thomasson and Woolsey [26] used a Lagrangian mechanics framework to extend Kirchhoff's equations to account for situations where a vehicle is operating in an unsteady and nonuniform flow field.

For a submerged craft operating near the surface, these models [25, 1, 26], as well as other standard submarine models [27, 28], would break down since they do not account for the additional physical phenomena that are essential in near-surface operations. Initially considering only calm-water scenarios, the presence of the free surface modifies the body-fluid interaction, affecting the fluid forcing in two primary ways. First, the free surface creates an asymmetry in the fluid volume, affecting the vehicle-induced fluid motion. This modifies the forces and moments that are commonly accounted for using added mass and inertia. Second, since the surface is free to deform, any vehicle motion generates surface waves, an irreversible process resulting in radiative damping. The persisting influence of these surface waves also incurs memory effects, as discussed in [19] and [29]. In general, motion near the free surface tends to force a submerged vehicle towards the surface and simultaneously generate a nose-down pitching moment. This "free surface suction," as well as radiative damping, were studied in [30] using the panel method outlined in [10]. Notably, Crook [30] quantifies the impact of the Froude number and the operating depth on the steady state lift, drag, and pitching moment experienced by the vehicle.

In addition to the free surface effects incurred by vehicle motion, the influence of surface waves acting on a submerged vehicle can also be significant. These wave excitation forces are usually incorporated using the Froude-Krylov and diffraction forces [8, 18]. Incident waves also result in second order "drift forces" which effectively modify the calm-water free surface suction effects [2]. Compared to the calm-water results, Crook [30] quantified the additional impact of incident wavelength, amplitude, and encounter angle on the free surface suction forces and moments. These second order drift forces and moments were included in the linearized control-oriented model in [31], where the authors developed control laws to mitigate heave and pitch motion for a submarine operating in ambient waves.

1.2 International Collaboration: Hypothesis, Objectives, and Approach

The work presented in this dissertation represents part of an international collaborative effort, with contributions primarily coming from researchers in Australia and the United States. We jointly hypothesize that nonlinear model-based control practices can expand the operating envelope for marine craft in elevated sea states. To test this hypothesis, the following objectives were proposed to the U. S. Office of Naval Research as the basis for the international collaborative research effort:

1. **Model design.** Develop a parametric model which incorporates parametric representations of the necessary fluid mechanics and is amenable to nonlinear control design practices.

2. **Model identification.** Design experiments (physical or numerical) and an identification algorithm that together may be used to populate the parametric model.

3. **Model validation.** Quantify the degree to which the identified model faithfully represents the true system behavior.

4. **Control design.** Construct a control law based on the identified model which places guaranteed bounds on the adverse wave-induced vehicle motions.

5. **Performance evaluation.** Evaluate the performance through simulation of the closed loop system subject to external wave forcing.

This dissertation addresses the model design objective using first principles modeling techniques. Specifically, this dissertation follows a Lagrangian mechanics approach to model the dynamics of marine craft operating in the presence of a free surface. The aim is to develop reduced order expressions for the potential flow hydrodynamic forces and moments with the expectation that additional phenomena like viscous drag may be incorporated using semi-empiricle methods [32].

In Lagrangian mechanics, one uses a scalar energy-like function to generate a set of ODEs which govern the system dynamics. This Lagrangian function is canonically defined as the system kinetic minus potential energy. To use the Lagrangian modeling approach, one first identifies a system to model. Past Lagrangian efforts [25, 33, 34] studied marine craft by considering a system composed of a rigid body and the ambient fluid, as illustrated on the left side of Figure 1.2. For a deeply submerged vehicle in an ideal fluid and in the absence of external forces, this system conserves energy. However, for a craft operating near or on the free surface, the free surface can also exchange energy with the vehicle.

As compared to prior works, this dissertation additionally considers the free surface as a system constituent. In the absence of external factors, the three-part system illustrated on the right side of Figure 1.2 conserves energy. In this case, the marine craft dynamics is governed by the transfer of energy between the remaining system constituents.

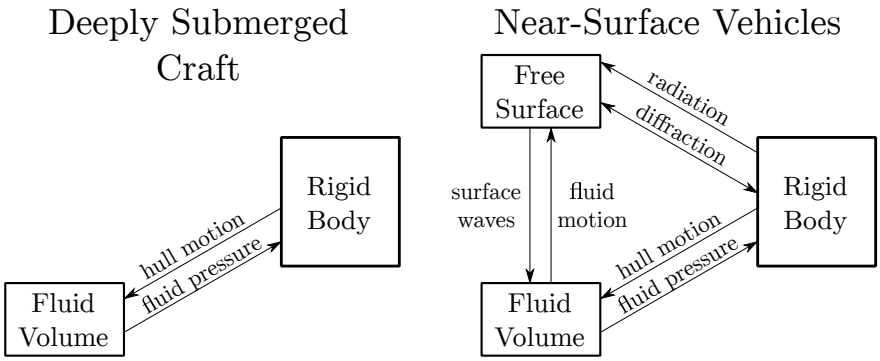

Figure 1.2: An illustration of some of the physical processes that take place for a deeply submerged craft and a near-surface vehicle.

1.3 Summary of Contributions

The principle contributions of this dissertation are Theorem 5.4.2 and Theorem 6.3.2. Theorem 5.4.2 presents a nonlinear model for a marine craft undergoing arbitrary maneuvers near a free surface. This maneuvering model can be interpreted as a nonlinear extension to the Cummins equations, which model the linearized dynamics of a marine craft. The Cummins equations serve as the basis for a number of models, including [21, 20, 24]. The nonlinear extension can improve the quality of these model predictions.

Theorem 6.3.2 presents a nonlinear unified maneuvering and seakeeping model. The benefit of this model is twofold. First, the maneuvering portion of the model captures the calm-water hydrodynamic effects which arise from nonlinear vehicle motions. This includes nonlinear expressions for the fluid memory effects. Second, the incident wave forces do not derive from RAOs which are obtained from linearized dynamics. In this model, the expressions for the generalized forces due to external fluid motion are inspired by a prior time-domain Lagrangian modeling approach [26]. The Lagrangian formulation also offers insight into how the traditional added mass matrices relate the calm-water radiation forces to the incident wave forces.

The additional contributions of this dissertation are summarized as follows.

Chapter 2:

- Rigid body mechanics is introduced using both Newtonian mechanics and Lagrangian mechanics.

Chapter 3:

- Standard expressions for the maneuvering and seakeeping equations are presented using the Lagrangian mechanics equations presented in Chapter 2.
- The governing equations of motion are introduced for a fluid volume. Special care is given to the fluid energy expressions which play a significant role in the remaining chapters.

Chapter 4:

- The Lagrangian approach to modeling fluid-vehicle interactions is rigorously defined for a vehicle in an ideal fluid. Special considerations are given to a vehicle near a free surface.
- The Lagrangian modeling approach is demonstrated to be equivalent to the more conventional Newtonian modeling approach.
- A theorem is given which proves that the fluid kinetic energy is invariant to translations and rotations of a rigid body which is submerged in an infinite volume of ideal and otherwise calm fluid.

Chapter 5:

- Velocity potential functions are constructed with and without memory effects to derive nonlinear, parametric equations of motion for a marine craft operating in the presence of an otherwise undisturbed free surface.

- The relationship between the fluid memory effects and the wave resistance forces is detailed.

Chapter 6:

- The model of Thomasson and Woolsey [26] is shown to be an appropriate parametric approach for incorporating wave excitation forces.
- A nonlinear, parametric, unified maneuvering and seakeeping model is derived

1.4 Overview

The organization of this dissertation follows the roadmap of standard guidance and navigation texts in the ship dynamics literature, for instance [1] and [2]. Chapters 2 and 3 introduce the tools necessary to analyze rigid body systems and fluid mechanic systems, respectively. Chapters 4, 5, and 6 then blend these analysis techniques to construct parametric models for fluid-body interactions. The following outline details the material contained within each chapter of this dissertation.

Chapter 2:

The fundamental concepts from dynamical systems theory that recur throughout this dissertation are introduced. The focus is primarily on rigid body dynamics, including the choice of reference frames and the corresponding kinematic descriptions. Both Newtonian and Lagrangian modeling approaches are also outlined, with more attention given to the latter. Several useful extensions of Lagrangian and Hamiltonian systems theory are also given.

Chapter 3:

The discussion of dynamical systems in Chapter 2 is expanded to include fluid dynamics and fluid-body interactions. Standard approaches to parametric modeling of

marine craft are introduced, and the commonly modeled physical phenomena are discussed. Ideal (potential) flow theory is introduced, as well as several useful properties which aid in control-oriented modeling of hydrodynamic phenomena. This chapter concludes with a discussion of ocean wave theory, including techniques for constructing realistic wave environments.

Chapter 4:

A Lagrangian mechanics framework for modeling fluid-body interactions is introduced. This framework is shown to be equivalent to the more conventional Newtonian modeling approach in three cases of interest: a rigid body operating in an unbounded fluid, a rigid body operating near a fixed wall, and a rigid body operating near a free surface. Chapter 4 concludes with several examples to demonstrate the Lagrangian modeling approach, including derivations of Kirchhoff's equations and Cummins' equations.

Chapter 5:

Extending the results in Chapter 4, a system Lagrangian is constructed to characterize the system energy for a near-surface underwater craft operating in an otherwise calm fluid. Using two variations of the modeling assumptions, two sets of near-surface maneuvering equations, one with memory effects and the other without. The importance of the memory effects is highlighted by contrasting these two calm water models.

Chapter 6:

The system Lagrangian function used to derive the maneuvering model presented in Chapter 5 is augmented to account for the energy due to externally generated fluid motion. The modified Lagrangian function is then used to construct a nonlinear unified maneuvering and seakeeping model.

Chapter 7:

The dissertation is summarized and future work is presented.

Chapter 2

Rigid Body Dynamics

In dynamical systems analysis, one uses physical laws to predict the behavior of a dynamic system. Analysis is often decomposed into *kinematics* and *kinetics*, which are briefly defined as

- *kinematics:* a mathematical model governing the geometry of a given motion, rather than the physical phenomena causing the motion.
- *kinetics:* a dynamic model which predicts the evolution of a system due to physical processes which result in forces and moments.

The mathematical representation of a dynamic system is typically driven by the modeling objective. The simplest mathematical models for vehicle motions are particle models, whose state is completely characterized using three coordinates in three dimensional Euclidean space. For a ship in littoral waters, one's objective might be planning a safe path which keeps the ship from any dangerously shallow water. Here, the safe trajectory can be modeled using a *kinematic particle*; using a bathymetric chart, one can generate a curve (for instance, using a technique outlined in [35]) which would guide the ship safely from one location to another. For stationkeeping of an ocean platform, one would instead model the system as

a *dynamic particle*, also incorporating the kinetics; the environmental forces and moments acting on the platform would to need be modeled and rejected via control design to mitigate platform motion.

More complex are multi-particle models. A system of N particles requires (in general) $3N$ coordinates to be completely characterized in state space. There are two special cases of multi-particle models studied in this dissertation: rigid body models and fluid models. A rigid body is a multi-particle system where the relative distances between each pair of particles are fixed. For a rigid body composed of $N > 2$ particles, the distance constraints simplify the system such that one need only locate three non-collinear particles (and correspondingly nine coordinates) to characterize the body [17, Sec. 4.1]. The total number of required coordinates is then reduced to six using the three unique distance constraints between each of the chosen three particles[1]. On the other hand, the relative distances between particles composing a fluid volume are free to vary. In general one must retain the $3N$ coordinates to characterize a fluid system, making fluid systems the more complex of the two cases. In this chapter, the focus is placed on rigid body models, deferring the discussion of fluid models to Chapter 3.

2.1 Mathematic Preliminaries

In this dissertation, the following reference frames are defined and are depicted in Figure 2.1. First, establish an inertial frame at O with right-handed basis $\{\boldsymbol{i}_1, \boldsymbol{i}_2, \boldsymbol{i}_3\}$ where $\boldsymbol{i}_3$ is aligned with the direction of gravity. Then, let the free vectors $\{\boldsymbol{b}_1, \boldsymbol{b}_2, \boldsymbol{b}_3\}$ form a basis for a body-fixed reference frame located at the body geometric center $\boldsymbol{x}_\mathrm{b} = [x_\mathrm{b}, y_\mathrm{b}, z_\mathrm{b}]^T$. Let $\boldsymbol{\theta}_\mathrm{b} = [\phi_\mathrm{b}, \theta_\mathrm{b}, \psi_\mathrm{b}]$ represent the standard roll, pitch, and yaw Euler angles, which are used in characterizing the orientation of the body frame. Finally, let $\boldsymbol{v} = [u, v, w]^T$ and $\boldsymbol{\omega} = [p, q, r]^T$

[1]Conceptually, once the first particle is located using three Cartesian coordinates, the second particle will lie along a sphere relative to the first, requiring two angles. The third particle can then be located along a circle perpendicular to the axis connecting the first and second point, requiring one additional angle.

respectively be the translational and rotational velocities of the body relative to O and expressed in the body frame, and let $\boldsymbol{\nu} = [\boldsymbol{v}^T, \boldsymbol{\omega}^T]^T$. Note that $\boldsymbol{\nu}$ does not integrate into a meaningful set of positions and angles since the velocities are defined with respect to the vectors $\{\boldsymbol{b}_1, \boldsymbol{b}_2, \boldsymbol{b}_3\}$ which are themselves undergoing motion.

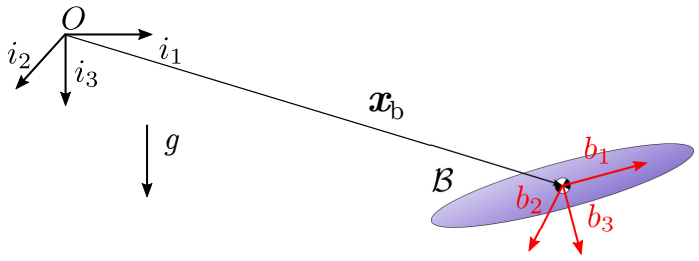

Figure 2.1: Reference frames defined for the equations of motion.

Let $\boldsymbol{e}_i \in \mathbb{R}^n$ define a unit vector with a 1 in the i^{th} position and whose dimension n will be clear from context. Let the hat operator $\hat{\cdot}$ define the cross product equivalent matrix

$$\boldsymbol{a} = \begin{pmatrix} a_1 \\ a_2 \\ a_3 \end{pmatrix} \quad \hat{\boldsymbol{a}} = \begin{pmatrix} 0 & -a_3 & a_2 \\ a_3 & 0 & -a_1 \\ -a_2 & a_1 & 0 \end{pmatrix}$$

satisfying $\hat{\boldsymbol{a}}\boldsymbol{b} = \boldsymbol{a} \times \boldsymbol{b}$ for $\boldsymbol{a}, \boldsymbol{b} \in \mathbb{R}^3$. At each instant, the orientation of the body fixed-frame may be defined using a sequence of principal rotations. In terms of the roll-pitch-yaw Euler angles, these principal rotation matrices are

$$\boldsymbol{R}_1(\phi_\mathrm{b}) = e^{\widehat{\boldsymbol{e}_1}\phi_\mathrm{b}} = \begin{pmatrix} 1 & 0 & 0 \\ 0 & \cos\phi_\mathrm{b} & -\sin\phi_\mathrm{b} \\ 0 & \sin\phi_\mathrm{b} & \cos\phi_\mathrm{b} \end{pmatrix} \quad \text{roll about } \boldsymbol{e}_1 \tag{2.1}$$

$$\boldsymbol{R}_2(\theta_\mathrm{b}) = e^{\widehat{\boldsymbol{e}_2}\theta_\mathrm{b}} = \begin{pmatrix} \cos\theta_\mathrm{b} & 0 & \sin\theta_\mathrm{b} \\ 0 & 1 & 0 \\ -\sin\theta_\mathrm{b} & 0 & \cos\theta_\mathrm{b} \end{pmatrix} \quad \text{pitch about } \boldsymbol{e}_2 \tag{2.2}$$

$$\boldsymbol{R}_3(\psi_\mathrm{b}) = e^{\widehat{\boldsymbol{e}_3}\psi_\mathrm{b}} = \begin{pmatrix} \cos\psi_\mathrm{b} & -\sin\psi_\mathrm{b} & 0 \\ \sin\psi_\mathrm{b} & \cos\psi_\mathrm{b} & 0 \\ 0 & 0 & 1 \end{pmatrix} \quad \text{yaw about } \boldsymbol{e}_3 \tag{2.3}$$

The matrices $\boldsymbol{R}_i$ are proper rotation matrices which belong to $SO(3)$, the special orthogonal group:

$$SO(3) \triangleq \{\boldsymbol{P} \in \mathbb{R}^{3\times 3} \;\; \big| \;\; \det(\boldsymbol{P}) = +1 \;\; \text{and} \;\; \boldsymbol{P}^{-1} = \boldsymbol{P}^T\} \tag{2.4}$$

Define $\boldsymbol{R} \in SO(3)$ as the proper rotation matrix which relates the orientation of the body fixed vectors $\{\boldsymbol{b}_1, \boldsymbol{b}_2, \boldsymbol{b}_3\}$ to the orientation of the inertially fixed axes $\{\boldsymbol{i}_1, \boldsymbol{i}_2, \boldsymbol{i}_3\}$. In other words, $\boldsymbol{R}$ maps free vectors from the body frame to the inertial frame. When parameterized by Euler angles, the rotation matrix is conventionally given by a "3-2-1" sequence for submerged vehicles [1]:

$$\boldsymbol{R}(\boldsymbol{\theta}_\text{b}) = e^{\widehat{\boldsymbol{e}_3}\psi_\text{b}} e^{\widehat{\boldsymbol{e}_2}\theta_\text{b}} e^{\widehat{\boldsymbol{e}_1}\phi_\text{b}} = \boldsymbol{R}_3(\psi_\text{b})\boldsymbol{R}_2(\theta_\text{b})\boldsymbol{R}_1(\phi_\text{b}) \tag{2.5}$$

or explicitly,

$$\boldsymbol{R} = \begin{pmatrix} \cos\theta_\text{b}\cos\psi_\text{b} & \sin\phi_\text{b}\sin\theta_\text{b}\cos\psi_\text{b} - \cos\phi_\text{b}\sin\psi_\text{b} & \cos\phi_\text{b}\sin\theta_\text{b}\cos\psi_\text{b} + \sin\phi_\text{b}\sin\psi_\text{b} \\ \cos\theta_\text{b}\sin\psi_\text{b} & \cos\phi_\text{b}\cos\psi_\text{b} + \sin\phi_\text{b}\sin\theta_\text{b}\sin\psi_\text{b} & -\sin\phi_\text{b}\cos\psi_\text{b} + \cos\phi_\text{b}\sin\theta_\text{b}\sin\psi_\text{b} \\ -\sin\theta_\text{b} & \sin\phi_\text{b}\cos\theta_\text{b} & \cos\phi_\text{b}\cos\theta_\text{b} \end{pmatrix} \tag{2.6}$$

The pair $(\boldsymbol{R}, \boldsymbol{x}_\text{b})$ enables a point $\bar{\boldsymbol{x}}$ expressed in the body frame to be equivalently expressed as a point $\boldsymbol{x}$ in the inertial frame:

$$\begin{pmatrix} \boldsymbol{x} \\ 1 \end{pmatrix} = \begin{pmatrix} \boldsymbol{R} & \boldsymbol{x}_\text{b} \\ \boldsymbol{0}^T & 1 \end{pmatrix} \begin{pmatrix} \bar{\boldsymbol{x}} \\ 1 \end{pmatrix}$$

2.2 Kinematics

Suppose Q is a configuration manifold. Then $\boldsymbol{q} \in Q$ completely characterizes the "configuration" or position and orientation of the system. Based on the choice of Q, kinematic equations are defined to relate the chosen body-fixed velocities to the rate of change of configuration variables. While position of the body can simply be given by $\boldsymbol{x}_\text{b}$, there are several choices to characterize the orientation of the body; Euler angles (as introduced above) or

quaternions are two common choices. One may also choose to use $\boldsymbol{R} \in SO(3)$ since each element in $SO(3)$ corresponds to a unique attitude.

2.2.1 Kinematic Relations using Euler Angles

Choosing to parameterize the orientation of the body in terms of the Euler angles,

$$\boldsymbol{q} = [\boldsymbol{x}_{\mathrm{b}}^T, \boldsymbol{\theta}_{\mathrm{b}}^T]^T \tag{2.7}$$

The translational velocities $\boldsymbol{v}$ are related to $\dot{\boldsymbol{x}}_{\mathrm{b}}$ as

$$\dot{\boldsymbol{x}}_{\mathrm{b}} = \boldsymbol{R}(\boldsymbol{\theta}_{\mathrm{b}})\boldsymbol{v} \tag{2.8}$$

Relating $\dot{\boldsymbol{\theta}}_{\mathrm{b}}$ to $\boldsymbol{\omega}$ has additional complexities since the Euler angles are themselves defined with respect to rotating axes. Using a series of proper rotation matrices, this relationship is

$$\boldsymbol{\omega} = \boldsymbol{e}_1\dot{\phi}_{\mathrm{b}} + \boldsymbol{R}_1^T(\phi_{\mathrm{b}})\boldsymbol{e}_2\dot{\theta}_{\mathrm{b}} + \boldsymbol{R}_1^T(\phi_{\mathrm{b}})\boldsymbol{R}_2^T(\theta_{\mathrm{b}})\boldsymbol{e}_3\dot{\psi}_{\mathrm{b}} \tag{2.9}$$

Define the matrix $\boldsymbol{L}(\boldsymbol{\theta}_{\mathrm{b}})$ as

$$\boldsymbol{L}(\boldsymbol{\theta}_{\mathrm{b}}) = \begin{pmatrix} 1 & \sin\phi_{\mathrm{b}}\tan\theta_{\mathrm{b}} & \cos\phi_{\mathrm{b}}\tan\theta_{\mathrm{b}} \\ 0 & \cos\phi_{\mathrm{b}} & -\sin\phi_{\mathrm{b}} \\ 0 & \sin\phi_{\mathrm{b}}\sec\theta_{\mathrm{b}} & \cos\phi_{\mathrm{b}}\sec\theta_{\mathrm{b}} \end{pmatrix} \tag{2.10}$$

and the rotational kinematics are compactly defined as

$$\dot{\boldsymbol{\theta}}_{\mathrm{b}} = \boldsymbol{L}(\boldsymbol{\theta}_{\mathrm{b}})\boldsymbol{\omega} \tag{2.11}$$

Define the combined kinematic transformation matrix

$$\boldsymbol{J} = \begin{pmatrix} \boldsymbol{R}(\boldsymbol{\theta}_{\mathrm{b}}) & \boldsymbol{0} \\ \boldsymbol{0} & \boldsymbol{L}(\boldsymbol{\theta}_{\mathrm{b}}) \end{pmatrix} \tag{2.12}$$

and the complete kinematic equations are

$$\dot{\boldsymbol{q}} = \boldsymbol{J}(\boldsymbol{\theta}_{\mathrm{b}})\boldsymbol{\nu} \tag{2.13}$$

One must be cognizant of the singularity which exists within $\boldsymbol{L}$ at $\theta_{\mathrm{b}} = \pm\frac{\pi}{2}$, corresponding to a pitch angle of ± 90 degrees. Fortunately, this is rarely a cause for concern when working with underwater vehicles, particularly when they operate near the free surface.

2.2.2 Kinematic Relations in $SE(3)$

The pair $(\boldsymbol{R}, \boldsymbol{x}_\mathrm{b})$ is an element in the special Euclidean group $SE(3)$ of three-dimensional rigid body rotations and translations. Choosing $Q = SE(3)$, the position and orientation of the body is given by

$$\boldsymbol{q} = \{\boldsymbol{R}, \boldsymbol{x}_\mathrm{b}\} \tag{2.14}$$

One may use the same expression as before to relate $\dot{\boldsymbol{x}}_\mathrm{b}$ and $\boldsymbol{v}$, though a new expression is required to relate $\dot{\boldsymbol{R}}$ to $\boldsymbol{\omega}$:

$$\dot{\boldsymbol{x}}_\mathrm{b} = \boldsymbol{R}\boldsymbol{v} \tag{2.15}$$

$$\dot{\boldsymbol{R}} = \boldsymbol{R}\hat{\boldsymbol{\omega}} \tag{2.16}$$

A derivation of $\dot{\boldsymbol{R}}$ is given in Appendix A.2. The chief advantage of this parameterization is that the kinematic equations for $\boldsymbol{R}$ are free of any singularities, unlike the kinematic equations for the the Euler angle rates (2.13). However, since there are only three rotational degrees of freedom, one may conclude that the nine elements in $\boldsymbol{R}$ are not independent from each other. One may therefore identify six constraint equations from the relationship $\boldsymbol{R}\boldsymbol{R}^T = \mathbb{I}$ to eliminate this redundancy.

2.3 Kinetics

Kinetic equations relate the forces and moments acting on a mechanical system to the velocities (or momenta) of the system. The foundation for modeling the kinetics of a single particle date back to 1687 with the first publication of Newton's *Principia*[2]. From Newton's second law, one could relate the motion of a particle to an externally applied force[3] [36, p83]:

[2]Sir Isaac Newton, 1642-1726.

[3]Note that the word "motion", as defined by Newton, refers to the system momentum: "The quantity of motion is the measure of the same, arising from the velocity and quantity of matter conjunctly"[36, p73].

> *The alteration of motion is ever proportional to the motive force impressed; and is made in the direction of the right line in which that force is impressed.*

It took almost 100 years for the complete rigid body equations of motion. The absence of a formal concept of angular momentum, as well as ambiguity in the understanding of rigid body rotations both contributed to this delay [37]. In 1776, Euler[4] presented his first and second axioms relating exogenous forces $\boldsymbol{f}$ and moments $\boldsymbol{\tau}$ to the translational momentum $\boldsymbol{p}$ and the angular momentum $\boldsymbol{h}$. For a rigid body with mass m_{b} and inertia matrix $\boldsymbol{I}_{\mathrm{b}}$, these equations are

$$\boldsymbol{f} = \frac{d}{dt}\boldsymbol{p}, \quad \boldsymbol{p} = m_{\mathrm{b}}\boldsymbol{v} \tag{2.17}$$

$$\boldsymbol{\tau} = \frac{d}{dt}\boldsymbol{h}, \quad \boldsymbol{h} = \boldsymbol{I}_{\mathrm{b}}\boldsymbol{\omega} \tag{2.18}$$

These equations represent the conservation of translational and angular momentum; in the absence of external forces and moments, $\boldsymbol{p}$ and $\boldsymbol{h}$ are conserved quantities. Assuming constant mass and inertia matrices, and evaluating the time derivative in a body-fixed frame which coincides with the center of mass, (2.17) and (2.18) become the *Newton-Euler equations*:

$$\begin{aligned} \boldsymbol{f} &= m_{\mathrm{b}}\dot{\boldsymbol{v}} + \boldsymbol{\omega} \times (m_{\mathrm{b}}\boldsymbol{v}) \\ \boldsymbol{\tau} &= \boldsymbol{I}_{\mathrm{b}}\dot{\boldsymbol{\omega}} + \boldsymbol{\omega} \times (\boldsymbol{I}_{\mathrm{b}}\boldsymbol{\omega}) \end{aligned} \tag{2.19}$$

In *Newtonian mechanics*, one derives the kinetic equations of motion by relating the external force and moment vectors to the time rate of change of the translational and angular momenta. The Newtonian approach is often called a *direct approach* or a *vectoral approach* because of the direct relationship between the imposed force and moment vectors and the system motion [37, 16]. A separate modeling approach was developed using principles of work and energy. In *Lagrangian mechanics*, one instead begins the system analysis with a scalar energy-like function, the *Lagrangian*[5]. Employing either D'Alembert's Principle of

[4] Leonhard Euler, 1707-1783.

[5] Joseph-Louis Lagrange, 1736-1813.

Virtual Work[6] or Hamilton's Principle of Least Action[7] then places a constraint on the system Lagrangian, yielding the equations of motion for the system [17, 16]. This energy-based approach is sometimes called an *indirect approach* or an *analytical approach* [37, 16].

2.3.1 Hamilton's Principle

Let $T(\boldsymbol{q}, \dot{\boldsymbol{q}}, t)$ represent the system kinetic energy and $V(\boldsymbol{q}, t)$ the system potential energy. Defining the Lagrangian as $\mathcal{L}(\boldsymbol{q}, \dot{\boldsymbol{q}}, t) = T - V$, *Hamilton's Principle of Least Action* states that the true trajectory of $\boldsymbol{q}(t)$ between known starting and ending points $\boldsymbol{q}(t_0)$ and $\boldsymbol{q}(t_1)$ will extremize the *action* I [38, 17], defined as

$$I = \int_{t_0}^{t_1} \mathcal{L}(\boldsymbol{q}, \dot{\boldsymbol{q}}, t) dt \tag{2.20}$$

While there are an infinite number of trajectories which might connect $\boldsymbol{q}_0$ and $\boldsymbol{q}_1$, the true system motion either minimizes or maximizes the time integral of $\mathcal{L}$ between an initial and final time. In Figure 2.2, the solid red line represents the true trajectory of a system, while the dashed blue lines depict arbitrary admissible variations.

Enforcing Hamilton's principle is done by setting the first *variation* of the action equal to zero:

$$\delta I = \delta \int_{t_0}^{t_1} \mathcal{L}(\boldsymbol{q}, \dot{\boldsymbol{q}}, t) dt = 0 \tag{2.21}$$

The variational operator δ is analogous to differentiation in multivariable calculus; it characterizes the sensitivity of I to changes in $\boldsymbol{q}(t)$. Setting the first variation equal to zero is then analogous to the process of searching for a functional extrema by computing the function's critical points.

[6] Jean le Rond d'Alembert, 1717-1783.

[7] William Rowan Hamilton, 1805-1865.

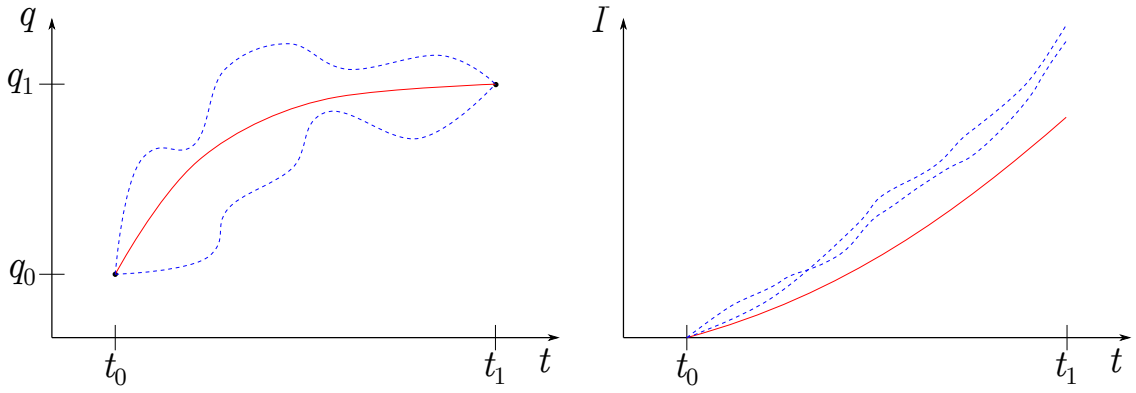

Figure 2.2: True trajectory (solid red line) and arbitrary variations (dashed blue lines) between initial and final value of $q(t)$.

2.3.2 Lagrangian Mechanics

The variational operator can be evaluated using a number of approaches: one may discretize the trajectory $\boldsymbol{q}(t)$ into a finite number of subintervals, as in [39, Ch. 1], one may employ a Taylor series expansion as in [38, Ch. 2], or one may introduce an *index* variable, as in [17, Ch. 2] and [40, Ch. 3]. Following [17], introduce an infinitesimal parameter α and a well-behaved function $\delta\boldsymbol{q}(t)$ which satisfies the initial and final conditions $\delta\boldsymbol{q}(t_0) = \delta\boldsymbol{q}(t_1) = \boldsymbol{0}$. The trajectory may then be rewritten as

$$\boldsymbol{q}(t,\alpha) = \boldsymbol{q}(t,0) + \alpha\ \delta\boldsymbol{q}(t) \tag{2.22}$$

In the above expression, $\boldsymbol{q}(t,0)$ is the true motion of the system and the term $\alpha\delta\boldsymbol{q}(t)$ represents a deviation from the true motion. Introducing the parameter α enables one to evaluate the first variation using a vector calculus framework:

$$\delta I = \frac{d}{d\alpha}\left[\int_{t_0}^{t_1} \mathcal{L}\left(\boldsymbol{q}(t,0) + \alpha\ \delta\boldsymbol{q}(t), \dot{\boldsymbol{q}}(t,0) + \alpha\ \delta\dot{\boldsymbol{q}}(t), t\right) dt\right]\Bigg|_{\alpha=0} = 0 \tag{2.23}$$

Assuming $\boldsymbol{q}(t) \in \mathbb{R}^n$, carrying out the differentiation yields

$$\begin{aligned}\frac{d}{d\alpha}\left[\int_{t_0}^{t_1} \mathcal{L}(\boldsymbol{q},\dot{\boldsymbol{q}},t)dt\right]\Bigg|_{\alpha=0} &= \sum_{i=1}^{n}\int_{t_0}^{t_1}\left[\frac{\partial\mathcal{L}}{\partial\dot{q}_i}\frac{\partial\dot{q}_i}{\partial\alpha} + \frac{\partial\mathcal{L}}{\partial q_i}\frac{\partial q_i}{\partial\alpha}\right]\Bigg|_{\alpha=0} dt \\ &= \sum_{i=1}^{n}\int_{t_0}^{t_1}\left[\frac{\partial\mathcal{L}}{\partial\dot{q}_i}\delta\dot{q}_i + \frac{\partial\mathcal{L}}{\partial q_i}\delta q_i\right] dt\end{aligned}$$

Integrating the first term by parts, one finds that the above expression is equivalent to

$$0 = \sum_{i=1}^{n} \left[\frac{\partial \mathcal{L}}{\partial \dot{q}_i} \cancel{\delta q_i} \Big|_{t_0}^{t_1} - \int_{t_0}^{t_1} \left[\frac{d}{dt} \left(\frac{\partial \mathcal{L}}{\partial \dot{q}_i} \right) \delta q_i - \frac{\partial \mathcal{L}}{\partial q_i} \delta q_i \right] dt \right]$$

$$0 = - \int_{t_0}^{t_1} \sum_{i=1}^{n} \left[\frac{d}{dt} \left(\frac{\partial \mathcal{L}}{\partial \dot{q}_i} \right) - \frac{\partial \mathcal{L}}{\partial q_i} \right] \delta q_i \; dt$$

For a set of independent generalized coordinates $\boldsymbol{q}$, the components δq_i will also be independent [17]. Moreover, since each δq_i represents an arbitrary variation, one may satisfy the above integral constraint equation by requiring

$$\frac{d}{dt} \left(\frac{\partial \mathcal{L}}{\partial \dot{q}_i} \right) - \frac{\partial \mathcal{L}}{\partial q_i} = 0 \quad t \in [t_0, t_1] \tag{2.24}$$

for each i. These n equations are known as the Euler-Lagrange equations. Concatenating them into a single vector equation, one writes

$$\frac{d}{dt} \left(\frac{\partial \mathcal{L}}{\partial \dot{\boldsymbol{q}}} \right) - \frac{\partial \mathcal{L}}{\partial \boldsymbol{q}} = 0 \quad t \in [t_0, t_1] \tag{2.25}$$

Comparison to Newtonian Mechanics

Hamilton's principle of least action enables an energy-based modeling approach, which differs fundamentally from the momentum-based Newtonian approach. Rather than studying how the system momenta evolve in response to imposed forces and moments, one instead studies how the system kinetic energy is altered in response to work performed on the system. This leads to a useful result in Lagrangian mechanics when considering that work is fundamentally defined as a force projected onto a resulting displacement: any force which does not result in a system displacement is inherently neglected, simplifying the system analysis.

To compare the Newtonian and Lagranian approaches, consider a particle of mass m located by the coordinates $\boldsymbol{x}_\mathrm{p} = (x_\mathrm{p}, y_\mathrm{p}, z_\mathrm{p})^T$ and subject to external forces $\boldsymbol{f}(\boldsymbol{x}_\mathrm{p})$. The particle's translational momentum is then $m\dot{\boldsymbol{x}}_\mathrm{p}$ and Newton's Second Law yields the following kinetic equations

$$\frac{d}{dt} \left(m\dot{\boldsymbol{x}}_\mathrm{p} \right) = \boldsymbol{f}(\boldsymbol{x}_\mathrm{p}) \tag{2.26}$$

The particle's kinetic energy is given by $\frac{1}{2}m\dot{\boldsymbol{x}}_{\mathrm{p}} \cdot \dot{\boldsymbol{x}}_{\mathrm{p}}$. If $\boldsymbol{f}$ is an irrotational vector field ($\nabla \times \boldsymbol{f} = 0$), then this force is said to be conservative and one may redefine $\boldsymbol{f}$ in terms of a scalar potential function [17, 41]. Let $V(\boldsymbol{x}_{\mathrm{b}})$ represent the potential energy associated with $\boldsymbol{f}$:

$$\frac{\partial V}{\partial \boldsymbol{x}_{\mathrm{p}}} = \boldsymbol{f}(\boldsymbol{x}_{\mathrm{p}}) \tag{2.27}$$

The Lagrangian function for the particle is then

$$\mathcal{L} = \frac{1}{2}m\dot{\boldsymbol{x}}_{\mathrm{p}} \cdot \dot{\boldsymbol{x}}_{\mathrm{p}} - V(\boldsymbol{x}_{\mathrm{p}}) \tag{2.28}$$

Using the Euler-Lagrange equations, the kinetic equations are found to be identical to those from Newton's Second Law

$$\frac{d}{dt}\left(m\dot{\boldsymbol{x}}_{\mathrm{p}}\right) = \boldsymbol{f}(\boldsymbol{x}_{\mathrm{p}}) \tag{2.29}$$

While this simple example illustrated the similarity between the Newtonian and Lagrangian approaches, it is somewhat restrictive to assume that a force may be associated with a corresponding potential energy. In the following section, several extensions of the Euler-Lagrange equations are presented which account for more general situations.

2.3.3 Extensions of the Euler-Lagrange Equations

Accounting for Nonconservative Forces

When deriving the Euler-Lagrange equations (2.25), it was assumed that the system was only subject to generalized forces which derived from a scalar potential, a somewhat limiting assumption in most practical cases. To account for additional generalized forces $\boldsymbol{Q}$, one modifies the action (2.20) to incorporate the work on the system due to the generalized forces W_{Q}

$$I = \int_{t_0}^{t_1} \left[\mathcal{L}(\boldsymbol{q}, \dot{\boldsymbol{q}}, t) + W_{\mathrm{Q}}\right] dt \tag{2.30}$$

The equations of motion are simply

$$\frac{d}{dt}\left(\frac{\partial \mathcal{L}}{\partial \dot{\boldsymbol{q}}}\right) - \frac{\partial \mathcal{L}}{\partial \boldsymbol{q}} = \boldsymbol{Q} \tag{2.31}$$

A rigorous derivation of (2.31) is given in [17, 16] using D'Alembert's Principle of Virtual Work. The generalized forces $\boldsymbol{Q}$ can accommodate more general forces, such as those arising from control inputs and viscosity.

Accounting for Quasivelocities: The Boltzmann-Hamel Equations

The Euler-Lagrange equations can also be modified to accommodate systems whose velocities are more conveniently given using a set of *quasivelocities*, a set of velocities which completely characterizes the system yet are not time-derivatives of the generalized coordinates [16, Sec. 4.1]. The body velocities $\boldsymbol{\nu}$ constitute a set of quasivelocities; they completely describe the rigid body velocities yet do not integrate to yield the generalized coordinates $\boldsymbol{q}$. (One may verify this using the kinematic relationship (2.13).) The use of quasivelocites is treated in several texts, for instance [16, Sec. 4.3] [42, Sec. 5.5].

The principal idea is that the kinetic energy has the same value when expressed using $\dot{\boldsymbol{q}}$ or $\boldsymbol{\nu}$ [16]:

$$T(\boldsymbol{q}, \dot{\boldsymbol{q}}, t) = T^*(\boldsymbol{q}, \boldsymbol{\nu}, t) \tag{2.32}$$

In terms of quasivelocities, the equations of motion are given by the *Boltzmann-Hamel* equations [16], though presented here in the matrix-vector form derived in [42]:

$$\frac{d}{dt}\left(\frac{\partial \mathcal{L}}{\partial \boldsymbol{\nu}}\right) + \boldsymbol{G}(\boldsymbol{q}, \boldsymbol{\nu})\frac{\partial \mathcal{L}}{\partial \boldsymbol{\nu}} - \boldsymbol{J}(\boldsymbol{q})^T \frac{\partial \mathcal{L}}{\partial \boldsymbol{q}} = \boldsymbol{J}(\boldsymbol{q})^T \boldsymbol{Q} \tag{2.33}$$

where

$$\boldsymbol{G}(\boldsymbol{q}, \boldsymbol{\nu}) = \sum_{i=1}^{n}\sum_{j=1}^{n}\sum_{k=1}^{n}\sum_{l=1}^{n}\sum_{m=1}^{n}\left(\boldsymbol{e}_i \boldsymbol{e}_j^T\right) J_{ki} J_{lm} \nu_m \left(\frac{\partial J_{kj}^{-T}}{\partial q_l} - \frac{\partial J_{lj}^{-T}}{\partial q_k}\right) \tag{2.34}$$

One may verify that in matrix form, the above expression for $\boldsymbol{G}$ is equivalent to

$$\boldsymbol{G}(\boldsymbol{q}, \boldsymbol{\nu}) = \boldsymbol{J}^T \left[\frac{d}{dt}\boldsymbol{J}^{-T} + \left(\frac{\partial}{\partial \boldsymbol{q}}\left(\boldsymbol{J}\boldsymbol{\nu}\right)\right)^T \boldsymbol{J}^{-T}\right] \tag{2.35}$$

For the chosen kinematic transformation matrix $\boldsymbol{J}$,

$$\boldsymbol{G}(\boldsymbol{\nu}) = \begin{pmatrix} \hat{\boldsymbol{\omega}} & \boldsymbol{0} \\ \hat{\boldsymbol{v}} & \hat{\boldsymbol{\omega}} \end{pmatrix} \tag{2.36}$$

Exploiting Ignorable Coordinates: Routhian Reduction

The structure of the Euler-Lagrange equations naturally gives rise to a process of identifying and eliminating *ignorable coordinates*[8]: generalized coordinates which do not appear in the system Lagrangian. For a system characterized by n generalized coordinates, assume that the Lagrangian does not depend on the first k coordinates, or $\mathcal{L}(q_{k+1}, \ldots, q_n, \dot{q}_1, \ldots, \dot{q}_n, t)$. Then (2.25) becomes

$$\frac{d}{dt}\left(\frac{\partial \mathcal{L}}{\partial \dot{q}_i}\right) = 0, \qquad i = 1, 2, \ldots, k \tag{2.37}$$

$$\frac{d}{dt}\left(\frac{\partial \mathcal{L}}{\partial \dot{q}_i}\right) = \frac{\partial \mathcal{L}}{\partial q_i}, \quad i = k+1, k+2, \ldots, n \tag{2.38}$$

For the first k equations, the quantity $\partial \mathcal{L}/\partial \dot{q}_i$ is conserved because it does not vary with time. It follows that

$$\frac{\partial \mathcal{L}}{\partial \dot{q}_i} = \beta_i, \quad i = 1, 2, \ldots k \tag{2.39}$$

where each constant β_i is uniquely determined from the initial conditions. Following [17, Sec. 8.3] or [16, Sec. 2.3], the constants β_i may be used to reduce the order of the system in a process known as *Routhian reduction*[9]. Define the *Routhian* function [16, Eq. 2.184][10]

$$\mathcal{R}(q_{k+1}, \ldots, q_n, \dot{q}_{k+1}, \ldots, \dot{q}_n, \beta_1, \ldots, \beta_k, t) = \mathcal{L} - \sum_{i=1}^{c} \beta_i \dot{q}_i \tag{2.40}$$

One may then show that the Euler-Lagrange equations apply to the Routhian, yielding a set of $n - k$ second order equations [16]:

$$\frac{d}{dt}\left(\frac{\partial \mathcal{R}}{\partial \dot{q}_i}\right) - \frac{\partial \mathcal{R}}{\partial q_i} = 0 \quad i = k+1, \ldots, n \tag{2.41}$$

The trajectories for the ignorable coordinates, though usually not of interest, may be determined from the following differential equation [16]:

$$\dot{q}_i = \frac{\partial \mathcal{R}}{\partial \beta_i} \tag{2.42}$$

[8] Also known as *cyclic* coordinates [17].

[9] Edward John Routh, 1831-1907.

[10] As compared to [16], the Routhian in [17] is defined as $-\mathcal{R}$. The multiplication by -1 does not affect the ensuing equations of motion in [17] because the authors do not consider external generalized forces – the system conserves energy.

Reducing the number of degrees of freedom simplifies the dynamic analysis. Other techniques for reducing a dynamic system exploit group symmetries. These processes, for instance Lie-Poisson[11] reduction and Euler-Poincaré[12] reduction, are detailed in [43].

2.3.4 Hamiltonian Mechanics

Similar to the Lagrangian approach, Hamiltonian systems are derived from a scalar energy function: the *Hamiltonian* $\mathcal{H}(\boldsymbol{q}, \boldsymbol{p}, t)$. In contrast to the Lagrangian, which is given in terms of the generalized coordinates $\boldsymbol{q}$ and the system velocities $\dot{\boldsymbol{q}}$ or $\boldsymbol{\nu}$, the Hamiltonian is given in terms of the generalized coordinates and the conjugate momenta $\boldsymbol{p}$, defined as

$$\boldsymbol{p} = \frac{\partial \mathcal{L}}{\partial \dot{\boldsymbol{q}}} \tag{2.43}$$

When the forces acting on the system are velocity-independent, the mechanical momentum $\boldsymbol{M}\dot{\boldsymbol{q}}$ is equivalent to the conjugate momenta [17].

Similar to the Routhian, the Hamiltonian is readily computed through a transformation of the system Lagrangian. Specifically, the Hamiltonian is generated using the *Legendre transformation*[13]:

$$\mathcal{H}(\boldsymbol{q}, \boldsymbol{p}, t) = \sum_{j=1}^{n} \dot{q}_j p_j - \mathcal{L}(\boldsymbol{q}, \dot{\boldsymbol{q}}, t) \tag{2.44}$$

For a time-invariant Lagrangian which is quadratic in the system velocities, the Hamiltonian simply becomes [17, Sec. 8.1]

$$\mathcal{H} = T(\boldsymbol{q}, \boldsymbol{p}) + V(\boldsymbol{q}), \tag{2.45}$$

the kinetic plus the potential energy, or the total system energy. Using the Hamiltonian, one may again use Hamilton's principle to derive the equations of motion. Using the Legendre transformation (2.44), one may rewrite the action (2.20) as

$$I = \int_{t_0}^{t_1} \left[\sum_{j=1}^{n} \dot{q}_j p_j - \mathcal{H}(\boldsymbol{q}, \boldsymbol{p}, t) \right] dt \tag{2.46}$$

[11] Marius Sophus Lie, 1842-1899. Siméon Denis Poisson, 1781-1840.

[12] Henri Poincaré, 1854-1912.

[13] Adrien-Marie Legendre, 1752-1833.

Enforcing Hamilton's principle, *i.e.* setting $\delta I = 0$, results in *Hamilton's Canonical Equations* [17, Sec. 8.5]

$$\dot{\boldsymbol{q}} = \frac{\partial \mathcal{H}}{\partial \boldsymbol{p}} \quad \text{and} \quad \dot{\boldsymbol{p}} = -\frac{\partial \mathcal{H}}{\partial \boldsymbol{q}} \tag{2.47}$$

Written compactly in first order form, the equations are

$$\frac{d}{dt}\begin{pmatrix} \boldsymbol{q} \\ \boldsymbol{p} \end{pmatrix} = \boldsymbol{S}\nabla\mathcal{H} \qquad \text{with} \qquad \boldsymbol{S} = \begin{pmatrix} \boldsymbol{0} & \mathbb{I}_n \\ -\mathbb{I}_n & \boldsymbol{0} \end{pmatrix} \tag{2.48}$$

The matrix $\boldsymbol{S}$ is known as the *symplectic* matrix, and encodes the canonical Hamiltonian structure. The equations (2.48) are a set of $2n$ first order differential equations, in contrast to the Euler-Lagrange equations which are given as a set of n second order differential equations.

Remark 2.3.1 *It is straightforward to show that $\mathcal{H}$ is conserved for a time-invariant Hamiltonian system:*

$$\frac{d\mathcal{H}}{dt} = (\nabla\mathcal{H})^T \frac{d}{dt}\begin{pmatrix} \boldsymbol{q} \\ \boldsymbol{p} \end{pmatrix} = (\nabla\mathcal{H})^T \boldsymbol{S}\,(\nabla\mathcal{H}) \tag{2.49}$$

By virtue of the skew symmetry of $\boldsymbol{S}$, the above quadratic form must evaluate to zero.

2.3.5 Non-Canonical Hamiltonian Systems

More generally, one may show that the canonical equations can be generated by a *Poisson Bracket* [17, Sec. 9.6] [38, Sec. 6.3]. For an arbitrary function of the state variables $a(\boldsymbol{q}, \boldsymbol{p})$, the Poisson bracket gives the time rate of change of a subject to the Hamiltonian dynamics:

$$\dot{a} = \{a, \mathcal{H}\} = \sum_{i=1}^{n} \left(\frac{\partial a}{\partial q_i}\frac{\partial \mathcal{H}}{\partial p_i} - \frac{\partial a}{\partial p_i}\frac{\partial \mathcal{H}}{\partial q_i} \right) = (\nabla a)^T \boldsymbol{S} \nabla\mathcal{H} \tag{2.50}$$

In terms of the Poisson bracket, the equations of motion are simply

$$\dot{\boldsymbol{q}} = \{\boldsymbol{q}, \mathcal{H}\} = \frac{\partial \mathcal{H}}{\partial \boldsymbol{p}} \tag{2.51}$$

$$\dot{\boldsymbol{p}} = \{\boldsymbol{p}, \mathcal{H}\} = -\frac{\partial \mathcal{H}}{\partial \boldsymbol{q}} \tag{2.52}$$

When the conjugate momenta are derived from quasi-velocities, the Hamiltonian structure takes on a modified, non-canonical form. In this case, the Poisson bracket yields

$$\dot{a} = \{a, \mathcal{H}\} = (\nabla a)^T \boldsymbol{\Lambda}(\boldsymbol{q}, \boldsymbol{p}) \nabla \mathcal{H} \tag{2.53}$$

where $\boldsymbol{\Lambda}(\boldsymbol{q}, \boldsymbol{p})$ is the *Poisson tensor*, a generalization of the symplectic matrix $\boldsymbol{S}$. Procedures for computing the Poisson tensor can be found in [43, Sec. 10.7]; these procedures were employed in [44] to compute the Poisson tensor for an underwater vehicle governed by Kirchhoff's equations[14].

The Poisson tensor is skew symmetric, which again enables one to conclude that the Hamiltonian is conserved:

$$\dot{\mathcal{H}} = (\nabla \mathcal{H})^T \boldsymbol{\Lambda} (\nabla \mathcal{H}) = 0 \tag{2.54}$$

If $\boldsymbol{\Lambda} \in \mathbb{R}^{n \times n}$ where n is odd, the Poisson tensor must be rank deficient [45], suggesting that one may identify additional conserved quantities. If a function $C(\boldsymbol{q}, \boldsymbol{p})$ satisfies

$$\dot{C} = \{C, \mathcal{H}\} = (\nabla C)^T \boldsymbol{\Lambda} (\nabla \mathcal{H}) = 0 \tag{2.55}$$

then C is a conserved quantity referred to as a *Casimir function*[15] [43]. The Casimir functions often prove useful in control design and stability analysis [44, 46, 47, 48].

2.4 Rigid Body Equations of Motion

In the most general case, the rigid body mass matrix $\boldsymbol{M}_\mathrm{b}$ may be defined with respect to any point fixed in the body frame. Let $\boldsymbol{x}_\mathrm{cm}$ locate the center of mass with respect to the arbitrary body-fixed point. Using the parallel axis theorem, the rigid body mass matrix will be of the form

$$\boldsymbol{M}_\mathrm{b} = \begin{pmatrix} m_\mathrm{b} \mathbb{I}_3 & -m_\mathrm{b} \hat{\boldsymbol{r}}_\mathrm{cm} \\ m_\mathrm{b} \hat{\boldsymbol{r}}_\mathrm{cm} & \boldsymbol{I}_\mathrm{b} - m_\mathrm{b} \hat{\boldsymbol{r}}_\mathrm{cm} \hat{\boldsymbol{r}}_\mathrm{cm} \end{pmatrix} \tag{2.56}$$

[14] Gustov Kirchhoff, 1824-1887.

[15] Hendrik Casimir, 1909-1990.

where $\boldsymbol{I}_{\mathrm{b}}$ is the inertia tensor about the center of mass and expressed relative to the body-fixed axes. The rigid body kinetic energy is then

$$T_{\mathrm{b}} = \frac{1}{2}\boldsymbol{\nu}^T \boldsymbol{M}_{\mathrm{b}} \boldsymbol{\nu} \tag{2.57}$$

For the system potential energy, only gravitational forces are considered. Assuming no significant change in altitude, the gravitational potential energy is given in terms of the sea-level acceleration due to gravity g:

$$V_{\mathrm{b}} = -m_{\mathrm{b}} g z_{\mathrm{b}} \tag{2.58}$$

For a translating and rotating rigid body under the influence of gravity, the rigid body Lagrangian is

$$\mathcal{L}_{\mathrm{b}} = \frac{1}{2}\boldsymbol{\nu}^T \boldsymbol{M}_{\mathrm{b}} \boldsymbol{\nu} + m_{\mathrm{b}} g z_{\mathrm{b}} \tag{2.59}$$

The kinetic equations of motion may now be derived using the system Lagrangian (2.59) and the Boltzmann-Hamel equations. Evaluating the terms on the left-hand side of (2.33), one finds

$$\begin{aligned}
\frac{d}{dt}\left(\frac{\partial \mathcal{L}_{\mathrm{b}}}{\partial \boldsymbol{\nu}}\right) &= \boldsymbol{M}_{\mathrm{b}} \dot{\boldsymbol{\nu}} \\
\begin{pmatrix} \hat{\boldsymbol{\omega}} & \boldsymbol{0} \\ \hat{\boldsymbol{v}} & \hat{\boldsymbol{\omega}} \end{pmatrix} \frac{\partial \mathcal{L}_{\mathrm{b}}}{\partial \boldsymbol{\nu}} &= \begin{pmatrix} \hat{\boldsymbol{\omega}} & \boldsymbol{0} \\ \hat{\boldsymbol{v}} & \hat{\boldsymbol{\omega}} \end{pmatrix} \boldsymbol{M}_{\mathrm{b}} \boldsymbol{\nu} \\
\boldsymbol{J}^T \frac{\partial \mathcal{L}_{\mathrm{b}}}{\partial \boldsymbol{q}} &= \boldsymbol{R}^T \boldsymbol{e}_3 m_{\mathrm{b}} g
\end{aligned}$$

Let $\boldsymbol{J}(\boldsymbol{q})^T \boldsymbol{Q} = \boldsymbol{F}$, the vector of exogenous forces and moments which do not derive from a scalar potential. Together, the kinematic equations (2.13) and the kinetic equations establish the complete equations of motion for a rigid body

$$\begin{aligned}
\dot{\boldsymbol{q}} &= \boldsymbol{J}(\boldsymbol{q})\boldsymbol{\nu} \\
\boldsymbol{M}_{\mathrm{b}} \dot{\boldsymbol{\nu}} + \begin{pmatrix} \hat{\boldsymbol{\omega}} & \boldsymbol{0} \\ \hat{\boldsymbol{v}} & \hat{\boldsymbol{\omega}} \end{pmatrix} \boldsymbol{M}_{\mathrm{b}} \boldsymbol{\nu} - \boldsymbol{R}^T \boldsymbol{e}_3 m_{\mathrm{b}} g &= \boldsymbol{F}
\end{aligned} \tag{2.60}$$

One may verify that when $\boldsymbol{x}_{\mathrm{cm}} = \boldsymbol{0}$, the kinetic equations reduce to the Newton-Euler equations (2.19).

Non-Canonical Representation of the Equations of Motion

Let $\boldsymbol{\pi}$ represent the generalized momenta associated with the quasivelocities $\boldsymbol{\nu}$:

$$\boldsymbol{\pi} = \frac{\partial \mathcal{L}}{\partial \boldsymbol{\nu}} = \boldsymbol{M}_{\mathrm{b}} \boldsymbol{\nu} \tag{2.61}$$

with

$$\boldsymbol{\pi}_v = \frac{\partial \mathcal{L}}{\partial \boldsymbol{v}} \quad \text{and} \quad \boldsymbol{\pi}_\omega = \frac{\partial \mathcal{L}}{\partial \boldsymbol{\omega}} \tag{2.62}$$

The rigid body Hamiltonian is then computed using the Legendre transformation (2.44):

$$\mathcal{H}_{\mathrm{b}} = \frac{1}{2} \boldsymbol{\pi}^T \boldsymbol{M}_{\mathrm{b}}^{-1} \boldsymbol{\pi} - m_{\mathrm{b}} g z_{\mathrm{b}} \tag{2.63}$$

The Hamiltonian equations for $\boldsymbol{q}$ may be derived from the kinematic relationship (2.13). Noting that $\boldsymbol{\nu} = \boldsymbol{M}_{\mathrm{b}}^{-1} \boldsymbol{\pi}$,

$$\dot{\boldsymbol{q}} = \boldsymbol{J} \boldsymbol{M}_{\mathrm{b}}^{-1} \boldsymbol{\pi} = \boldsymbol{J} \frac{\partial \mathcal{H}}{\partial \boldsymbol{\pi}} \tag{2.64}$$

Substituting $\boldsymbol{\pi}$ into the Boltzmann-Hamel equations (2.33), one may derive the Hamiltonian equations for the generalized momenta:

$$\frac{d}{dt} \boldsymbol{\pi} = -\boldsymbol{G} \boldsymbol{\pi} + \boldsymbol{J}^T \frac{\partial \mathcal{L}}{\partial \boldsymbol{q}} \tag{2.65}$$

The term $-\boldsymbol{G}\boldsymbol{\pi}$ may be rewritten as

$$- \begin{pmatrix} \hat{\boldsymbol{\omega}} & \boldsymbol{0} \\ \hat{\boldsymbol{v}} & \hat{\boldsymbol{\omega}} \end{pmatrix} \begin{pmatrix} \boldsymbol{\pi}_v \\ \boldsymbol{\pi}_\omega \end{pmatrix} = \boldsymbol{C} \boldsymbol{\nu} \quad \text{with} \quad \boldsymbol{C} = \begin{pmatrix} \boldsymbol{0} & \hat{\boldsymbol{\pi}}_v \\ \hat{\boldsymbol{\pi}}_v & \hat{\boldsymbol{\pi}}_\omega \end{pmatrix} \tag{2.66}$$

Finally, using the Legendre transformation to relate the system Lagrangian to the Hamiltonian, one finds

$$\frac{\partial \mathcal{L}_{\mathrm{b}}}{\partial \boldsymbol{q}} = \frac{\partial (\boldsymbol{\pi} \cdot \boldsymbol{\nu} - \mathcal{H}_{\mathrm{b}})}{\partial \boldsymbol{q}} = -\frac{\partial \mathcal{H}_{\mathrm{b}}}{\partial \boldsymbol{q}} \tag{2.67}$$

Combine the equations for $\boldsymbol{q}$ and $\boldsymbol{\pi}$ as

$$\frac{d}{dt} \begin{pmatrix} \boldsymbol{q} \\ \boldsymbol{\pi} \end{pmatrix} = \begin{pmatrix} \boldsymbol{0} & \boldsymbol{J} \\ -\boldsymbol{J}^T & \boldsymbol{C} \end{pmatrix} \begin{pmatrix} \partial \mathcal{H}_{\mathrm{b}} / \partial \boldsymbol{q} \\ \partial \mathcal{H}_{\mathrm{b}} / \partial \boldsymbol{\pi} \end{pmatrix} \tag{2.68}$$

For rigid body motion, the Poisson tensor is

$$\boldsymbol{\Lambda} = -\boldsymbol{\Lambda}^T = \begin{pmatrix} \mathbf{0} & \boldsymbol{J} \\ -\boldsymbol{J}^T & \boldsymbol{C} \end{pmatrix} \tag{2.69}$$

and note that $\boldsymbol{\Lambda}$ has full rank. The non-canonical Hamiltonaian equations are simply

$$\frac{d}{dt}\begin{pmatrix} \boldsymbol{q} \\ \boldsymbol{\pi} \end{pmatrix} = \boldsymbol{\Lambda}\nabla\mathcal{H}_{\mathrm{b}} \tag{2.70}$$

Chapter 3

Fluid Mechanics

Fluid systems are modeled using the same principles introduced in Chapter 2: conservation laws are applied to a fluid volume which yield a governing set of dynamic equations. The mechanics of a fluid system are more intricate than of a rigid body, however, since the relative distances between the fluid particles are not fixed. One is therefore tasked with characterizing the behavior of an infinite collection of fluid particles which are individually free to react to both internal and external forces.

Discretizing the fluid volume into a finite number of cells enables CFD, a numerical approach to predicting the fluid behavior. High fidelity CFD approaches use different schemes to approximate solutions to the Navier-Stokes equations and can model complex fluid dynamic phenomena including boundary layer mechanics and turbulent flow [49]. Panel and strip methods are lower fidelity CFD approaches which solve the Bernoulli equation, a simplified governing equation which neglects viscosity, vorticity, and compressibility effects. Even in the low fidelity case, the time required to sufficiently predict the fluid behavior can be excessive.

There are a number of applications which require reduced-order representations of the hydrodynamic forces and moments. Typical model-based control design and state estimation methodologies, such as LQR and Kalman filtering, require a parametric ODE model of the

system dynamics. The gain parameters in the resulting controller or observer must then be iteratively tuned through a repeated cycle of system simulation and performance evaluation; this iterative process would be infeasible using high fidelity CFD. Other iterative processes which benefit from reduced order models include design optimization schemes, where one must rapidly characterize how the vessel response or stability margins are affected by varying the hull shape or actuator configuration. Finally, reduced-order models are also required for training simulators which must respond in real time to the actions of a helmsmen. The traditional reduced order models used for these applications are maneuvering models and seakeeping models, each addressing different parts of the ship modeling problem.

In this chapter, the standard "parts" of ship dynamics modeling are introduced, beginning with a discussion of commonly identified forces in ship dynamics. These forces are then combined with the dynamical systems theory described in Chapter 2 to present the common mathematical structures for maneuvering and seakeeping models. In the remainder of this chapter, potential flow theory and wave mechanics are introduced to give context to how these standard parts are identified in the first place.

3.1 Common Forces

In this treatment, the commonly used forces and moments are decomposed into primary and secondary effects. Primary effects are the "potential flow" effects incurred by an unappended hull interacting with the ambient fluid. These effects often establish a baseline for preliminary hull design. Secondary effects are more often associated with the addition of hull appendages (control surfaces, fins, etc.). These effects, for instance, account for generalized forces due to control inputs, circulation effects and boundary layer effects.

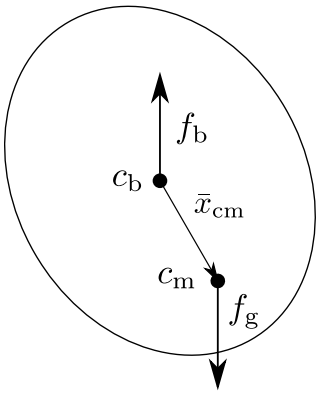

Figure 3.1: Depiction of the pendulum-like restoring torque which arises for a neutrally buoyant and fully submerged vehicle with offset centers of mass (c_m) and buoyancy (c_b).

3.1.1 Primary Effects

Hydrostatics

The hydrostatic force results from Archimedes' Principle[1] and is defined as the buoyancy force equal to the weight of the fluid displaced by the vehicle [8]. The hydrostatic force acts at the centroid of the displaced fluid, or the center of buoyancy, and for a fully submerged vehicle, the center of buoyancy is stationary in a body fixed frame. If the vehicle is neutrally buoyant, the hydrostatic buoyancy force exactly counteracts the gravitational force. Though when the center of mass does not align with the center of buoyancy, a pendulum-like restoring torque occurs, tending to swing the center of mass below the center of buoyancy; see Figure 3.1. For a floating vessel however, the center of buoyancy moves as the free surface deforms around the vessel. Moreover, the magnitude of the buoyancy force changes as the volume of displaced fluid varies with vertical oscillatory motions of the vehicle. The buoyancy force is sometimes referred to as the hydrostatic stiffness because of its analogous behavior to a mechanical spring.

[1] Archimedes of Syracuse, 287 BC to 212 BC.

Radiation Effects: Added Mass, Damping, Memory Effects, and Surface Suction

As compared to vehicle motion in a vacuum, a vehicle moving through an ambient fluid must push the fluid out of the way, driving fluid motion in a neighborhood of the vehicle. This induced fluid motion implies that additional kinetic energy is required in the fluid-vehicle system as compared to a vehicle undergoing the same motion through a vacuum. This vehicle-induced fluid motion is known as a radiation effect because it accounts for the transfer of kinetic energy from the craft into the surrounding fluid.

For marine craft operating in the presence of a free surface, the radiation effects appear in two primary ways [8, Sec. 6.15]. The first is added mass, a physical phenomenon which manifests as an apparent increase in the system inertia. The added mass forces and moments are closely related to the fluid kinetic energy induced by the instantaneous motion of the vehicle, and these effects exist even in the absence of a free surface. The second effect is radiative damping, which acts like a velocity-dependent dissipative force and is due to the generation of waves along the free surface. In the absence of any dissipative phenomena (like viscosity), the total energy of the vehicle-fluid system will remain constant. However, a portion of the vehicle energy is irreversibly used to generate surface waves, resulting in an apparent non-conservative force acting on the vehicle.

The radiative damping effects are closely related to the memory effects. While there is some ambiguity in the definition of memory effects within the literature, this dissertation adopts a definition based on the discussion of Cummins [19] and Ogilvie [29]. To summarize, a vehicle motion in the presence of a free surface will incur both an instantaneous fluid response and a longer lasting fluid response. Ogilvie [29] explains this process through a simple example: when a pebble is tossed into a pond, the initial impact generates an almost instantaneous fluid response. This initial response then results in a longer lasting series of ripples. In line with this discussion, any fluid effects past the instantaneous fluid response are considered memory effects in this dissertation. This includes the fluid motion due to fully developed, steady-state wake patterns. For a fully submerged vehicle operating near the free surface, the

radiation effects also incur free surface suction forces and moments. As the fluid is pinched between the vehicle and the free surface, the vehicle-induced fluid motion generates a region of low pressure, tending to deform the free surface and draw the vehicle upwards towards the surface.

Wave Excitations: Froude-Krylov, Diffraction

Wave excitation forces are proportional to the wave amplitude and are assumed to act on a vessel which is restrained from all motion [18]. Given that velocity fields associated with surface waves are both unsteady (temporally varying) and nonuniform (spatially varying), the pressure field acting on the vehicle's hull will be unsteady and nonuniform. Froude-Krylov forces derive from the time-varying pressure distribution due to an incident wave field acting on the hull, but assuming that the hull does not impact the ambient flow.

Surface waves also induce diffraction forces which result from the incident waves interacting with the hull. The presence of the hull essentially modifies the characteristics of an ambient wave field in a neighborhood of the body. Waves tend to both scatter around the hull (refraction) and bounce off of the hull (reflection), resulting in an exchange of momentum between the wave and the vessel. These effects tend to be significant only when the characteristic length[2] of the ship is on the same order as the ambient waves: very large waves tend to be unaffected by the vessel, while very small waves tend to be negated by the inertial characteristics of the ship.

Second-Order Drift Effects

Second order drift forces are "time-averaged" forces which also arise in the presence of surface waves. These forces typically result in lateral drift for a floating or submerged craft. They also tend to modify the suction forces for a fully submerged vehicle [31, 30].

[2]In head/following seas, the characteristic length would be the ship length; in beam seas it would be the beam.

3.1.2 Secondary Effects

Circulation Forces

Lift (or side) forces in an ideal fluid are given by the Kutta-Joukowski Theorem [41, Sec. 13.7]. The theorem predicts a lift force proportional to the circulation about the vehicle and which acts perpendicular to the direction of free-stream velocity (flow-relative vehicle velocity). The lift force predicted by the Kutta-Joukowski Theorem is remarkably accurate for airfoils or hydrofoils at small angles of attack (where viscous effects are minimal). For submerged craft and surface ships, the lift force is most often used in predicting hydrodynamic forces due to fins and control surfaces (rudders, bow planes, etc). At large sideslip angles however, lift forces due to the hull itself may become significant. Additionally, in certain operating conditions, interactions between the hull and the hydrofoils can have substantial impacts on the accuracy of these ideal-flow predictions.

Viscous Effects

Viscous forces result from shear stress induced by boundary layer mechanics. In a viscous fluid, it is realistic to prescribe a "no-slip" boundary condition: the fluid particles adjacent to the hull have zero velocity relative to the hull [49, Sec. 1.2]. As a result, there exists a thin region of fluid (the boundary layer) where the flow increases up to its nominal speed over the body. By Newton's Third Law, the decrease in hull-relative fluid momentum in the boundary layer implies that the boundary layer exerts a "skin friction" force on the hull. Skin friction forces depend on the "smoothness" of the surface over which the fluid is flowing [49].

Another effect associated with boundary layer mechanics is flow separation due to adverse pressure gradients. Adverse pressure gradients arise when a fluid flow is required to turn over a convex surface such as an airfoil or hydrofoil. Flow separation leads to a low pressure wake region which induces additional drag forces and can lead to more complex fluid dynamic

phenomena like stall.

Slowly Varying Effects

Perez [2] describes "slowly varying forces" as those that can be taken as constant over the course of a simulation. Examples include wind forces which act on the superstructure of a vessel, and forces due to underwater currents. In both cases, forces arise from the modified pressure field due to the the presence of a constant, background flow field.

Control Inputs

Control forces and moments result from a helmsman or a control scheme utilizing the craft's actuators. There are several types of actuators typically employed for marine craft. Bow planes, stern planes, and rudders are control surfaces which manipulate the circulation to generate lift forces to control the orientation of a vehicle. Engine driven propellers or water jets are used to generate thrust. Certain classes of submerged craft also have ballast control to regulate the gravitational forces and moments acting on the vehicle. For instance, underwater gliders utilize ballast control to generate extremely efficient motion for extended periods of time. Surface vessels sometimes use anti-roll tanks or control moment gyroscopes (CMGs) to actively reject roll and pitch perturbations due to ambient waves.

3.2 Standard Classes of Models

Reduced-order motion models for surface ships are traditionally divided into maneuvering and seakeeping models. Maneuvering models address the calm water response of a marine craft, quantifying how the vessel interacts with an otherwise stationary or uniformly moving fluid. Seakeeping models instead treat the response of a vessel due to incoming waves, albeit only for motion about a linearized forward trajectory. Separately, maneuvering and

seakeeping models cover many reasonable operating conditions experienced by ships; the fundamental assumptions of each model differ, allowing for their respective operating envelopes. In terms of the primary forces, these models are generally decomposed as in Table 3.1.

Table 3.1: Decomposition of the primary forces for maneuvering and seakeeping models.

Physical effect	Maneuvering	Seakeeping
Hydrostatic	✓	✓
Added Mass	✓	✓
Damping	✓	✓
Froude-Krylov		✓
Diffraction		✓
2^{nd} Order Drift		✓

3.2.1 Maneuvering Models

Neglecting ambient waves, maneuvering models address the calm-water characteristics of surface ships, typically through standard maneuvering tests. Examples of standard maneuvering tests include the steady turn test, where the rudder is given a prescribed deflection and both the transient and steady turning radii are computed, and the crash stop where the stopping distance and heading deflection are measured for a vessel traveling at cruise speed [6]. Essentially, maneuvering models require that external forcing functions be slowly varying.

Using the rigid body equations of motion from Chapter 2 (2.60), the maneuvering equations take the form

$$\boldsymbol{M}_{\text{b}}\dot{\boldsymbol{\nu}} + \boldsymbol{G}(\boldsymbol{\nu})\boldsymbol{M}_{\text{b}}\boldsymbol{\nu} = \boldsymbol{F}_{\text{h}}(\boldsymbol{q}, \boldsymbol{\nu}, \dot{\boldsymbol{\nu}}) \tag{3.1}$$

where $\boldsymbol{F}_{\mathrm{h}}$ represents the generalized fluid forces acting on the vehicle. Note that the gravitational forces are absent from this expression; they are typically combined with the hydrostatic effects. According to Table 3.1, the exogenous force and moment vector can be decomposed in terms of the hydrostatic contributions $\boldsymbol{g}$, the radiation contributions $\boldsymbol{F}_{\mathrm{rad}}$, and any other contributions from the secondary forces $\boldsymbol{F}$:

$$\boldsymbol{F}_{\mathrm{h}} = -\boldsymbol{g}(\boldsymbol{q}) - \boldsymbol{F}_{\mathrm{rad}}(\boldsymbol{\nu}, \dot{\boldsymbol{\nu}}) + \boldsymbol{F} \tag{3.2}$$

In the absence of unsteady external fluid behavior (*e.g.* ambient waves), one may employ standard assumptions for the structure of the radiation forces, enabling the following representation [1, 2]:

$$\boldsymbol{F}_{\mathrm{rad}} = \boldsymbol{M}_{\mathrm{f}}\dot{\boldsymbol{\nu}} + \boldsymbol{C}_{\mathrm{f}}(\boldsymbol{\nu})\boldsymbol{\nu} + \boldsymbol{D}_{\mathrm{f}}(\boldsymbol{\nu})\boldsymbol{\nu} \tag{3.3}$$

Here, $\boldsymbol{M}_{\mathrm{f}}$ is the constant added mass matrix, $\boldsymbol{C}_{\mathrm{f}}$ accounts for the Munk moments, and $\boldsymbol{D}_{\mathrm{f}}$ is the radiative damping matrix. Hydrodynamic parameters which appear in maneuvering models are sometimes referred to as slow motion derivatives [21]. The standard nonlinear form of the maneuver equations are [1, 2]

$$\dot{\boldsymbol{q}} = \boldsymbol{J}(\boldsymbol{q})\boldsymbol{\nu} \tag{3.4}$$

$$\left[\boldsymbol{M}_{\mathrm{b}} + \boldsymbol{M}_{\mathrm{f}}\right]\dot{\boldsymbol{\nu}} + \left[\boldsymbol{G}(\boldsymbol{\nu})\boldsymbol{M}_{\mathrm{b}} + \boldsymbol{C}_{\mathrm{f}}(\boldsymbol{\nu})\right]\boldsymbol{\nu} + \boldsymbol{D}_{\mathrm{f}}(\boldsymbol{\nu})\boldsymbol{\nu} + \boldsymbol{g}(\boldsymbol{q}) = \boldsymbol{F} \tag{3.5}$$

In these equations, the added mass modifies the rigid body inertia matrix, affecting the inertial characteristics of the dynamic system. The radiative damping forces are akin to "frictional" damping forces that appear in the modeling of mechanical systems, and account for the resistive forces due to the generation of surface waves.

Special case: Deeply Submerged Vehicle Models

Submerged craft models can be considered a subset of maneuvering models. The principal difference is that standard submerged craft models neglect the free surface effects since they typically operate whilst deeply submerged. This simplification immensely simplifies the fluid

mechanics of the modeling problem. As in the maneuvering model, the hydrodynamic forces are decomposed into a hydrostatics component $\boldsymbol{g}$, a radiation component $\boldsymbol{F}_{\text{rad}}$, as well as contributions from any secondary forces $\boldsymbol{F}$:

$$\boldsymbol{F}_{\text{h}} = -\boldsymbol{g}(\boldsymbol{q}) - \boldsymbol{F}_{\text{rad}}(\boldsymbol{\nu}, \dot{\boldsymbol{\nu}}) + \boldsymbol{F} \tag{3.6}$$

Assuming neutral buoyancy, a submerged craft experiences no net hydrostatic force; the hydrostatic force is counteracted by the gravitational force. However, in the case of offset centers of mass and buoyancy, the vehicle experiences an orientation-dependent hydrostatic restoring torque. In this case, $\boldsymbol{g}$ is only a function of the Euler angles $\boldsymbol{\theta}_{\text{b}}$.

In the absence of a free surface, the vehicle experiences no radiative damping forces, implying that the radiation effects are completely characterized by the added mass and the Munk moments:

$$\boldsymbol{F}_{\text{rad}} = \boldsymbol{M}_{\text{f}}\dot{\boldsymbol{\nu}} + \boldsymbol{C}_{\text{f}}(\boldsymbol{\nu})\boldsymbol{\nu} \tag{3.7}$$

The kinetic equations of motion for a deeply submerged craft in an ideal fluid are [1]

$$\left[\boldsymbol{M}_{\text{b}} + \boldsymbol{M}_{\text{f}}\right]\dot{\boldsymbol{\nu}} + \left[\boldsymbol{G}(\boldsymbol{\nu})\boldsymbol{M}_{\text{b}} + \boldsymbol{C}_{\text{f}}(\boldsymbol{\nu})\right]\boldsymbol{\nu} + \boldsymbol{g}(\boldsymbol{\theta}_{\text{b}}) = \boldsymbol{F} \tag{3.8}$$

These equations are a modified form of Kirchhoff's equations[3] [25] for deeply submerged vehicle motion.

3.2.2 Seakeeping Models

To accommodate a reduced-order representation of the excitation forces, seakeeping models are subject to the following set of simplifying assumptions [2, Sec. 4.2].

Assumption 3.2.1 *Standard seakeeping models assume:*

1. *The ocean waves may be thought of as a realization of a power spectral density.*

[3]Kirchhoff's equations assume coincident centers of mass and buoyancy. In that case, the hydrostatic term $\boldsymbol{g}(\boldsymbol{\theta}_{\text{b}})$ would vanish.

2. *The hydrodynamics are well approximated using linear wave theory.*

3. *The ship makes only small deviations from a nominal forward trajectory with constant speed.*

The traditional seakeeping model is the result of linearity assumptions in both the hydrodynamics and the rigid body dynamics. To present the seakeeping model, Perez [2] introduces the "h-frame", a reference frame which remains fixed with respect to the steady forward motion of the ship at a constant speed U. The coordinates used to represent a linear model are then called "perturbation coordinates", representing the small perturbations from the nominal forward speed. Let $\boldsymbol{q}^* = \boldsymbol{q} - \boldsymbol{q}_{\mathrm{e}}$, the difference between the true configuration and the equilibrium configuration, which is defined as $\boldsymbol{q}_{\mathrm{e}}(t) = [Ut, 0, 0, 0, 0, 0]^T$. The seakeeping equations are

$$\boldsymbol{M}_{\mathrm{b}}\ddot{\boldsymbol{q}}^* = \boldsymbol{F}_{\mathrm{h}}(\boldsymbol{q}^*, \dot{\boldsymbol{q}}^*, \ddot{\boldsymbol{q}}^*, \omega_{\mathrm{e}}) \tag{3.9}$$

For excitation forces due to ambient waves at a single frequency ω, the external force vector can be decomposed into (linearized) hydrostatic forces $\boldsymbol{G}\boldsymbol{q}^*$, radiation forces $\boldsymbol{F}_{\mathrm{rad}}$, and excitation forces $\boldsymbol{F}_{\mathrm{w}}$:

$$\boldsymbol{F}_{\mathrm{h}} = -\boldsymbol{G}\boldsymbol{q}^* - \boldsymbol{F}_{\mathrm{rad}}(\dot{\boldsymbol{q}}^*, \ddot{\boldsymbol{q}}^*, \omega_{\mathrm{e}}) - \boldsymbol{F}_{\mathrm{w}}(\omega_{\mathrm{e}}) \tag{3.10}$$

In the seakeeping case, the hydrodynamic forces are functions of the encounter frequency ω_{e}, the frequency at which the vehicle encounters the incident waves:

$$\omega_{\mathrm{e}} = \omega - \frac{\omega^2 U}{g}\cos\chi \tag{3.11}$$

The encounter frequency is a function of the wave frequency ω, the constant forward speed U, and the relative wave heading χ. For a linear system, the vehicle must oscillate sinusoidally at the frequency of excitation ω_{e}. In this case,

$$\boldsymbol{q}^*(t) = \mathrm{real}\left[\tilde{\boldsymbol{q}}^* e^{i\omega_{\mathrm{e}} t}\right] \tag{3.12}$$

where $\tilde{\boldsymbol{q}}^*$ is the amplitude of oscillation and $i = \sqrt{-1}$.

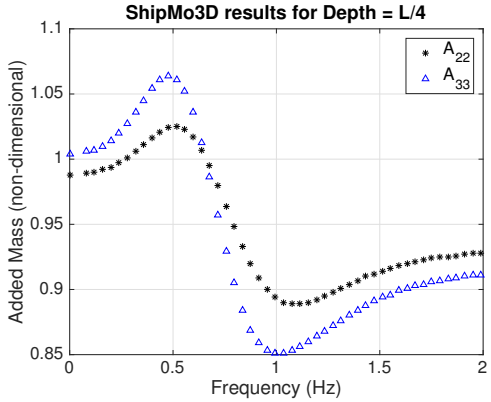

(a) Plot of the added mass values $A_{22}(\omega_e)$ (sway acceleration into sway force) and $A_{33}(\omega_e)$ (heave acceleration into heave force). Values non-dimensionalized by the body's mass m_b.

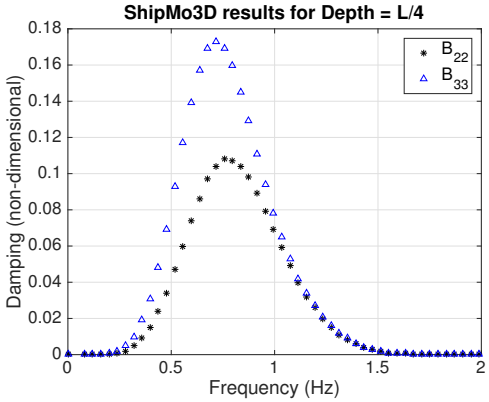

(b) Plot of the added mass values $B_{22}(\omega_e)$ (sway velocity into sway force) and $B_{33}(\omega_e)$ (heave velocity into heave force). Values non-dimensionalized by the quantity $m_b\sqrt{g/L}$.

Figure 3.2: Added mass and damping results computed using a 3-D panel method (ShipMo3D) for a fully submerged spheroidal body with a fineness ratio of 6:1 and with a centerline depth of one quarter body length below the free surface.

Again, one may further decompose the radiation forces into added mass and damping, though in this case the parameters depend of the encounter frequency. In line with standard seakeeping notation, different symbols are employed for the added mass $\boldsymbol{A}(\omega_e)$ and damping $\boldsymbol{B}(\omega_e)$ matrices to stress that these parameters now depend on the frequency of excitation:

$$\boldsymbol{F}_{\text{rad}} = \boldsymbol{A}(\omega_e)\ddot{\boldsymbol{q}}^* + \boldsymbol{B}(\omega_e)\dot{\boldsymbol{q}}^* \tag{3.13}$$

Bailey *et al.* [21] refer to these frequency dependent parameters as hydrodynamic coefficients. At certain oscillation frequencies, the vehicle imparts more energy into the surrounding fluid corresponding to larger added mass and damping values, as seen in Figure 3.2. This varied transfer of energy may be thought of as a "resonance" of sorts between the vehicle and the free surface. Expressed in the frequency domain, the seakeeping equations of motion are [2]

$$-\omega_e^2\left[\boldsymbol{M}_b + \boldsymbol{A}(\omega_e)\right]\tilde{\boldsymbol{q}}^* + i\omega_e\boldsymbol{B}(\omega_e)\tilde{\boldsymbol{q}}^* + \boldsymbol{G}\tilde{\boldsymbol{q}}^* = \boldsymbol{F}_w(\omega_e) \tag{3.14}$$

It is then straightforward to solve for the motion amplitudes:

$$\tilde{\boldsymbol{q}}^* = \left(-\omega_{\mathrm{e}}^2 \left[\boldsymbol{M}_{\mathrm{b}} + \boldsymbol{A}(\omega_{\mathrm{e}})\right] + i\omega_{\mathrm{e}}\boldsymbol{B}(\omega_{\mathrm{e}}) + \boldsymbol{G}\right)^{-1} \boldsymbol{F}_{\mathrm{w}}(\omega_{\mathrm{e}}) \tag{3.15}$$

This "frequency domain response" to a single wave train is known as a motion Response Amplitude Operator (RAO), a transfer function-like operator which maps a set of wave characteristics (frequency, amplitude, heading) to a corresponding vessel motion. (One may similarly obtain a set of force RAOs.) Under linear systems theory, these motion RAOs may be superimposed to yield the more complex vessel motions observed in a random seaway.

At first glance, the seakeeping model is more comprehensive than the maneuvering model because it accounts for each of the primary forces. However, it is the underlying linearity assumption inherent to seakeeping models which enables the reduced-order representations of the primary forces. Moreover, the system must be linear so that one may superimpose the RAOs to predict the vessel's response in a seaway. If the unmodeled (nonlinear and non-oscillatory) dynamics become significant, the seakeeping predictions will be erroneous.

3.3 Potential Flow Theory

In the prior sections, conventional structures for the maneuvering and seakeeping models were presented in terms of hydrodynamic forces and moments. Here, the underlying fluid behavior which leads to these forces and moments is detailed. To model the motion of a fluid system, one typically invokes the conservation of mass, momentum, and energy to generate a set of governing equations. For a fluid with a density $\rho(\boldsymbol{x}, t)$, Eulerian velocity field $\boldsymbol{V}_{\mathrm{f}}(\boldsymbol{x}, t)$, and internal energy e, the conservation equations for an infinitesimal fluid volume dV are

$$\begin{aligned} 0 &= \frac{D}{Dt}(\rho\ dV) \\ \boldsymbol{F} &= \frac{D}{Dt}\left(\rho\ dV\ \boldsymbol{V}_{\mathrm{f}}\right) \\ P &= \frac{D}{Dt}\left(\rho\ dV\left(\frac{1}{2}\boldsymbol{V}_{\mathrm{f}} \cdot \boldsymbol{V}_{\mathrm{f}} + e\right)\right) \end{aligned}$$

The conservation of mass states that mass cannot be created or destroyed, the momentum equations relate the fluid momenta to the forces $\boldsymbol{F}$ acting on the fluid, and the energy equation relates the fluid energy to the rate of work P done on the fluid. The material derivative describes how a property associated with an element of fluid material evolves with time:

$$\frac{D}{Dt}Q(\boldsymbol{x},t) = \frac{\partial Q}{\partial t} + \boldsymbol{V}_{\mathrm{f}} \cdot \nabla Q \tag{3.16}$$

The first term, $\partial Q/\partial t$, is the local derivative accounting for the material change of Q due to time variations of the material element. The convective derivative $\boldsymbol{V}_{\mathrm{f}} \cdot \nabla Q$ accounts for the material change of Q due to the instantaneous motion of the material element.

Before studying the governing equations in detail, the fluid behavior is simplified using the following set of assumptions:

Assumption 3.3.1 (Potential Flow Theory) *The fluid is incompressible ($\rho = \text{constant}$) and the fluid velocity field is irrotational ($\nabla \times \boldsymbol{V}_{\mathrm{f}} = \boldsymbol{0}$).*

For a thorough treatment of potential flow theory, one may reference [8] or [41]. With the latter portion of Assumption 3.3.1, one may uniquely define the fluid velocity field in terms of a scalar potential ϕ [8, 41]:

$$\boldsymbol{V}_{\mathrm{f}}(\boldsymbol{x}) = \nabla\phi(\boldsymbol{x}) \tag{3.17}$$

Remark 3.3.2 *This is the second time in this dissertation that a vector field has been defined in terms of a scalar potential function. The first instance was in the presentation of Lagrangian Mechanics in Section 2.3.2, where a potential energy function was used to represent an irrotational force field.*

3.3.1 Conservation of Mass

For an infinitesimal fluid volume dV, conservation of mass implies that

$$\frac{D}{Dt}(\rho\, dV) = 0 \tag{3.18}$$

That is, the material change in mass at an arbitrary position in the fluid must be zero. Evaluating the material derivative in the above expression yields

$$dV\frac{D\rho}{Dt} + \rho\frac{D(dV)}{Dt} = dV\left(\frac{\partial\rho}{\partial t} + \boldsymbol{V}_{\mathrm{f}}\cdot\nabla\rho\right) + \rho\ dV\nabla\cdot\boldsymbol{V}_{\mathrm{f}} \tag{3.19}$$

Substituting the above expression into (3.18),

$$\frac{D\rho}{Dt} = -\rho\nabla\cdot\boldsymbol{V}_{\mathrm{f}} \tag{3.20}$$

Equation (3.20) is the continuity equation [8, 41] and it states that the material transport of fluid density is proportional to the divergence of the fluid velocity. Making use of the incompressibility assumption and the definition of the velocity field in terms of a scalar potential,

$$0 = -\rho\nabla\cdot(\nabla\phi)$$

Conservation of mass for an incompressible fluid thus reduces to Laplace's equation:

$$\nabla^2\phi = 0 \tag{3.21}$$

3.3.2 Conservation of Momentum

Applying the conservation of momentum to a fluid volume results in the Navier-Stokes equations[4]. Beginning again by considering an infinitesimal volume of fluid, one may use Newton's second law to relate the material change in fluid momentum to the sum of internal and external forces $\boldsymbol{F}$:

$$\frac{D}{Dt}\left(\rho\ dV\boldsymbol{V}_{\mathrm{f}}\right) = \boldsymbol{F} \tag{3.22}$$

From the conservation of mass, the term ρdV must be constant. The material derivative may additionally be reduced using the irrotational flow assumption as

$$\frac{D}{Dt}\left(\rho\ dV\boldsymbol{V}_{\mathrm{f}}\right) = \rho\ dV\left(\frac{\partial\boldsymbol{V}_{\mathrm{f}}}{\partial t} + \frac{1}{2}\nabla(\boldsymbol{V}_{\mathrm{f}}\cdot\boldsymbol{V}_{\mathrm{f}})\right) \tag{3.23}$$

[4]Claude-Louis Navier, 1785-1836. Sir George Gabriel Stokes, 1819-1903.

Studying the forces $\boldsymbol{F}$, any effects due to viscosity are ignored. Considering only pressure force and body force contributions [41]:

$$\boldsymbol{F} = \boldsymbol{f}_{\mathrm{p}} + \boldsymbol{f}_{\mathrm{b}} \tag{3.24}$$

The pressure forces act along the surface δS of the infinitesimal fluid volume dV and the net pressure force acting on a fluid element is given by [41, Sec 5.2]

$$\boldsymbol{f}_{\mathrm{p}} = -\iint_{\delta S} p\boldsymbol{n} dS = -dV\nabla p \tag{3.25}$$

For the body forces, only the effects of gravity acting on the fluid are considered:

$$\boldsymbol{f}_{\mathrm{b}} = dV\nabla(\rho g z) = \begin{pmatrix} 0 \\ 0 \\ dV\rho g \end{pmatrix} \tag{3.26}$$

(Note that z is measured positive "down"; see Figure 2.1.) Incorporating all of the simplifications thus far, the momentum equations are

$$\rho\left(\frac{\partial \boldsymbol{V}_{\mathrm{f}}}{\partial t} + \frac{1}{2}\nabla(\boldsymbol{V}_{\mathrm{f}}\cdot\boldsymbol{V}_{\mathrm{f}})\right) = \nabla(\rho g z) - \nabla p \tag{3.27}$$

Using the definition of the fluid velocity in terms of the scalar potential, (3.27) may be rewritten as

$$\nabla\left(\rho\frac{\partial\phi}{\partial t} + \frac{1}{2}\rho(\nabla\phi)\cdot(\nabla\phi) - \rho g z + p\right) = \boldsymbol{0} \tag{3.28}$$

Since this relationship holds for every infinitesimal volume of fluid, the quantity in parenthesis must be constant everywhere within the fluid at a given instant in time. The previous expression may be integrated to yield the unsteady Bernoulli equation[5] [41, Sec. 8.4]:

$$\rho\frac{\partial\phi}{\partial t} + \frac{1}{2}\rho(\nabla\phi)\cdot(\nabla\phi) - \rho g z + p = C(t) \tag{3.29}$$

In (3.29) $C(t)$ is a term which depends only on time, and represents the effects of additional work performed on the fluid volume; typically, $C(t) = 0$. In this case, we recover what [50] refers to as the Bernoulli pressure or total pressure:

$$-p = \rho\frac{\partial\phi}{\partial t} + \frac{\rho}{2}(\nabla\phi)\cdot(\nabla\phi) - \rho g z \tag{3.30}$$

[5]Daniel Bernoulli, 1700-1782.

This relationship holds everywhere in the fluid continuum, though when prescribing a circulation, the relationship holds only along streamlines [41].

In steady flow, the standard Bernoulli equation is recovered

$$\frac{1}{2}\rho(\nabla\phi)\cdot(\nabla\phi) - \rho g z + p = 0 \tag{3.31}$$

Though it was derived using the conservation of momentum, Karamcheti remarks that Bernoulli's equation is also a statement of conservation of energy [41, Sec. 8.6]. The expression $\rho/2(\nabla\phi)\cdot(\nabla\phi)$ is the fluid kinetic energy per unit volume. The expression $\rho g z$, which derives from the external gravitational body force, is the hydrostatic potential energy per unit volume. Karamcheti additionally remarks that since p is an irrotational scalar field, it may be also be interpreted as a pressure potential. The total potential energy of the system is thus $(p - \rho g z)$. Further, in the absence of hydrostatic effects, Lamb [25] remarks that fluid motion is driven by pressure work; this remark has immediate physical meaning since the fluid kinetic energy must balance the pressure potential in a closed system.

3.3.3 Conservation of Energy

The conservation of energy characterizes the transport of energy within a fluid volume due to both internal and external factors. Consider the total fluid energy for an infinitesimal fluid volume

$$E = \rho\, dV \left(\frac{1}{2}\boldsymbol{V}_{\mathrm{f}}\cdot\boldsymbol{V}_{\mathrm{f}} + e\right) \tag{3.32}$$

with contributions from both the fluid kinetic energy $\rho\frac{1}{2}\boldsymbol{V}_{\mathrm{f}}\cdot\boldsymbol{V}_{\mathrm{f}}dV$ and the internal fluid energy $\rho e dV$. The fluid kinetic energy is analogous to the mechanical kinetic energy discussed in Chapter 2, while the internal energy accounts for thermal energy within the fluid [41]. The conservation of energy then relates the material change in fluid energy to the rate of work done on the fluid volume:

$$\frac{DE}{Dt} = P \tag{3.33}$$

Again, note that the quantity ρdV is constant. Evaluating the substantial derivative of E yields

$$\frac{D}{Dt}\left(\rho\ dV\left(\frac{1}{2}\boldsymbol{V}_{\mathrm{f}}\cdot\boldsymbol{V}_{\mathrm{f}}+e\right)\right)=\rho\ dV\left(\frac{1}{2}\frac{D(\boldsymbol{V}_{\mathrm{f}}\cdot\boldsymbol{V}_{\mathrm{f}})}{Dt}+\frac{De}{Dt}\right)$$

Expanding the material change of the fluid kinetic energy, one finds

$$\frac{1}{2}\frac{D(\boldsymbol{V}_{\mathrm{f}}\cdot\boldsymbol{V}_{\mathrm{f}})}{Dt}=\frac{1}{2}\frac{\partial(\boldsymbol{V}_{\mathrm{f}}\cdot\boldsymbol{V}_{\mathrm{f}})}{\partial t}+\frac{1}{2}\boldsymbol{V}_{\mathrm{f}}\cdot\nabla(\boldsymbol{V}_{\mathrm{f}}\cdot\boldsymbol{V}_{\mathrm{f}})$$

Using the definition of the fluid velocity in terms of a scalar potential,

$$\frac{1}{2}\frac{D(\boldsymbol{V}_{\mathrm{f}}\cdot\boldsymbol{V}_{\mathrm{f}})}{Dt}=\nabla\left(\frac{\partial\phi}{\partial t}+\frac{1}{2}\nabla\phi\cdot\nabla\phi\right)\cdot\boldsymbol{V}_{\mathrm{f}} \tag{3.34}$$

Again, only the rates of work done by body forces P_{b} and pressure forces P_{p} are considered. From the fundamental definition of power, the rate of work due to body forces is given by projecting the body force onto the fluid velocity:

$$P_{\mathrm{b}}=\boldsymbol{f}_{\mathrm{b}}\cdot\boldsymbol{V}_{\mathrm{f}}=dV\nabla(\rho gz)\cdot\boldsymbol{V}_{\mathrm{f}} \tag{3.35}$$

Additional care must be taken when computing the rate of work due to pressure forces. Recalling the definition of the pressure force as a surface integral over the fluid element (3.25), work contributions from translations and dilations of the fluid element must both be included. Karamcheti [41, Sec. 5.4] gives the following expression for the pressure power

$$P_{\mathrm{p}}=-\iint_{\delta S}p\boldsymbol{V}_{\mathrm{f}}\cdot\boldsymbol{n}dS=-dV\nabla\cdot(p\boldsymbol{V})=-dV\left(\nabla p\cdot\boldsymbol{V}_{\mathrm{f}}+p\nabla\cdot\boldsymbol{V}_{\mathrm{f}}\right) \tag{3.36}$$

The term $-dV\nabla p\cdot\boldsymbol{V}_{\mathrm{f}}$ is simply $\boldsymbol{f}_{\mathrm{p}}\cdot\boldsymbol{V}_{\mathrm{f}}$ and accounts for the portion of pressure work which results in motions of a fluid element. The term $-dV\nabla\cdot\boldsymbol{V}_{\mathrm{f}}$ then accounts for an expansion or contraction of the fluid element.

Dividing through by the infinitesimal volume dV, the energy equation becomes

$$\rho\nabla\left(\frac{\partial\phi}{\partial t}+\frac{1}{2}\nabla\phi\cdot\nabla\phi\right)\cdot\boldsymbol{V}_{\mathrm{f}}+\rho\frac{\partial e}{\partial t}+\boldsymbol{V}_{\mathrm{f}}\cdot\nabla e=\nabla(\rho gz)\cdot\boldsymbol{V}_{\mathrm{f}}-\nabla p\cdot\boldsymbol{V}_{\mathrm{f}}-p\nabla\cdot\boldsymbol{V}_{\mathrm{f}} \tag{3.37}$$

Additional simplifications can be made by taking the dot product of (3.28) with $\boldsymbol{V}_{\mathrm{f}}$:

$$\nabla\left(\rho\frac{\partial\phi}{\partial t}+\frac{1}{2}\rho(\nabla\phi)\cdot(\nabla\phi)-\rho gz+p\right)\cdot\boldsymbol{V}_{\mathrm{f}}=0 \tag{3.38}$$

Subtracting (3.38) from the complete energy equation (3.37) yields

$$\rho\left(\frac{\partial e}{\partial t}+\boldsymbol{V}_{\mathrm{f}}\cdot\nabla e\right)=-p\nabla\cdot\boldsymbol{V}_{\mathrm{f}} \tag{3.39}$$

Together, (3.38) and (3.39) govern the material transport of fluid energy. The first equation (3.38) relates the rate of change of fluid kinetic energy (per unit volume) to the rate of work done by gravitational and pressure forces:

$$\frac{D}{Dt}\left(\frac{\rho}{2}\nabla\phi\cdot\nabla\phi\right)=\nabla(\rho gz-p)\cdot\nabla\phi \tag{3.40}$$

The second equation (3.39) relates the rate of change of internal energy to the changes in fluid volume:

$$\rho\frac{De}{Dt}=-p\nabla\cdot\nabla\phi \tag{3.41}$$

Karamcheti [41] remarks that this expression is a form of the first law of thermodynamics for an adiabatic system. From (3.21), however, the Laplacian term $\nabla\cdot\boldsymbol{V}_{\mathrm{f}}$ must equal zero. Thus, for an incompressible fluid, the internal energy is a constant of motion:

$$\frac{De}{Dt}=0 \tag{3.42}$$

The Bernoulli equation (3.29) has decoupled the material change of internal energy from the material change of fluid kinetic energy. Further, the internal energy is constant for a fluid governed by potential flow theory. This result will be important in the coming chapters where fluid energy functions are used to derive equations which model fluid-body interactions.

3.3.4 Boundary Conditions

Up to this point, we have not considered how a fluid interacts with other entities. While Laplace's equation (3.21) and Bernoulli's equation (3.29) constrain the fluid behavior, it isn't immediately clear how the fluid is affected, for instance, by a rigid wall, a moving body, or another fluid. To accommodate these effects, additional constraints are prescribed along the

boundaries of the fluid. Any impermeable boundary must satisfy a zero-penetration condition, while any freely deforming boundary must additionally satisfy a dynamic boundary condition.

The boundary conditions for a free surface flow are typically derived using the approaches outlined in [8] and [18]. One may also employ Hamilton's principle, as in [51] and [50], to derive the fluid boundary conditions. Following [51], consider a fluid which is bounded above by a free surface and below by a rigid wall. Define the fluid Lagrangian to be the Bernoulli pressure (3.30) integrated over the fluid volume:

$$\mathcal{L}_{\mathrm{f}} = \int_{x_1}^{x_2} \int_{y_1}^{y_2} \int_{\eta(x,y,t)}^{z_1} \left[\frac{1}{2} (\nabla \phi) \cdot (\nabla \phi) + \frac{\partial \phi}{\partial t} + gz \right] dz dy dx \tag{3.43}$$

In the above limits of integration, x_1, x_2, y_1, and y_2 represent the boundaries of the fluid volume perpendicular to the plane of the undisturbed free surface; here, the limiting case is studied where the boundary locations tend to infinity in each of these directions. The term z_1 represents the location of the sea floor, assumed to be constant in this case, and $\eta(x, y, t)$ represents the free surface elevation.

Select the scalar fields $\phi(x, y, z, t)$ and $\eta(x, y, t)$ to represent the system configuration. Note that this choice of configuration completely characterizes the fluid system since the fluid velocity can be determined everywhere from ϕ and η. Following the discussion in Section 2.3.1, define the action

$$I(\phi, \eta) = \int_{t_0}^{t_1} \mathcal{L}_{\mathrm{f}}(\phi, \eta, t) dt \tag{3.44}$$

and set the first variation equal to zero

$$\delta I = 0 \tag{3.45}$$

From the derivation given in Appendix A.3, applying Hamilton's principle yields

$$
\begin{aligned}
0 = \delta I = \int_{t_0}^{t_1} \Bigg\{ & \\
& \int_{x_1}^{x_2}\int_{y_1}^{y_2}\int_{z_1}^{\eta} -\left(\frac{\partial^2\phi}{\partial x^2}+\frac{\partial^2\phi}{\partial y^2}+\frac{\partial^2\phi}{\partial z^2}\right)\delta\phi \; dzdydx \\
& + \int_{x_1}^{x_2}\int_{y_1}^{y_2}\left[\left(\frac{\partial\phi}{\partial x}\frac{\partial\eta}{\partial x}+\frac{\partial\phi}{\partial y}\frac{\partial\eta}{\partial y}-\frac{\partial\phi}{\partial z}+\frac{\partial\eta}{\partial t}\right)\delta\phi\right]\Bigg|_{z=\eta} dydx \\
& + \int_{x_1}^{x_2}\int_{y_1}^{y_2}\left[\frac{1}{2}\left(\frac{\partial\phi}{\partial x}^2+\frac{\partial\phi}{\partial y}^2+\frac{\partial\phi}{\partial z}^2\right)+\frac{\partial\phi}{\partial t}-gz\right]\Bigg|_{z=\eta}\delta\eta \; dydx \\
& + \int_{x_1}^{x_2}\int_{y_1}^{y_2}\left[-\frac{\partial\phi}{\partial z}\delta\phi\right]\Bigg|_{z=z_1} dydx \\
& \Bigg\} dt
\end{aligned}
$$

Since $\delta\phi$ and $\delta\eta$ are arbitrary, the following conditions hold within the fluid volume:

$$0 = \frac{\partial^2\phi}{\partial x^2}+\frac{\partial^2\phi}{\partial y^2}+\frac{\partial^2\phi}{\partial z^2} \tag{3.46}$$

$$0 = \left[\frac{\partial\phi}{\partial x}\frac{\partial\eta}{\partial x}+\frac{\partial\phi}{\partial y}\frac{\partial\eta}{\partial y}-\frac{\partial\phi}{\partial z}+\frac{\partial\eta}{\partial t}\right]\Bigg|_{z=\eta} \tag{3.47}$$

$$0 = \left[\frac{1}{2}\left(\frac{\partial\phi}{\partial x}^2+\frac{\partial\phi}{\partial y}^2+\frac{\partial\phi}{\partial z}^2\right)+\frac{\partial\phi}{\partial t}-gz\right]\Bigg|_{z=\eta} \tag{3.48}$$

$$0 = \frac{\partial\phi}{\partial z}\Bigg|_{z=z_1} \tag{3.49}$$

From the first line (3.46), one recovers Laplace's equation (3.21), which represents conservation of mass within the fluid volume

$$\nabla^2\phi = 0 \tag{3.50}$$

Compared to [8, Sec 6.1], (3.47) and (3.48) respectively define the kinematic and dynamic free surface boundary conditions:

$$\left[\frac{D}{Dt}(z-\eta)\right]\Bigg|_{z=\eta} = \left[\frac{\partial\phi}{\partial z}-\frac{\partial\eta}{\partial t}-\frac{\partial\phi}{\partial x}\frac{\partial\eta}{\partial x}-\frac{\partial\phi}{\partial y}\frac{\partial\eta}{\partial y}\right]\Bigg|_{z=\eta} = 0 \tag{3.51}$$

$$\left[-\frac{p-p_{\mathrm{a}}}{\rho}\right]\Bigg|_{z=\eta} = \left[\frac{\partial\phi}{\partial t}+\frac{1}{2}\nabla\phi\cdot\nabla\phi-gz\right]\Bigg|_{z=\eta} = 0 \tag{3.52}$$

The kinematic boundary condition (3.51) states that the fluid particles along the surface move with the same vertical velocity as the free surface, implying that the free surface is a streamline of the flow. The dynamic boundary condition (3.52) constrains the surface pressure of the fluid to be constant and equal to the sea-level atmospheric pressure, p_{a}.

The final expression (3.49) is the sea floor boundary condition. This kinematic condition states that the fluid velocity normal to the sea floor must equal zero, or that the fluid does not penetrate the rigid boundary:

$$\left.\frac{\partial \phi}{\partial z}\right|_{z=z_1} = 0 \tag{3.53}$$

Together, (3.50)-(3.53) completely govern the fluid behavior in an ideal fluid which is bounded above by a free surface and below by a rigid boundary. In this dissertation, it is assumed that the sea floor extends infinitely far, enabling (3.53) to be neglected altogether.

The Linearized Combined Free Surface Boundary Condition

At first glance, the free surface boundary conditions provide a complete set of equations governing the evolution of the free surface: (3.52) provides an equation for the location of η

$$\eta = \left[\frac{1}{2g}\nabla\phi\cdot\nabla\phi + \frac{1}{g}\frac{\partial\phi}{\partial t}\right]\Bigg|_{z=\eta}$$

and (3.51) provides an expression for the temporal evolution

$$\frac{\partial\eta}{\partial t} = \left[\frac{\partial\phi}{\partial z} - \frac{\partial\phi}{\partial x}\frac{\partial\eta}{\partial x} - \frac{\partial\phi}{\partial y}\frac{\partial\eta}{\partial y}\right]\Bigg|_{z=\eta}$$

However, upon closer examination, the expression for η is defined in terms of functions which are themselves evaluated along the free surface. Since the location of the free surface is generally unknown *a priori*, the boundary conditions (3.51) and (3.52) are not immediately useful. To address the question of where to evaluate the free surface boundary conditions, one may employ a linearization assumption to simplify the problem [8, 18]. By assuming small amplitude free surface perturbations (and consequently small free surface slopes), one can ignore the higher order terms involving the spatial derivatives in (3.51) and (3.52). Further,

neglecting higher order terms justifies a first-order approximation of the free surface as the undisturbed free surface, given by the plane $z = 0$. Lewandowski [18, Ch. 4, Sec. 3] remarks that in shallow water, the small amplitude assumption is rather stringent. In deep water, however, the predictions remain quite reasonable even in the presence of larger free surface deformations. The linearized boundary conditions are

$$\left.\frac{\partial \phi}{\partial z}\right|_{z=0} = \left.\frac{\partial \eta}{\partial t}\right|_{z=0} \tag{3.54}$$

$$\left.\frac{\partial \phi}{\partial t}\right|_{z=0} = \left. g\eta \right|_{z=0} \tag{3.55}$$

Differentiating the simplified dynamic condition (3.55) with respect to time and substituting it into the simplified kinematic condition (3.54) yields the linearized, combined free surface boundary condition

$$\left.\frac{\partial^2 \phi}{\partial t^2}\right|_{z=0} - g\left.\frac{\partial \phi}{\partial z}\right|_{z=0} = 0 \tag{3.56}$$

The Kinematic Rigid Body Boundary Condition

For a rigid body, the fluid velocity normal to the hull must equal the normal velocity of the hull at each point. Karamcheti [41, p. 252] remarks that problems which solve Laplace's equation in conjunction with this kinematic body boundary condition are called *Neumann exterior problems*. Let $\boldsymbol{r}_{\mathrm{h}}$ represent a point along the hull expressed relative to the origin of the body-fixed frame, and let $\boldsymbol{n}_+$ represent the corresponding unit normal vector directed from the fluid into the vehicle. Then, define the set $\mathcal{B} = \{\bar{\boldsymbol{x}} \mid \bar{\boldsymbol{x}} = \boldsymbol{r}_{\mathrm{h}}\}$, which gives the location of the rigid hull. The kinematic rigid body boundary condition is

$$\left[\nabla\phi \cdot \boldsymbol{n}_+\right]\big|_{\mathcal{B}} = \left[(\boldsymbol{v} + \boldsymbol{\omega} \times \boldsymbol{r}_{\mathrm{h}})\right] \cdot \boldsymbol{n}_+ \tag{3.57}$$

If one defines the body geometry vector $\boldsymbol{b}$ as

$$\boldsymbol{b} = \begin{pmatrix} \boldsymbol{n}_+ \\ \boldsymbol{r}_{\mathrm{h}} \times \boldsymbol{n}_+ \end{pmatrix} \tag{3.58}$$

then the body boundary condition may be rewitten as

$$(\nabla\phi \cdot \boldsymbol{n}_+)\,\big|_{\mathcal{B}} = \boldsymbol{b} \cdot \boldsymbol{\nu} \tag{3.59}$$

This boundary condition constrains the velocity perpendicular to the rigid hull. It's important to understand that we have given up the ability to prescribe the flow tangent to the hull under potential flow theory. In a viscous fluid, a more realistic prescription is the "no-slip" boundary condition, which additionally constrains the fluid velocity tangent to the hull. For streamlined bodies operating at low angles of attack, the hydrodynamics are dominated by potential flow effects and the no-slip condition can often be neglected.

3.3.5 Useful Results in Potential Flow Theory

Superposition

Since the Laplacian operator is a linear operator, if two solutions to Laplace's equation exist

$$\nabla^2\phi_1 = 0 \qquad \text{and} \qquad \nabla^2\phi_2 = 0$$

then the superposition of these solutions also satisfy Laplace's equation

$$\nabla^2\left(\phi_1 + \phi_2\right) = 0$$

This implies that independent solutions can be linearly superimposed to generate additional hydrodynamic solutions. It is generally non-trivial to analytically satisfy a fluid boundary condition with a single scalar potential. However, combinations of simple functions can be used to construct hydrodynamic solutions with relative ease. Panel-based algorithms, for instance, use this concept of superposition to model fluid-body interactions.

Impulsive Motions

For any state of irrotational fluid motion, one may interpret the motion as being instantaneously generated from rest by a set of impulsive body and pressure forces [41, Sec. 9.9].

Moreover, since only irrotational body and pressure forces are considered, the fluid motion will remain irrotational for all time. Lamb [25, Art. 40] further remarks that the velocity potential in a simply connected fluid can be completely determined when ϕ, $\nabla\phi\cdot\boldsymbol{n}_+$, or some combination is given over the boundaries of the fluid volume. The importance of impulsively generated motions will be highlighted throughout the remainder of this dissertation. Conceptually, it provides insight into how fluid-vehicle systems evolve with time. This idea is also foundational for Cummins' description of the fluid memory effects [19].

3.4 Wave Mechanics

The ocean is governed by random and chaotic processes, leading to seemingly unpredictable behavior. Ocean waves depend on a variety of environmental factors, including wind speed, wind direction, as well as geographic factors like ocean depth and distance from a coastline [52]. However, with certain statistical assumptions, one can use potential flow theory to construct realistic wave realizations.

3.4.1 Plane Progressive Waves

A plane progressive wave is a gravity-induced surface wave which propagates in a single direction at a single frequency. Following [8, Sec. 6.2], consider a wave for which the surface elevation is purely sinusoidal:

$$\eta(x,t) = A\sin(kx - \omega t + \varepsilon) \tag{3.60}$$

The surface elevation is given in terms of the wave amplitude A, the wavenumber k, the wave frequency ω, and an arbitrary phase angle ε; see Figure 3.3. The wave height is then defined by $H = 2A$.

For a fluid of infinite depth, the scalar potential governing a plane progressive wave is

$$\phi_{\mathrm{w}}(x,z,t) = \frac{gA}{\omega}e^{-kz}\cos(kx - \omega t + \varepsilon) \tag{3.61}$$

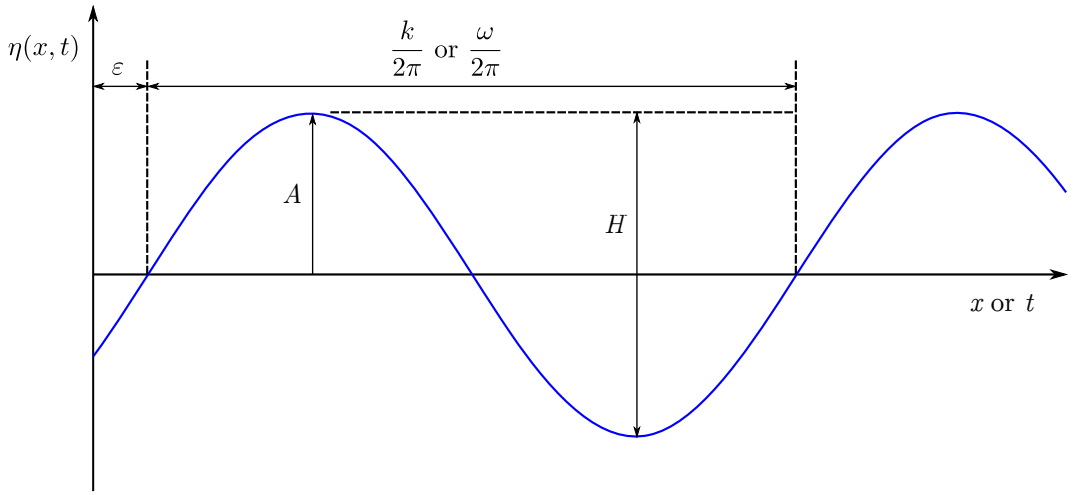

Figure 3.3: Depictions of the constants required to initialize a plane progressive wave. Note that the abscissa can represent either distance or time.

A derivation of this potential function is given in [8], though one may easily verify that this potential satisfies each of the boundary conditions given in Section 3.3.4. Studying Laplace's equation first, one finds

$$\nabla^2\phi_{\mathrm{w}} = -\frac{gAk^2}{\omega}e^{-kz}\cos(kx-\omega t+\varepsilon) + \frac{gAk^2}{\omega}e^{-kz}\cos(kx-\omega t+\varepsilon) = 0 \tag{3.62}$$

Using the linearized kinematic free surface boundary condition (3.54), the free surface elevation matches (3.60):

$$\eta = \frac{1}{g}\frac{\partial\phi_{\mathrm{w}}}{\partial t}\bigg|_{z=0} = A\sin(kx-\omega t+\varepsilon)$$

Substituting the potential (3.61) into the combined free surface boundary condition (3.56), one finds

$$\frac{\partial^2\phi_{\mathrm{w}}}{\partial t^2}\bigg|_{z=0} - g\frac{\partial\phi_{\mathrm{w}}}{\partial z}\bigg|_{z=0} = -gA\omega\cos(kx-\omega t+\varepsilon) + \frac{g^2Ak}{\omega}\cos(kx-\omega t+\varepsilon)$$

The boundary condition is only satisfied when the deep water dispersion relation holds [8]

$$\omega^2 = gk \tag{3.63}$$

This equation defines the relationship between the wave frequency and the wavenumber for gravity-driven surface waves. Finally, in the limit as the sea floor tends to infinite depth,

the sea floor boundary condition is also satisfied

$$\lim_{z_1\to\infty} \frac{\partial \phi_{\mathrm{w}}}{\partial z}\bigg|_{z=z_1} = \lim_{z_1\to\infty} -\frac{gAk}{\omega} e^{-kz_1}\cos(kx-\omega t+\varepsilon) = 0 \tag{3.64}$$

Taking the gradient of the scalar potential yields the corresponding fluid velocity field in inertial space:

$$\boldsymbol{V}_{\mathrm{f}}(\boldsymbol{x},t) = A\omega e^{-kz}\begin{pmatrix} -\sin(kx-\omega t+\varepsilon) \\ 0 \\ -\cos(kx-\omega t+\varepsilon) \end{pmatrix} \tag{3.65}$$

A snapshot of the velocity field is given in Figure 3.4. The plane progressive wave exhibits periodic behavior in the x direction and exponential decay with increasing depth.

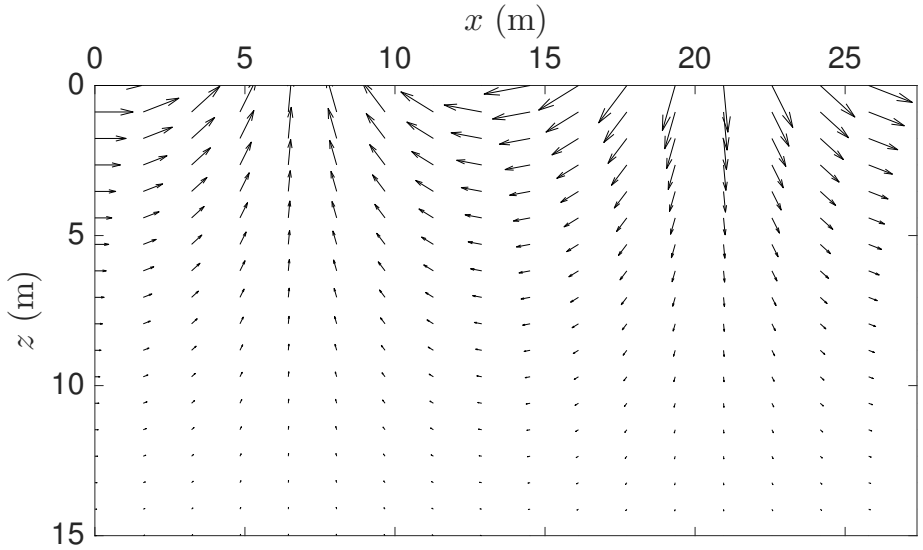

Figure 3.4: Snapshot of a plane progressive wave in the $x-z$ plane.

3.4.2 Ocean Wave Nomenclature and Statistics

In the ocean, there exists a continuous spectrum of wave frequencies which propagate across a continuous range of headings, exhibiting both spatially and temporally random behavior.

However, if the free surface evolves on a much faster time scale than the stochastic properties of the waves themselves, we can model the wave system as a stationary, zero-mean Gaussian[6] process [2, Sec. 2.4]:

$$E[\eta(t)] = 0 \tag{3.66}$$

$$E[\eta^2(t)] = \int_0^\infty S(\omega) d\omega \tag{3.67}$$

Here, $E[\,]$ denotes the expected value of a function and $S(\omega)$ is the wave spectrum, the power spectral density (PSD) of the wave energy.

Several spectra have been developed over the years, including the Pierson-Moskowitz and Bretschneither spectra [1, 2] and more recently the Elfouhaily spectrum [52]. These spectra map environmental characteristics, like the wind speed, to an energy density function. For instance, the one-parameter Pierson-Moskowitz spectrum is defined below in terms of the wind speed U_{w}:

$$S(\omega) = \frac{0.0081 g^2}{\omega^5} \exp\left[-0.74 \left(\frac{g}{U_{\mathrm{w}}\omega}\right)^4\right] \tag{3.68}$$

In Figure 3.5, it is apparent that the spectrum becomes more energetic with increasing wind-speed, leading to rougher seas. The intensity of a wave realization is characterized in terms of a sea state. In terms of the significant wave height, defined as the average of the one-third largest waves in a given realization, the sea states and their descriptions are given in Table 3.2 [2].

3.4.3 Long-Crested Wave Realizations

A long-crested wave realization employs a wave spectrum to model a wave system in two-dimensions[7]. To construct a wave realization from a sea spectrum, one superimposes a series

[6] Carl Friedrich Gauss, 1777-1855.

[7] Extruding the wave realization into three-dimensions, one finds that the wave crests extend infinitely far since the wave headings are all aligned, hence the name "long-crested waves"; see Figure 3.6

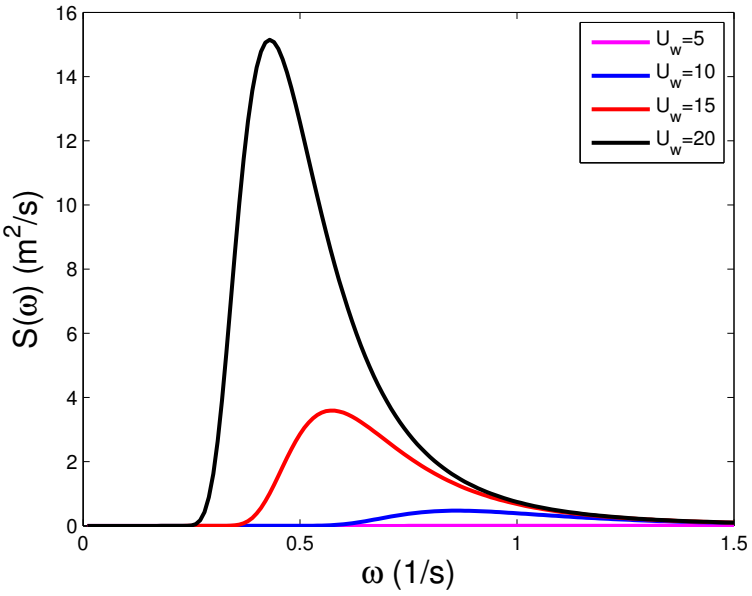

Figure 3.5: The Pierson-Moskowitz spectrum (3.68) plotted for wind speeds of 5ms^{-1}, 10ms^{-1}, 15ms^{-1}, 20ms^{-1}.

Table 3.2: World Meteorological Organization (WMO) sea state code.

Sea state code	Significant wave height	Seaway description
0	0m	Calm (glassy)
1	0.00m to 0.10m	Calm (rippled)
2	0.10m to 0.50m	Smooth (wavelets)
3	0.50m to 1.25m	Slight
4	1.25m to 2.50m	Moderate
5	2.50m to 4.00m	Rough
6	4.00m to 6.00m	Very rough
7	6.00m to 9.00m	High
8	9.00m to 14.0m	Very high
9	>14.0m	Phenomenal

of plane progressive waves with correctly chosen frequencies and amplitudes. Since the area under a the spectral density curve $S(\omega)$ gives the mean-square of the wave height, one can compute pairs of wave frequencies and amplitudes which approximate the spectral density curve [2].

To realize a wave field for the Pierson-Moskowitz spectrum, one first selects a wind velocity U_{w} to model a desired sea state. One then chooses a set of interpolation frequencies ω_i where the spectral density curve is nonzero. These correspond to the frequencies of the superimposed waves. Next, approximate the area under the spectral density curve using a Riemann sum. For an approximation using rectangular slices, the area of each slice is $S(\omega_i)\Delta\omega_i$ where $S(\omega_i)$ represents the height at the i^{th} interpolation frequency and the term $\Delta\omega_i$ represents the corresponding distance between successive interpolation frequencies. Then each of the wave amplitudes can be computed as

$$A_i = \sqrt{2S(\omega_i)\Delta\omega_i} \tag{3.69}$$

Lastly, generate a random phase ε_i for each wave. The resulting free surface corresponding to a Pierson-Moskowitz spectrum with a wind speed of $10\mathrm{ms}^{-1}$ ($\sim$20 knots) and 51 frequencies evenly spaced between $\omega = 0.5\mathrm{s}^{-1}$ and $\omega = 3\mathrm{s}^{-1}$ is plotted in Figure 3.6.

3.4.4 Short-Crested Wave Realizations

As compared to long-crested wave realizations, which superpose plane progressive waves along the same direction, short crested waves also superpose waves across a variety of headings. To achieve this, one may augment the sea spectrum with a spreading function [2]:

$$S_{\mathrm{sc}}(\omega, \chi) = S(\omega)M(\chi) \tag{3.70}$$

The spreading function $M(\chi)$ disperses the wave energy across a range of headings, generating a short-crested wave spectrum $S_{\mathrm{sc}}(\omega, \chi)$. Perez [2, Sec. 2.8] presents a commonly used

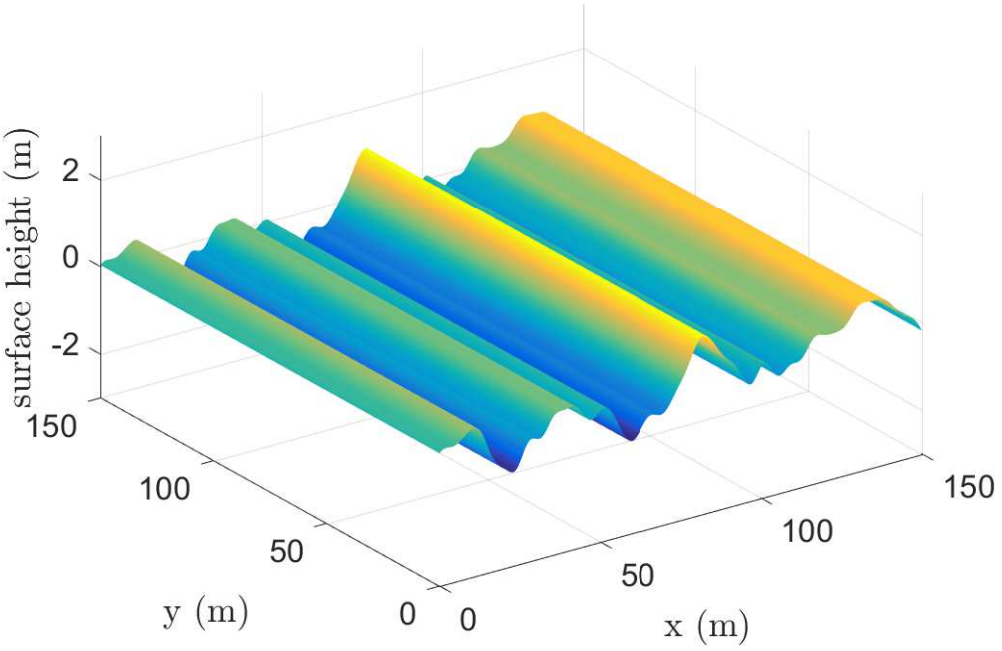

Figure 3.6: A snapshot of the free surface generated by a Pierson-Moskowitz spectrum with a wind speed of 10ms^{-1} and 51 evenly space frequencies between 0.5s^{-1} and 3s^{-1}.

spreading function

$$M(\chi) = \frac{2^{(2n-1)}n!(n-1)!}{\pi(2n-1)!}\cos^{2n}(\chi-\chi_0) \quad \text{for } -\frac{\pi}{2} < \chi - \chi_0 < \frac{\pi}{2} \tag{3.71}$$

where larger values of n correspond to a narrower concentration of wave headings.

To construct a short-crested wave realization, one must prescribe a set of interpolation headings χ_i in addition to a set of interpolation frequencies ω_i. The Pierson-Moskowitz spectrum with a wind speed of 10ms^{-1} and with a spreading function parameter $n = 2$ is visualized in Figure 3.7. Based on this spectrum, 26 interpolation frequencies were applied to 11 different headings to construct the short crested wave realization depicted in Figure 3.8.

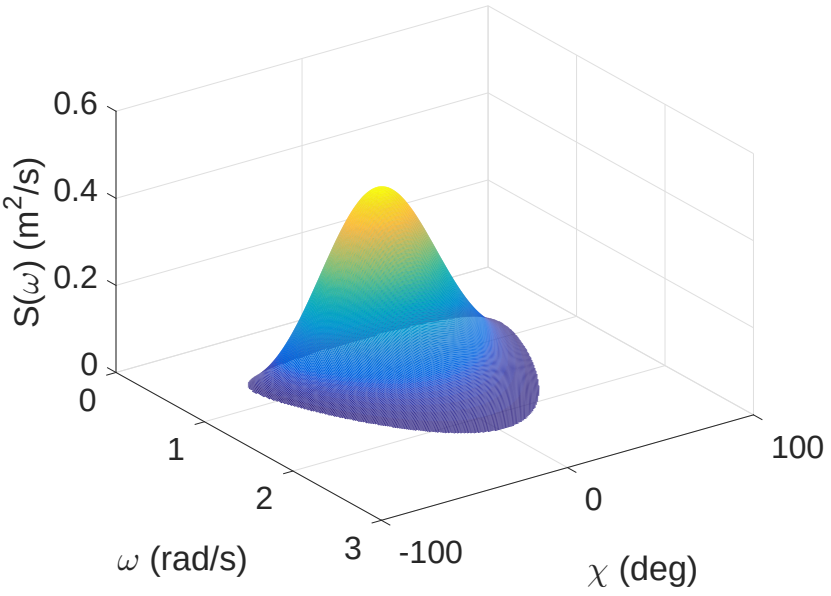

Figure 3.7: Pierson-Moskowitz spectrum with $U = 10\text{ms}^{-1}$ and the spreading function parameter $n = 2$.

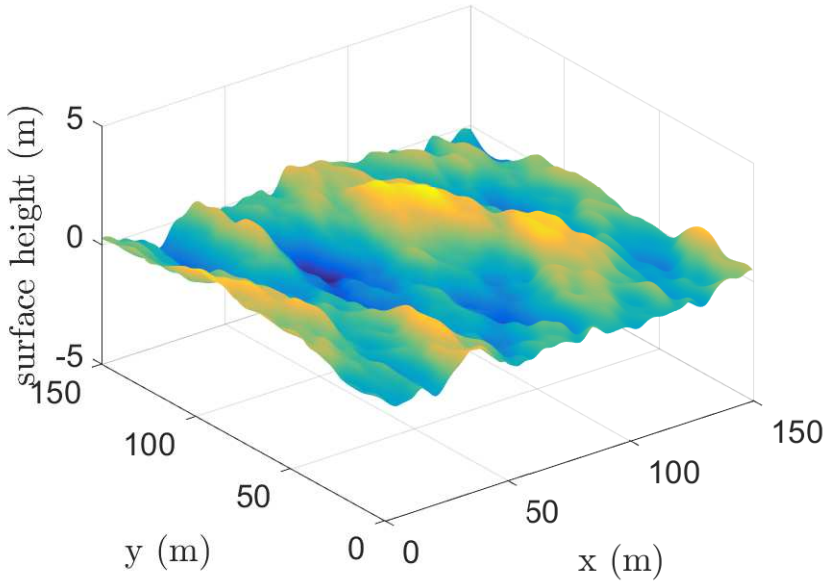

Figure 3.8: Surface height snapshot using 286 plane progressive waves to approximate the Pierson-Moskowitz spectrum with $U_{\text{w}} = 10\text{ms}^{-1}$.

Chapter 4

Lagrangian Mechanics for Fluid-Body Interactions

As discussed in the treatment of Lagrangian mechanics in Chapter 2, if one can construct a Lagrangian function for a given system, this function may be used to generate a set of ODEs which govern the system motion. Additional physical effects which aren't incorporated using the system Lagrangian can then be modeled as generalized forces. This approach was followed when presenting the maneuvering and seakeeping models in Chapter 3: the rigid body equations of motion were derived using Lagrangian mechanics and the hydrodynamics were incorporated as generalized forces. In this chapter, some of these generalized forces are instead derived from fluid Lagrangian functions.

As an interesting observation, Lagrangian mechanics is largely absent from many of the modern introductory texts in ship dynamics, including the works of Newman [8], Fossen [1], Lewandowski [18], and Perez [2]; with the exception of some minor notes given in [1], these four works almost exclusively follow the Newtonian modeling approach[1]. In this chapter, Lagrangian modeling of fluid-body interactions is introduced in the context of the more familiar

[1]Earlier works by Lamb [25], and to a lesser extent, Milne-Thomson [53], outline several applications for Lagrangian mechanics in fluid systems.

Newtonian modeling approach. This chapter begins with a review of force and moment expressions used for Newtonian modeling. Transitioning to Lagrangian mechanics, the relevant system energy functions are identified. These energies are then used to derive expressions for the hydrodynamic forces and moments acting on a vehicle, and the Lagrangian expressions are compared to those from Newtonian mechanics. This chapter concludes with four examples which demonstrate the Lagrangian modeling process for a variety of applications.

4.1 Newtonian Mechanics

From the discussion of radiation effects in Section 3.1, the motion of a rigid body immersed in a fluid must induce fluid motion. This fluid motion is primarily driven by the pressure along the hull. Let $\boldsymbol{n}_+$ represent a unit normal vector directed out of the fluid and let $\boldsymbol{n}_- = -\boldsymbol{n}_+$ (a unit normal vector directed into the fluid). The transfer of momentum from the body into the fluid is

$$\boldsymbol{f}_{\mathrm{b}} = \iint_{\mathcal{B}} p\boldsymbol{n}_- dS \tag{4.1}$$

In this expression, one may interpret the pressure acting on the fluid as the inertial force per unit area due to the combination of rigid body translations and rotations. The resulting force is analogous to the pressure force acting on an infinitesimal volume of fluid (3.25). In this case, however, it represents the integrated total effect of the body acting on each infinitesimal fluid element adjacent to the hull. Note that the body does not induce a fluid torque as a direct consequence of the conservation of vorticity within a fluid volume [41].

Conversely, Newton's third law requires that the fluid also exerts a force back onto the body. The expressions for force and moment due to the fluid pressure acting on a rigid body are [8]

$$\boldsymbol{f}_{\mathrm{p}} = \iint_{\mathcal{B}} p\boldsymbol{n}_+ dS \tag{4.2}$$

$$\boldsymbol{\tau}_{\mathrm{p}} = \iint_{\mathcal{B}} p(\boldsymbol{r}_{\mathrm{h}} \times \boldsymbol{n}_+) dS \tag{4.3}$$

where $\boldsymbol{r}_{\mathrm{h}}$ is the location of the point along the hull corresponding to $\boldsymbol{n}_{+}$. The pressure here is given by the unsteady Bernoulli equation (3.29). Neglecting the hydrostatics (appropriate without a free surface), the equations are commonly written as

$$\boldsymbol{f}_{\mathrm{p}} = -\iint_{\mathcal{B}} \left(\rho \frac{\partial \phi}{\partial t} + \rho \frac{1}{2} \nabla\phi \cdot \nabla\phi\right) \boldsymbol{n}_{+} dS \tag{4.4}$$

$$\boldsymbol{\tau}_{\mathrm{p}} = -\iint_{\mathcal{B}} \left(\rho \frac{\partial \phi}{\partial t} + \rho \frac{1}{2} \nabla\phi \cdot \nabla\phi\right) (\boldsymbol{r}_{\mathrm{h}} \times \boldsymbol{n}_{+}) dS \tag{4.5}$$

These expressions (4.4)-(4.5) simply evaluate the total effect of the fluid pressure acting along the hull of the vehicle. The fluid pressure adjacent to the body is affected by the remainder of the fluid volume, however – the pressure distribution over the vehicle in an unbounded fluid would differ from that over a vehicle operating near a rigid wall. To recast the fluid force in a way that takes into account the fluid volume, consider the application of the gradient theorem (A.1) to the fluid pressure:

$$\iiint_{\mathcal{F}} \nabla p \; dV = \iint_{\mathcal{B}} p\boldsymbol{n}_{+} \; dS + \iint_{\mathcal{E}} p\boldsymbol{n}_{+} \; dS \tag{4.6}$$

Rearranging the terms, the fluid force can equivalently be expressed as

$$\boldsymbol{f}_{\mathrm{p}} = \iiint_{\mathcal{F}} \nabla p \; dV - \iint_{\mathcal{E}} p\boldsymbol{n}_{+} \; dS \tag{4.7}$$

While arguably less useful from a computational standpoint[2], expressing the force equation in this form reinforces the idea that the entire fluid volume, including any other fluid boundaries, directly influences the force acting on a submerged vehicle.

A more useful form for the force and moment equations comes from Newman [8, Ch. 4.12]. Consider a submerged body suspended in an infinite volume of fluid. Let $\mathcal{F}$ represent only a portion of the fluid, bounded externally by a fictitious yet stationary envelope $\mathcal{E}$ and internally by the rigid hull of the body $\mathcal{B}$. The boundaries $\mathcal{E}$ and $\mathcal{B}$ are depicted in Figure 4.1. Let $\boldsymbol{p}_{\mathrm{f}}$ represent the fluid momentum per unit volume:

$$\boldsymbol{p}_{\mathrm{f}} = \rho \boldsymbol{V}_{\mathrm{f}} = \rho \nabla\phi \tag{4.8}$$

[2]As per the discussion in [54], computing gradients numerically is typically computationally intensive and the fluid volume is typically quite large.

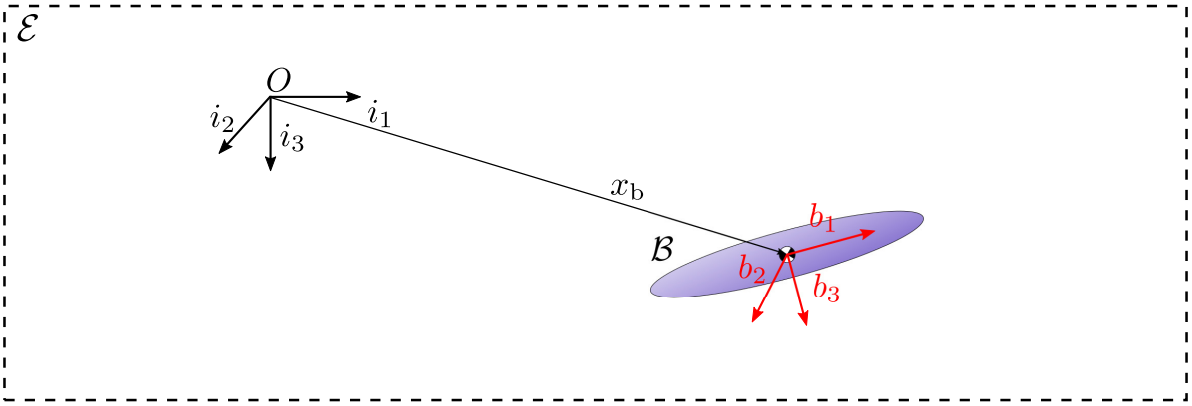

Figure 4.1: An underwater vehicle suspended in a volume of fluid $\mathcal{F}$ contained within an envelope $\mathcal{E}$.

Then the total fluid momentum contained in the volume $\mathcal{F}$ is

$$\boldsymbol{P}_{\mathrm{f}} = \iiint_{\mathcal{F}} \boldsymbol{p}_{\mathrm{f}} \, dV = \iiint_{\mathcal{F}} \rho \nabla \phi \, dV \tag{4.9}$$

Applying the gradient theorem to the right-hand side, and taking the time derivative of both sides yields

$$\frac{d}{dt}\boldsymbol{P}_{\mathrm{f}} = \rho \frac{d}{dt}\left[\iint_{\mathcal{B}} \phi \boldsymbol{n}_{+} \, dS + \iint_{\mathcal{E}} \phi \boldsymbol{n}_{+} \, dS \right] \tag{4.10}$$

Using this identity, Newman [8, Sec. 4.12] derives the following alternate expressions for the hydrodynamic force and moment.

Proposition 4.1.1 (Alternate forms for the hydrodynamic force and moment.) *The hydrodynamic force and moment acting on a rigid body can be equivalently defined as*

$$\boldsymbol{f}_{\mathrm{p}} = -\rho \frac{d}{dt} \iint_{\mathcal{B}} \phi \boldsymbol{n}_{+} \, dS - \rho \iint_{\mathcal{E}} \left[\nabla \phi \left(\nabla \phi \cdot \boldsymbol{n}_{+} \right) - \frac{1}{2} \left(\nabla \phi \cdot \nabla \phi \right) \boldsymbol{n}_{+} \right] dS \tag{4.11}$$

$$\boldsymbol{\tau}_{\mathrm{p}} = -\rho \frac{d}{dt} \iint_{\mathcal{B}} \phi \left(\boldsymbol{r}_{\mathrm{h}} \times \boldsymbol{n}_{+} \right) dS - \rho \iint_{\mathcal{E}} \boldsymbol{r} \times \left[\nabla \phi (\nabla \phi \cdot \boldsymbol{n}_{+}) - \frac{1}{2} (\nabla \phi \cdot \nabla \phi) \boldsymbol{n}_{+} \right] dS \tag{4.12}$$

□

For a proof of this proposition, see Appendix A.4.

Remark 4.1.2 (Incorporating hydrostatic effects.) *Equating (4.4) to (4.11) and (4.5) to (4.12), the corresponding hydrostatic force and moment may be incorporated by adding the terms*

$$\iint_{\mathcal{B}} \rho g z \boldsymbol{n}_+ dS \quad \text{and} \quad \iint_{\mathcal{B}} \rho g z (\boldsymbol{r}_{\text{h}} \times \boldsymbol{n}_+) dS$$

to (4.11) and (4.12), respectively.

To interpret the new force expression (4.11), first add (4.10) to (4.11):

$$\boldsymbol{f}_{\text{p}} = -\frac{d}{dt}\boldsymbol{P}_{\text{f}} + \iint_{\mathcal{E}} \rho \left[\frac{\partial \phi}{\partial t}\boldsymbol{n}_+ + \frac{1}{2}\nabla\phi \cdot \nabla\phi \boldsymbol{n}_+ - \nabla\phi(\nabla\phi \cdot \boldsymbol{n}_+) \right] dS \tag{4.13}$$

This expression relates that the total force acting on the vehicle to the time rate of change of fluid momentum contained within $\mathcal{F}$. To interpret the remainder of (4.13), consider an additional surface $\mathcal{E}_1$ which completely contains $\mathcal{E}$. The above approach may be iterated to relate the surface integral over $\mathcal{E}$ to a surface integral over $\mathcal{E}_1$ and a volume integral over the fluid contained between $\mathcal{E}$ and $\mathcal{E}_1$. Thus, the terms evaluated along the surface $\mathcal{E}$ in (4.13) account for any fluid effects external to $\mathcal{F}$ which may additionally have an impact on the vehicle dynamics.

Recall that the location of $\mathcal{E}$ has not yet been specified; it simply represents an arbitrary closed surface which is fixed in inertial space. It is often convenient to let $\mathcal{E}$ coincide with the fluid boundaries where the corresponding boundary conditions can be used to further simplify the expressions. Newman [8] remarks that $\mathcal{E}$ may also be placed within the surface of the body, so long as it remains exterior to any singularities within the body[3]. Allowing $\mathcal{E}$ to shrink arbitrarily close to a singularity enables one to derive the *Lagally Theorem* [55, 56]. If a body is simulated in a fluid using elementary potential flow building blocks, such as sources or doublets, the Lagally Theorem relates the strengths of these singularities to the corresponding force and moment over the body.

[3]Potential flow codes typically resolve the fluid behavior using a collection of singularities placed outside of the fluid.

4.1.1 Alternate Force and Moment Expressions in an Unbounded Fluid

When studying vehicle induced fluid motion in an unbounded fluid, consider the following remark, which summarizes the discussion in [25, Art. 117].

Remark 4.1.3 *When considering a system which is initialized by an impulsive body motion and which undergoes motion for a finite time, the fluid velocity $\nabla\phi$ must decay to zero infinitely far from the vessel, and the fluid velocity must decay sufficiently fast. Otherwise, a finite impulse applied to the body would result in an infinite system energy.*

Proposition 4.1.4 *When $\mathcal{E}$ extends infinitely far from the vehicle in all directions, the force and moment expressions become*

$$\boldsymbol{f}_{\mathrm{p}} = -\rho \frac{d}{dt} \iint_{\mathcal{B}} \phi \boldsymbol{n}_{+} \, dS \tag{4.14}$$

$$\boldsymbol{\tau}_{\mathrm{p}} = -\rho \frac{d}{dt} \iint_{\mathcal{B}} \phi \left(\boldsymbol{r}_{\mathrm{h}} \times \boldsymbol{n}_{+} \right) dS \tag{4.15}$$

□

Proof. From Remark 4.1.3, the integrals along $\mathcal{E}$ in (4.11) and (4.12) must equal zero. ■

Proposition 4.1.5 *Considering an unbounded fluid whose motion is due solely to the motion of a submerged vehicle, the following relationship holds*

$$\iint_{\mathcal{E}} \left. \frac{\partial \phi}{\partial t} \right|_{t=t_1} \boldsymbol{n}_{+} dS = 0 \tag{4.16}$$

for any time t_1 and in the limit that $\mathcal{E}$ extends infinitely far from the vehicle.

□

Proof. With the property that $\nabla\phi = \mathbf{0}$ infinitely far from the vehicle, any temporal changes in the velocity potential ϕ must correspond to uniform changes in the velocity potential. This

implies that for any time t_1,

$$\left.\frac{\partial \phi}{\partial t}\right|_{\boldsymbol{x}\in\mathcal{E},\ t=t_1} = c$$

where c is a constant. This enables one to write

$$\iint_{\mathcal{E}} \left.\frac{\partial \phi}{\partial t}\right|_{t=t_1} \boldsymbol{n}_+ dS = \iint_{\mathcal{E}} c\ \boldsymbol{n}_+\ dS \tag{4.17}$$

Let $\mathcal{V}$ represent the entire volume contained within $\mathcal{E}$ (including the volume contained within the hull of the rigid body). Application of the gradient theorem then yields

$$\iint_{\mathcal{E}} c\boldsymbol{n}_+ dS = \iiint_{\mathcal{V}} \nabla c\ dV = 0 \tag{4.18}$$

■

To interpret the force expression (4.14), consider again the relationship between the force and the fluid momentum given in (4.13). As a result of Proposition 4.1.5, (4.13) becomes

$$\boldsymbol{f}_{\mathrm{p}} = -\frac{d}{dt}\boldsymbol{P}_{\mathrm{f}} \tag{4.19}$$

The net hydrodynamic force acting on a vehicle in an unbounded fluid is thus equivalent to the time rate of change of fluid momentum. Recall (2.17) (Euler's first axiom for rigid body motion)

$$\boldsymbol{f} = \frac{d}{dt}\boldsymbol{p}_{\mathrm{b}}$$

where $\boldsymbol{p}_{\mathrm{b}}$ represents the translational momentum of a rigid body and $\boldsymbol{f}$ represents the sum of externally applied forces.

Remark 4.1.6 (Conserved quantities.) *For a neutrally buoyant vehicle in an unbounded fluid, Euler's first axiom of rigid body motion implies that the sum of the mechanical translational momenta and fluid momenta are constants of motion:*

$$\frac{d}{dt}\left(\boldsymbol{p}_{\mathrm{b}} + \boldsymbol{P}_{\mathrm{f}}\right) = \boldsymbol{0} \quad \Longrightarrow \quad \boldsymbol{p}_{\mathrm{b}} + \boldsymbol{P}_{\mathrm{f}} = \boldsymbol{c} \tag{4.20}$$

4.1.2 Alternate Force and Moment Expressions in a Fluid with a Rigid Boundary

Assume now that the fluid volume is bounded by a rigid wall which is a finite distance from the vehicle in at least one direction.

Proposition 4.1.7 *In the case where $\mathcal{E}$ coincides with a rigid boundary, the force and moment expressions become*

$$\boldsymbol{f}_{\mathrm{p}} = -\rho \frac{d}{dt} \iint_{\mathcal{B}} \phi \boldsymbol{n}_{+} \, dS + \rho \iint_{\mathcal{E}} \frac{1}{2} \left(\nabla \phi \cdot \nabla \phi \right) \boldsymbol{n}_{+} dS \tag{4.21}$$

$$\boldsymbol{\tau}_{\mathrm{p}} = -\rho \frac{d}{dt} \iint_{\mathcal{B}} \phi \left(\boldsymbol{r}_{\mathrm{h}} \times \boldsymbol{n}_{+} \right) dS + \rho \iint_{\mathcal{E}} \frac{1}{2} (\nabla \phi \cdot \nabla \phi) \boldsymbol{r} \times \boldsymbol{n}_{+} dS \tag{4.22}$$

□

Proof. Along any rigid boundary, the fluid must satisfy the kinematic zero-penetration boundary condition, which requires $\nabla \phi \cdot \boldsymbol{n}_{+} = 0$ in (4.11) and (4.12). ■

4.1.3 Alternate Force and Moment Expressions in a Fluid with a Free Surface

In the final case considered, the "top" of $\mathcal{E}$ now coincides with a free surface $\mathcal{S}$, as depicted in Figure 4.2. (The combination of $\mathcal{E}$ and $\mathcal{S}$ defines the external bounding surface of the fluid volume $\mathcal{F}$.) Explicitly, $\mathcal{S} = \left\{ \boldsymbol{x} \;\middle|\; z = \eta(x, y, t) \right\}$ and represents the collection of fluid particles along the free surface. As compared to the prior sections where $\mathcal{E}$ was assumed to be stationary, the free surface will generally be in motion. From the discussion on boundary conditions in Section 3.3.4, the free surface evolves such that the pressure remains constant along it. In this case, the hydrostatic pressure can no longer be neglected. Sclavounos [54] re-derives (4.11)-(4.12) for a body floating on a free surface, though the results additionally hold for a submerged vehicle.

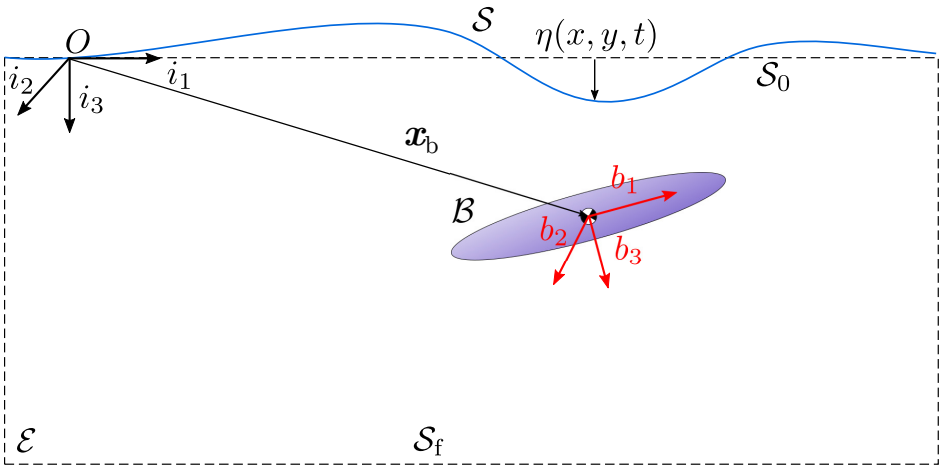

Figure 4.2: Depiction of the various surfaces for a submerged vehicle maneuvering near a free surface. The fluid volume is bounded below and on the sides by $\mathcal{E}$ and above by the free surface $\mathcal{S}$. The plane $\mathcal{S}_0$ represents the undisturbed free surface located at $z = 0$ and the plane $\mathcal{S}_\mathrm{f}$ represents the sea floor located at a large depth $z = z_\mathrm{f}$.

Proposition 4.1.8 (Alternate force and moment expressions for a vehicle near a free surface.) *For a vehicle operating in the presence of a free surface, the force and moment acting on the vehicle are*

$$\begin{aligned}\boldsymbol{f}_\mathrm{p} = &-\rho\frac{d}{dt}\iint_{\mathcal{B}}\phi\boldsymbol{n}_+dS - \rho\frac{d}{dt}\iint_{\mathcal{S}}\phi\boldsymbol{n}_+dS\\ &+\rho g\iint_{\mathcal{B}}z\boldsymbol{n}_+dS + \rho g\iint_{\mathcal{S}}z\boldsymbol{n}_+dS \qquad (4.23)\\ \boldsymbol{\tau}_\mathrm{p} = &-\rho\frac{d}{dt}\iint_{\mathcal{B}}\phi\boldsymbol{r}_\mathrm{h}\times\boldsymbol{n}_+dS - \rho\frac{d}{dt}\iint_{\mathcal{S}}\phi\boldsymbol{r}\times\boldsymbol{n}_+dS\\ &+\rho g\iint_{\mathcal{B}}z\boldsymbol{r}_\mathrm{h}\times\boldsymbol{n}_+dS + \rho g\iint_{\mathcal{S}}z\boldsymbol{r}\times\boldsymbol{n}_+dS \qquad (4.24)\end{aligned}$$

□

Proof. See [54, Sec. 2].

To interpret the terms in the first line of the force expression (4.23), consider the following application of the gradient theorem.

$$-\frac{d}{dt}\iiint_{\mathcal{F}}\rho\nabla\phi\,dV = -\rho\frac{d}{dt}\iint_{\mathcal{B}}\phi\boldsymbol{n}_+dS - \rho\frac{d}{dt}\iint_{\mathcal{S}}\phi\boldsymbol{n}_+dS - \rho\frac{d}{dt}\iint_{\mathcal{E}}\phi\boldsymbol{n}_+dS$$

Because $\mathcal{E}$ is stationary and assumed to be infinitely far from the vehicle, the time rate of change of the integral over $\mathcal{E}$ is zero by Proposition 4.1.5. The terms on the top line of (4.23) therefore represent the time rate of change of fluid momentum:

$$-\rho\frac{d}{dt}\iint_{\mathcal{B}}\phi\boldsymbol{n}_{+}dS-\rho\frac{d}{dt}\iint_{\mathcal{S}}\phi\boldsymbol{n}_{+}dS=-\frac{d}{dt}\boldsymbol{P}_{\mathrm{f}} \tag{4.25}$$

The terms on the second line of (4.23) are related to the gravitational force acting on the fluid. The integral over the body is simply the buoyancy force acting on the rigid body, which is easily seen from the following application of the gradient theorem

$$\iint_{\mathcal{B}}\rho gz\boldsymbol{n}_{+}dS=-\iint_{\mathcal{B}}\rho gz\boldsymbol{n}_{-}dS=-\iiint_{\forall}\nabla(\rho gz)dV=-\rho g\forall\boldsymbol{i}_{3} \tag{4.26}$$

Here, the term $\forall$ represents the volume of fluid displaced by the rigid body. To interpret the integral over $\mathcal{S}$, consider the following identity which again leverages the gradient theorem

$$\iiint_{\mathcal{F}}\nabla(\rho gz)dV=\iint_{\mathcal{B}}\rho gz\boldsymbol{n}_{+}dS+\iint_{\mathcal{S}}\rho gz\boldsymbol{n}_{+}dS+\iint_{\mathcal{E}}\rho gz\boldsymbol{n}_{+}dS \tag{4.27}$$

In Section 3.3.2, the quantity $\nabla(\rho gz)dV$ represented the force of gravity acting on an infinitesimally small fluid element; integrating this quantity over the fluid volume then represents the cumulative effect of gravity on on the fluid volume. Explicitly defining limits of integration, the volume integral in (4.27) becomes

$$\iiint_{\mathcal{F}}\nabla(\rho gz)dV=\int_{x_1}^{x_2}\int_{y_1}^{y_2}\int_{\eta}^{z_{\mathrm{f}}}\nabla(\rho gz)dzdydx$$

where the limits of integration x_1, x_2, y_1 and y_2 coincide with the infinite boundary $\mathcal{E}$, η coincides with the free surface $\mathcal{S}$, and z_{f} coincides with the sea floor $\mathcal{S}_{\mathrm{f}}$. These surfaces are illustrated in Figure 4.2. Noting that $z=0$ along $\mathcal{S}_0$, one may rewrite (4.27) as

$$\begin{aligned}\boldsymbol{0}=&\left(\int_{x_1}^{x_2}\int_{y_1}^{y_2}\int_{0}^{z_{\mathrm{f}}}\nabla(\rho gz)\;dz\;dy\;dx-\iint_{\mathcal{B}}\rho gz\boldsymbol{n}_{+}dS-\iint_{\mathcal{E}}\rho gz\boldsymbol{n}_{+}dS-\iint_{\mathcal{S}_0}\rho gz\boldsymbol{n}_{+}dS\right)\\&+\left(\int_{x_1}^{x_2}\int_{y_1}^{y_2}\int_{\eta}^{0}\nabla(\rho gz)\;dz\;dy\;dx-\iint_{\mathcal{S}}\rho gz\boldsymbol{n}_{+}dS\right)\end{aligned}$$

The first expression in parenthesis vanishes by application of the gradient theorem, leaving simply

$$\iint_{\mathcal{S}}\rho gz\boldsymbol{n}_{+}dS=-\int_{x_1}^{x_2}\int_{y_1}^{y_2}\rho g\eta(x,y,t)\boldsymbol{i}_{3}\;dy\;dx=-\iint_{\mathcal{S}}\rho g\eta(x,y,t)\boldsymbol{i}_{3}dS \tag{4.28}$$

Thus, the integral over $\mathcal{S}$ corresponds to an additional buoyancy-like force acting on the rigid body due to deformations of the free surface. Define the total gravitational force

$$\boldsymbol{F}_{\mathrm{g}} = -\rho g \left(\forbar + \iint_{\mathcal{S}} \eta(x,y,t) dS \right) \boldsymbol{i}_3 \tag{4.29}$$

Because $\boldsymbol{F}_{\mathrm{g}}$ is an irrotational vector field, one may identify a corresponding potential energy function

$$V_{\mathrm{g}}(z,t) = \rho g \left(\forbar + \iint_{\mathcal{S}} \eta(x,y,t) dS \right) z \tag{4.30}$$

which satisfies

$$\boldsymbol{F}_{\mathrm{g}} = -\frac{\partial V_{\mathrm{g}}}{\partial \boldsymbol{x}} \tag{4.31}$$

Also, define a kinetic energy-like function

$$T_{\mathrm{f}}(\dot{\boldsymbol{x}}, t) = \boldsymbol{P}_{\mathrm{f}} \cdot \dot{\boldsymbol{x}}$$

where $\dot{\boldsymbol{x}}$ represents the instantaneous fluid velocity at a point $\boldsymbol{x}$, *i.e* $\dot{\boldsymbol{x}} = \boldsymbol{V}_{\mathrm{f}}(\boldsymbol{x}, t)$. Then one may define a Lagrangian function

$$\mathcal{L}_{\mathrm{f}} = T_{\mathrm{f}}(\dot{\boldsymbol{x}}, t) - V_{\mathrm{g}}(z,t) \tag{4.32}$$

and the force equations (4.23) is simply

$$\boldsymbol{f}_{\mathrm{p}} = -\frac{d}{dt}\frac{\partial \mathcal{L}_{\mathrm{f}}}{\partial \dot{\boldsymbol{x}}} + \frac{\partial \mathcal{L}_{\mathrm{f}}}{\partial \boldsymbol{x}} \tag{4.33}$$

In this form, the hydrodynamic forces resemble a Lagrangian mechanical system. However, the partial derivatives in (4.33) aren't taken with respect to the generalized coordinates $\boldsymbol{q}$, so (4.33) doesn't represent a true set of Lagrangian equations. In the coming sections, the hydrodynamic forces are generated by rigorous application of the Euler-Lagrange equations.

4.2 Lagrangian Mechanics

Briefly revisiting the key results from Section 2.3.2, let T represent the system kinetic energy and V the system potential energy. The system Lagrangian is then $\mathcal{L} = T - V$. For a set

of independent generalized coordinates $\boldsymbol{q}$, the equations of motion for a dynamic system are given by the Euler-Lagrange equations

$$\frac{d}{dt}\frac{\partial \mathcal{L}}{\partial \dot{\boldsymbol{q}}} - \frac{\partial \mathcal{L}}{\partial \boldsymbol{q}} = \boldsymbol{0}$$

In Lagrangian mechanics, the task of modeling the fluid-body system essentially reduces to correctly identifying the scalar energy functions T and V.

In Section 4.1, the fluid momentum was closely related to the rigid body momentum. From Remark 4.1.6, it was specifically observed that the rigid body translational momentum combined with the fluid momentum was a conserved quantity. This should not come as any surprise since both the rigid body and the fluid equations obey the conservation of momentum. Because we are only considering the fluid acting on the vehicle and *vice versa*, it makes sense that the combined fluid-body system should conserve momentum. Similar results may be realized under the Lagrangian approach, where the equations of motion instead derive from the conservation of energy. Consider a system which is composed of both a rigid body and the ambient fluid. One may correspondingly decompose the system Lagrangian in terms of the rigid body contributions $\mathcal{L}_{\mathrm{b}}$ and the fluid contributions $\mathcal{L}_{\mathcal{F}}$

$$\mathcal{L} = \mathcal{L}_{\mathrm{b}} + \mathcal{L}_{\mathcal{F}} \tag{4.34}$$

where

$$\mathcal{L}_{\mathrm{b}} = T_{\mathrm{b}} - V_{\mathrm{b}}$$
$$\mathcal{L}_{\mathcal{F}} = T_{\mathcal{F}} - V_{\mathcal{F}}$$

With the aim of characterizing how the fluid impacts the rigid body motion, apply the Euler-Lagrange equations to (4.34) and separate the contributions from the fluid Lagrangian:

$$\frac{d}{dt}\frac{\partial \mathcal{L}_{\mathrm{b}}}{\partial \dot{\boldsymbol{q}}} - \frac{\partial \mathcal{L}_{\mathrm{b}}}{\partial \boldsymbol{q}} = -\frac{d}{dt}\frac{\partial \mathcal{L}_{\mathcal{F}}}{\partial \dot{\boldsymbol{q}}} + \frac{\partial \mathcal{L}_{\mathcal{F}}}{\partial \boldsymbol{q}} \tag{4.35}$$

In this form, one readily finds that the generalized hydrodynamic force acting on the rigid body is

$$\boldsymbol{F}_{\mathrm{h}} = -\frac{d}{dt}\frac{\partial \mathcal{L}_{\mathcal{F}}}{\partial \dot{\boldsymbol{q}}} + \frac{\partial \mathcal{L}_{\mathcal{F}}}{\partial \boldsymbol{q}} \tag{4.36}$$

In the following sections, expressions for the fluid kinetic energy $T_{\mathcal{F}}$ and potential energy $V_{\mathcal{F}}$ are given.

Fluid Kinetic Energy without a Free Surface

Consider the fluid contained within an inertially-fixed, closed surface $\mathcal{E}$ and exterior to the hull of the rigid body $\mathcal{B}$; see Figure 4.1. For an Eulerian fluid velocity field $\boldsymbol{V}_{\mathrm{f}}(\boldsymbol{x},t)$, the fluid kinetic energy contained within this fluid volume $\mathcal{F}$ is

$$T_{\mathcal{F}} = \iiint_{\mathcal{F}} \frac{1}{2}\rho \boldsymbol{V}_{\mathrm{f}} \cdot \boldsymbol{V}_{\mathrm{f}} dV \tag{4.37}$$

Essentially, $T_{\mathcal{F}}$ represents the combined kinetic energy of each infinitesimal mass ρdV of fluid contained within $\mathcal{F}$. Note the following vector calculus identity (A.10)

$$\nabla \cdot (\phi \nabla \phi) = \nabla \phi \cdot \nabla \phi + \phi \nabla^2 \phi$$

For an incompressible fluid, the term involving the Laplacian vanishes, and the kinetic energy may be rewritten as

$$T_{\mathcal{F}} = \iiint_{\mathcal{F}} \frac{1}{2}\rho \nabla \cdot (\phi \nabla \phi)\, dV$$

The kinetic energy may be further simplified using Gauss's divergence theorem (A.2)

$$T_{\mathcal{F}} = \frac{1}{2}\rho \iint_{\mathcal{B}} (\phi \nabla \phi) \cdot \boldsymbol{n}_+ dS + \frac{1}{2}\rho \iint_{\mathcal{E}} (\phi \nabla \phi) \cdot \boldsymbol{n}_+ dS \tag{4.38}$$

In this form, the fluid kinetic energy is the flux of the abstract quantity $\phi \nabla \phi$ through the fluid bounding surfaces. If $\mathcal{E}$ extends infinitely far from the body in all directions, the surface integral over $\mathcal{E}$ in (4.38) vanishes.

Fluid Kinetic Energy with a Free Surface

If the "top" of $\mathcal{E}$ coincides with the free surface $\mathcal{S}$ (as in Figure 4.2) and extends infinitely far from the vehicle in the remaining directions, (4.38) becomes

$$T_{\mathcal{F}} = \frac{1}{2}\rho \iint_{\mathcal{B}} (\phi \nabla \phi) \cdot \boldsymbol{n}_+ dS + \frac{1}{2}\rho \iint_{\mathcal{S}} (\phi \nabla \phi) \cdot \boldsymbol{n}_+ dS \tag{4.39}$$

There exists added complexity in (4.39) since $\boldsymbol{n}_+$ is a function of the free surface slopes $\partial\eta/\partial x$ and $\partial\eta/\partial y$.

Fluid Potential Energy without a Free Surface

One may consider a number of different potential energies associated with irrotational body forces or thermal energies. Since the only body force considered in Section 3.3.2 was due to gravity, the only potential due to exogenous forces considered in this dissertation is the gravitational potential energy. Moreover, the discussion in Section 3.3.3 suggests that under potential flow assumptions, one may neglect any thermal energy contributions related to internal energies. From Section 3.3.2, the fluid potential energy for an infinitesimal fluid element is $-\rho g z dV$. This may be integrated to yield the total fluid potential energy contained within $\mathcal{F}$

$$V_{\mathcal{F}} = -\iiint_{\mathcal{F}} \rho g z dV \tag{4.40}$$

The integrand in (4.40) is simple enough to integrate directly, though there is an issue with the limits of integration since $\mathcal{F}$ contains a void corresponding to the fluid displaced by the vehicle. This issue may be circumvented using the following identity

$$\iiint_{\mathcal{F}} \rho g z \; dV = \iiint_{\mathcal{F}_1} \rho g z \; dV - \iiint_{\forall} \rho g z \; dV \tag{4.41}$$

From Figure 4.3a, the volume $\mathcal{F}_1$ represents the fluid contained within $\mathcal{E}$, absent the vehicle, and $\forall$ represents the fluid volume displaced by the vehicle. Since $\mathcal{E}$ is fixed, the first integral on the right-hand side of (4.41) is simply

$$\iiint_{\mathcal{F}_1} \rho g z \; dV = c \tag{4.42}$$

where c is a constant. One may verify that the second integral yields

$$\iiint_{\forall} \rho g z \; dV = \rho g \forall z_{\mathrm{b}} \tag{4.43}$$

where quantity $\rho g \forall$ represents the weight of the displaced fluid. Thus, the fluid potential energy contained within $\mathcal{E}$ is

$$V_{\mathcal{F}} = \rho g \forall z_{\mathrm{b}} - c \tag{4.44}$$

Note that a potential energy function, much like the fluid velocity potential, is unique only to an additive constant [57, Sec. 3.4]. Since $\nabla V_{\mathcal{F}}$ appears in the equations of motion rather than just $V_{\mathcal{F}}$, the constant c will not impact the dynamics. In future expressions, take $c = 0$.

Remark 4.2.1 (Buoyancy force) *The hydrostatic buoyancy force acting on a body is given by*

$$\boldsymbol{f}_{\text{buoyancy}} = -\frac{\partial V_{\mathcal{F}}}{\partial \boldsymbol{q}} = -\boldsymbol{i}_3 \rho g \forbar{V} \tag{4.45}$$

The magnitude of this force is equal to the weight of the displaced fluid and the direction opposes that of gravity. Conceptually, the buoyancy force is a consequence of Newton's third law: the gravitational force acting on the fluid displaced by the vehicle produces an equal and opposite force on the body.

Remark 4.2.2 (Neutrally buoyant vehicles) *For a vehicle with coincident centers of mass and buoyancy immersed in a fluid without a free surface, the system potential energy is*

$$V_{\text{b}} + V_{\mathcal{F}} = g\left(\rho \forbar{V} - m_{\text{b}}\right) z_{\text{b}} \tag{4.46}$$

This expression vanishes when the vehicle is neutrally buoyant, i.e. $m_{\text{b}} = \rho \forbar{V}$. *In this case, the effect of gravity on both the vehicle and the fluid exactly cancel each other, and it is appropriate to neglect both effects.*

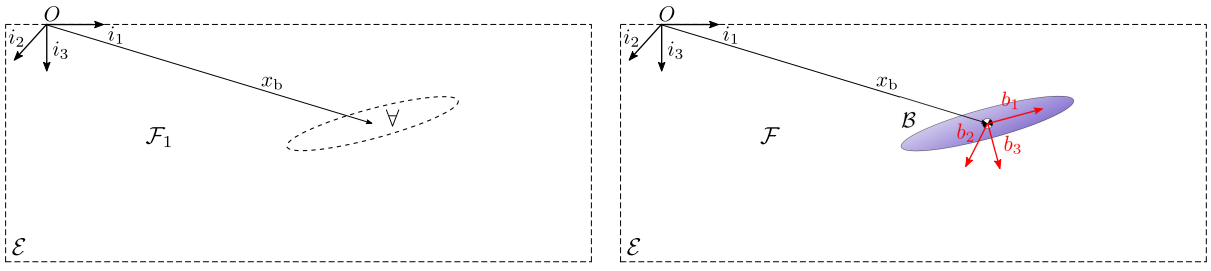

(a) Depiction of the fluid volume $\mathcal{F}_1$.

(b) Depiction of the fluid volume $\mathcal{F}$.

Figure 4.3: Comparing the fluid volumes $\mathcal{F}_1$ and $\mathcal{F}$ without a free surface.

Fluid Potential Energy with a Free Surface

When the fluid volume is bounded above by a free surface, one of the boundaries of $\mathcal{F}$ is now free to move. In this case, the volume integral over $\mathcal{F}_1$ must be adjusted accordingly. If $\mathcal{F}_1$ is bounded by the free surface elevation $\eta(x,y,t)$, as well as 5 other arbitrary limits of integration (in Cartesian coordinates, for instance, x_1, x_2, y_1, y_2, z_f), the integral is[4]

$$\iiint_{\mathcal{F}_1} \rho g z \; dV = \int_{x_1}^{x_2} \int_{y_1}^{y_2} \int_{\eta(x,y,t)}^{z_\mathrm{f}} \rho g z \; dz \; dy \; dx \tag{4.47}$$

Note that with the defined reference frame (see, for instance Figure 4.3), it makes sense to define η as the lower limit of integration since z is positive "down". One may again integrate the fluid potential energy with respect to z, though the unknown location of η precludes the complete integral of the potential energy as before:

$$\iiint_{\mathcal{F}_1} \rho g z \; dV = \iint_{\mathcal{S}_0} \frac{1}{2} \rho g \left(z_\mathrm{f}^2 - \eta^2 \right) dS = c - \iint_{\mathcal{S}_0} \frac{1}{2} \rho g \eta^2(x,y,t) dS \tag{4.48}$$

When a free surface is present, the fluid potential energy is thus

$$V_{\mathcal{F}} = \rho g \forbar z_\mathrm{b} + \iint_{\mathcal{S}_0} \frac{1}{2} \rho g \eta^2(x,y,t) dS \tag{4.49}$$

Remark 4.2.3 (Free surface potential energy) *From the definition of the kinematic free surface boundary condition (3.51), the free surface is a streamline of the flow. Therefore, under potential flow theory, $\mathcal{S}$ is an invariant set; fluid particles which begin on the free surface remain on the free surface. Thus, fluid particles may not join or leave the free surface. This implies that a free surface elevation "stretches" the fluid continuum along the surface, and one may physically interpret the integral in (4.49) as an elastic potential energy with a "hydrostatic spring stiffness" of $\rho g dS$.*

[4]Cartesian coordinates are employed here for ease of presentation, though any number of parameterizations could be used without affecting the evaluation of the integral.

General Lagrangian Expressions

In integral form, the fluid Lagrangian is

$$\mathcal{L}_{\mathcal{F}} = \iiint_{\mathcal{F}} \left[\frac{1}{2}\rho \nabla\phi \cdot \nabla\phi + \rho g z \right] dV \tag{4.50}$$

Combining the kinetic and potential energy expressions (4.38) and (4.44), the Lagrangian expression for the fluid contained within $\mathcal{E}$ is

$$\mathcal{L}_{\mathcal{F}} = \frac{1}{2}\rho \iint_{\mathcal{B}} (\phi \nabla\phi) \cdot \boldsymbol{n}_+ dS + \frac{1}{2}\rho \iint_{\mathcal{E}} (\phi \nabla\phi) \cdot \boldsymbol{n}_+ dS - \rho g \forbar z_{\mathrm{b}} \tag{4.51}$$

For a semi-infinite fluid volume which is bounded above by a free surface, combining (4.39) and (4.49) yields

$$\mathcal{L}_{\mathcal{F}} = \frac{1}{2}\rho \iint_{\mathcal{B}} (\phi \nabla\phi) \cdot \boldsymbol{n}_+ dS + \frac{1}{2}\rho \iint_{\mathcal{S}} (\phi \nabla\phi) \cdot \boldsymbol{n}_+ dS - \frac{1}{2}\rho \iint_{\mathcal{S}_0} g\eta^2(x,y,t) dS - \rho g \forbar z_{\mathrm{b}} \tag{4.52}$$

4.2.1 Force and Moment Expressions in an Unbounded Fluid

Prior to deriving the generalized forces, the following theorem is presented regarding the fluid kinetic energy in an unbounded fluid.

Theorem 4.2.4 *For an unbounded volume of fluid whose motion is due solely to the motion of a rigid body, the fluid kinetic energy is invariant under shifts in position and orientation of the body:*

$$\frac{\partial T_{\mathcal{F}}}{\partial \boldsymbol{q}} = \boldsymbol{0} \tag{4.53}$$

□

Proof. Begin with the following identity, which follows from (A.10)

$$\nabla \cdot \left(\phi \nabla \frac{\partial \phi}{\partial q_i} \right) = \nabla \cdot \left(\frac{\partial \phi}{\partial q_i} \nabla \phi \right) \tag{4.54}$$

and the fact that

$$\nabla^2\left(\frac{\partial\phi}{\partial q_i}\right) = \frac{\partial}{\partial q_i}\left(\nabla^2\phi\right) = 0$$

The following integral relationship then holds

$$\frac{1}{2}\rho\iiint_{\mathcal{F}}\nabla\cdot\left(\phi\nabla\frac{\partial\phi}{\partial q_i}\right)dV = \frac{1}{2}\rho\iiint_{\mathcal{F}}\nabla\cdot\left(\frac{\partial\phi}{\partial q_i}\nabla\phi\right)dV \tag{4.55}$$

Applying the divergence theorem to both sides,

$$\begin{aligned}\frac{1}{2}\rho\iint_{\mathcal{B}}\phi\nabla\frac{\partial\phi}{\partial q_i}\cdot\boldsymbol{n}_+dS + \frac{1}{2}\rho\iint_{\mathcal{E}}\phi\nabla\frac{\partial\phi}{\partial q_i}\cdot\boldsymbol{n}_+dS = \\ \frac{1}{2}\rho\iint_{\mathcal{B}}\frac{\partial\phi}{\partial q_i}\nabla\phi\cdot\boldsymbol{n}_+dS + \frac{1}{2}\rho\iint_{\mathcal{E}}\frac{\partial\phi}{\partial q_i}\nabla\phi\cdot\boldsymbol{n}_+dS\end{aligned}$$

In the limit that $\mathcal{E}$ extends infinitely far from the body in all directions, the integrals over $\mathcal{E}$ vanish, and thus

$$\frac{1}{2}\rho\iint_{\mathcal{B}}\phi\nabla\frac{\partial\phi}{\partial q_i}\cdot\boldsymbol{n}_+dS = \frac{1}{2}\rho\iint_{\mathcal{B}}\frac{\partial\phi}{\partial q_i}\nabla\phi\cdot\boldsymbol{n}_+dS \tag{4.56}$$

Using the body boundary condition (3.59)

$$\left(\nabla\phi\cdot\boldsymbol{n}_+\right)\big|_{\mathcal{B}} = \boldsymbol{b}\cdot\boldsymbol{\nu} \quad \text{where} \quad \boldsymbol{b} = \begin{pmatrix}\boldsymbol{n}_+ \\ \boldsymbol{r}_{\mathrm{h}}\times\boldsymbol{n}_+\end{pmatrix}$$

and noting that neither $\boldsymbol{n}_+$, $\boldsymbol{b}$, nor $\boldsymbol{\nu}$ depends on $\boldsymbol{q}$, the following relationship must hold

$$\frac{\partial}{\partial q_i}\left(\nabla\phi\cdot\boldsymbol{n}_+\right)\big|_{\mathcal{B}} = \left(\nabla\frac{\partial\phi}{\partial q_i}\cdot\boldsymbol{n}_+\right) = 0$$

Substituting these relationships into (4.56) yields

$$\frac{1}{2}\rho\iint_{\mathcal{B}}\frac{\partial\phi}{\partial q_i}\boldsymbol{b}\cdot\boldsymbol{\nu}dS = 0 \tag{4.57}$$

Because the limits of integration do not depend on q_i, the above expression may be rewritten as

$$\frac{\partial}{\partial q_i}\left(\frac{1}{2}\rho\iint_{\mathcal{B}}\phi\boldsymbol{b}\cdot\boldsymbol{\nu}dS\right) = 0 \tag{4.58}$$

Finally, in the limit that $\mathcal{E}$ extends infinitely far from the vehicle, the quantity in parenthesis is the fluid kinetic energy, and thus

$$\frac{\partial T_{\mathcal{F}}}{\partial q_i} = 0 \tag{4.59}$$

■

Corollary 4.2.5 *Since $\boldsymbol{\nu}$ may be taken as arbitrary and independent of q_i, (4.57) enables us to further conclude that ϕ must be independent of the rigid body generalized coordinates for an infinite volume of fluid whose motion is due solely to the vehicle.*

Assuming a neutrally buoyant vehicle with coincident centers of mass and buoyancy, the fluid Lagrangian is composed solely of the fluid kinetic energy:

$$\mathcal{L}_{\mathcal{F}} = \frac{1}{2}\rho \iiint_{\mathcal{F}} \nabla\phi \cdot \nabla\phi dV \tag{4.60}$$

In this case, one may use Theorem 4.2.4 to show that

$$\frac{\partial \mathcal{L}_{\mathcal{F}}}{\partial \boldsymbol{q}} = 0 \tag{4.61}$$

Next, compute

$$\frac{\partial \mathcal{L}_{\mathcal{F}}}{\partial \boldsymbol{\nu}} = \rho \iiint_{\mathcal{F}} \nabla\phi \cdot \nabla \frac{\partial \phi}{\partial \boldsymbol{\nu}} dV = \rho \iint_{\mathcal{B}} \phi \nabla \frac{\partial \phi}{\partial \boldsymbol{\nu}} \cdot \boldsymbol{n}_+ dS \tag{4.62}$$

Again using the body boundary condition, the following relationship must hold

$$\left(\nabla \frac{\partial \phi}{\partial \boldsymbol{\nu}} \cdot \boldsymbol{n}_+ \right) \Big|_{\mathcal{B}} = \boldsymbol{b} \tag{4.63}$$

The hydrodynamic force and moment acting on a vehicle in an unbounded fluid is

$$\boldsymbol{f}_{\mathrm{p}} = -\rho \frac{d}{dt} \iint_{\mathcal{B}} \phi \boldsymbol{n}_+ \, dS \tag{4.64}$$

$$\boldsymbol{\tau}_{\mathrm{p}} = -\rho \frac{d}{dt} \iint_{\mathcal{B}} \phi \left(\boldsymbol{r}_{\mathrm{h}} \times \boldsymbol{n}_+ \right) dS \tag{4.65}$$

Remark 4.2.6 (Conserved Quantities) *For a neutrally buoyant vehicle with coincident centers of mass and buoyancy,*

$$\frac{\partial}{\partial \boldsymbol{q}} \left(\mathcal{L}_{\mathrm{b}} + \mathcal{L}_{\mathcal{F}} \right) = 0 \tag{4.66}$$

This implies that

$$\frac{d}{dt} \left(\frac{\partial (\mathcal{L}_{\mathrm{b}} + \mathcal{L}_{\mathcal{F}})}{\partial \dot{\boldsymbol{q}}} \right) = 0 \quad \Longrightarrow \quad \frac{\partial (\mathcal{L}_{\mathrm{b}} + \mathcal{L}_{\mathcal{F}})}{\partial \dot{\boldsymbol{q}}} = \boldsymbol{c} \tag{4.67}$$

The equations of motion for a body in an unbounded fluid may be further simplified, for instance, using Routhian reduction. Additionally, one may use Noether's theorem[5] *[43] to show that this system invariance corresponds to the conservation of linear and angular momentum for the fluid-body system.*

4.2.2 Force and Moment Expressions in a Fluid with a Rigid Boundary

Starting again with the same Lagrangian function

$$\mathcal{L}_{\mathcal{F}} = \frac{1}{2}\rho \iiint_{\mathcal{F}} \nabla\phi \cdot \nabla\phi dV \tag{4.68}$$

compute

$$\frac{\partial \mathcal{L}_{\mathcal{F}}}{\partial \boldsymbol{\nu}} = \rho \iiint_{\mathcal{F}} \nabla\phi \cdot \nabla \frac{\partial \phi}{\partial \boldsymbol{\nu}} dV = \rho \iint_{\mathcal{B}} \rho\phi \; \boldsymbol{b} \; dS + \rho \iint_{\mathcal{E}} \rho\phi \nabla \frac{\partial \phi}{\partial \boldsymbol{\nu}} \cdot \boldsymbol{n}_+ dS$$

Since the boundary $\mathcal{E}$ is fixed,

$$\nabla \frac{\partial \phi}{\partial \boldsymbol{\nu}} \cdot \boldsymbol{n}_+ \Big|_{\boldsymbol{x}=\mathcal{E}} = \frac{\partial}{\partial \boldsymbol{\nu}} \nabla\phi \cdot \boldsymbol{n}_+ \Big|_{\boldsymbol{x}=\mathcal{E}} = \boldsymbol{0}$$

The first contribution to the generalized hydrodynamic force is thus

$$-\frac{d}{dt}\left(\frac{\partial \mathcal{L}_{\mathcal{F}}}{\partial \boldsymbol{\nu}}\right) = -\rho \frac{d}{dt} \iint_{\mathcal{B}} \phi \begin{pmatrix} \boldsymbol{n}_+ \\ \boldsymbol{r}_{\mathrm{h}} \times \boldsymbol{n}_+ \end{pmatrix} dS \tag{4.69}$$

For a vehicle maneuvering near a rigid wall, the fluid Lagrangian depends on the vehicle's generalized coordinates – the vehicle's distance and orientation relative to the boundary now affects the fluid kinetic energy. In this case, the boundaries of $\mathcal{F}$ also depend on the generalized coordinates. Evaluating the derivative of $\mathcal{L}_{\mathcal{F}}$ with respect to $\boldsymbol{q}$ therefore requires one to employ the Leibniz rule[6]. Explicitly, one finds

$$\frac{\partial \mathcal{L}_{\mathcal{F}}}{\partial \boldsymbol{q}} = \rho \iiint_{\mathcal{F}} \nabla\phi \cdot \nabla \frac{\partial \phi}{\partial \boldsymbol{q}} dV + \frac{1}{2}\rho \iint_{\mathcal{E}} \nabla\phi \cdot \nabla\phi \begin{pmatrix} \boldsymbol{n}_+ \\ \boldsymbol{r} \times \boldsymbol{n}_+ \end{pmatrix} dS \tag{4.70}$$

[5]Emmy Noether, 1882-1935

[6]Gottfried Wilhelm Leibniz, 1646-1716.

The generalized hydrodynamic forces acting on a neutrally buoyant rigid body near a fixed boundary are

$$\boldsymbol{f}_{\mathrm{p}} = -\rho \frac{d}{dt} \iint_{\mathcal{B}} \phi \boldsymbol{n}_{+} \, dS + \frac{1}{2}\rho \iint_{\mathcal{E}} (\nabla\phi \cdot \nabla\phi)\, \boldsymbol{n}_{+} dS \tag{4.71}$$

$$\boldsymbol{\tau}_{\mathrm{p}} = -\rho \frac{d}{dt} \iint_{\mathcal{B}} \phi \left(\boldsymbol{r}_{\mathrm{h}} \times \boldsymbol{n}_{+}\right) dS + \frac{1}{2}\rho \iint_{\mathcal{E}} (\nabla\phi \cdot \nabla\phi) \boldsymbol{r} \times \boldsymbol{n}_{+} dS \tag{4.72}$$

These expressions are identical to those derived from Newtonian mechanics (4.21)-(4.22).

4.2.3 Force and Moment Expressions in a Fluid with a Free Surface

For a vehicle near a free surface, consider the fluid kinetic and potential energies

$$T_{\mathcal{F}} = \iiint_{\mathcal{F}} \frac{1}{2}\rho \nabla\phi \cdot \nabla\phi \, dV$$

$$V_{\mathcal{F}} = -\iiint_{\mathcal{F}} \rho g z \, dV$$

First, compute

$$\frac{\partial V_{\mathcal{F}}}{\partial \boldsymbol{\nu}} = \mathbf{0}$$

Then, using the Leibniz rule, one finds that

$$-\frac{\partial V_{\mathcal{F}}}{\partial \boldsymbol{q}} = \iint_{\mathcal{B}} \rho g z \begin{pmatrix} \boldsymbol{n}_{+} \\ \boldsymbol{r}_{\mathrm{h}} \times \boldsymbol{n}_{+} \end{pmatrix} dS + \iint_{\mathcal{S}} \rho g z \begin{pmatrix} \boldsymbol{n}_{+} \\ \boldsymbol{r} \times \boldsymbol{n}_{+} \end{pmatrix} dS \tag{4.73}$$

Next, compute

$$\frac{\partial T_{\mathcal{F}}}{\partial \boldsymbol{\nu}} = \rho \iiint_{\mathcal{F}} \nabla\phi \cdot \nabla \frac{\partial \phi}{\partial \boldsymbol{\nu}} dV = \rho \iint_{\mathcal{B}} \rho\phi \, \boldsymbol{b} \, dS + \rho \iint_{\mathcal{S}} \rho\phi \frac{\partial}{\partial \boldsymbol{\nu}} \nabla\phi \cdot \boldsymbol{n}_{+} dS$$

Taking the time rate of change yields

$$-\frac{\partial T_{\mathcal{F}}}{\partial \boldsymbol{\nu}} = -\rho \frac{d}{dt} \iint_{\mathcal{B}} \rho\phi \begin{pmatrix} \boldsymbol{n}_{+} \\ \boldsymbol{r} \times \boldsymbol{n}_{+} \end{pmatrix} dS - \rho \frac{d}{dt} \iint_{\mathcal{S}} \rho\phi \frac{\partial}{\partial \boldsymbol{\nu}} \nabla\phi \cdot \boldsymbol{n}_{+} dS \tag{4.74}$$

Finally, compute

$$\begin{aligned}\frac{\partial T_{\mathcal{F}}}{\partial \boldsymbol{q}} &= \rho \iint_{\mathcal{B}} \phi \frac{\partial}{\partial \boldsymbol{q}} \nabla\phi \cdot \boldsymbol{n}_+ dS + \rho \iint_{\mathcal{S}} \phi \frac{\partial}{\partial \boldsymbol{q}} \nabla\phi \cdot \boldsymbol{n}_+ dS \\ &= \rho \iint_{\mathcal{S}} \phi \frac{\partial}{\partial \boldsymbol{q}} \nabla\phi \cdot \boldsymbol{n}_+ dS \end{aligned} \tag{4.75}$$

Combining (4.73), (4.74), and (4.75), one finds

$$\begin{aligned}\boldsymbol{f}_{\mathrm{p}} = &-\rho \frac{d}{dt} \iint_{\mathcal{B}} \phi \boldsymbol{n}_+ \, dS - \left(\rho \frac{d}{dt} \iint_{\mathcal{S}} \rho\phi \frac{\partial}{\partial \boldsymbol{v}} \nabla\phi \cdot \boldsymbol{n}_+ dS - \rho \iint_{\mathcal{S}} \phi \frac{\partial}{\partial \boldsymbol{x}_{\mathrm{b}}} \nabla\phi \cdot \boldsymbol{n}_+ dS \right) \\ &+ \rho g \iint_{\mathcal{B}} z \boldsymbol{n}_+ dS + \rho g \iint_{\mathcal{S}} z \boldsymbol{n}_+ dS \end{aligned} \tag{4.76}$$

$$\begin{aligned}\boldsymbol{\tau}_{\mathrm{p}} = &-\rho \frac{d}{dt} \iint_{\mathcal{B}} \phi \boldsymbol{r}_{\mathrm{h}} \times \boldsymbol{n}_+ dS - \left(\rho \frac{d}{dt} \iint_{\mathcal{S}} \rho\phi \frac{\partial}{\partial \boldsymbol{\omega}} \nabla\phi \cdot \boldsymbol{n}_+ dS - \rho \iint_{\mathcal{S}} \phi \frac{\partial}{\partial \boldsymbol{\theta}_{\mathrm{b}}} \nabla\phi \cdot \boldsymbol{n}_+ dS \right) \\ &+ \rho g \iint_{\mathcal{B}} z \boldsymbol{r}_{\mathrm{h}} \times \boldsymbol{n}_+ dS + \rho g \iint_{\mathcal{S}} z \boldsymbol{r} \times \boldsymbol{n}_+ dS \end{aligned} \tag{4.77}$$

For (4.76) and (4.77) to match the expressions (4.23) and (4.23), it must be true that

$$\begin{aligned} -\rho \frac{d}{dt} \iint_{\mathcal{S}} \phi \boldsymbol{n}_+ dS &= -\left(\rho \frac{d}{dt} \iint_{\mathcal{S}} \rho\phi \frac{\partial}{\partial \boldsymbol{v}} \nabla\phi \cdot \boldsymbol{n}_+ dS - \rho \iint_{\mathcal{S}} \phi \frac{\partial}{\partial \boldsymbol{x}_{\mathrm{b}}} \nabla\phi \cdot \boldsymbol{n}_+ dS \right) \\ -\rho \frac{d}{dt} \iint_{\mathcal{S}} \phi \boldsymbol{r} \times \boldsymbol{n}_+ dS &= -\left(\rho \frac{d}{dt} \iint_{\mathcal{S}} \rho\phi \frac{\partial}{\partial \boldsymbol{\omega}} \nabla\phi \cdot \boldsymbol{n}_+ dS - \rho \iint_{\mathcal{S}} \phi \frac{\partial}{\partial \boldsymbol{\theta}_{\mathrm{b}}} \nabla\phi \cdot \boldsymbol{n}_+ dS \right) \end{aligned}$$

However, it is unclear how to prove these identities without explicitly choosing a functional form for ϕ.

4.3 Examples

The expressions given in the previous sections apply to general scenarios. The geometry of the problem, including the hull shape and any external boundaries, is incorporated through the potential function. For simple cases, techniques exist for finding analytical functions for ϕ. For instance, the Milne-Thomson circle theorem[7] may be used to generate a closed-form solution for a circle immersed in a prescribed background flow [53] and the Joukowski

[7]Louis Melville Milne-Thomson, 1891-1974.

mapping[8] enables one to simulate inviscid flow over an airfoil [41]. However, with increasing complexity analytical solutions can seldom be found. In the following examples, several cases are studied which admit simple potential flow solutions to further explore the Lagrangian modeling approach.

Until now, no mention has been given to how the fluid kinetic energy is affected by expressing the energy in different reference frames. In this dissertation, the rigid body equations of motion are expressed in a body-fixed frame. The ambient fluid expressed in a body-fixed frame will appear to undergo motion opposite the body motion. For example, to a ship traveling at a constant velocity along a straight trajectory, the fluid far ahead of the ship will appear to be moving towards the ship at precisely the ship's speed. This apparent fluid motion, if not properly recognized, will drastically impact any calculations of the fluid kinetic energy. Since the rigid body kinetic energy is defined with respect to a stationary reference frame, the fluid kinetic energy must be similarly defined. The importance of this concept will become apparent in the following example.

4.3.1 Equations of Motion for a Circle in an Unbounded Fluid

The potential governing a circle is given by a free stream with an opposing doublet [41], an equivalent scenario to a cylinder moving through an otherwise stationary fluid[9]. As depicted in Figure 4.4, the circle has radius a and the center of the circle is located at $\boldsymbol{x}_{\rm b} = [x_{\rm b},\ z_{\rm b}]^T$. Relative to a reference frame fixed to the center of the circle, the velocity potential is

$$\phi = (-\dot{x}_{\rm b}x - \dot{z}_{\rm b}z) + a^2\frac{\dot{x}_{\rm b}x + \dot{z}_{\rm b}z}{x^2+z^2} \tag{4.78}$$

The first term in parenthesis in (4.78) accounts for the free stream velocity, while the second represents the doublet. Per the earlier remarks, the free stream term represents only the

[8] Nikolay Yegorovich Zhukovsky, 1847-1921

[9] Some subtle differences exist, as outlined in [8, Table 4.2], though they do not affect the present formulation.

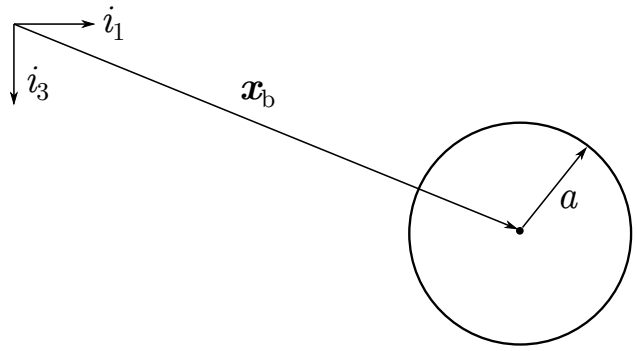

Figure 4.4: An illustration of the reference frames used to define the circle example.

apparent fluid velocity seen in the body-fixed frame, and should be disregarded when computing the fluid kinetic energy; if one did not neglect the free stream term, it would result in an infinite fluid kinetic energy. The term due to the doublet then represents the influence of the circle on the ambient fluid. The fluid kinetic energy is

$$T_\mathcal{F} = \iint_\mathcal{F} \frac{1}{2}\rho \nabla\phi \cdot \nabla\phi = \iint_\mathcal{F} \frac{1}{2}\rho a^4 \frac{\dot{x}_\mathrm{b}^2 + \dot{z}_\mathrm{b}^2}{(x^2+z^2)^2} dS \tag{4.79}$$

Recognizing that the kinetic energy integral will be more easily computed in polar coordinates, one may employ the following coordinate transformation:

$$x \mapsto r\cos\theta \quad z \mapsto r\sin\theta \quad dS \mapsto r dr d\theta$$

In polar coordinates, the fluid kinetic energy is

$$T_\mathcal{F} = \lim_{b\to\infty} \int_0^{2\pi} \int_a^b \frac{1}{2}\rho a^4 \frac{\dot{x}_\mathrm{b}^2 + \dot{z}_\mathrm{b}^2}{r^4} r dr d\theta = \frac{1}{2}\rho\pi a^2 (\dot{x}_\mathrm{b}^2 + \dot{z}_\mathrm{b}^2) \tag{4.80}$$

Assuming a neutrally buoyant body with coincident centers of mass and buoyancy, one may neglect the hydrostatic effects per Remark 4.2.2. The fluid Lagrangian is then simply

$$\mathcal{L}_\mathcal{F} = \frac{1}{2}\begin{pmatrix} \dot{x}_\mathrm{b} & \dot{z}_\mathrm{b} \end{pmatrix} \begin{pmatrix} \rho\pi a^2 & 0 \\ 0 & \rho\pi a^2 \end{pmatrix} \begin{pmatrix} \dot{x}_\mathrm{b} \\ \dot{z}_\mathrm{b} \end{pmatrix} \tag{4.81}$$

Applying the Euler-Lagrange equations to the fluid Lagrangian then yields the hydrodynamic force. First compute

$$\frac{\partial \mathcal{L}_\mathcal{F}}{\partial \dot{\boldsymbol{x}}_\mathbf{b}} = \begin{pmatrix} \rho\pi a^2 & 0 \\ 0 & \rho\pi a^2 \end{pmatrix} \begin{pmatrix} \dot{x}_\mathrm{b} \\ \dot{z}_\mathrm{b} \end{pmatrix}$$

which represents the fluid momentum induced by the motion of the circle. Then compute

$$\frac{d}{dt}\frac{\partial \mathcal{L}_{\mathcal{F}}}{\partial \dot{\boldsymbol{x}}_{\mathrm{b}}} = \begin{pmatrix} \rho\pi a^2 & 0 \\ 0 & \rho\pi a^2 \end{pmatrix} \begin{pmatrix} \ddot{x}_{\mathrm{b}} \\ \ddot{z}_{\mathrm{b}} \end{pmatrix}$$

Finally, by Theorem 4.2.4,

$$\frac{\partial \mathcal{L}_{\mathcal{F}}}{\partial \boldsymbol{x}_{\mathrm{b}}} = \begin{pmatrix} 0 \\ 0 \end{pmatrix}$$

The total hydrodynamic force acting on the circle due to the motion of the circle through otherwise calm water is

$$\boldsymbol{F}_{\mathrm{h}} = -\frac{d}{dt}\frac{\partial \mathcal{L}_{\mathcal{F}}}{\partial \dot{\boldsymbol{x}}_{\mathrm{b}}} + \frac{\partial \mathcal{L}_{\mathcal{F}}}{\partial \boldsymbol{x}_{\mathrm{b}}} = -\begin{pmatrix} \rho\pi a^2 & 0 \\ 0 & \rho\pi a^2 \end{pmatrix} \begin{pmatrix} \ddot{x}_{\mathrm{b}} \\ \ddot{z}_{\mathrm{b}} \end{pmatrix} \tag{4.82}$$

Consistent with existing results for the motion of a circle in an unbounded fluid [8], the Lagrangian approach predicts a hydrodynamic force which is only proportional to the body accelerations; in steady motion, the circle will experience no net force. This is in agreement with Remarks 4.1.6 and 4.2.6. The complete equations of motion are

$$\begin{pmatrix} m_{\mathrm{b}} + \rho\pi a^2 & 0 \\ 0 & m_{\mathrm{b}} + \rho\pi a^2 \end{pmatrix} \begin{pmatrix} \ddot{x}_{\mathrm{b}} \\ \ddot{z}_{\mathrm{b}} \end{pmatrix} = \begin{pmatrix} 0 \\ 0 \end{pmatrix} \tag{4.83}$$

4.3.2 Equations of Motion for a Circle near a Rigid Wall

To approximate the fluid motion due to a circle near a wall, one may use the method of images [8, 41]. Briefly, one can model a rigid boundary in a potential flow by imposing an *image potential*, a reflection of the original system potential function across the boundary. As illustrated in Figure 4.5, let z_{w} represent the location of the wall and then the distance between the circle and the wall is given by z_{bw}. Explicitly,

$$z_{\mathrm{bw}} = z_{\mathrm{w}} - z_{\mathrm{b}} \quad \text{and} \quad \dot{z}_{\mathrm{bw}} = -\dot{z}_{\mathrm{b}}$$

The image potential is

$$\phi_{\mathrm{i}} = a^2 \frac{x\dot{x}_{\mathrm{b}} + (z - 2z_{\mathrm{bw}})\dot{z}_{\mathrm{b}}}{x^2 + (z - 2z_{\mathrm{bw}})^2} \tag{4.84}$$

The complete velocity potential is then

$$\phi = a^2 \left(\frac{\dot{x}_\mathrm{b} x + \dot{z}_\mathrm{b} z}{x^2 + z^2} + \frac{x\dot{x}_\mathrm{b} + (z - 2z_\mathrm{bw})\dot{z}_\mathrm{b}}{x^2 + (z - 2z_\mathrm{bw})^2} \right) \tag{4.85}$$

Note that this approach only approximates the fluid flow over a circle near a rigid wall; the presence of the image warps the circle into an ellipse [25]. The total fluid kinetic energy is

$$T_\mathcal{F} = \iint_\mathcal{F} \frac{1}{2}\rho a^4 \left(\dot{x}_\mathrm{b}^2 + \dot{z}_\mathrm{b}^2\right) \left(\frac{1}{(x^2 + z^2)^2} + \frac{1}{(x^2 + (z - 2z_\mathrm{bw})^2)^2} \right) dS \tag{4.86}$$

Again, the kinetic energy is evaluated in polar coordinates, though in this case one must be careful to ensure that the integral is only evaluated over the semi-infinite fluid volume bounded by the rigid wall and the circle:

$$T_\mathcal{F} = \frac{1}{2}\rho\pi a^2 (\dot{x}_\mathrm{b}^2 + \dot{z}_\mathrm{b}^2) \left(1 + \frac{1}{2}\frac{a^2}{z_\mathrm{bw}^2} \right) \tag{4.87}$$

Assuming again that the circle is neutrally buoyant, the fluid Lagrangian is

$$\mathcal{L}_\mathcal{F} = \frac{1}{2} \begin{pmatrix} \dot{x}_\mathrm{b} & \dot{z}_\mathrm{b} \end{pmatrix} \begin{pmatrix} \rho\pi a^2 \left(1 + \frac{1}{2}\frac{a^2}{z_\mathrm{bw}^2}\right) & 0 \\ 0 & \rho\pi a^2 \left(1 + \frac{1}{2}\frac{a^2}{z_\mathrm{bw}^2}\right) \end{pmatrix} \begin{pmatrix} \dot{x}_\mathrm{b} \\ \dot{z}_\mathrm{b} \end{pmatrix} \tag{4.88}$$

As compared to the previous case, there exists an explicit dependence on the position z_b relative to the rigid boundary. Note that if the circle were to move infinitely far from the wall, one would recover (4.81).

One may then apply the Euler-Lagrange equations to (4.88) to compute the hydrodynamic force. First, compute

$$-\frac{d}{dt}\frac{\partial \mathcal{L}_\mathcal{F}}{\partial \dot{\boldsymbol{x}}_\mathrm{b}} = - \begin{pmatrix} \rho\pi a^2 \left(1 + \frac{1}{2}\frac{a^2}{z_\mathrm{bw}^2}\right) & 0 \\ 0 & \rho\pi a^2 \left(1 + \frac{1}{2}\frac{a^2}{z_\mathrm{bw}^2}\right) \end{pmatrix} \begin{pmatrix} \ddot{x}_\mathrm{b} \\ \ddot{z}_\mathrm{b} \end{pmatrix} - \begin{pmatrix} \rho\pi a^2 \frac{a^2}{z_\mathrm{b}^3} & 0 \\ 0 & \rho\pi a^2 \frac{a^2}{z_\mathrm{b}^3} \end{pmatrix} \begin{pmatrix} \dot{x}_\mathrm{b}\dot{z}_\mathrm{b} \\ \dot{z}_\mathrm{b}^2 \end{pmatrix}$$

Then,

$$\frac{\partial \mathcal{L}_\mathcal{F}}{\partial \boldsymbol{x}_\mathrm{b}} = \begin{pmatrix} 0 \\ \frac{1}{2}\rho\pi a^2 \frac{a^2}{z_\mathrm{bw}^3} \left(\dot{x}_\mathrm{b} + z_\mathrm{b}\right) \end{pmatrix}$$

The hydrodynamic force is

$$\boldsymbol{F}_\mathrm{h} = -\rho\pi a^2 \left(1 + \frac{1}{2}\frac{a^2}{z_\mathrm{bw}^2}\right) \begin{pmatrix} \ddot{x}_\mathrm{b} \\ \ddot{z}_\mathrm{b} \end{pmatrix} - \rho\pi a^2 \frac{a^2}{z_\mathrm{bw}^3} \begin{pmatrix} \dot{x}_\mathrm{b}\dot{z}_\mathrm{b} \\ \frac{1}{2}(\dot{z}_\mathrm{b}^2 - \dot{x}_\mathrm{b}^2) \end{pmatrix} \tag{4.89}$$

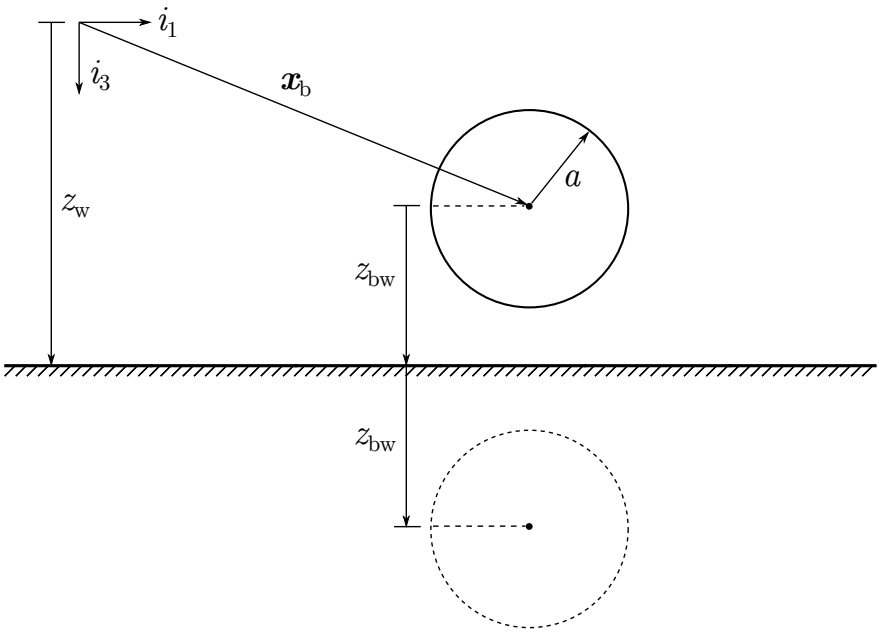

Figure 4.5: An illustration of the circle near a rigid wall.

In this case, the circle experiences forces which depend on it's acceleration, velocity, and position. The complete equations of motion are

$$\begin{pmatrix} m_\mathrm{b} + \rho\pi a^2\left(1+\frac{1}{2}\frac{a^2}{z_\mathrm{bw}^2}\right) & 0 \\ 0 & m_\mathrm{b} + \rho\pi a^2\left(1+\frac{1}{2}\frac{a^2}{z_\mathrm{bw}^2}\right) \end{pmatrix} \begin{pmatrix} \ddot{x}_\mathrm{b} \\ \ddot{z}_\mathrm{b} \end{pmatrix} = -\rho\pi a^2 \frac{a^2}{z_\mathrm{bw}^3} \begin{pmatrix} \dot{x}_\mathrm{b}\dot{z}_\mathrm{b} \\ \frac{1}{2}(\dot{z}_\mathrm{b}^2 - \dot{x}_\mathrm{b}^2) \end{pmatrix} \tag{4.90}$$

The simulation results for a circle with $a = 1\mathrm{m}$ are shown in Figure 4.6. As expected, the wall tends to "pull" the circle towards it. Also, by studying the closed circle-fluid system, the total system energy remains constant throughout the simulation. Had one just studied the circle subject to generalized forces, the kinetic energy would appear to fluctuate as the body interacts with the fluid.

4.3.3 Deeply Submerged Vehicles: Kirchhoff's Equations

While the first two examples focused on problems with specific geometries, the final two examples are more general, considering structures of the velocity potential that may apply

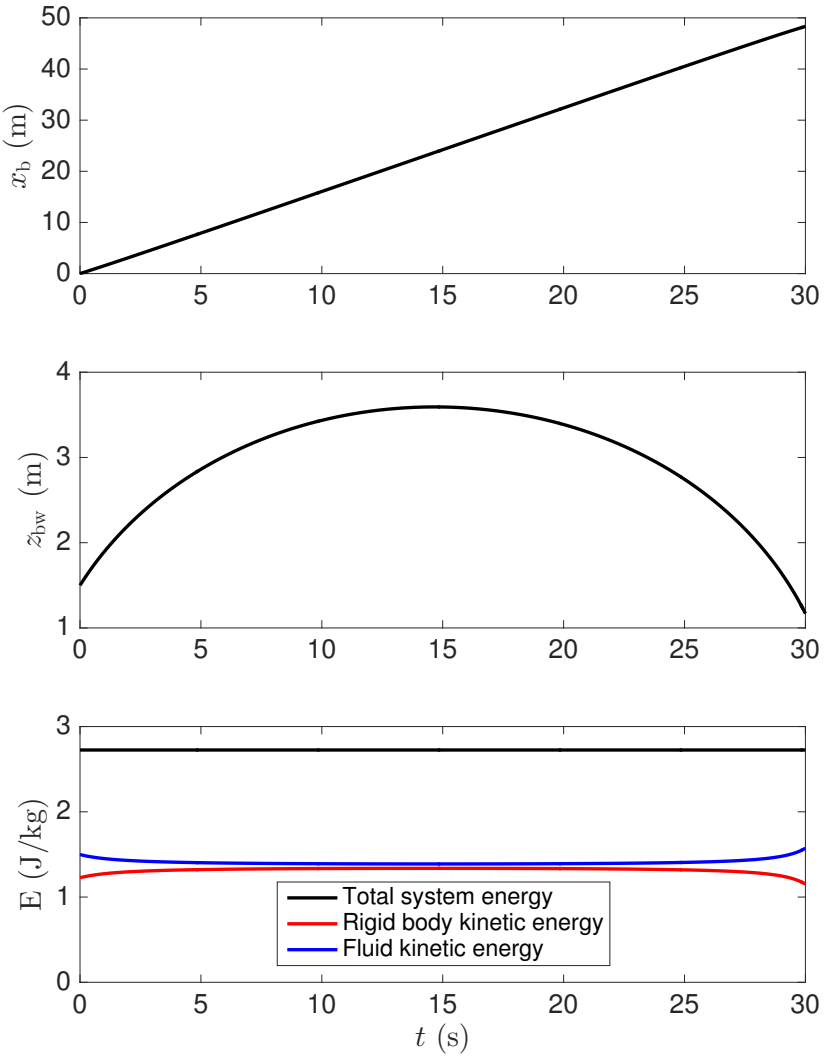

Figure 4.6: Simulation results for a circle moving near a rigid wall. The initial conditions are $x_{b0} = 0\text{m}$, $z_{bw0} = 1.5\text{m}$, $\dot{x}_{b0} = 1.5\text{m/s}$, and $\dot{z}_{b0} = -0.45\text{m/s}$.

to a wide variety of geometries and operating conditions.

Kirchhoff's equations govern the motion of a rigid body traveling through an ideal volume of otherwise calm fluid which extends infinitely far in all directions from the body [25]. Again, consider the case depicted in Figure 4.1: a rigid body suspended in a volume of fluid $\mathcal{F}$ which

is externally bounded by an envelope $\mathcal{E}$. Kirchhoff also assumed that the body is neutrally buoyant with coincident centers of mass and buoyancy. By Remark 4.2.2 we may therefore neglect the effects of gravity and hydrostatics altogether. The expressions for the rigid body Lagrangian and fluid Lagrangian are thus:

$$\mathcal{L}_{\mathrm{b}} = \frac{1}{2}\boldsymbol{\nu}^T \boldsymbol{M}_{\mathrm{b}} \boldsymbol{\nu} \tag{4.91}$$

$$\mathcal{L}_{\mathcal{F}} = \iiint_{\mathcal{F}} \frac{\rho}{2} \nabla\phi \cdot \nabla\phi \; dV \tag{4.92}$$

As before, the divergence theorem may be used to rewrite the fluid kinetic energy

$$\mathcal{F}_{\mathcal{F}} = \frac{1}{2}\rho \iint_{\mathcal{B}} (\phi \nabla\phi) \cdot \boldsymbol{n}_+ dS + \frac{1}{2}\rho \iint_{\mathcal{E}} (\phi \nabla\phi) \cdot \boldsymbol{n}_+ dS \tag{4.93}$$

In the limit that $\mathcal{E}$ extends infinitely far from the body in all directions, the surface integral over $\mathcal{E}$ must vanish. The surface integral over $\mathcal{B}$ may also be simplified using the body boundary condition (3.59)

$$\mathcal{F}_{\mathcal{F}} = \frac{1}{2}\rho \iint_{\mathcal{B}} \phi \boldsymbol{b}^T dS \; \boldsymbol{\nu} \tag{4.94}$$

It is at this point that one must select a form for the scalar potential. So far, we know that ϕ cannot depend on the generalized coordinates (from Corollary 4.2.5) and that the potential function must somehow depend on the vehicle velocity. Kirchhoff proposed the following velocity potential [25]

$$\phi_{\mathrm{K}} = \boldsymbol{\varphi}_{\mathrm{K}} \cdot \boldsymbol{\nu} = \boldsymbol{\phi}_{\mathrm{K}} \cdot \boldsymbol{v} + \boldsymbol{\chi}_{\mathrm{K}} \cdot \boldsymbol{\omega} \tag{4.95}$$

Define ϕ_{K} as "Kirchhoff's potential", and the terms $\boldsymbol{\phi}_{\mathrm{K}}$ and $\boldsymbol{\chi}_{\mathrm{K}}$ are vector potentials which scale the individual components of the body velocity. Note that the velocity potential for a circle in an unbounded fluid used in the example in Section 4.3.1 may be factored into this form. Substituting (4.95) into (4.94), the fluid Lagrangian may be factored into a quadratic form

$$\mathcal{L}_{\mathcal{F}} = \frac{1}{2}\begin{pmatrix} \boldsymbol{v} \\ \boldsymbol{\omega} \end{pmatrix}^T \left[\rho \iint_{\mathcal{B}} \begin{pmatrix} \boldsymbol{\phi}_{\mathrm{K}} \boldsymbol{n}_+^T & \boldsymbol{\phi}_{\mathrm{K}} (\bar{\boldsymbol{x}}_{\mathrm{h}} \times \boldsymbol{n}_+)^T \\ \boldsymbol{\chi}_{\mathrm{K}} \boldsymbol{n}_+^T & \boldsymbol{\chi}_{\mathrm{K}} (\bar{\boldsymbol{x}}_{\mathrm{h}} \times \boldsymbol{n}_+)^T \end{pmatrix} dS \right] \begin{pmatrix} \boldsymbol{v} \\ \boldsymbol{\omega} \end{pmatrix}$$

Define the *added mass* matrix

$$\boldsymbol{M}_{\mathcal{B}} = \rho \iint_{\mathcal{B}} \begin{pmatrix} \boldsymbol{\phi}_{\mathrm{K}} \boldsymbol{n}_+^T & \boldsymbol{\phi}_{\mathrm{K}} (\bar{\boldsymbol{x}}_{\mathrm{h}} \times \boldsymbol{n}_+)^T \\ \boldsymbol{\chi}_{\mathrm{K}} \boldsymbol{n}_+^T & \boldsymbol{\chi}_{\mathrm{K}} (\bar{\boldsymbol{x}}_{\mathrm{h}} \times \boldsymbol{n}_+)^T \end{pmatrix} dS \tag{4.96}$$

and the fluid kinetic energy may be written compactly as

$$\mathcal{L}_{\mathcal{F}} = \frac{1}{2}\boldsymbol{\nu}^T \boldsymbol{M}_{\mathcal{B}} \boldsymbol{\nu} \tag{4.97}$$

Proposition 4.3.1 *The added mass for a deeply submerged rigid body is constant and symmetric positive definite.*

A proof of Proposition 4.3.1 is given by Newman [8, Sec. 4.14].

Altogether, the system Lagrangian which governs Kirchhoff's equations is

$$\mathcal{L}_{\mathrm{K}} = \frac{1}{2}\boldsymbol{\nu}^T \left(\boldsymbol{M}_{\mathrm{b}} + \boldsymbol{M}_{\mathcal{B}}\right) \boldsymbol{\nu} \tag{4.98}$$

Physically, the rigid body mass matrix $\boldsymbol{M}_{\mathrm{b}}$ defines the relationship between the vehicle velocity and the rigid body kinetic energy. In the same light, the added mass matrix $\boldsymbol{M}_{\mathrm{b}}$ defines the relationship between the vehicle velocity and the fluid kinetic energy. Moreover, we observe that the effect of the fluid manifests as a modification to the inertial characteristics of the body in (4.98).

Using the Boltzmann-Hamel equations (2.33), Kirchhoff's equations are

$$\dot{\boldsymbol{q}} = \boldsymbol{J}\boldsymbol{\nu} \tag{4.99}$$

$$\left(\boldsymbol{M}_{\mathrm{b}} + \boldsymbol{M}_{\mathcal{B}}\right) \begin{pmatrix} \dot{\boldsymbol{v}} \\ \dot{\boldsymbol{\omega}} \end{pmatrix} + \begin{pmatrix} \hat{\boldsymbol{\omega}} & \boldsymbol{0} \\ \hat{\boldsymbol{v}} & \hat{\boldsymbol{\omega}} \end{pmatrix} \left(\boldsymbol{M}_{\mathrm{b}} + \boldsymbol{M}_{\mathcal{B}}\right) \begin{pmatrix} \boldsymbol{v} \\ \boldsymbol{\omega} \end{pmatrix} = \begin{pmatrix} \boldsymbol{f} \\ \boldsymbol{\tau} \end{pmatrix} \tag{4.100}$$

As expected, these equations match the Newtonian approach followed in [8, 44] and the Lagrangian approach in [25, 33, 44].

Remark 4.3.2 *Because both the rigid body Lagrangian and the fluid Lagrangian were used to derive Kirchhoff's equations, (4.100) governs both the rigid body motion and the fluid motion. This implies that the motion of the infinite dimensional fluid continuum is completely characterized by only the six degrees of freedom associated with the rigid body.*

Lie-Poisson Representation of Kirchhoff's Equations

Since the equations of motion are invariant to the generalized coordinates $\boldsymbol{q}$, one may identify a corresponding set of conserved quantities which may be used to simplify the equations of motion. Lamb [25, Art. 139-140] employed Routhian reduction to remove the ignorable coordinates. Leonard's approach [44] is instead followed here, which uses Lie-Poisson reduction to remove the ignorable coordinates and obtain a reduced-dimensional system with a non-canonical Hamiltonian structure. Employing the Legendre transformation, the momenta conjugate to the quasivelocities are

$$\boldsymbol{\pi} = \begin{pmatrix} \boldsymbol{\pi}_v \\ \boldsymbol{\pi}_\omega \end{pmatrix} = \frac{\partial \mathcal{L}_{\mathrm{K}}}{\partial \boldsymbol{\nu}} = (\boldsymbol{M}_{\mathrm{b}} + \boldsymbol{M}_{\mathcal{B}}) \begin{pmatrix} \boldsymbol{v} \\ \boldsymbol{\omega} \end{pmatrix} \tag{4.101}$$

The system Hamiltonian is

$$\mathcal{H} = \frac{1}{2} \boldsymbol{\pi}^T \left(\boldsymbol{M}_{\mathrm{b}} + \boldsymbol{M}_{\mathcal{B}}\right)^{-1} \boldsymbol{\pi} \tag{4.102}$$

and the Poisson tensor is [44]

$$\boldsymbol{\Lambda}(\boldsymbol{\pi}) = \begin{pmatrix} \boldsymbol{0} & \hat{\boldsymbol{\pi}}_v \\ \hat{\boldsymbol{\pi}}_v & \hat{\boldsymbol{\pi}}_\omega \end{pmatrix} \tag{4.103}$$

The equations of motion are then given by the Poisson bracket

$$\dot{\boldsymbol{\pi}} = \{\boldsymbol{\pi}, \mathcal{H}\} = \boldsymbol{\Lambda} \nabla \mathcal{H} \tag{4.104}$$

Leonard [44] also identified two Casimir functions

$$C_1 = \boldsymbol{\pi}_\omega \cdot \boldsymbol{\pi}_v \quad \text{and} \quad C_2 = \boldsymbol{\pi}_v \cdot \boldsymbol{\pi}_v \tag{4.105}$$

which satisfy the relationship

$$\dot{C}_i = \{C_i, \mathcal{H}\} = 0 \ \text{ for } i = 1, 2 \tag{4.106}$$

4.3.4 The Cummins Equations for Zero Forward Speed

The Cummins equations model the radiation forces for a surface craft which experiences either small perturbations from a stationary position or small perturbations from a straight-

ahead trajectory at a constant speed [19, 29]. As compared to Kirchhoff's equations, the small motion assumption simplifies the body boundary condition since one may enforce this condition along the nominal hull position rather than the true (constantly perturbed) location. However, additional complexity arises because the fluid behavior in Cummins' equations must satisfy the free surface boundary condition. The free surface incurs *memory effects*, persisting hydrodynamic forces and moments due to the vehicle's motion history [29]. For the sake of brevity, only the Cummins equations for zero forward speed are derived, recognizing that the following procedure may be used for the forward speed equations as well.

Cummins uses the concept of a rest-to-rest impulsive motion to establish the necessary velocity potential [19, 29]. This process may be decomposed into the four phases illustrated in Figure 4.7.

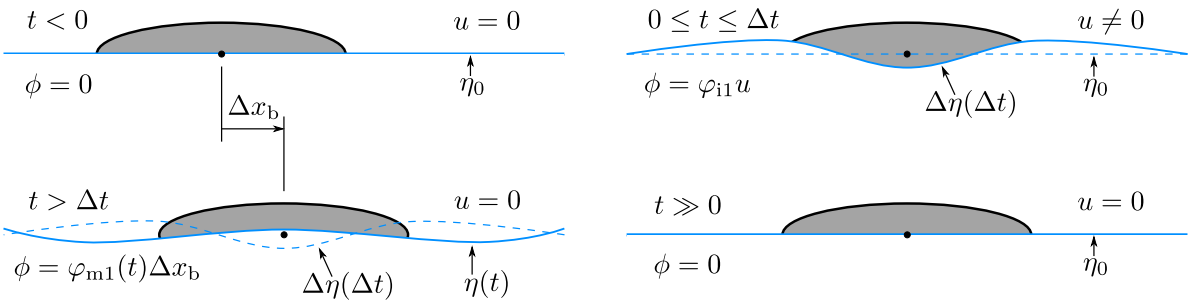

Figure 4.7: Illustration of the Cummins impulse.

Before the impulse ($t < 0$), the vehicle is at rest floating on the free surface and both the fluid and the free surface are undisturbed.

During the impulse ($0 \le t \le \Delta t$), the vehicle undergoes an impulsive displacement Δx_b during a small time Δt. Cummins [19] remarks that the time history of the impulse is irrelevant, though one may visualize the process by considering a vehicle motion to consist of a large, uniform velocity over the impulse time Δt. In the case depicted in Figure 4.7, the

impulse is in surge, and the corresponding impulsive velocity is given by

$$u = \frac{\Delta x_{\mathrm{b}}}{\Delta t}$$

Let $\boldsymbol{e}_i$ represent a unit vector with a 1 in the i^{th} position, and the velocity potential during an impulsive motion is [25, 19, 58]

$$\phi = (u\boldsymbol{e}_1) \cdot \boldsymbol{\varphi}_{\mathrm{i}} = u\varphi_{\mathrm{i}1} \tag{4.107}$$

Cummins assumes that the potential satisfies the kinematic body boundary condition along the nominal hull location

$$(\nabla(u\varphi_{\mathrm{i}1}) \cdot \boldsymbol{n}_+) \big|_{\mathcal{B}_0} = (\boldsymbol{n}_+ \cdot (u\boldsymbol{e}_1)) \big|_{\mathcal{B}_0} \tag{4.108}$$

Using the linearized kinematic free surface boundary condition (3.54),

$$\left.\frac{\partial \eta}{\partial t}\right|_{z=0} = \left.\frac{\partial \phi}{\partial z}\right|_{z=0}$$

the free surface elevation during the impulse is given by

$$\Delta\eta = -\left.\frac{\partial \varphi_{\mathrm{i}1}}{\partial z}\right|_{z=0} \Delta x_{\mathrm{b}} \tag{4.109}$$

After the impulse ($t > \Delta t$), the vehicle is arrested, though the free surface perturbation $\Delta\eta$ serves as the initial conditions for a surface wave. Since $u = 0$ after the impulse, the velocity potential corresponding to the impulsive motion is also zero. The ensuing gravity wave is generated by a *memory effect velocity potential*

$$\phi = \boldsymbol{\varphi}_{\mathrm{m}}(t) \cdot (\Delta x_{\mathrm{b}}\boldsymbol{e}_1) = \varphi_{\mathrm{m}1}(t)\Delta x_{\mathrm{b}} \tag{4.110}$$

From the linearized dynamic free surface boundary condition (3.55)

$$\left.\frac{\partial \phi}{\partial t}\right|_{z=0} = g\eta$$

the memory effect potential satisfies the initial condition

$$\Delta x_{\mathrm{b}} \left.\frac{\partial \varphi_{\mathrm{m}1}}{\partial t}\right|_{z=0,t=0^+} = g\Delta\eta \quad \text{or} \quad \left.\frac{\partial \varphi_{\mathrm{m}1}}{\partial t}\right|_{z=0,t=0^+} = g\left.\frac{\partial \varphi_{\mathrm{i}1}}{\partial z}\right|_{z=0} \tag{4.111}$$

The potential function subsequently evolves according to the linearized combined free surface boundary condition (3.56)

$$\left.\frac{\partial^2 \varphi_{\mathrm{m1}}}{\partial t^2}\right|_{z=0} \Delta x_{\mathrm{b}} - g \left.\frac{\partial \varphi_{\mathrm{m1}}}{\partial z}\right|_{z=0} \Delta x_{\mathrm{b}} = 0 \tag{4.112}$$

Long after the impulse ($t \gg 0$), the fluid again comes to rest in a neighborhood of the vehicle.

In discrete time, the fluid motion due to the arbitrary motion of a marine craft can be thought of as the sum of the responses to a series of impulses, each with the appropriate time lag [29]. Consider a discrete time system with time step Δt. Then let $u(i\Delta t)$ represent the impulsive velocity at $t = i\Delta t$ and assume that u remains constant during each time interval[10]. The corresponding impulsive displacement $\Delta x_{\mathrm{b}}(i\Delta t)$ is then

$$\Delta x_{\mathrm{b}}(i\Delta t) = u(i\Delta t)\Delta t \tag{4.113}$$

The velocity potential for the first several time steps with the initial condition $\phi(0) = 0$ is

$$\begin{aligned}
\phi(0) &= 0 \\
\phi(\Delta t) &= \varphi_{\mathrm{i1}} u(\Delta t) \\
\phi(2\Delta t) &= \varphi_{\mathrm{i1}} u(2\Delta t) + \varphi_{\mathrm{m1}}(\Delta t)\Delta x_{\mathrm{b}}(\Delta t) \\
\phi(3\Delta t) &= \varphi_{\mathrm{i1}} u(3\Delta t) + \varphi_{\mathrm{m1}}(2\Delta t)\Delta x_{\mathrm{b}}(\Delta t) + \varphi_{\mathrm{m1}}(\Delta t)\Delta x_{\mathrm{b}}(2\Delta t) \\
\phi(4\Delta t) &= \varphi_{\mathrm{i1}} u(4\Delta t) + \varphi_{\mathrm{m1}}(3\Delta t)\Delta x_{\mathrm{b}}(\Delta t) + \varphi_{\mathrm{m1}}(2\Delta t)\Delta x_{\mathrm{b}}(2\Delta t) + \varphi_{\mathrm{m1}}(\Delta t)\Delta x_{\mathrm{b}}(3\Delta t) \\
&\vdots \\
\phi(k\Delta t) &= \varphi_{\mathrm{i1}} u(k\Delta t) + \sum_{i=1}^{k} \varphi_{\mathrm{m1}}(k\Delta t - i\Delta t)\Delta x_{\mathrm{b}}(i\Delta t)
\end{aligned}$$

Because the memory terms persist from one time step to another, each line gains an additional memory effect term from the vehicle impulse at the prior time. In discrete time, the memory potential is

$$\phi_{\mathrm{m}} = \sum_{i=1}^{k} \varphi_{\mathrm{m1}}(k\Delta t - i\Delta t)\Delta x_{\mathrm{b}}(i\Delta t)$$

[10]The zero-order hold assumption [59].

In continuous time, one may interpret these impulses as occurring infinitesimally close so that the impulse responses are integrated rather than summed [29]. To derive the continuous time memory potential, rewrite ϕ_{m} using (4.113)

$$\phi_{\mathrm{m}} = \sum_{i=1}^{k} \varphi_{\mathrm{m1}}(k\Delta t - i\Delta t)u(i\Delta t)\Delta t \tag{4.114}$$

Then, one may study the limiting case where Δt represents an infinitesimal change in time. As the discrete time case approaches continuous time, let $\Delta t \to d\tau$, $i\Delta t \to \tau$, and $k\Delta t \to t$:

$$\phi_{\mathrm{m}} = \int_0^t \varphi_{\mathrm{m1}}(t-\tau)u(\tau)d\tau \tag{4.115}$$

The complete velocity potential is thus

$$\phi(t) = \varphi_{\mathrm{i1}}u(t) + \int_0^t \varphi_{\mathrm{m1}}(t-\tau)u(\tau)d\tau \tag{4.116}$$

Since the vehicle is assumed to only undergo small motions from a nominal (stationary) position, one may choose to characterize the system in terms of the coordinate velocities $\dot{\boldsymbol{q}}$ rather than the quasivelocities $\boldsymbol{\nu}$. Extending (4.116) to six degrees of freedom, one recovers Cummins' potential

$$\phi_{\mathrm{C}}(\dot{\boldsymbol{q}}, t) = \boldsymbol{\varphi}_{\mathrm{i}} \cdot \dot{\boldsymbol{q}}(t) + \int_0^t \boldsymbol{\varphi}_{\mathrm{m}}(t-\tau) \cdot \dot{\boldsymbol{q}}(\tau)d\tau \tag{4.117}$$

Recall that the kinematic body boundary condition may be evaluated along the stationary hull $\mathcal{B}_0$ rather than the true, constantly perturbed hull location $\mathcal{B}$. This enables ϕ_{C} to be defined independent of the generalized coordinates $\boldsymbol{q}$. Cummins also places the following restrictions on the potential functions

$$\boldsymbol{\varphi}_{\mathrm{i}}\big|_{z=0} = \mathbf{0} \tag{4.118}$$

$$\boldsymbol{\varphi}_{\mathrm{m}}\big|_{t\leq 0} = \mathbf{0} \tag{4.119}$$

The first condition is consistent with the linearization assumption, while the second implies that there are no memory effects before the system motion is initialized at $t = 0$. The potential functions also satisfy the following relationship, which is the vector form of (4.111)

$$\left.\frac{\boldsymbol{\varphi}_{\mathrm{i}}}{\partial z}\right|_{z=0} = \frac{1}{g}\left.\frac{\partial \boldsymbol{\varphi}_{\mathrm{m}}(0)}{\partial t}\right|_{z=0} \tag{4.120}$$

The equations of motion are given by

$$\frac{d}{dt}\frac{\partial \mathcal{L}}{\partial \dot{\boldsymbol{q}}} = -\boldsymbol{g}(\boldsymbol{q}) \tag{4.121}$$

Here, $\boldsymbol{g}$ represents the hydrostatic restoring force. (Expressions for the hydrostatics are more complex for surface craft since the center of buoyancy is free to move.) Since the contributions from the rigid body Lagrangian to the complete equations of motion were already addressed in the prior example, the focus here is placed on the fluid Lagrangian. First, from the definition of the fluid kinetic energy (4.37),

$$\begin{aligned}\frac{\partial \mathcal{L}_{\mathcal{F}}}{\partial \dot{q}_j} &= \rho \iiint_{\mathcal{F}} \nabla\phi \cdot \nabla\left(\frac{\partial \phi}{\partial \dot{q}_j}\right) \\ &= \rho \iint_{\mathcal{B}_0} \phi \nabla\left(\frac{\partial \phi}{\partial \dot{q}_j}\right) \cdot \boldsymbol{n}_+ dS + \rho \iint_{\mathcal{S}_0} \phi \nabla\left(\frac{\partial \phi}{\partial \dot{q}_j}\right) \cdot \boldsymbol{n}_+ dS\end{aligned}$$

From the body boundary condition, the integral over the body reduces to

$$\rho \iint_{\mathcal{B}_0} \phi \nabla\left(\frac{\partial \phi}{\partial \dot{q}_j}\right) \cdot \boldsymbol{n}_+ dS = \rho \iint_{\mathcal{B}_0} \phi(\boldsymbol{b} \cdot \boldsymbol{e}_j)\, dS \tag{4.122}$$

One may also simplify the integral along the surface, noting that

$$\nabla\left(\frac{\partial \phi_{\mathrm{C}}}{\partial \dot{q}_j}\right)\bigg|_{z=0} \cdot \boldsymbol{n}_+ = -\frac{\partial \varphi_{\mathrm{i}j}}{\partial z}\bigg|_{z=0} = -\frac{1}{g}\frac{\partial \varphi_{\mathrm{m}j}(0)}{\partial t}\bigg|_{z=0} \tag{4.123}$$

Altogether, one finds

$$\begin{aligned}\frac{\partial \mathcal{L}_{\mathcal{F}}}{\partial \dot{\boldsymbol{q}}} &= \rho \iint_{\mathcal{B}_0} \left[\boldsymbol{\varphi}_{\mathrm{i}} \cdot \dot{\boldsymbol{q}}(t) + \int_0^t \boldsymbol{\varphi}_{\mathrm{m}}(t-\tau) \cdot \dot{\boldsymbol{q}}(\tau) d\tau\right] \boldsymbol{b}\, dS \\ &\quad - \frac{\rho}{g} \iint_{\mathcal{S}_0} \int_0^t \boldsymbol{\varphi}_{\mathrm{m}}(t-\tau) \cdot \dot{\boldsymbol{q}}(\tau) d\tau\, \frac{\partial \boldsymbol{\varphi}_{\mathrm{m}}(0)}{\partial t}\, dS\end{aligned} \tag{4.124}$$

Because $\mathcal{B}_0$ and $\mathcal{S}_0$ do not depend on time, the orders of the integrals in (4.124) may be interchanged. Define the following matrices

$$\boldsymbol{M}_{\mathcal{B}_0} = \rho \iint_{\mathcal{B}_0} \boldsymbol{b}\, \boldsymbol{\varphi}_{\mathrm{i}}^T\, dS \tag{4.125}$$

$$\boldsymbol{K}_{\mathcal{B}_0}(t) = \rho \iint_{\mathcal{B}_0} \boldsymbol{b}\, \frac{\partial \boldsymbol{\varphi}_{\mathrm{m}}^T(t)}{\partial t}\, dS \tag{4.126}$$

$$\boldsymbol{K}_{\mathcal{S}_0}(t) = \frac{\rho}{g} \iint_{\mathcal{S}_0} \frac{\partial \boldsymbol{\varphi}_{\mathrm{m}}(0)}{\partial t}\, \frac{\partial \boldsymbol{\varphi}_{\mathrm{m}}^T(t)}{\partial t}\, dS \tag{4.127}$$

The equations of motion are

$$(\boldsymbol{M}_{\mathrm{b}} + \boldsymbol{M}_{\mathcal{B}_0})\,\ddot{\boldsymbol{q}}(t) + \int_0^t [\boldsymbol{K}_{\mathcal{B}_0}(t-\tau) - \boldsymbol{K}_{\mathcal{S}_0}(t-\tau)]\,\dot{\boldsymbol{q}}(\tau)d\tau + \boldsymbol{g}(\boldsymbol{q}) = \boldsymbol{0} \tag{4.128}$$

As compared to Cummins' results [19], these equations have additional generalized forces due to the matrix $\boldsymbol{K}_{\mathcal{S}_0}$. This is a result of Cummins' decision to only use the linearized Bernoulli pressure, rather than the full Bernoulli pressure, when computing the equations of motion.

4.4 Closing Remarks

Perhaps the most important conclusion we may draw from this chapter is that each expression given for the hydrodynamic forces and moments is equivalent to

$$\boldsymbol{f}_{\mathrm{p}} = \iint_{\mathcal{B}} p\boldsymbol{n}_+ dS \tag{4.129}$$

$$\boldsymbol{\tau}_{\mathrm{p}} = \iint_{\mathcal{B}} p(\boldsymbol{r}_{\mathrm{h}} \times \boldsymbol{n}_+) dS \tag{4.130}$$

Elegant and concise, these expressions serve as the basis for the Kutta-Joukowski lift force [8, 41], the Lagally Theorem [55, 56], Kirchhoff's equations [25], the Cummins equations [19], and Sclavonous' impulse theory [54]. By showing that the forces and moments derived from Lagrangian mechanics reduce to (4.129) and (4.130) in several scenarios of interest, it has been demonstrated at a general level how Lagrangian modeling techniques are related to some of the more common frameworks used in potential flow.

Also of interest, Theorem 4.2.4 proved that a submerged vehicle's position and orientation do not affect the scalar velocity potential or the fluid kinetic energy in an unbounded fluid. While this is generally assumed to be true, the author is unaware of any earlier proof of such a result.

Chapter 5

Near-Surface Maneuvering

In this chapter, two nonlinear models for a marine craft maneuvering near a free surface are derived. The models assume that the fluid motion is due solely to the motion of the vehicle; hydrodynamic effects due to incident waves are deferred to Chapter 6. The first model is an extension of Kirchhoff's equations and neglects the fluid memory effects. By augmenting the potential function used to derive Kirchhoff's equations, one can incorporate the fluid forces and moments which act on a rigid body due to the instantaneous response of a fluid with a free surface. The second model draws from both Kirchhoff's equations and Cummins's equations. The model incorporates the fluid memory effects using a potential function structure similar to that used to derive the Cummins equations. By constructing models with and without the fluid memory effects, one can isolate exactly how the fluid memory affects the vehicle dynamics.

5.1 Statement of Assumptions

Assumption 5.1.1 (Modeling assumptions) *1. The fluid is incompressible and inviscid and the fluid velocity is irrotational (the potential flow assumptions).*

2. *The linearized free surface boundary conditions are valid.*

3. *The fluid motion is due solely to the motion of the rigid body.*

5.2 General Lagrangian Functions

In Chapter 4, Lagrangian expressions were presented which resulted in forces and moments that more easily compare to those from Newtonian mechanics. Here, a more intuitive decomposition of the fluid energy functions is presented:

$$\mathcal{L} = \mathcal{L}_{\mathrm{b}} + \mathcal{L}_{\mathcal{B}} + \mathcal{L}_{\mathcal{S}} \tag{5.1}$$

As compared to the two-part system Lagrangian presented in Chapter 4, the fluid Lagrangian is decomposed into a *fluid body Lagrangian* $\mathcal{L}_{\mathcal{B}}$ and a *free surface Lagrangian* $\mathcal{L}_{\mathcal{S}}$. The definitions and physical meanings of these terms will be given in the coming sections.

Rigid Body Lagrangian

Briefly revisiting Section 2.4, the rigid body kinetic energy takes the form:

$$T_{\mathrm{b}} = \frac{1}{2}\boldsymbol{\nu}^T \boldsymbol{M}_{\mathrm{b}} \boldsymbol{\nu}$$

Let the origin of the body fixed frame coincide with the vehicle's center of buoyancy and let $\boldsymbol{r}_{\mathrm{cm}}$ locate the center of mass in the body-fixed frame. The rigid body mass matrix is then

$$\boldsymbol{M}_{\mathrm{b}} = \begin{pmatrix} m_{\mathrm{b}}\mathbb{I}_3 & -m_{\mathrm{b}}\hat{\boldsymbol{r}}_{\mathrm{cm}} \\ m_{\mathrm{b}}\hat{\boldsymbol{r}}_{\mathrm{cm}} & \boldsymbol{I}_{\mathrm{b}} - m_{\mathrm{b}}\hat{\boldsymbol{r}}_{\mathrm{cm}}\hat{\boldsymbol{r}}_{\mathrm{cm}} \end{pmatrix} \tag{5.2}$$

where $\mathbb{I}_3$ is the 3-by-3 identity matrix. The rigid body potential energy is

$$V_{\mathrm{b}} = -m_{\mathrm{b}} g z_{\mathrm{b}} - m_{\mathrm{b}} g \boldsymbol{r}_{\mathrm{cm}} \cdot \left(\boldsymbol{R}^T \boldsymbol{i}_3\right) \tag{5.3}$$

The first term accounts for the gravitational potential energy of the body while the second term accounts for the gravity-induced torque which tends to swing the center of mass below

the center of buoyancy; this term vanishes for a vehicle with coincident centers of mass and buoyancy. The rigid body Lagrangian is then the difference between rigid body kinetic and potential energies:

$$\mathcal{L}_{\mathrm{b}} = \frac{1}{2}\boldsymbol{\nu}^T \boldsymbol{M}_{\mathrm{b}} \boldsymbol{\nu} + m_{\mathrm{b}} g z_{\mathrm{b}} + m_{\mathrm{b}} g \boldsymbol{x}_{\mathrm{cm}} \cdot \left(\boldsymbol{R}^T \boldsymbol{i}_3\right) \tag{5.4}$$

Fluid Energy Contributions

In Chapter 4, the Lagrangian function for a fluid volume $\mathcal{F}$ was defined as

$$\mathcal{L}_{\mathcal{F}} = \iiint_{\mathcal{F}} \left(\frac{1}{2}\rho \nabla\phi \cdot \nabla\phi + \rho g z\right) dV$$

Rewrite the integrand as

$$\mathcal{L}_{\mathcal{F}} = \iiint_{\mathcal{F}} \nabla \cdot \left(\frac{1}{2}\rho\phi\nabla\phi + \frac{1}{2}\rho g z^2 \boldsymbol{i}_3\right) dV$$

and this expression may be defined in terms of surface integrals over the hull $\mathcal{B}$ and the free surface $\mathcal{S}$:

$$\mathcal{L}_{\mathcal{F}} = \iint_{\mathcal{B}} \left(\frac{1}{2}\rho\phi\nabla\phi + \frac{1}{2}\rho g z^2 \boldsymbol{i}_3\right) \cdot \boldsymbol{n}_+ dS + \iint_{\mathcal{S}} \left(\frac{1}{2}\rho\phi\nabla\phi + \frac{1}{2}\rho g z^2 \boldsymbol{i}_3\right) \cdot \boldsymbol{n}_+ dS$$

This enables the following definitions of the fluid energy functions:

$$T_{\mathcal{B}} = \frac{1}{2}\rho \iint_{\mathcal{B}} (\phi\nabla\phi) \cdot \boldsymbol{n}_+ dS \tag{5.5}$$

$$V_{\mathcal{B}} = -\frac{1}{2}\rho g \iint_{\mathcal{B}} z^2 \boldsymbol{i}_3 \cdot \boldsymbol{n}_+ dS \tag{5.6}$$

$$T_{\mathcal{S}} = \frac{1}{2}\rho \iint_{\mathcal{S}} (\phi\nabla\phi) \cdot \boldsymbol{n}_+ dS \tag{5.7}$$

$$V_{\mathcal{S}} = -\frac{1}{2}\rho g \iint_{\mathcal{S}} z^2 \boldsymbol{i}_3 \cdot \boldsymbol{n}_+ dS \tag{5.8}$$

Let $T_{\mathcal{B}}$ denote the "fluid body kinetic energy" and denote $V_{\mathcal{B}}$ the "fluid body potential energy"; these terms represent the contributions to the fluid kinetic and potential energies which are integrated over the body. Similarly, let $T_{\mathcal{S}}$ denote the "free surface kinetic energy"

and denote $V_{\mathcal{S}}$ the "free surface potential energy". Then, one may decompose the fluid Lagrangian into the "fluid body Lagrangian"

$$\mathcal{L}_{\mathcal{B}} = \iint_{\mathcal{B}} \left(\frac{1}{2}\rho\phi\nabla\phi + \frac{1}{2}\rho g z^2 \boldsymbol{i}_3 \right) \cdot \boldsymbol{n}_+ dS \tag{5.9}$$

and the "free surface Lagrangian"

$$\mathcal{L}_{\mathcal{S}} = \iint_{\mathcal{S}} \left(\frac{1}{2}\rho\phi\nabla\phi + \frac{1}{2}\rho g z^2 \boldsymbol{i}_3 \right) \cdot \boldsymbol{n}_+ dS \tag{5.10}$$

Fluid Body Lagrangian

As in Section 4.3.3, the fluid body kinetic energy may be simplified using the body boundary condition (3.59). Recall that the geometry vector $\boldsymbol{b}$ is

$$\boldsymbol{b} = \begin{pmatrix} \boldsymbol{n}_+ \\ \boldsymbol{r}_{\mathrm{h}} \times \boldsymbol{n}_+ \end{pmatrix}$$

where $\boldsymbol{r}_{\mathrm{h}}$ denotes the point on the hull at which the unit normal vector $\boldsymbol{n}_+$ is defined. (A subscript + implies that the unit normal vector $\boldsymbol{n}_+$ is directed out of the fluid volume.) The fluid body kinetic energy is then

$$T_{\mathcal{B}} = \frac{1}{2}\rho \iint_{\mathcal{B}} \phi \boldsymbol{b}^T dS \; \boldsymbol{\nu} \tag{5.11}$$

One may relate the fluid body potential energy to a volume integral within the body:

$$V_{\mathcal{B}} = -\frac{1}{2}\rho g \iint_{\mathcal{B}} z^2 \boldsymbol{i}_3 \cdot \boldsymbol{n}_+ dS = \frac{1}{2}\rho g \iint_{\mathcal{B}} z^2 \boldsymbol{i}_3 \cdot \boldsymbol{n}_- dS = \iiint_{\forall} \rho g z \; dV \tag{5.12}$$

The integral over the volume fluid displaced by the body $\forall$ is simply the potential energy associated with the buoyancy force:

$$V_{\mathcal{B}} = \rho g \forall z_{\mathrm{b}} \tag{5.13}$$

Altogether, the fluid body Lagrangian is

$$\mathcal{L}_{\mathcal{B}} = \frac{1}{2}\rho \iint_{\mathcal{B}} \phi \boldsymbol{b}^T dS \; \boldsymbol{\nu} - \rho g \forall z_{\mathrm{b}} \tag{5.14}$$

Free Surface Lagrangian

The linearization assumption enables the free surface integrals appearing in (5.10) to be evaluated along the undisturbed free surface $\mathcal{S}_0$ rather than the true location of the surface $\mathcal{S}$. Denote $\mathcal{L}_{\mathcal{S}_0}$ the "linearized free surface Lagrangian":

$$\mathcal{L}_{\mathcal{S}_0} = \iint_{\mathcal{S}_0} \left(\frac{1}{2}\rho\phi\nabla\phi + \frac{1}{2}\rho g\eta^2(x,y,t)\boldsymbol{i}_3 \right) \cdot \boldsymbol{n}_+ dS \tag{5.15}$$

(For brevity, $\mathcal{L}_{\mathcal{S}_0}$ will simply be referred to as the free surface Lagrangian for the remainder of this dissertation.) From the linearized dynamic free surface boundary condition (3.55), the free surface elevation is

$$\eta(x,y,t) = \frac{1}{g}\frac{\partial\phi}{\partial t}\bigg|_{\mathcal{S}_0} \tag{5.16}$$

and should be thought of as a "small perturbation" from $\mathcal{S}_0$. Moreover, along the undisturbed free surface, $\boldsymbol{n}_+ = -\boldsymbol{i}_3$. Substituting the expressions for η and $\boldsymbol{n}_+$ into (5.15), the free surface Lagrangian becomes

$$\mathcal{L}_{\mathcal{S}_0} = -\frac{\rho}{2}\iint_{\mathcal{S}_0} \left[\phi\frac{\partial\phi}{\partial z} + \frac{1}{g}\left(\frac{\partial\phi}{\partial t}\right)^2 \right] dS$$

Using the following identity

$$\frac{1}{2}\frac{\partial^2\phi^2}{\partial t^2} = \left(\frac{\partial\phi}{\partial t}\right)^2 + \phi\frac{\partial^2\phi}{\partial t^2}$$

the free surface Lagrangian becomes

$$\mathcal{L}_{\mathcal{S}_0} = -\frac{\rho}{2}\iint_{\mathcal{S}_0} \left[\frac{-\phi}{g}\left(\frac{\partial^2\phi}{\partial t^2} - g\frac{\partial\phi}{\partial z}\right) + \frac{1}{2g}\frac{\partial^2\phi^2}{\partial t^2} \right] dS$$

Recognizing the quantity in parentheses as the free surface boundary condition (3.56), that term must equal zero everywhere along $\mathcal{S}_0$. This observation reduces the free surface Lagrangian to

$$\mathcal{L}_{\mathcal{S}_0} = -\frac{\rho}{4g}\iint_{\mathcal{S}_0} \frac{\partial^2\phi^2}{\partial t^2} dS \tag{5.17}$$

Remark 5.2.1 *The expression for the free surface Lagrangian (5.17) holds for arbitrary potential functions when the linearized free surface boundary condition is applicable.*

The General Scalar Potential

To determine an appropriate form for the fluid potential, revisit the potentials used to derive Kirchhoff's equations (4.95) and Cummins' equations (4.117):

$$\phi_{\mathrm{K}}(\boldsymbol{\nu}) = \boldsymbol{\varphi}_{\mathrm{K}} \cdot \boldsymbol{\nu}$$
$$\phi_{\mathrm{C}}(\dot{\boldsymbol{q}}, t) = \boldsymbol{\varphi}_{\mathrm{i}} \cdot \dot{\boldsymbol{q}} + \int_0^t \boldsymbol{\varphi}_{\mathrm{m}}(t-\tau) \cdot \dot{\boldsymbol{q}}(\tau) d\tau$$

For an unbounded fluid, the vector potential $\boldsymbol{\varphi}_{\mathrm{K}}$ is independent of the body's generalized coordinates. In the presence of any fluid boundaries, the body's position and orientation relative to the boundary will affect the vector potential; this was the case for the example given in Section 4.3.2. However, noting that $\boldsymbol{\nu} = \mathbf{0}$ implies $\phi_{\mathrm{K}} = 0$, this particular structure only captures the instantaneous fluid motion resulting from the vehicle motion and neglects any memory effects. For a body-fluid system with a free surface, Cummins decomposed the velocity potential into an impulse potential and a memory potential; the former accounts for the instantaneous fluid response while the latter captures any persisting fluid memory effects. The potential, however, only accounts for small perturbations from a nominal position or pure surge trajectory. Combining the approaches of Kirchhoff and Cummins, define a general potential of the form

$$\phi(\boldsymbol{q}, \boldsymbol{\nu}, t) = \phi_{\mathrm{K}}(\boldsymbol{\nu}) + \phi_{\mathrm{s}}(\boldsymbol{q}, \boldsymbol{\nu}) + \phi_{\mathrm{m}}(\boldsymbol{q}, \boldsymbol{\nu}, t) \tag{5.18}$$

Kirchhoff's potential ϕ_{K} is augmented by a state-dependent free-surface potential ϕ_{s} and a state- and time-dependent memory effect potential ϕ_{m}.

5.3 Memory-Free Impulse Model

The fluid memory effects add considerable complexity to a resulting model; in the Cummins equations (4.128), the memory effects led to convolution integrals in the equations of the motion. One would ideally neglect the memory effects in a control-oriented model to

circumvent this added complexity. The memory effects, however, are found to be essential in the equations of motion. To illustrate their importance, a memory-free model is first constructed.

Assumption 5.3.1 *Neglecting memory effects, a scalar potential $\phi(\boldsymbol{q}, \boldsymbol{\nu})$ that describes fluid motion corresponding to the motion of a rigid body near a free surface satisfies the following criteria:*

1. $\lim_{z_\mathrm{b} \to \infty} \phi(\boldsymbol{q}, \boldsymbol{\nu}) = \phi_\mathrm{K}$
2. $\boldsymbol{\nu} = \mathbf{0} \implies \phi = 0$

The first criterion in Assumption 5.3.1 follows from the expectation that, in the limit of deep submergence, fluid behavior consistent with Kirchhoff's equations should be recovered. The second criterion implies that at each instant, the fluid motion is due solely to the motion of the vehicle. This explicitly precludes the incorporation of memory effects, where the fluid remains in motion even if the vessel is brought to rest. Assuming a free surface potential of the form

$$\phi_\mathrm{s}(\boldsymbol{q}, \boldsymbol{\nu}) = \boldsymbol{\varphi}_\mathrm{s}(\boldsymbol{q}) \cdot \boldsymbol{\nu} = \boldsymbol{\phi}_\mathrm{s}(\boldsymbol{q}) \cdot \boldsymbol{v} + \boldsymbol{\chi}_\mathrm{s}(\boldsymbol{q}) \cdot \boldsymbol{\omega}, \tag{5.19}$$

the complete velocity potential is

$$\phi(\boldsymbol{q}, \boldsymbol{\nu}) = \left(\boldsymbol{\varphi}_\mathrm{K} + \boldsymbol{\varphi}_\mathrm{s}(\boldsymbol{q})\right)^T \boldsymbol{\nu} \tag{5.20}$$

The vector function $\boldsymbol{\varphi}_\mathrm{s}(\boldsymbol{q})$ accounts for the modifications to the vehicle-induced fluid motion due to the presence of the free surface. The superposition of $\boldsymbol{\varphi}_\mathrm{K}$ and $\boldsymbol{\varphi}_\mathrm{s}$ corresponds to the impulsive fluid response potential in Cummins' equations. Note from Assumption 5.3.1, it must be true that $\boldsymbol{\varphi}_\mathrm{s} \to \mathbf{0}$ as $z_\mathrm{b} \to \infty$.

5.3.1 Memory-Free System Lagrangian

Fluid Body Lagrangian

Substituting the scalar potential (5.20) into the fluid body Lagrangian (4.50), one finds

$$\mathcal{L}_{\mathcal{B}} = \frac{1}{2}\begin{pmatrix}\boldsymbol{v}\\ \boldsymbol{\omega}\end{pmatrix}^T \left[\rho \iint_{\mathcal{B}} \begin{pmatrix}\boldsymbol{\phi}_{\mathrm{K}}\boldsymbol{n}_+^T & \boldsymbol{\phi}_{\mathrm{K}}(\boldsymbol{r}_{\mathrm{h}}\times\boldsymbol{n}_+)^T\\ \boldsymbol{\chi}_{\mathrm{K}}\boldsymbol{n}_+^T & \boldsymbol{\chi}_{\mathrm{K}}(\boldsymbol{r}_{\mathrm{h}}\times\boldsymbol{n}_+)^T\end{pmatrix} dS\right]\begin{pmatrix}\boldsymbol{v}\\ \boldsymbol{\omega}\end{pmatrix}$$
$$+\frac{1}{2}\begin{pmatrix}\boldsymbol{v}\\ \boldsymbol{\omega}\end{pmatrix}^T \left[\rho \iint_{\mathcal{B}} \begin{pmatrix}\boldsymbol{\phi}_{\mathrm{s}}\boldsymbol{n}_+^T & \boldsymbol{\phi}_{\mathrm{s}}(\boldsymbol{r}_{\mathrm{h}}\times\boldsymbol{n}_+)^T\\ \boldsymbol{\chi}_{\mathrm{s}}\boldsymbol{n}_+^T & \boldsymbol{\chi}_{\mathrm{s}}(\boldsymbol{r}_{\mathrm{h}}\times\boldsymbol{n}_+)^T\end{pmatrix} dS\right]\begin{pmatrix}\boldsymbol{v}\\ \boldsymbol{\omega}\end{pmatrix} - \rho g \forall z_{\mathrm{b}}$$

The first term in brackets is the deeply submerged added mass $\boldsymbol{M}_{\mathcal{B}}$ (4.96) which completely characterizes the effects of the fluid volume in Kirchhoff's equations. Defining the additional matrix

$$\boldsymbol{M}_2(\boldsymbol{q}) = \rho \iint_{\mathcal{B}} \begin{pmatrix}\boldsymbol{\phi}_{\mathrm{s}}\boldsymbol{n}_+^T & \boldsymbol{\phi}_{\mathrm{s}}(\boldsymbol{r}_{\mathrm{h}}\times\boldsymbol{n}_+)^T\\ \boldsymbol{\chi}_{\mathrm{s}}\boldsymbol{n}_+^T & \boldsymbol{\chi}_{\mathrm{s}}(\boldsymbol{r}_{\mathrm{h}}\times\boldsymbol{n}_+)^T\end{pmatrix} dS \tag{5.21}$$

the fluid body Lagrangian may be written compactly as

$$\mathcal{L}_{\mathcal{B}} = \frac{1}{2}\boldsymbol{\nu}^T\left[\boldsymbol{M}_{\mathcal{B}} + \boldsymbol{M}_2(\boldsymbol{q})\right]\boldsymbol{\nu} - \rho g \forall z_{\mathrm{b}}$$

Note that $\boldsymbol{M}_2(\boldsymbol{q})$ is not necessarily symmetric. However, since the term $\boldsymbol{M}_2(\boldsymbol{q})$ appears in a quadratic form in the expression for $\mathcal{L}_{\mathcal{B}}$, it may (and should) be made symmetric without loss of generality (see [59, ch. 1], for instance). One may accordingly define the *surface-perturbed added mass* $\Delta\boldsymbol{M}_{\mathcal{B}}(\boldsymbol{q})$ as the symmetric part of $\boldsymbol{M}_2(\boldsymbol{q})$:

$$\Delta\boldsymbol{M}_{\mathcal{B}}(\boldsymbol{q}) = \frac{1}{2}\left(\boldsymbol{M}_2(\boldsymbol{q}) + \boldsymbol{M}_2^T(\boldsymbol{q})\right) \tag{5.22}$$

and the fluid body Lagrangian is

$$\mathcal{L}_{\mathcal{B}} = \frac{1}{2}\boldsymbol{\nu}^T\left[\boldsymbol{M}_{\mathcal{B}} + \Delta\boldsymbol{M}_{\mathcal{B}}(\boldsymbol{q})\right]\boldsymbol{\nu} - \rho g \forall z_{\mathrm{b}} \tag{5.23}$$

Although the skew symmetric part of $\boldsymbol{M}_2(\boldsymbol{q})$ does not contribute to the system energy, it does have physical significance. From the perspective of dynamical systems theory, the fluid

motion corresponding to the skew component of $\boldsymbol{M}_2(\boldsymbol{q})$ reflects a *workless constraint* [16]; this fluid motion is necessary to satisfy the fluid boundary conditions, though it doesn't result in a generalized force acting on the rigid body.

Free Surface Lagrangian

Using the definition of the scalar potential (5.20), the term ϕ^2 in the integrand of the free surface Lagrangian (5.17) can be written as

$$\phi^2(\boldsymbol{q},\boldsymbol{\nu}) = \boldsymbol{\nu}^T \left(\boldsymbol{\varphi}_{\mathrm{K}}\boldsymbol{\varphi}_{\mathrm{K}}^T + \left[\boldsymbol{\varphi}_{\mathrm{s}}\boldsymbol{\varphi}_{\mathrm{K}}^T + \boldsymbol{\varphi}_{\mathrm{K}}\boldsymbol{\varphi}_{\mathrm{s}}^T\right] + \boldsymbol{\varphi}_{\mathrm{s}}\boldsymbol{\varphi}_{\mathrm{s}}^T\right)\boldsymbol{\nu}$$

Since $\mathcal{S}_0$ does not depend on time, the time derivatives in (5.17) may be moved outside of the integral. Rewrite $\mathcal{L}_{\mathcal{S}_0}$ as

$$\mathcal{L}_{\mathcal{S}_0} = \frac{1}{2}\frac{\partial^2}{\partial t^2}\left(\boldsymbol{\nu}^T\left[\boldsymbol{A}_{\mathcal{S}0} + \boldsymbol{B}_{\mathcal{S}0}(\boldsymbol{q}) + \boldsymbol{C}_{\mathcal{S}0}(\boldsymbol{q})\right]\boldsymbol{\nu}\right)$$

where

$$\begin{aligned}
\boldsymbol{A}_{\mathcal{S}0} &= -\frac{\rho}{2g}\iint_{\mathcal{S}_0} \boldsymbol{\varphi}_{\mathrm{K}}\boldsymbol{\varphi}_{\mathrm{K}}^T dS \\
\boldsymbol{B}_{\mathcal{S}0}(\boldsymbol{q}) &= -\frac{\rho}{2g}\iint_{\mathcal{S}_0} \left(\boldsymbol{\varphi}_{\mathrm{s}}\boldsymbol{\varphi}_{\mathrm{K}}^T + \boldsymbol{\varphi}_{\mathrm{K}}\boldsymbol{\varphi}_{\mathrm{s}}^T\right) dS \\
\boldsymbol{C}_{\mathcal{S}0}(\boldsymbol{q}) &= -\frac{\rho}{2g}\iint_{\mathcal{S}_0} \boldsymbol{\varphi}_{\mathrm{s}}\boldsymbol{\varphi}_{\mathrm{s}}^T dS
\end{aligned}$$

Care must be taken when evaluating the partial time derivatives. From the discussion in Section 3.3.5, the fluid motion at any instant can be thought of as being initialized from rest by a suitable set of impulsive pressures. For vehicle models in potential flow, the fluid motion has historically been evaluated as a result of an impulsive vessel motion [19] [25]. We may therefore interpret the fluid velocity at each instant in time as being generated by an impulsive (instantaneous) vessel motion, and during this impulse the vessel velocity $\boldsymbol{\nu}$ may be taken as constant. (See, for instance [19, p. 4] or the discussion in [29, pp. 25-26].)

A more conceptual way to reason that the vehicle velocities should be constant during a vehicle impulse comes from the fluid boundary conditions. Since the fluid motion in a simply

connected fluid volume is completely determined by the flow normal to the boundaries, one may completely characterize the fluid behavior using kinematic body and free surface boundary conditions. Moreover, the body boundary condition (3.59) only depends on the vehicle velocities, so higher derivatives of $\boldsymbol{\nu}$ should not impact the fluid velocity. This rationale justifies the following definition of the *free surface added mass* $\boldsymbol{M}_{\mathcal{S}_0}$

$$\begin{aligned}\boldsymbol{M}_{\mathcal{S}_0}(\boldsymbol{q},\boldsymbol{\nu}) &= \frac{\partial^2}{\partial t^2}\left[\iint_{\mathcal{S}_0}(\boldsymbol{\varphi}_{\mathrm{K}}+\boldsymbol{\varphi}_{\mathrm{s}})(\boldsymbol{\varphi}_{\mathrm{K}}+\boldsymbol{\varphi}_{\mathrm{s}})^T\,dS\right] \\ &= \sum_{i=1}^{6}\sum_{j=1}^{6}\frac{\partial^2(\boldsymbol{B}_{\mathcal{S}0}+\boldsymbol{C}_{\mathcal{S}0})}{\partial q_i\partial q_j}(\boldsymbol{J}_i^T\boldsymbol{\nu})(\boldsymbol{J}_j^T\boldsymbol{\nu}) + \frac{\partial(\boldsymbol{B}_{\mathcal{S}0}+\boldsymbol{C}_{\mathcal{S}0})}{\partial q_i}\frac{\partial \boldsymbol{J}_i^T}{\partial q_j}\boldsymbol{\nu}(\boldsymbol{J}_j^T\boldsymbol{\nu}) \qquad (5.24)\end{aligned}$$

where $\boldsymbol{J}_i^T$ is the i^{th} row of the kinematic transformation matrix $\boldsymbol{J}$. Then, the free surface Lagrangian is

$$\mathcal{L}_{\mathcal{S}_0} = \frac{1}{2}\boldsymbol{\nu}^T\boldsymbol{M}_{\mathcal{S}_0}(\boldsymbol{q},\boldsymbol{\nu})\boldsymbol{\nu} \qquad (5.25)$$

Remark 5.3.2 *Each term in (5.24) depends quadratically on the rigid body velocity. For mechanical systems, the system mass is rarely velocity-dependent. Perhaps the most common natural occurrence of a velocity-dependent mass is in special relativity where a particle's mass increases as its velocity approaches the speed of light [17, 38].*

One almost always finds that the kinetic energy in a mechanical system depends quadratically on the velocity. However, the free surface Lagrangian explicitly features a quartic dependence on the rigid body velocity. A quartic velocity dependence is significant when relating a system Lagrangian to a corresponding Hamiltonian function. Generating a system Hamiltonian using the Legendre transformation (2.44) is straightforward when the system kinetic energy is at most quadratic in the body velocity. For a time-invariant Lagrangian that depends quadratically on the body velocity, the corresponding Hamiltonian function also defines the total system energy [38]. While the Legendre transformation is still well defined for a Lagrangian with quartic velocity dependence, generating a Hamiltonian function becomes a more complicated process, and it may no longer be interpreted as the total system energy.

The System Lagrangian for Memory-Free Motion

For a rigid body moving through an ideal fluid near an otherwise calm free surface without memory effects, the total system Lagrangian is

$$\begin{aligned}\mathcal{L} = \frac{1}{2}\boldsymbol{\nu}^T\big(\boldsymbol{M}_{\mathrm{b}} + \boldsymbol{M}_{\mathcal{B}} + \Delta\boldsymbol{M}_{\mathcal{B}}(\boldsymbol{q}) + \boldsymbol{M}_{\mathcal{S}_0}(\boldsymbol{q},\boldsymbol{\nu})\big)\boldsymbol{\nu} \\ + g\left(m_{\mathrm{b}} - \rho\forall\right) z_{\mathrm{b}} + m_{\mathrm{b}} g \boldsymbol{r}_{\mathrm{cm}} \cdot \left(\boldsymbol{R}^T \boldsymbol{i}_3\right)\end{aligned} \tag{5.26}$$

The terms in (5.26) have the following interpretations:

- $\boldsymbol{\nu}^T(\boldsymbol{M}_{\mathrm{b}} + \boldsymbol{M}_{\mathcal{B}})\boldsymbol{\nu}/2$ is the system kinetic energy which results in Kirchhoff's equations for deeply submerged motion.
- $\boldsymbol{\nu}^T\Delta\boldsymbol{M}_{\mathcal{B}}\boldsymbol{\nu}/2$ accounts for the asymmetry in the fluid volume due to the free surface boundary; as compared to a deeply submerged vehicle, a near-surface vehicle will experience asymmetric forcing since there is more fluid below the vehicle than above.
- $\boldsymbol{\nu}^T\boldsymbol{M}_{\mathcal{S}_0}\boldsymbol{\nu}/2$ accounts for the fact that the bounding surface deforms in response to any vehicle motion.
- $g\left(\rho\forall - m_{\mathrm{b}}\right) z_{\mathrm{b}}$ accounts for non-neutral buoyancy.
- $m_{\mathrm{b}} g \boldsymbol{r}_{\mathrm{cm}} \cdot \left(\boldsymbol{R}^T \boldsymbol{i}_3\right)$ accounts for offset centers of mass and buoyancy [44].

Recognizing the physical contributions of each term, it is straightforward to extend this formulation to other operating conditions. For instance, if the vessel were to operate in the presence of a rigid, stationary boundary (such as the sea floor), the contributions from $\Delta\boldsymbol{M}_{\mathcal{B}}$ would remain, while $\boldsymbol{M}_{\mathcal{S}_0}$ would vanish. In this case, the vector potential function $\boldsymbol{\varphi}_{\mathrm{s}}$ could be approximated using the method of images, as in Section 4.3.2.

5.3.2 Memory-Free Equations of Motion

Prior to deriving the equations of motion, note the following vector differentiation identities which enable one to retain the convenient vector and matrix structure used in the system Lagrangian.

$$\frac{d}{d\boldsymbol{z}}\left(\frac{1}{2}\boldsymbol{z}^T\boldsymbol{P}\boldsymbol{z}\right)=\boldsymbol{P}\boldsymbol{z}, \qquad \boldsymbol{z}\in\mathbb{R}^n, \qquad \boldsymbol{P}=\boldsymbol{P}^T\in\mathbb{R}^{n\times n} \tag{5.27}$$

$$\frac{d}{dt}\boldsymbol{P}(\boldsymbol{z}(t))=\sum_{i=1}^{n}\frac{\partial\boldsymbol{P}}{\partial z_i}\frac{dz_i}{dt}, \qquad \boldsymbol{z}:\mathbb{R}\to\mathbb{R}^n, \qquad \boldsymbol{P}:\mathbb{R}^n\to\mathbb{R}^{n\times n} \tag{5.28}$$

$$\frac{\partial}{\partial\boldsymbol{\zeta}}\left(\boldsymbol{z}^T\boldsymbol{P}(\boldsymbol{\zeta})\boldsymbol{z}\right)=\sum_{i=1}^{n}\left[\left(\boldsymbol{e}_i\boldsymbol{z}^T\right)\frac{\partial\boldsymbol{P}}{\partial\zeta_i}\right]\boldsymbol{z}, \qquad \boldsymbol{\zeta},\boldsymbol{z},\boldsymbol{e}_i\in\mathbb{R}^n, \qquad \boldsymbol{P}:\mathbb{R}^n\to\mathbb{R}^{n\times n} \tag{5.29}$$

In (5.29), $\boldsymbol{e}_i$ is a unit vector with conforming dimensions and with a 1 in the i^{th} position. The equations of motion are then given by the Boltzman-Hamel equations (2.33), rewritten here for convenience:

$$\frac{d}{dt}\left(\frac{\partial\mathcal{L}}{\partial\boldsymbol{\nu}}\right)+\boldsymbol{G}(\boldsymbol{q},\boldsymbol{\nu})\frac{\partial\mathcal{L}}{\partial\boldsymbol{\nu}}-\boldsymbol{J}(\boldsymbol{q})^T\frac{\partial\mathcal{L}}{\partial\boldsymbol{q}}=\boldsymbol{F}$$

In the coming sections, the contributions to the equations of motion from each of the three Lagrangian functions are derived assuming the vehicle is neutrally buoyant.

Rigid Body Lagrangian

Beginning with the terms in the rigid body Lagrangian (2.33), compute

$$\frac{\partial\mathcal{L}_{\text{b}}}{\partial\boldsymbol{\nu}}=\boldsymbol{M}_{\text{b}}\boldsymbol{\nu}$$

Using the kinematic relations (2.13), one finds that

$$\boldsymbol{L}^T\frac{\partial(\boldsymbol{R}^T\boldsymbol{i}_3)}{\partial\boldsymbol{\theta}_{\text{b}}}^T=\widehat{\boldsymbol{R}^T\boldsymbol{i}_3}, \text{ and therefore, } -\boldsymbol{J}^T\frac{\partial\mathcal{L}_{\text{b}}}{\partial\boldsymbol{q}}=\begin{pmatrix}\boldsymbol{0}\\ -mg\boldsymbol{r}_{\text{cm}}\times(\boldsymbol{R}^T\boldsymbol{i}_3)\end{pmatrix}$$

The rigid body contribution to the equations of motion are

$$\boldsymbol{M}_{\text{b}}\dot{\boldsymbol{\nu}}+\boldsymbol{G}\boldsymbol{M}_{\text{b}}\boldsymbol{\nu}+\begin{pmatrix}\boldsymbol{0}\\ -mg\boldsymbol{r}_{\text{cm}}\times(\boldsymbol{R}^T\boldsymbol{i}_3)\end{pmatrix} \tag{5.30}$$

Fluid Body Lagrangian

Moving on to the contributions from the fluid body Lagrangian (5.23), compute

$$\frac{\partial \mathcal{L}_{\mathcal{B}}}{\partial \boldsymbol{\nu}} = \big(\boldsymbol{M}_{\mathcal{B}} + \Delta \boldsymbol{M}_{\mathcal{B}}(\boldsymbol{q})\big)\boldsymbol{\nu}$$

Using (5.28), and recalling that $\boldsymbol{J}_{\mathrm{i}}^T$ represents the i^{th} row of $\boldsymbol{J}$, evaluate

$$\frac{d}{dt}\left(\frac{\partial \mathcal{L}_{\mathcal{B}}}{\partial \boldsymbol{\nu}}\right) = \big(\boldsymbol{M}_{\mathcal{B}} + \Delta \boldsymbol{M}_{\mathcal{B}}(\boldsymbol{q})\big)\dot{\boldsymbol{\nu}} + \left[\sum_{i=1}^{6}(\boldsymbol{J}_i^T\boldsymbol{\nu})\frac{\partial \Delta \boldsymbol{M}_{\mathcal{B}}}{\partial q_i}\right]\boldsymbol{\nu}$$

With (5.29), one then finds

$$\boldsymbol{J}^T\frac{\partial \mathcal{L}_{\mathcal{B}}}{\partial \boldsymbol{q}} = \frac{1}{2}\left[\sum_{i=1}^{6}(\boldsymbol{J}_i\boldsymbol{\nu}^T)\frac{\partial \Delta \boldsymbol{M}_{\mathcal{B}}}{\partial q_i}\right]\boldsymbol{\nu}$$

The fluid body contributions to the equations of motion are

$$\big(\boldsymbol{M}_{\mathcal{B}} + \Delta \boldsymbol{M}_{\mathcal{B}}(\boldsymbol{q})\big)\dot{\boldsymbol{\nu}} + \boldsymbol{G}\big(\boldsymbol{M}_{\mathcal{B}} + \Delta \boldsymbol{M}_{\mathcal{B}}(\boldsymbol{q})\big)\boldsymbol{\nu} + \left[\sum_{i=1}^{6}\left(\boldsymbol{J}_i^T\boldsymbol{\nu}\mathbb{I} - \frac{1}{2}\boldsymbol{J}_i\boldsymbol{\nu}^T\right)\frac{\partial \Delta \boldsymbol{M}_{\mathcal{B}}}{\partial q_i}\right]\boldsymbol{\nu} \quad (5.31)$$

where $\mathbb{I}$ is the six-by-six identity matrix.

Free Surface Lagrangian

Moving to the free surface Lagrangian (5.25), compute

$$\frac{\partial \mathcal{L}_{\mathcal{S}_0}}{\partial \boldsymbol{\nu}} = \boldsymbol{M}_{\mathcal{S}_0}\boldsymbol{\nu} + \frac{1}{2}\left[\sum_{i=1}^{6}(\boldsymbol{e}_i\boldsymbol{\nu}^T)\frac{\partial \boldsymbol{M}_{\mathcal{S}_0}}{\partial \nu_i}\right]\boldsymbol{\nu}$$

Evaluating the time rate of change yields

$$\begin{aligned}\frac{d}{dt}\left(\frac{\partial \mathcal{L}_{\mathcal{S}_0}}{\partial \boldsymbol{\nu}}\right) = &\left[\boldsymbol{M}_{\mathcal{S}_0} + \sum_{i=1}^{6}\left((\boldsymbol{e}_i\boldsymbol{\nu}^T)\frac{\partial \boldsymbol{M}_{\mathcal{S}_0}}{\partial \nu_i} + \frac{\partial \boldsymbol{M}_{\mathcal{S}_0}}{\partial \nu_i}(\boldsymbol{\nu}\boldsymbol{e}_i^T)\right) + \frac{1}{2}\sum_{i=1}^{6}\sum_{j=1}^{6}(\boldsymbol{e}_i\boldsymbol{\nu}^T)\frac{\partial^2 \boldsymbol{M}_{\mathcal{S}_0}}{\partial \nu_i \partial \nu_j}(\boldsymbol{\nu}\boldsymbol{e}_j^T)\right]\dot{\boldsymbol{\nu}} \\ &+ \left[\sum_{i=1}^{6}(\boldsymbol{J}_i^T\boldsymbol{\nu})\frac{\partial \boldsymbol{M}_{\mathcal{S}_0}}{\partial q_i} + \frac{1}{2}\sum_{i=1}^{6}\sum_{j=1}^{6}(\boldsymbol{e}_i\boldsymbol{\nu}^T)\frac{\partial^2 \boldsymbol{M}_{\mathcal{S}_0}}{\partial \nu_i \partial q_j}(\boldsymbol{J}_j^T\boldsymbol{\nu})\right]\boldsymbol{\nu}\end{aligned}$$

Similar to the fluid body Lagrangian, compute

$$\boldsymbol{J}^T\frac{\partial \mathcal{L}_{\mathcal{S}_0}}{\partial \boldsymbol{q}} = \frac{1}{2}\left[\sum_{i=1}^{6}(\boldsymbol{J}_i\boldsymbol{\nu}^T)\frac{\partial \boldsymbol{M}_{\mathcal{S}_0}}{\partial q_i}\right]\boldsymbol{\nu}$$

The contribution from the free surface Lagrangian to the equations of motion is

$$\left[\boldsymbol{M}_{\mathcal{S}_0}+\sum_{i=1}^{6}\left((\boldsymbol{e}_i\boldsymbol{\nu}^T)\frac{\partial \boldsymbol{M}_{\mathcal{S}_0}}{\partial \nu_i}+\frac{\partial \boldsymbol{M}_{\mathcal{S}_0}}{\partial \nu_i}(\boldsymbol{\nu}\boldsymbol{e}_i^T)\right)+\frac{1}{2}\sum_{i=1}^{6}\sum_{j=1}^{6}(\boldsymbol{e}_i\boldsymbol{\nu}^T)\frac{\partial^2 \boldsymbol{M}_{\mathcal{S}_0}}{\partial \nu_i\partial \nu_j}(\boldsymbol{\nu}\boldsymbol{e}_j^T)\right]\dot{\boldsymbol{\nu}} \tag{5.32}$$
$$+\left[\sum_{i=1}^{6}\left(\boldsymbol{J}_i^T\boldsymbol{\nu}\mathbb{I}-\frac{1}{2}\boldsymbol{J}_i\boldsymbol{\nu}^T\right)\frac{\partial \boldsymbol{M}_{\mathcal{S}_0}}{\partial q_i}+\frac{1}{2}\sum_{i=1}^{6}\sum_{j=1}^{6}(\boldsymbol{e}_i\boldsymbol{\nu}^T)\frac{\partial^2 \boldsymbol{M}_{\mathcal{S}_0}}{\partial \nu_i\partial q_j}(\boldsymbol{J}_j^T\boldsymbol{\nu})\right]\boldsymbol{\nu}$$
$$+\boldsymbol{G}\left[\boldsymbol{M}_{\mathcal{S}_0}\boldsymbol{\nu}+\frac{1}{2}\sum_{i=1}^{6}(\boldsymbol{e}_i\boldsymbol{\nu}^T)\frac{\partial \boldsymbol{M}_{\mathcal{S}_0}}{\partial \nu_i}\right]\boldsymbol{\nu}$$

Kinetic Equations for Memory-Free Motion

Combining (5.30), (5.31), and (5.32) in (2.33), the dynamic equations for a marine craft moving in the presence of an otherwise undisturbed free surface are

$$\left(\boldsymbol{M}_{\mathrm{b}}+\boldsymbol{M}_{\mathrm{I}}(\boldsymbol{q},\boldsymbol{\nu})\right)\dot{\boldsymbol{\nu}}+\left(\boldsymbol{C}_{\mathrm{b}}(\boldsymbol{\nu})+\boldsymbol{C}_{\mathrm{I}}(\boldsymbol{q},\boldsymbol{\nu})\right)\boldsymbol{\nu}+\boldsymbol{D}_{\mathrm{I}}(\boldsymbol{q},\boldsymbol{\nu})\boldsymbol{\nu}+\boldsymbol{g}(\boldsymbol{\theta}_{\mathrm{b}})=\boldsymbol{F} \tag{5.33}$$

The system matrices are defined as follows. First, $\boldsymbol{C}_{\mathrm{b}}$ is the so-called Coriolis and centripetal matrix, defined as

$$\boldsymbol{C}_{\mathrm{b}}(\boldsymbol{\nu})=\boldsymbol{G}\boldsymbol{M}_{\mathrm{b}} \tag{5.34}$$

and the term $\boldsymbol{C}_{\mathrm{b}}(\boldsymbol{\nu})\boldsymbol{\nu}$ accounts for the fact that the equations of motion are expressed in a non-inertial reference frame. The "instantaneous fluid response matrices" $\boldsymbol{M}_{\mathrm{I}}$, $\boldsymbol{C}_{\mathrm{I}}$, and $\boldsymbol{D}_{\mathrm{I}}$

are defined as

$$\boldsymbol{M}_{\mathrm{I}}(\boldsymbol{q},\boldsymbol{\nu}) = \boldsymbol{M}_{\mathcal{B}} + \Delta\boldsymbol{M}_{\mathcal{B}} + \boldsymbol{M}_{\mathcal{S}_0} + \sum_{i=1}^{6}\left((\boldsymbol{e}_i\boldsymbol{\nu}^T)\frac{\partial \boldsymbol{M}_{\mathcal{S}_0}}{\partial \nu_i} + \frac{\partial \boldsymbol{M}_{\mathcal{S}_0}}{\partial \nu_i}(\boldsymbol{\nu}\boldsymbol{e}_i^T)\right) + \frac{1}{2}\sum_{i=1}^{6}\sum_{j=1}^{6}(\boldsymbol{e}_i\boldsymbol{\nu}^T)\frac{\partial^2 \boldsymbol{M}_{\mathcal{S}_0}}{\partial \nu_i \partial \nu_j}(\boldsymbol{\nu}\boldsymbol{e}_j^T) \tag{5.35}$$

$$\boldsymbol{C}_{\mathrm{I}}(\boldsymbol{q},\boldsymbol{\nu}) = \boldsymbol{G}\left[\boldsymbol{M}_{\mathcal{B}} + \Delta\boldsymbol{M}_{\mathcal{B}} + \boldsymbol{M}_{\mathcal{S}_0} + \frac{1}{2}\sum_{i=1}^{6}(\boldsymbol{e}_i\boldsymbol{\nu}^T)\frac{\partial \boldsymbol{M}_{\mathcal{S}_0}}{\partial \nu_i}\right] \tag{5.36}$$

$$\boldsymbol{D}_{\mathrm{I}}(\boldsymbol{q},\boldsymbol{\nu}) = \sum_{i=1}^{6}\left(\boldsymbol{J}_i^T\boldsymbol{\nu}\mathbb{I} - \frac{1}{2}\boldsymbol{J}_i\boldsymbol{\nu}^T\right)\left(\frac{\partial \Delta\boldsymbol{M}_{\mathcal{B}}}{\partial q_i} + \frac{\partial \boldsymbol{M}_{\mathcal{S}_0}}{\partial q_i}\right) + \frac{1}{2}\sum_{i=1}^{6}\sum_{j=1}^{6}\left(\boldsymbol{J}_j^T\boldsymbol{\nu}\right)\left(\boldsymbol{e}_i\boldsymbol{\nu}^T\right)\frac{\partial^2 \boldsymbol{M}_{\mathcal{S}_0}}{\partial \nu_i \partial q_j} \tag{5.37}$$

These matrices incorporate the hydrodynamic effects due to the instantaneous fluid response. The matrix $\boldsymbol{M}_{\mathrm{I}}$ represents the fluid added mass, and accounts for the acceleration-dependent hydrodynamic forces and moments. The Munk moments [8, 41] due to the instantaneous fluid response are captured by the matrix $\boldsymbol{C}_{\mathrm{I}}$. The matrix $\boldsymbol{D}_{\mathrm{I}}$ accounts for the velocity-dependent hydrodynamic effects incurred by the free surface; these effects persist for steady motions where the vehicle acceleration is zero. The vector $\boldsymbol{g}$ accounts for the hydrostatic restoring torque due to offset centers of mass and buoyancy and is defined as

$$\boldsymbol{g}(\boldsymbol{\theta}_{\mathrm{b}}) = \begin{pmatrix} \boldsymbol{0} \\ -m_{\mathrm{b}} g \boldsymbol{r}_{\mathrm{cm}} \times (\boldsymbol{R}^T \boldsymbol{i}_3) \end{pmatrix} \tag{5.38}$$

Referring to [1, Property 2.3], the matrices $\boldsymbol{C}_{\mathrm{b}}$ and $\boldsymbol{C}_{\mathrm{I}}$ can be redefined such that they are skew symmetric, a useful property in Lyapunov stability analysis.

Proposition 5.3.3 *One may define* $(\boldsymbol{C}_{\mathrm{b}}(\boldsymbol{\nu}) + \boldsymbol{C}_{\mathrm{I}}(\boldsymbol{q},\boldsymbol{\nu}))\,\boldsymbol{\nu} = \boldsymbol{C}_2(\boldsymbol{q},\boldsymbol{\nu})\boldsymbol{\nu}$ *where* $\boldsymbol{C}_2(\boldsymbol{q},\boldsymbol{\nu})$ *is skew symmetric:*

$$\boldsymbol{C}_2(\boldsymbol{q},\boldsymbol{\nu}) = \begin{pmatrix} \boldsymbol{0} & -\widehat{(\partial \mathcal{L}/\partial \boldsymbol{v})} \\ -\widehat{(\partial \mathcal{L}/\partial \boldsymbol{v})} & -\widehat{(\partial \mathcal{L}/\partial \boldsymbol{\omega})} \end{pmatrix} \tag{5.39}$$

Proof. Comparing (5.33) with (2.33), one recognizes that

$$(\boldsymbol{C}_{\mathrm{b}}(\boldsymbol{\nu})+\boldsymbol{C}_{\mathrm{I}}(\boldsymbol{q},\boldsymbol{\nu}))\boldsymbol{\nu}=\boldsymbol{G}(\boldsymbol{\nu})\frac{\partial\mathcal{L}}{\partial\boldsymbol{\nu}}=\begin{pmatrix}\hat{\boldsymbol{\omega}} & \mathbf{0}\\ \hat{\boldsymbol{v}} & \hat{\boldsymbol{\omega}}\end{pmatrix}\begin{pmatrix}\partial\mathcal{L}/\partial\boldsymbol{v}\\ \partial\mathcal{L}/\partial\boldsymbol{\omega}\end{pmatrix}$$

Noting that $\hat{\boldsymbol{a}}\boldsymbol{b}=-\hat{\boldsymbol{b}}\boldsymbol{a}$, write

$$(\boldsymbol{C}_{\mathrm{b}}(\boldsymbol{\nu})+\boldsymbol{C}_{\mathrm{I}}(\boldsymbol{q},\boldsymbol{\nu}))\boldsymbol{\nu}=\begin{pmatrix}-(\widehat{\partial\mathcal{L}/\partial\boldsymbol{v}})\boldsymbol{\omega}\\ -(\widehat{\partial\mathcal{L}/\partial\boldsymbol{v}})\boldsymbol{v}-(\widehat{\partial\mathcal{L}/\partial\boldsymbol{\omega}})\boldsymbol{\omega}\end{pmatrix}=\boldsymbol{C}_2(\boldsymbol{q},\boldsymbol{\nu})\boldsymbol{\nu}\quad\blacksquare$$

Remark 5.3.4 *Underwater vehicle motion in calm water without memory effects is invariant with respect to the coordinates x_{b}, y_{b}, and ψ_{b}. That is, the system Lagrangian (5.26) is invariant to displacements which are parallel to the undisturbed free surface, implying that x_{b}, y_{b}, and ψ_{b} are ignorable coordinates.*

Some mention should be made concerning the extent to which the free surface is correctly resolved in this model. Unlike the Cummins equations [19], memory effects are neglected in this model. An impulsive rest-to-rest perturbation in the body's position and orientation, for example, would leave no residual fluid motion in the form of radiated surface waves. This model only satisfies an "instantaneous" free surface boundary condition, truncating the ensuing fluid motion and its effect on the vessel.

5.3.3 Captive Model Equations: Motion in Pure Surge

To see more clearly what physical effects are incorporated in the memory-free model, the equations of motion are specialized to the case of pure surge motion parallel to the undisturbed free surface. This is analogous to a "captive" model scenario, where a vehicle undergoes a prescribed motion and the resultant forces and moments are computed. The equations of motion for a submerged vehicle which maintains pure surge motion are presented to study the resulting forces and moments in the longitudinal degrees of freedom (surge, heave, and pitch).

Assumption 5.3.5 *For forward motion parallel to the undisturbed free surface, let* $\boldsymbol{\nu} = u\boldsymbol{e}_1$ *and let* $\boldsymbol{\theta}_\mathrm{b} = \mathbf{0}$*. Also, assume that the vehicle has coincident centers of mass and buoyancy and assume that the hull exhibits port-starboard symmetry so that the equations in surge, heave, and pitch may be decoupled from the equations in yaw, roll, and sway.*

Using symbolic mathematics software, one may simplify the equations to specified operating conditions. Define the auxiliary matrix

$$\bar{\boldsymbol{M}}_{\mathcal{S}_0} = -\frac{\rho}{2}\iint_{\mathcal{S}_0} (\boldsymbol{\varphi}_\mathrm{K} + \boldsymbol{\varphi}_\mathrm{s})\,(\boldsymbol{\varphi}_\mathrm{K} + \boldsymbol{\varphi}_\mathrm{s})^T\, dA \tag{5.40}$$

For the conditions given in Assumption 5.3.5, the reduced impulsive response matrices in the surge, heave, and pitch directions are

$$\begin{aligned}\boldsymbol{M}_\mathrm{I} = &\begin{pmatrix} M_{\mathcal{B}11} + \Delta M_{\mathcal{B}11} & M_{\mathcal{B}31} + \Delta M_{\mathcal{B}31} & M_{\mathcal{B}51} + \Delta M_{\mathcal{B}51} \\ M_{\mathcal{B}31} + \Delta M_{\mathcal{B}31} & M_{\mathcal{B}33} + \Delta M_{\mathcal{B}33} & M_{\mathcal{B}53} + \Delta M_{\mathcal{B}53} \\ M_{\mathcal{B}51} + \Delta M_{\mathcal{B}51} & M_{\mathcal{B}53} + \Delta M_{\mathcal{B}53} & M_{\mathcal{B}55} + \Delta M_{\mathcal{B}55} \end{pmatrix} \\ &+ \frac{u^2}{g}\begin{pmatrix} 0 & 0 & -\frac{3}{2}\bar{M}_{\mathcal{S}_0 11,z_\mathrm{b}} \\ 0 & \bar{M}_{\mathcal{S}_0 11,z_\mathrm{b}z_\mathrm{b}} & \bar{M}_{\mathcal{S}_0 11,z_\mathrm{b}\theta_\mathrm{b}} - \bar{M}_{\mathcal{S}_0 31,z_\mathrm{b}} \\ -\frac{3}{2}\bar{M}_{\mathcal{S}_0 11,z_\mathrm{b}} & \bar{M}_{\mathcal{S}_0 11,z_\mathrm{b}\theta_\mathrm{b}} - \bar{M}_{\mathcal{S}_0 31,z_\mathrm{b}} & \bar{M}_{\mathcal{S}_0 11,\theta_\mathrm{b}\theta_\mathrm{b}} - 2\bar{M}_{\mathcal{S}_0 51,z_\mathrm{b}} \end{pmatrix}\end{aligned} \tag{5.41}$$

$$\boldsymbol{C}_\mathrm{I} = -u\begin{pmatrix} 0 & 0 & 0 \\ 0 & 0 & 0 \\ M_{\mathcal{B}31} + \Delta M_{\mathcal{B}31} & M_{\mathcal{B}33} + \Delta M_{\mathcal{B}33} & M_{\mathcal{B}35} + \Delta M_{\mathcal{B}35} \end{pmatrix} \tag{5.42}$$

$$\boldsymbol{D}_\mathrm{I} = -\frac{u}{2}\begin{pmatrix} 0 & 0 & 0 \\ \Delta M_{\mathcal{B}11,z_\mathrm{b}} & \Delta M_{\mathcal{B}31,z_\mathrm{b}} & \Delta M_{\mathcal{B}51,z_\mathrm{b}} \\ \Delta M_{\mathcal{B}11,\theta_\mathrm{b}} & \Delta M_{\mathcal{B}31,\theta_\mathrm{b}} & \Delta M_{\mathcal{B}51,\theta_\mathrm{b}} \end{pmatrix} \tag{5.43}$$

In the above expressions, a subscript ij denotes the (i,j) element of the corresponding matrix and a subscript $,q_i$ denotes a partial derivative with respect to q_i. For instance, $\Delta M_{\mathcal{B}11,z_\mathrm{b}}$ is shorthand for

$$\Delta M_{\mathcal{B}11,z_\mathrm{b}} = \boldsymbol{e}_1^T \frac{\partial \Delta \boldsymbol{M}_\mathcal{B}}{\partial z_\mathrm{b}} \boldsymbol{e}_1 \tag{5.44}$$

Note that $\boldsymbol{M}_{\mathcal{S}_0} = \mathbf{0}$ for a vehicle undergoing pure surge parallel to the undisturbed free surface. This occurs because the system is being excited in a direction corresponding to an ignorable coordinate, as discussed in Remark 5.3.4. Note that when $\boldsymbol{M}_{\mathcal{S}_0} = \mathbf{0}$, it does not imply that there is no free surface deformation. Rather, it implies that the free surface kinetic and potential energies must balance each other:

$$\frac{1}{2}\boldsymbol{\nu}^T \boldsymbol{M}_{\mathcal{S}_0}\boldsymbol{\nu} = T_{\mathcal{S}} - V_{\mathcal{S}} = 0 \tag{5.45}$$

At a constant depth and orientation, the elements in $\Delta\boldsymbol{M}_{\mathcal{B}}$ and $\bar{\boldsymbol{M}}_{\mathcal{S}_0}$ will be constant, though their gradients will be nonzero. These gradient terms populate the matrix $\boldsymbol{D}_{\mathrm{I}}$ and also add additional terms to the added mass matrix $\boldsymbol{M}_{\mathrm{I}}$. Interestingly, the terms on the second line of (5.41) are multiplied by the factor u^2/g, which resembles the square of the Froude number

$$Fr = \frac{u}{\sqrt{gL}} \tag{5.46}$$

The Froude number is often used to characteriz the portion of the radiation forces associated with wave making.

The equations in surge, heave, and pitch for a vehicle constrained to pure surge motion are

$$\begin{aligned}
&\begin{pmatrix} M_{\mathcal{B}11}+\Delta M_{\mathcal{B}11} & M_{\mathcal{B}31}+\Delta M_{\mathcal{B}31} & M_{\mathcal{B}51}+\Delta M_{\mathcal{B}51} \\ M_{\mathcal{B}31}+\Delta M_{\mathcal{B}31} & M_{\mathcal{B}33}+\Delta M_{\mathcal{B}33} & M_{\mathcal{B}53}+\Delta M_{\mathcal{B}53} \\ M_{\mathcal{B}51}+\Delta M_{\mathcal{B}51} & M_{\mathcal{B}53}+\Delta M_{\mathcal{B}53} & M_{\mathcal{B}55}+\Delta M_{\mathcal{B}55} \end{pmatrix}\begin{pmatrix} \dot{u} \\ 0 \\ 0 \end{pmatrix} \\
&+\frac{u^2}{g}\begin{pmatrix} 0 & 0 & -\frac{3}{2}\bar{M}_{\mathcal{S}11,z_{\mathrm{b}}} \\ 0 & \bar{M}_{\mathcal{S}11,z_{\mathrm{b}}z_{\mathrm{b}}} & \bar{M}_{\mathcal{S}11,z_{\mathrm{b}}\theta_{\mathrm{b}}}-\bar{M}_{\mathcal{S}31,z_{\mathrm{b}}} \\ -\frac{3}{2}\bar{M}_{\mathcal{S}11,z_{\mathrm{b}}} & \bar{M}_{\mathcal{S}11,z_{\mathrm{b}}\theta_{\mathrm{b}}}-\bar{M}_{\mathcal{S}31,z_{\mathrm{b}}} & \bar{M}_{\mathcal{S}11,\theta_{\mathrm{b}}\theta_{\mathrm{b}}}-2\bar{M}_{\mathcal{S}51,z_{\mathrm{b}}} \end{pmatrix}\begin{pmatrix} \dot{u} \\ 0 \\ 0 \end{pmatrix} \\
&= u^2\begin{pmatrix} 0 \\ \frac{1}{2}\Delta M_{\mathcal{B}11,z_{\mathrm{b}}} \\ M_{\mathcal{B}31}+\Delta M_{\mathcal{B}31}+\frac{1}{2}\Delta M_{\mathcal{B}11,\theta_{\mathrm{b}}} \end{pmatrix} - \begin{pmatrix} f_{\mathrm{surge}} \\ f_{\mathrm{heave}} \\ \tau_{\mathrm{pitch}} \end{pmatrix}
\end{aligned} \tag{5.47}$$

The expressions f_{surge}, f_{heave} and τ_{pitch} are the generalized constraint forces which are necessary to maintain the straight ahead motion.

Assuming constant velocity, the resulting hydrodynamic forces in surge and heave and the hydrodynamic moment in pitch are

$$\begin{pmatrix} f_{\text{surge}} \\ f_{\text{heave}} \\ \tau_{\text{pitch}} \end{pmatrix} = u^2 \begin{pmatrix} 0 \\ \frac{1}{2}\Delta M_{\mathcal{B}11,z_{\text{b}}} \\ M_{\mathcal{B}31} + \Delta M_{\mathcal{B}31} + \frac{1}{2}\Delta M_{\mathcal{B}11,\theta_{\text{b}}} \end{pmatrix} \tag{5.48}$$

Though only motion in surge is considered, (5.48) indicates that a suction force and a pitching moment result from straight-ahead motion. These terms may be interpreted as the free surface suction effects described by Crook [30]. For a submerged body traveling straight ahead at constant speed near the free surface, the analytical expression for the free surface suction force is simply

$$f_{\text{suction}} = \frac{1}{2}u^2 \frac{\partial \Delta M_{\mathcal{B}11}}{\partial z_{\text{b}}} \tag{5.49}$$

Second-order drift forces [30, 31] could be obtained by prescribing an additional oscillatory motion in heave. One effect absent from this model is a traditional wave-resistance force. Without surge accelerations $\dot{u}$, no hydrodynamic forces exist in the surge equation. This is contrary to numerical and physical results, which predict velocity-dependent wave resistance forces opposing the surge motion [30, 12]. This absence underscores the shortcoming of the memory-free model: because the model does not explicitly capture the vehicle-induced wake pattern, the corresponding wake-induced forces do not appear in the equations of motion.

5.3.4 Equations of Motion for a Circle near a Rigid Wall

Additional insights to the memory-free model are gained by returning to the example in Section 4.3.2. For a circle near a rigid wall, $\mathcal{L}_{\mathcal{S}_0} = 0$ and the only matrices required to simulate the equations are $\boldsymbol{M}_{\mathcal{B}}$ and $\Delta\boldsymbol{M}_{\mathcal{B}}$. Though not explicitly defined in Section 4.3.2,

the analytical expressions for the added mass matrices are

$$\boldsymbol{M}_{\mathcal{B}} = \begin{pmatrix} \rho\pi a^2 & 0 \\ 0 & \rho\pi a^2 \end{pmatrix} \tag{5.50}$$

$$\Delta\boldsymbol{M}_{\mathcal{B}} = \begin{pmatrix} \frac{1}{2}\rho\pi a^2 \frac{a^2}{z_{\mathrm{bw}}^2} & 0 \\ 0 & \frac{1}{2}\rho\pi a^2 \frac{a^2}{z_{\mathrm{bw}}^2} \end{pmatrix} \tag{5.51}$$

$$\tag{5.52}$$

Recall that a is the radius of the cylinder and z_{bw} represents the distance between the cylinder center and the rigid wall. Since the circle was assumed to be neutrally buoyant, $\rho\pi a^2 = m_{\mathrm{b}}$. One may then define the rigid body and the fluid body kinetic energy functions:

$$T_{\mathrm{b}} = \frac{1}{2}\dot{\boldsymbol{x}}_{\mathrm{b}}^T \boldsymbol{M}_{\mathrm{b}} \dot{\boldsymbol{x}}_{\mathrm{b}} = \frac{1}{2} m_{\mathrm{b}} \left(\dot{x}_{\mathrm{b}}^2 + \dot{z}_{\mathrm{b}}^2\right) \tag{5.53}$$

$$T_{\mathcal{B}} = \frac{1}{2}\dot{\boldsymbol{x}}_{\mathrm{b}}^T \left(\boldsymbol{M}_{\mathcal{B}} + \Delta\boldsymbol{M}_{\mathcal{B}}\right) \dot{\boldsymbol{x}}_{\mathrm{b}} = \frac{1}{2} m_{\mathrm{b}} \left(1 + \frac{1}{2}\frac{a^2}{z_{\mathrm{bw}}^2}\right) \left(\dot{x}_{\mathrm{b}}^2 + \dot{z}_{\mathrm{b}}^2\right) \tag{5.54}$$

The surface-perturbed added mass matrix characterizes how the fluid kinetic energy is affected by changes in distance relative to the wall; as the circle moves closer to the wall, $T_{\mathcal{B}}$ will increase. The resulting suction force when $\dot{z}_{\mathrm{b}} = 0$ is given by (5.49):

$$f_{\mathrm{suction}} = \frac{1}{2} m_{\mathrm{b}} \dot{x}_{\mathrm{b}}^2 \frac{a^2}{z_{\mathrm{bw}}^3} \tag{5.55}$$

Note that sign of the above expression indicates that the force is directed towards the wall. In the absence of external forces, the circle-fluid system conserves energy. This implies that an increase in fluid kinetic energy incurs a decrease in rigid body kinetic energy, ultimately decreasing the velocity of the circle. We observed this phenomenon in Figure 4.6.

These results enable additional insights into the surface-perturbed added mass matrix: $\Delta\boldsymbol{M}_{\mathcal{B}}$ defines how much additional work the circle must exert to accelerate the ambient fluid near the wall, and its gradient defines how quickly the circle accelerates towards the wall. While the surface-perturbed added mass matrix was computed for a rigid wall in this example, is is expected that one will observe similar effects for a rigid body near a free surface.

5.3.5 Remarks on System Identification

While it far exceeds the scope of this dissertation to develop an identification technique for the proposed model, one can make preliminary observations based on the model structure. Assuming that $\boldsymbol{M}_{\mathrm{b}}$ is known, and that $\boldsymbol{M}_{\mathcal{B}}$ can be computed by conventional means, there are 42 state dependent parameters that must be identified, 21 each from $\Delta\boldsymbol{M}_{\mathcal{B}}(\boldsymbol{q})$ and $\boldsymbol{M}_{\mathcal{S}_0}(\boldsymbol{q},\boldsymbol{\nu})$. In the absence of functional forms for the state dependencies, it may be necessary to compile parameters into a multi-dimensional lookup table prior to simulating the equations of motion. Fortunately, physical intuition suggests some simplifications. From Remark 5.3.4, the partial derivatives with respect to x_{b}, y_{b}, and ψ_{b} are zero. Further, if the vessel is axisymmetric about the $\boldsymbol{b}_1$ axis, the partial derivatives with respect to ϕ_{b} will be zero. This is often a reasonable assumption for un-appended underwater vehicles. In the very special case of a spherical geometry, the only non-zero partial derivatives will be with respect to the depth and the translational velocities.

One approach to computing $\Delta\boldsymbol{M}_{\mathcal{B}}$ and $\boldsymbol{M}_{\mathcal{S}_0}$ is to compute the potential functions $\boldsymbol{\varphi}_{\mathrm{k}}$ and $\boldsymbol{\varphi}_{\mathrm{s}}$ which satisfy the specified boundary conditions (3.59) and (3.56). This approach was taken in [60] to achieve a partial solution for the case of a 2-D circular cylinder. However, it would be more practical to use a panel method to numerically compute these potential functions. One could also use experimental data to populate the parameters. For instance, one could employ planar motion mechanism (PMM) testing (physical or virtual) [61] to generate data for combinations of operating conditions of interest. Leveraging the fact that $\boldsymbol{M}_{\mathcal{B}}$ only depends on the configuration and $\boldsymbol{M}_{\mathcal{S}_0}$ depends on both the configuration and velocity, one could expand conventional identification techniques (see, for instance, [6]) to extract these parameters from the data. One could then use finite difference techniques to approximate the derivatives of the hydrodynamic terms.

Another approach leverages the relationship between the hydrodynamic parameters and the system energy functions. Note that the following relationship holds, regardless of the vehicle

motions

$$\frac{1}{2}\boldsymbol{\nu}^T\left(\boldsymbol{M}_{\mathcal{B}}+\Delta\boldsymbol{M}_{\mathcal{B}}(\boldsymbol{q})+\boldsymbol{M}_{\mathcal{S}_0}(\boldsymbol{q},\boldsymbol{\nu})\right)\boldsymbol{\nu}=T_{\mathcal{F}}(\boldsymbol{q},u)-V_{\mathcal{F}}(\boldsymbol{q},u) \tag{5.56}$$

If the vehicle were to undergo pure surge motion, this relationship would isolate the (1,1) element of each matrix:

$$\frac{1}{2}\left(M_{\mathcal{B}11}+\Delta M_{\mathcal{B}11}(\boldsymbol{q})+M_{\mathrm{s}11}(\boldsymbol{q},u)\right)u^2=T_{\mathcal{F}}(\boldsymbol{q},u)-V_{\mathcal{F}}(\boldsymbol{q},u) \tag{5.57}$$

While it would be challenging (if not impossible) to measure the fluid kinetic and potential energies in a physical experiment[1], the fluid velocity and free surface deformations are typically computed in CFD[2]. Assuming $\boldsymbol{M}_{\mathcal{B}}$ is computed *a priori*, then (5.57) represents a single equation for two unknowns. These terms may be isolated when considering the physical meanings of each term. If the free surface were replaced by a rigid wall, $M_{\mathcal{S}_0 11}$ would vanish in (5.57). This enables a two-part identification procedure where one computes $\Delta M_{\mathcal{B}11}$ by simulating the vehicle near a rigid boundary, then computes $M_{\mathcal{S}_0 11}$ by simulating the vehicle near a free surface. After identifying the (1,1) elements, this procedure could be sequentially carried out in the other degrees of freedom to populate the complete matrices. It remains to show, however, if and when the elements of $\Delta\boldsymbol{M}_{\mathcal{B}}$ can be reasonably approximated from a fluid with a rigid wall. In the trivial case that the body is deeply submerged, $\Delta\boldsymbol{M}_{\mathcal{B}}=\boldsymbol{0}$ whether the boundary is a rigid wall or a free surface. One would therefore expect a range of depths where this approximation would be valid. Even in cases where the rigid wall approximation is poor, the energy balance (5.56) still yields an additional equation to aid in the identification process; this relationship would not be apparent if one followed a Newtonian modeling approach.

[1] Also, a physical experiment would include viscous effects that are not included in this energy balance.

[2] One would have to be wary of discretization errors when numerically integrating the fluid kinetic energy.

5.4 Memory-Affected Impulse Model

The absence of wave resistance forces is the primary shortcoming of the memory-free model. By only studying the instantaneous response of the ambient fluid, the free surface evolution is effectively truncated. These effects are depicted in Figure 5.1. In Figure 5.1a, the instantaneous fluid response to pure surge motion of an ellipse is computed using a 2-D panel method. Since the body has fore-aft symmetry, the free surface elevation and the corresponding fluid force distribution are also both symmetric. The free surface trough results in a low pressure region which tends to pull the vehicle towards the free surface, though because the pressure distribution is symmetric, no net drag force is experienced by the vehicle. On the other hand, Figure 5.1b depicts the surface elevation and pressure distribution when the free surface is allowed to evolve. As the body undergoes forward motion, the free surface trough tends to lag behind. This moves the low pressure region towards the aft of the body, which causes a portion of this "suction" force to project into the surge direction and also causes a nose down pitching moment. This comparison highlights the importance of the memory effects for computing wave resistance forces. It also suggests that the free surface suction force is closely related to the wave resistance forces, two hydrodynamic phenomena which are typically treated separately.

To capture the memory effects in the Lagrangian model, one must define a suitable velocity potential which governs the memory effects. Recall Cummins' velocity potential (4.117), which incorporated the memory effects for small vessel motions:

$$\phi_{\mathrm{C}}(\dot{\boldsymbol{q}},t)=\boldsymbol{\varphi}_{\mathrm{i}}\cdot\dot{\boldsymbol{q}}(t)+\int_0^t\boldsymbol{\varphi}_{\mathrm{m}}(t-\tau)\cdot\dot{\boldsymbol{q}}(\tau)d\tau$$

Comparing ϕ_{C} to the memory-free velocity potential (5.20), one finds that the impulsive velocity potential must be a function of the generalized coordinates $\boldsymbol{q}(t)$:

$$\boldsymbol{\varphi}_{\mathrm{i}}(\boldsymbol{q}(t))=\boldsymbol{\varphi}_{\mathrm{K}}+\boldsymbol{\varphi}_{\mathrm{s}}(\boldsymbol{q}(t)) \tag{5.58}$$

Moreover, since each impulse also initializes a component of the memory potential, the

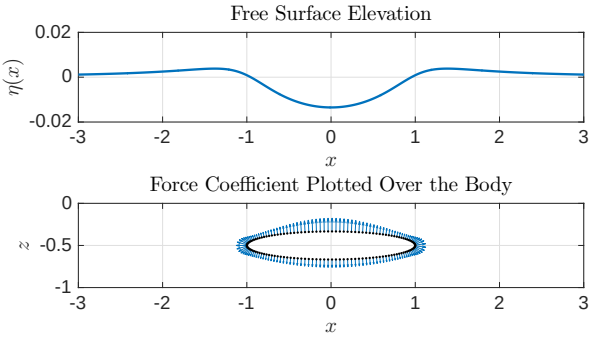

(a) Memory-free depiction of the free surface and distribution of the force coefficient over the vehicle.

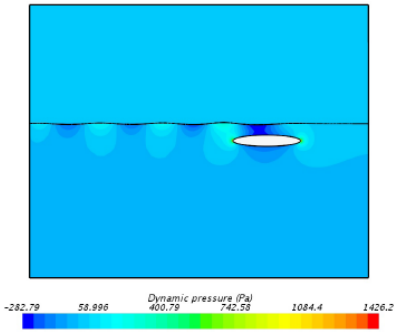

(b) Memory-affected depiction of the free surface and distribution of the pressure over the vehicle.

Figure 5.1: Comparison of the free surface computed from a 2-D panel method without memory effects and a memory-affected free surface computed from an unsteady Euler solver.

memory potential must also be a function of the generalized coordinates:

$$\phi_{\mathrm{m}}(t) = \int_0^t \boldsymbol{\varphi}_{\mathrm{m}}(\boldsymbol{q}(\tau), t-\tau) \cdot \boldsymbol{\nu}(\tau) d\tau \tag{5.59}$$

The complete velocity potential for a submerged craft operating near the free surface with memory effects is

$$\phi(\boldsymbol{q}(t), \boldsymbol{\nu}(t), t) = (\boldsymbol{\varphi}_{\mathrm{k}} + \boldsymbol{\varphi}_{\mathrm{s}}(\boldsymbol{q}(t))) \cdot \boldsymbol{\nu}(t) + \int_0^t \boldsymbol{\varphi}_{\mathrm{m}}(\boldsymbol{q}(\tau), t-\tau) \cdot \boldsymbol{\nu}(\tau) d\tau \tag{5.60}$$

Prior to deriving the equations of motion, note the following notation which will be used in the remainder of this chapter. Because the potential function (5.60) has state variables evaluated at both time t and time τ, the expressions which appear in the equations of motion will similarly have these dependencies. Since it will be tedious to constantly specify, for instance $\boldsymbol{q}(t)$ versus $\boldsymbol{q}(\tau)$, the following simplification is employed for the sake of brevity. A state variable appearing without a functional dependency will be assumed to be evaluated at time t: $\boldsymbol{q} = \boldsymbol{q}(t)$ or $\boldsymbol{\nu} = \boldsymbol{\nu}(t)$. If a functional dependency is given, the state variable is to be evaluated at the time indicated: $\boldsymbol{q}(\tau)$ refers to the value of $\boldsymbol{q}$ evaluated at time τ.

5.4.1 Memory-Affected System Lagrangian

Fluid Body Lagrangian

Beginning with the fluid body Lagrangian (5.14), substitute in the assumed velocity potential (5.60)

$$\mathcal{L}_{\mathcal{B}} = \frac{1}{2}\rho \iint_{\mathcal{B}} \left[(\boldsymbol{\varphi}_{\mathrm{K}} + \boldsymbol{\varphi}_{\mathrm{s}}(\boldsymbol{q})) \cdot \boldsymbol{\nu} + \int_0^t \boldsymbol{\varphi}_{\mathrm{m}}(\boldsymbol{q}(\tau), t-\tau) \cdot \boldsymbol{\nu}(\tau) d\tau \right] \boldsymbol{b}^T dS \; \boldsymbol{\nu} - \rho g \forall z_{\mathrm{b}} \tag{5.61}$$

Recall the following matrices from Section 5.3

$$\boldsymbol{M}_{\mathcal{B}} = \rho \iint_{\mathcal{B}} \boldsymbol{\varphi}_{\mathrm{K}} \boldsymbol{b}^T dS$$
$$\Delta \boldsymbol{M}_{\mathcal{B}}(\boldsymbol{q}) = \mathrm{sym}\left(\rho \iint_{\mathcal{B}} \boldsymbol{\varphi}_{\mathrm{s}}(\boldsymbol{q}) \boldsymbol{b}^T dS \right)$$

Similar to the Cummins equations (4.128), define the fluid kernel matrix

$$\boldsymbol{K}_{\mathcal{B}}(\boldsymbol{q}(\tau), t-\tau) = \frac{\rho}{2} \iint_{\mathcal{B}} \boldsymbol{b} \; \boldsymbol{\varphi}_{\mathrm{m}}^T(\boldsymbol{q}(\tau), t-\tau) dS \tag{5.62}$$

The fluid body Lagrangian is

$$\mathcal{L}_{\mathcal{B}} = \frac{1}{2}\boldsymbol{\nu}^T \left(\boldsymbol{M}_{\mathcal{B}} + \Delta \boldsymbol{M}_{\mathcal{B}}(\boldsymbol{q}) \right) \boldsymbol{\nu} + \boldsymbol{\nu}^T \int_0^t \boldsymbol{K}_{\mathcal{B}}(\boldsymbol{q}(\tau), t-\tau) \boldsymbol{\nu}(\tau) d\tau - \rho g \forall z_{\mathrm{b}} \tag{5.63}$$

As compared to the fluid body Lagrangian in Section 5.3, the memory effects potential contributes to the fluid kinetic energy in the form of a convolution integral. This term accounts for the past motions $\boldsymbol{\nu}(\tau)$ of the vehicle. One should note that the quantity

$$\boldsymbol{\nu}^T(t) \boldsymbol{K}_{\mathcal{B}}(\boldsymbol{q}(\tau), t-\tau) \boldsymbol{\nu}(\tau)$$

is *not* a quadratic form – unless $\boldsymbol{\nu}$ is a constant, $\boldsymbol{\nu}(t)$ and $\boldsymbol{\nu}(\tau)$ are two different vectors. Thus, one cannot claim anything about the symmetry of $\boldsymbol{K}_{\mathcal{B}}$.

Free Surface Lagrangian

Moving on to the free surface Lagrangian, evaluate

$$-\frac{\rho}{4g}\iint_{\mathcal{S}_0}\phi^2 dS = -\frac{\rho}{4g}\iint_{\mathcal{S}_0}\Big[\boldsymbol{\nu}^T\left(\boldsymbol{\varphi}_{\mathrm{K}}\boldsymbol{\varphi}_{\mathrm{K}}^T + \boldsymbol{\varphi}_{\mathrm{K}}\boldsymbol{\varphi}_{\mathrm{s}}^T(\boldsymbol{q}) + \boldsymbol{\varphi}_{\mathrm{s}}\boldsymbol{\varphi}_{\mathrm{K}}^T + \boldsymbol{\varphi}_{\mathrm{s}}(\boldsymbol{q})\boldsymbol{\varphi}_{\mathrm{s}}^T(\boldsymbol{q})\right)\boldsymbol{\nu}$$
$$+ 2\boldsymbol{\nu}^T\left(\boldsymbol{\varphi}_{\mathrm{K}} + \boldsymbol{\varphi}_{\mathrm{s}}(\boldsymbol{q})\right)\int_0^t \boldsymbol{\varphi}_{\mathrm{m}}^T(\boldsymbol{q}(\tau), t-\tau)\boldsymbol{\nu}(\tau)d\tau$$
$$+ \left(\int_0^t \boldsymbol{\varphi}_{\mathrm{m}}^T(\boldsymbol{q}(\tau), t-\tau)\boldsymbol{\nu}(\tau)d\tau\right)^2\Big]dS \tag{5.64}$$

Again, revisit the matrix definitions from Section 5.3:

$$\boldsymbol{A}_{\mathcal{S}_0} = -\frac{\rho}{2g}\iint_{\mathcal{S}_0}\boldsymbol{\varphi}_{\mathrm{K}}\boldsymbol{\varphi}_{\mathrm{K}}^T dS$$
$$\boldsymbol{B}_{\mathcal{S}_0}(\boldsymbol{q}) = -\frac{\rho}{2g}\iint_{\mathcal{S}_0}\left(\boldsymbol{\varphi}_{\mathrm{s}}(\boldsymbol{q})\boldsymbol{\varphi}_{\mathrm{K}}^T + \boldsymbol{\varphi}_{\mathrm{K}}\boldsymbol{\varphi}_{\mathrm{s}}^T(\boldsymbol{q})\right)dS$$
$$\boldsymbol{C}_{\mathcal{S}_0}(\boldsymbol{q}) = -\frac{\rho}{2g}\iint_{\mathcal{S}_0}\boldsymbol{\varphi}_{\mathrm{s}}(\boldsymbol{q})\boldsymbol{\varphi}_{\mathrm{s}}^T(\boldsymbol{q})dS$$

To simplify the additional terms featuring the memory potential, define

$$\boldsymbol{D}_{\mathcal{S}_0}(\boldsymbol{q}, \boldsymbol{q}(\tau), t-\tau) = -\frac{\rho}{2g}\iint_{\mathcal{S}_0}\left[\boldsymbol{\varphi}_{\mathrm{K}} + \boldsymbol{\varphi}_{\mathrm{s}}(\boldsymbol{q})\right]\boldsymbol{\varphi}_{\mathrm{m}}^T(\boldsymbol{q}(\tau), t-\tau)dS$$
$$\varepsilon_{\mathcal{S}_0}(t) = \iint_{\mathcal{S}_0}\left(\int_0^t \boldsymbol{\varphi}_{\mathrm{m}}^T(\boldsymbol{q}(\tau), t-\tau)\boldsymbol{\nu}(\tau)d\tau\right)^2 dS$$
$$= \iint_{\mathcal{S}_0}\phi_{\mathrm{m}}(t)^2 dS$$

Note that $\boldsymbol{D}_{\mathcal{S}_0}$ couples the impulsive potentials $\boldsymbol{\varphi}_{\mathrm{K}}$ and $\boldsymbol{\varphi}_{\mathrm{s}}$ with the memory potential $\boldsymbol{\varphi}_{\mathrm{m}}$. Altogether, the free surface Lagrangian takes the form

$$\mathcal{L}_{\mathcal{S}_0} = \frac{\partial^2}{\partial t^2}\left[\frac{1}{2}\boldsymbol{\nu}^T\left[\boldsymbol{A}_{\mathcal{S}_0} + \boldsymbol{B}_{\mathcal{S}_0}(\boldsymbol{q}) + \boldsymbol{C}_{\mathcal{S}_0}(\boldsymbol{q})\right]\boldsymbol{\nu} + \int_0^t \boldsymbol{\nu}^T\boldsymbol{D}_{\mathcal{S}_0}(\boldsymbol{q}, \boldsymbol{q}(\tau), t-\tau)\boldsymbol{\nu}(\tau)d\tau + \varepsilon_{\mathcal{S}_0}(t)\right]$$

The same approach used in Section 5.3 is used here to evaluate the time derivatives; during each impulse, the vehicle velocities are assumed to be constant. This enabled the definition of the free surface added mass matrix:

$$\boldsymbol{M}_{\mathcal{S}_0}(\boldsymbol{q}, \boldsymbol{\nu}) = \frac{\partial^2}{\partial t^2}\left[\boldsymbol{A}_{\mathcal{S}_0} + \boldsymbol{B}_{\mathcal{S}_0}(\boldsymbol{q}) + \boldsymbol{C}_{\mathcal{S}_0}(\boldsymbol{q})\right]$$

Additionally, define the terms

$$\begin{aligned}\boldsymbol{K}_{\mathcal{S}_0 1}(\boldsymbol{q},\boldsymbol{\nu},\boldsymbol{q}(\tau),t-\tau) &= \frac{\partial^2}{\partial t^2}\boldsymbol{D}_{\mathcal{S}_0}(\boldsymbol{q},\boldsymbol{q}(\tau),t-\tau)\\ &= \frac{\partial^2 \boldsymbol{D}_{\mathcal{S}_0}(\boldsymbol{q},\boldsymbol{q}(\tau),t-\tau)}{\partial(t-\tau)^2}\\ &\quad+\sum_{i=1}^{6}\sum_{j=1}^{6}\Bigg[\frac{\partial^2 \boldsymbol{D}_{\mathcal{S}_0}(\boldsymbol{q},\boldsymbol{q}(\tau),t-\tau)}{\partial q_i \partial q_j}(\boldsymbol{J}_i^T\boldsymbol{\nu})(\boldsymbol{J}_j^T\boldsymbol{\nu})\\ &\quad+\frac{\partial \boldsymbol{D}_{\mathcal{S}_0}(\boldsymbol{q},\boldsymbol{q}(\tau),t-\tau)}{\partial q_i}\frac{\partial \boldsymbol{J}_i^T}{\partial q_j}\boldsymbol{\nu}(\boldsymbol{J}_j^T\boldsymbol{\nu})\Bigg] \qquad (5.65)\\ \gamma_{\mathcal{S}_0}(\boldsymbol{q},\boldsymbol{\nu},t) &= \frac{\partial^2 \varepsilon_{\mathrm{s}}(t)}{\partial t^2}\\ &= 2\iint_{\mathcal{S}_0}\Bigg[\left(\frac{\partial \phi_{\mathrm{m}}(t)}{\partial t}\right)^2+\phi_{\mathrm{m}}(t)\int_0^t \frac{\partial^2 \boldsymbol{\varphi}_{\mathrm{m}}^T(\boldsymbol{q}(\tau),t-\tau)}{\partial t^2}\boldsymbol{\nu}(\tau)d\tau\\ &\quad+\phi_{\mathrm{m}}(t)\frac{\partial \boldsymbol{\varphi}_{\mathrm{m}}^T(\boldsymbol{q},0)}{\partial t}\boldsymbol{\nu}\Bigg]dS \qquad (5.66)\end{aligned}$$

The free surface Lagrangian is then

$$\mathcal{L}_{\mathcal{S}_0}=\frac{1}{2}\boldsymbol{\nu}^T\boldsymbol{M}_{\mathcal{S}_0}(\boldsymbol{q},\boldsymbol{\nu})\boldsymbol{\nu}+\boldsymbol{\nu}^T\int_0^t \boldsymbol{K}_{\mathcal{S}_0 1}(\boldsymbol{q},\boldsymbol{\nu},\boldsymbol{q}(\tau),t-\tau)\boldsymbol{\nu}(\tau)d\tau+\gamma_{\mathcal{S}_0}(t) \qquad (5.67)$$

Property 5.4.1 (System Invariance) *One may show by direct substitution that Lagrangian equations of motion are invariant to transformations of the form*

$$\mathcal{L}_1(q,\dot{q},t)=\mathcal{L}(q,\dot{q},t)+f(t) \qquad (5.68)$$

where f is any scalar function of t. Note that this transformation does alter the relationship between the Lagrangian and the system energy, however.

By Property 5.4.1, one may effectively redefine $\gamma_{\mathcal{S}_0}$ since the first line of (5.66) will not impact the system dynamics:

$$\gamma_{\mathcal{S}_0}(\boldsymbol{q},\boldsymbol{\nu},t)=2\iint_{\mathcal{S}_0}\boldsymbol{\nu}^T\frac{\partial \boldsymbol{\varphi}_{\mathrm{m}}(\boldsymbol{q},0)}{\partial t}\int_0^t \boldsymbol{\varphi}_{\mathrm{m}}(\boldsymbol{q}(\tau),t-\tau)\boldsymbol{\nu}(\tau)d\tau dS$$

Define the matrix

$$\boldsymbol{K}_{\mathcal{S}_0 2}(\boldsymbol{q},\boldsymbol{q}(\tau),t-\tau)=2\iint_{\mathcal{S}_0}\frac{\partial \boldsymbol{\varphi}_{\mathrm{m}}(\boldsymbol{q},0)}{\partial t}\boldsymbol{\varphi}_{\mathrm{m}}^T(\boldsymbol{q}(\tau),t-\tau)dS \qquad (5.69)$$

and $\gamma_{\mathcal{S}_0}$ becomes

$$\gamma_{\mathcal{S}_0}(\boldsymbol{q},\boldsymbol{\nu},t) = \boldsymbol{\nu}^T \int_0^t \boldsymbol{K}_{\mathcal{S}_0 2}(\boldsymbol{q},\boldsymbol{q}(\tau),t-\tau)\boldsymbol{\nu}(\tau)d\tau \tag{5.70}$$

Define the complete free surface kernel matrix $\boldsymbol{K}_{\mathcal{S}_0}$:

$$\boldsymbol{K}_{\mathcal{S}_0}(\boldsymbol{q},\boldsymbol{\nu},\boldsymbol{q}(\tau),t-\tau) = \boldsymbol{K}_{\mathcal{S}_0 1}(\boldsymbol{q},\boldsymbol{\nu},\boldsymbol{q}(\tau),t-\tau) + \boldsymbol{K}_{\mathcal{S}_0 2}(\boldsymbol{q},\boldsymbol{q}(\tau),t-\tau) \tag{5.71}$$

The free surface Lagrangian then may be compactly written as

$$\mathcal{L}_{\mathcal{S}_0} = \frac{1}{2}\boldsymbol{\nu}^T \boldsymbol{M}_{\mathcal{S}_0}(\boldsymbol{q},\boldsymbol{\nu})\boldsymbol{\nu} + \boldsymbol{\nu}^T \int_0^t \boldsymbol{K}_{\mathcal{S}_0}(\boldsymbol{q},\boldsymbol{\nu},\boldsymbol{q}(\tau),t-\tau)\boldsymbol{\nu}(\tau)d\tau \tag{5.72}$$

The System Lagrangian for Memory-Affected Motion

Combining the rigid body Lagrangian with the updated expressions for the fluid body Lagrangian and the free surface Lagrangian, the complete system Lagrangian is

$$\begin{aligned}\mathcal{L} = &\frac{1}{2}\boldsymbol{\nu}^T\big(\boldsymbol{M}_{\mathrm{b}} + \boldsymbol{M}_{\mathcal{B}} + \Delta\boldsymbol{M}_{\mathcal{B}}(\boldsymbol{q}) + \boldsymbol{M}_{\mathcal{S}_0}(\boldsymbol{q},\boldsymbol{\nu})\big)\boldsymbol{\nu} \\ &+ \boldsymbol{\nu}^T \int_0^t \left[\boldsymbol{K}_{\mathcal{B}}(\boldsymbol{q}(\tau),t-\tau) + \boldsymbol{K}_{\mathcal{S}_0}(\boldsymbol{q},\boldsymbol{\nu},\boldsymbol{q}(\tau),t-\tau)\right]\boldsymbol{\nu}(\tau)d\tau \\ &+ g\left(m_{\mathrm{b}} - \rho\forall\right) z_{\mathrm{b}} + m_{\mathrm{b}} g \boldsymbol{r}_{\mathrm{cm}} \cdot \left(\boldsymbol{R}^T \boldsymbol{i}_3\right)\end{aligned} \tag{5.73}$$

The terms on the first and third lines model the memory-free motion of the fluid-vehicle system, while the terms on the second line account for the memory effects incurred by vehicle motion.

5.4.2 Memory-Affected Equations of Motion

Since the equations of motion due to the first and third lines of (5.73) are given by (5.33), only the additional contributions from the memory effects need to be computed. For ease of notation, let $\mathcal{L}_{\mathrm{m}}$ represent the portion of the system Lagrangian corresponding to the memory effects:

$$\mathcal{L}_{\mathrm{m}}(\boldsymbol{q},\boldsymbol{\nu},t) = \boldsymbol{\nu}^T \int_0^t \left[\boldsymbol{K}_{\mathcal{B}}(\boldsymbol{q}(\tau),t-\tau) + \boldsymbol{K}_{\mathcal{S}_0}(\boldsymbol{q},\boldsymbol{\nu},\boldsymbol{q}(\tau),t-\tau)\right]\boldsymbol{\nu}(\tau)d\tau \tag{5.74}$$

First, compute

$$\frac{\partial \mathcal{L}_{\rm m}}{\partial \boldsymbol{\nu}} = \int_0^t \left[\boldsymbol{K}_{\mathcal{B}}(\boldsymbol{q}(\tau), t-\tau) + \boldsymbol{K}_{\mathcal{S}_0}(\boldsymbol{q}, \boldsymbol{\nu}, \boldsymbol{q}(\tau), t-\tau)\right] \boldsymbol{\nu}(\tau) d\tau + \int_0^t \sum_{i=1}^{6} \left(\boldsymbol{e}_i \boldsymbol{\nu}^T\right) \frac{\partial \boldsymbol{K}_{\mathcal{S}_0}(\boldsymbol{q}, \boldsymbol{\nu}, \boldsymbol{q}(\tau), t-\tau)}{\partial \nu_i} \boldsymbol{\nu}(\tau) d\tau$$

Taking the time rate of change yields

$$\begin{aligned}
\frac{d}{dt}\frac{\mathcal{L}_{\rm m}}{\partial \boldsymbol{\nu}} = & \int_0^t \sum_{i=1}^{6} \left(\boldsymbol{e}_i \boldsymbol{\nu}^T(\tau) \frac{\partial \boldsymbol{K}_{\mathcal{S}_0}^T(\boldsymbol{q}, \boldsymbol{\nu}, \boldsymbol{q}(\tau), t-\tau)}{\partial \nu_i} + \frac{\partial \boldsymbol{K}_{\mathcal{S}_0}(\boldsymbol{q}, \boldsymbol{\nu}, \boldsymbol{q}(\tau), t-\tau)}{\partial \nu_i} \boldsymbol{\nu}(\tau) \boldsymbol{e}_i^T \right) d\tau \; \dot{\boldsymbol{\nu}} \\
& + \int_0^t \sum_{i=1}^{6} \sum_{j=1}^{6} \boldsymbol{e}_i \boldsymbol{\nu}^T \frac{\partial^2 \boldsymbol{K}_{\mathcal{S}_0}(\boldsymbol{q}, \boldsymbol{\nu}, \boldsymbol{q}(\tau), t-\tau)}{\partial \nu_i \partial \nu_j} \boldsymbol{\nu}(\tau) \boldsymbol{e}_j^T d\tau \; \dot{\boldsymbol{\nu}} \\
& + \int_0^t \frac{\partial (\boldsymbol{K}_{\mathcal{B}}(\boldsymbol{q}(\tau), t-\tau) + \boldsymbol{K}_{\mathcal{S}_0}(\boldsymbol{q}, \boldsymbol{\nu}, \boldsymbol{q}(\tau), t-\tau))}{\partial (t-\tau)} \boldsymbol{\nu}(\tau) d\tau \\
& + \int_0^t \sum_{i=1}^{6} \left(\frac{\partial \boldsymbol{K}_{\mathcal{S}_0}(\boldsymbol{q}, \boldsymbol{\nu}, \boldsymbol{q}(\tau), t-\tau)}{\partial q_i} \boldsymbol{J}_i^T \boldsymbol{\nu} + \boldsymbol{e}_i \boldsymbol{\nu}^T \frac{\partial^2 \boldsymbol{K}_{\mathcal{S}_0}(\boldsymbol{q}, \boldsymbol{\nu}, \boldsymbol{q}(\tau), t-\tau)}{\partial \nu_i \partial (t-\tau)} \right) \boldsymbol{\nu}(\tau) d\tau \\
& + \int_0^t \sum_{i=1}^{6} \sum_{j=1}^{6} (\boldsymbol{J}_j^T \boldsymbol{\nu}) \boldsymbol{e}_i \boldsymbol{\nu}^T \frac{\partial^2 \boldsymbol{K}_{\mathcal{S}_0}(\boldsymbol{q}, \boldsymbol{\nu}, \boldsymbol{q}(\tau), t-\tau)}{\partial q_j \partial \nu_i} \boldsymbol{\nu}(\tau) d\tau
\end{aligned}$$

Also, evaluate

$$\begin{aligned}
\boldsymbol{G}\frac{\partial \mathcal{L}_{\rm m}}{\partial \boldsymbol{\nu}} = & \boldsymbol{G} \int_0^t \left[\boldsymbol{K}_{\mathcal{B}}(\boldsymbol{q}(\tau), t-\tau) + \boldsymbol{K}_{\mathcal{S}_0}(\boldsymbol{q}, \boldsymbol{\nu}, \boldsymbol{q}(\tau), t-\tau)\right] \boldsymbol{\nu}(\tau) d\tau \\
& + \boldsymbol{G} \int_0^t \sum_{i=1}^{6} \left(\boldsymbol{e}_i \boldsymbol{\nu}^T(\tau)\right) \frac{\partial \boldsymbol{K}_{\mathcal{S}_0}(\boldsymbol{q}, \boldsymbol{\nu}, \boldsymbol{q}(\tau), t-\tau)}{\partial \nu_i} d\tau \; \boldsymbol{\nu}
\end{aligned} \tag{5.75}$$

In an effort to maintain the same structure as the memory free model (5.33), one must factor $\boldsymbol{\nu}$ from the first line of (5.75). Define the 3×6 auxiliary matrices $\boldsymbol{K}_1, \boldsymbol{K}_2$ as

$$\begin{aligned}
\boldsymbol{K}_1(\boldsymbol{q}, \boldsymbol{\nu}, \boldsymbol{q}(\tau), t-\tau) &= (\mathbb{I}_{3\times 3} \;\; \boldsymbol{0}_{3\times 3}) \left(\boldsymbol{K}_{\mathcal{B}}(\boldsymbol{q}(\tau), t-\tau) + \boldsymbol{K}_{\mathcal{S}_0}(\boldsymbol{q}, \boldsymbol{\nu}, \boldsymbol{q}(\tau), t-\tau)\right) \\
\boldsymbol{K}_2(\boldsymbol{q}, \boldsymbol{\nu}, \boldsymbol{q}(\tau), t-\tau) &= (\boldsymbol{0}_{3\times 3} \;\; \mathbb{I}_{3\times 3}) \left(\boldsymbol{K}_{\mathcal{B}}(\boldsymbol{q}(\tau), t-\tau) + \boldsymbol{K}_{\mathcal{S}_0}(\boldsymbol{q}, \boldsymbol{\nu}, \boldsymbol{q}(\tau), t-\tau)\right)
\end{aligned}$$

where $\mathbb{I}_{3\times 3}$ is the three-by-three identity matrix and $\boldsymbol{0}_{3\times 3}$ is a three-by-three matrix of zeros. Note that $\boldsymbol{K}_1$ simply represents the first three rows of $\boldsymbol{K}_{\mathcal{B}} + \boldsymbol{K}_{\mathcal{S}_0}$ while $\boldsymbol{K}_2$ represents the

latter three. Then, using Proposition 5.3.3, one may reparameterize the top line of (5.75) as

$$\boldsymbol{G}\int_0^t \left[\boldsymbol{K}_{\mathcal{B}}(\boldsymbol{q}(\tau),t-\tau)+\boldsymbol{K}_{\mathcal{S}_0}(\boldsymbol{q},\boldsymbol{\nu},\boldsymbol{q}(\tau),t-\tau)\right]\boldsymbol{\nu}(\tau)d\tau = -\int_0^t \begin{pmatrix} \boldsymbol{0} & \boldsymbol{K}_1(\widehat{t-\tau})\boldsymbol{\nu}(\tau) \\ \boldsymbol{K}_1(\widehat{t-\tau})\boldsymbol{\nu}(\tau) & \boldsymbol{K}_2(\widehat{t-\tau})\boldsymbol{\nu}(\tau) \end{pmatrix} d\tau\ \boldsymbol{\nu}$$

Finally, compute

$$\boldsymbol{J}(\boldsymbol{q})^T\frac{\partial \mathcal{L}_{\mathrm{m}}}{\partial \boldsymbol{q}} = \int_0^t \sum_{i=1}^{6}\left(\boldsymbol{J}_i\boldsymbol{\nu}^T\right)\frac{\partial \boldsymbol{K}_{\mathcal{S}_0}(t-\tau)}{\partial q_i}\boldsymbol{\nu}(\tau)d\tau \tag{5.76}$$

To organize the above contributions to the equations of motion, define the "memory fluid response matrices" $\boldsymbol{M}_{\mathrm{M}}$, $\boldsymbol{C}_{\mathrm{M}}$, $\boldsymbol{D}_{\mathrm{M}}$, and $\boldsymbol{K}_{\mathrm{M}}$

$$\begin{aligned}\boldsymbol{M}_{\mathrm{M}}(\boldsymbol{q},\boldsymbol{\nu},t) &= \int_0^t\left[\sum_{i=1}^{6}\boldsymbol{e}_i\boldsymbol{\nu}^T(\tau)\frac{\partial \boldsymbol{K}_{\mathcal{S}_0}^T(t-\tau)}{\partial \nu_i}+\frac{\partial \boldsymbol{K}_{\mathcal{S}_0}(t-\tau)}{\partial \nu_i}\boldsymbol{\nu}(\tau)\boldsymbol{e}_i^T\right]d\tau \\ &\quad+\int_0^t\left[\sum_{i=1}^{6}\sum_{j=1}^{6}\boldsymbol{e}_i\boldsymbol{\nu}^T\frac{\partial^2 \boldsymbol{K}_{\mathcal{S}_0}(t-\tau)}{\partial \nu_i\partial \nu_j}\boldsymbol{\nu}(\tau)\boldsymbol{e}_j^T\right]d\tau \end{aligned}\tag{5.77}$$

$$\begin{aligned}\boldsymbol{C}_{\mathrm{M}}(\boldsymbol{q},\boldsymbol{\nu},t) &= \boldsymbol{G}\int_0^t\sum_{i=1}^{6}\boldsymbol{e}_i\boldsymbol{\nu}^T(\tau)\frac{\partial \boldsymbol{K}_{\mathcal{S}_0}^T(t-\tau)}{\partial \nu_i}d\tau \\ &\quad-\int_0^t\begin{pmatrix}\boldsymbol{0} & \boldsymbol{K}_1(\widehat{t-\tau})\boldsymbol{\nu}(\tau)\\ \boldsymbol{K}_1(\widehat{t-\tau})\boldsymbol{\nu}(\tau) & \boldsymbol{K}_2(\widehat{t-\tau})\boldsymbol{\nu}(\tau)\end{pmatrix}d\tau\end{aligned}\tag{5.78}$$

$$\begin{aligned}\boldsymbol{D}_{\mathrm{M}}(\boldsymbol{q},\boldsymbol{\nu},t) &= \int_0^t\sum_{i=1}^{6}\left(\frac{\partial \boldsymbol{K}_{\mathcal{S}_0}(t-\tau)}{\partial q_i}\boldsymbol{\nu}(\tau)\boldsymbol{J}_i^T-\boldsymbol{J}_i\boldsymbol{\nu}(\tau)^T\frac{\partial \boldsymbol{K}_{\mathcal{S}_0}^T(t-\tau)}{\partial q_i}\right)d\tau \\ &\quad+\int_0^t\sum_{i=1}^{6}\sum_{j=1}^{6}\boldsymbol{e}_i\boldsymbol{\nu}^T(\tau)\left[(\boldsymbol{J}_j^T\boldsymbol{\nu})\frac{\partial^2 \boldsymbol{K}_{\mathcal{S}_0}^T(t-\tau)}{\partial q_j\partial \nu_i}+\frac{\partial^2 \boldsymbol{K}_{\mathcal{S}_0}^T(t-\tau)}{\partial \nu_i\partial(t-\tau)}\right]d\tau\end{aligned}\tag{5.79}$$

$$\boldsymbol{K}_{\mathrm{M}}(\boldsymbol{q},\boldsymbol{\nu},\boldsymbol{q}(\tau),t-\tau) = \frac{\partial\left(\boldsymbol{K}_{\mathcal{B}}(t-\tau)+\boldsymbol{K}_{\mathcal{S}_0}(t-\tau)\right)}{\partial(t-\tau)}\tag{5.80}$$

Note that the in the above definitions, the functional dependencies on $\boldsymbol{q}(\tau)$, $\boldsymbol{q}$, and $\boldsymbol{\nu}$ in $\boldsymbol{K}_{\mathcal{B}}$ and $\boldsymbol{K}_{\mathcal{S}_0}$ have been omitted for brevity.

Theorem 5.4.2 (A nonlinear maneuvering model with memory effects) *For a fluid which obeys the modeling assumptions given in Assumption 5.1.1, the kinetic equations for*

a neutrally buoyant rigid body are

$$\begin{aligned}\boldsymbol{F} = &\left(\boldsymbol{M}_{\mathrm{b}} + \boldsymbol{M}_{\mathrm{I}}(\boldsymbol{q},\boldsymbol{\nu}) + \boldsymbol{M}_{\mathrm{M}}(\boldsymbol{q},\boldsymbol{\nu},t)\right)\dot{\boldsymbol{\nu}} \\ &+ \left(\boldsymbol{C}_{\mathrm{b}}(\boldsymbol{\nu}) + \boldsymbol{C}_{\mathrm{I}}(\boldsymbol{q},\boldsymbol{\nu}) + \boldsymbol{C}_{\mathrm{M}}(\boldsymbol{q},\boldsymbol{\nu},t)\right)\boldsymbol{\nu} \\ &+ \left(\boldsymbol{D}_{\mathrm{I}}(\boldsymbol{q},\boldsymbol{\nu}) + \boldsymbol{D}_{\mathrm{M}}(\boldsymbol{q},\boldsymbol{\nu},t)\right)\boldsymbol{\nu} \\ &+ \boldsymbol{g}(\boldsymbol{\theta}_{\mathrm{b}}) + \int_0^t \boldsymbol{K}_{\mathrm{M}}(\boldsymbol{q},\boldsymbol{\nu},\boldsymbol{q}(\tau),t-\tau)\boldsymbol{\nu}(\tau)d\tau \end{aligned} \tag{5.81}$$

where $\boldsymbol{M}_{\mathrm{I}}$, $\boldsymbol{C}_{\mathrm{I}}$ *and* $\boldsymbol{D}_{\mathrm{I}}$ *are defined in (5.35)-(5.37),* $\boldsymbol{M}_{\mathrm{M}}$, $\boldsymbol{C}_{\mathrm{M}}$, $\boldsymbol{D}_{\mathrm{M}}$, *and* $\boldsymbol{K}_{\mathrm{M}}$ *are defined in (5.77)-(5.80), and* $\boldsymbol{g}$ *is defined in (5.38).* □

Corollary 5.4.3 (Non-neutrally buoyant vehicles) *For a vehicle which isn't neutrally buoyant, one may instead use the following definition of the hydrostatic vector in the equations of motion(5.81):*

$$\boldsymbol{g}(\boldsymbol{\theta}_{\mathrm{b}}) = -\begin{pmatrix} g(m_{\mathrm{b}} - \rho\forall)\left(\boldsymbol{R}^T\boldsymbol{i}_3\right) \\ m_{\mathrm{b}}g\boldsymbol{r}_{\mathrm{cm}} \times \left(\boldsymbol{R}^T\boldsymbol{i}_3\right) \end{pmatrix} \tag{5.82}$$

The equations of motion (5.81) include the temporal evolution of the free surface. The added functionality comes with a price, however. The equations of motion now feature an explicit dependence on time as well as the time history of vehicle position and velocity. This increases the complexity involved with identifying this model as compared to the memory-free model; one must now identify the kernel functions $\boldsymbol{K}_{\mathcal{B}}$ and $\boldsymbol{K}_{\mathcal{S}_0}$. Perhaps the greatest advantage of (5.81) is that the model makes no assumptions which restrict the vehicle motion. As compared to the Cummins equations, this model is not limited to small perturbations from a nominal (straight-ahead) trajectory.

5.4.3 Captive Model Equations with Memory Effects

The equations (5.81) address the shortcomings present in the memory-free model. Without the memory effects, the equations (5.33) were unable to capture any wave resistance forces since only the instantaneous exchange of energy between the body and the free surface was

modeled. To verify that the addition of the fluid memory effects explicitly leads to wave resistance forces, the captive model equations for a vehicle restricted to pure surge motion are again presented (motion corresponding to Assumption 5.3.5). Assuming a constant velocity parallel to the free surface, one finds

$$f_{\text{surge}} = -u\int_0^t \frac{\partial\left(K_{\mathcal{S}_0 11}(t-\tau)+K_{\mathcal{B}11}(t-\tau)\right)}{\partial(t-\tau)}d\tau \tag{5.83}$$

$$\begin{aligned} f_{\text{heave}} = {} & \frac{1}{2}u^2\frac{\partial\Delta M_{\mathcal{B}11}}{\partial z_{\text{b}}} + u\int_0^t \frac{\partial K_{\mathcal{S}_0 11}(t-\tau)}{\partial z_{\text{b}}}d\tau \\ & - u\int_0^t \frac{\partial\left(K_{\mathcal{S}_0 31}(t-\tau)+K_{\mathcal{B}31}(t-\tau)\right)}{\partial(t-\tau)}d\tau \end{aligned} \tag{5.84}$$

$$\begin{aligned} \tau_{\text{pitch}} = {} & u^2(M_{\mathcal{B}31}+\Delta M_{\mathcal{B}31}) + \frac{1}{2}u^2\frac{\Delta M_{\mathcal{B}11}}{\partial\theta_{\text{b}}} \\ & u^2\int_0^t \left(K_{\mathcal{S}_0 31}(t-\tau)+K_{\mathcal{B}31}(t-\tau)\right)d\tau + u\int_0^t \frac{\partial K_{\mathcal{S}_0 11}(t-\tau)}{\partial\theta_{\text{b}}}d\tau \\ & - u\int_0^t \frac{\partial\left(K_{\mathcal{S}_0 51}(t-\tau)+K_{\mathcal{B}51}(t-\tau)\right)}{\partial(t-\tau)}d\tau - u\int_0^t 6\frac{\partial^2 K_{\mathcal{S}_0 11}(t-\tau)}{\partial q\partial(t-\tau)} \end{aligned} \tag{5.85}$$

In this case, one explicitly finds a force in the surge due to the fluid memory effects. (5.83) may be interpreted as the wave resistance force for a marine craft advancing in otherwise calm seas. Additional terms also appear in the heave force and pitching moment. As one might expect, this reveals that the memory effects also impact the free surface suction force and moment.

5.4.4 Comparison to the Cummins Equations

Recall the definition of the Cummins Equations given in Section 4.3.4:

$$\left(\boldsymbol{M}_{\text{b}}+\boldsymbol{M}_{\mathcal{B}_0}\right)\ddot{\boldsymbol{q}}(t) + \int_0^t \left[\boldsymbol{K}_{\mathcal{B}_0}(t-\tau)-\boldsymbol{K}_{\mathcal{S}_0}(t-\tau)\right]\dot{\boldsymbol{q}}(\tau)d\tau + \boldsymbol{g}(\boldsymbol{q}) = \boldsymbol{0}$$

where

$$\boldsymbol{M}_{\mathcal{B}_0} = \rho \iint_{\mathcal{B}_0} \boldsymbol{b}\, \boldsymbol{\varphi}_{\mathrm{i}}^T \, dS$$
$$\boldsymbol{K}_{\mathcal{B}_0}(t) = \rho \iint_{\mathcal{B}_0} \boldsymbol{b}\, \frac{\partial \boldsymbol{\varphi}_{\mathrm{m}}^T(t)}{\partial t} \, dS$$
$$\boldsymbol{K}_{\mathcal{S}_0}(t) = \frac{\rho}{g} \iint_{\mathcal{S}_0} \frac{\partial \boldsymbol{\varphi}_{\mathrm{m}}(0)}{\partial t}\, \frac{\partial \boldsymbol{\varphi}_{\mathrm{m}}^T(t)}{\partial t} \, dS$$

Though the Cummins equations and (5.81) were derived using different velocity potential functions, they both derive from the same general energy functions. One may therefore interpret the Cummins equations as the linearized version of (5.81).

In the Cummins equations, $\boldsymbol{M}_{\mathcal{B}_0}$ is the only matrix which accounts for the instantaneous fluid response. One may therefore interpret the matrices $(\boldsymbol{M}_{\mathrm{I}} - \boldsymbol{M}_{\mathcal{B}} - \Delta\boldsymbol{M}_{\mathcal{B}})$, $\boldsymbol{C}_{\mathrm{I}}$ and $\boldsymbol{D}_{\mathrm{I}}$ as the nonlinear terms neglected in the Cummins equations. A similar observation may be made for the memory effects. The matrix $\boldsymbol{K}_{\mathrm{M}}$ corresponds to the memory effect matrices $\boldsymbol{K}_{\mathcal{B}_0} + \boldsymbol{K}_{\mathcal{S}_0}$ in the Cummins equations. One may therfore interpret the matrices $\boldsymbol{M}_{\mathrm{M}}$, $\boldsymbol{C}_{\mathrm{M}}$ and $\boldsymbol{D}_{\mathrm{M}}$ as the nonlinear memory terms neglected in the Cummins equations.

5.4.5 Remarks on the Memory Effects

The challenges associated with identifying the memory effects have been well documented [19, 29, 21, 22, 62]. Early results from Cummins [19] and Ogilvie [29] related the memory effects to the frequency dependent added mass parameters by treating the convolution integrals as impulse response functions. The memory effects could then be mapped into the frequency domain using Fourier transforms[3] [29, 62], resulting in

$$\boldsymbol{A}(\omega) = \boldsymbol{A}(\infty) - \frac{1}{\omega}\int_0^\infty \boldsymbol{K}(t)\sin(\omega t)dt \tag{5.86}$$
$$\boldsymbol{B}(\omega) = \int_0^\infty \boldsymbol{K}(t)\cos(\omega t)dt \tag{5.87}$$

[3]Joseph Fourier, 1768-1830.

(Recall from Section 3.2.2 that the matrices $\boldsymbol{A}$ and $\boldsymbol{B}$ refer to the frequency dependent added mass and damping parameters which traditionally appear in the seakeeping equations.) While these expressions offer one method to accommodate the memory effects, mapping the model to the frequency domain would negate many of the benefits of (5.81), as outlined in [19]. Inverse relationships appear in [21, 22, 20, 62], which instead map the frequency dependent parameters to the kernel functions:

$$\boldsymbol{K}(t) = \frac{2}{\pi}\int_0^\infty \omega\left(\boldsymbol{A}(\infty) - \boldsymbol{A}(\omega)\right)\sin(\omega t)d\omega \tag{5.88}$$

$$\boldsymbol{K}(t) = \frac{2}{\pi}\int_0^\infty \left(\boldsymbol{B}(\omega) - \boldsymbol{B}(\infty)\right)\cos(\omega t)d\omega \tag{5.89}$$

The authors in [22] remark that the integral in (5.89) typically converges faster than in (5.88), so (5.89) is more commonly implemented. These expressions are more valuable since the terms $\boldsymbol{A}(\omega)$ and $\boldsymbol{B}(\omega)$ can easily be computed, for instance, from conventional seakeeping codes. However, [21] remarks that there is a practical issue with this approach: one typically does not have the frequency dependent parameters across the complete range of integration. With both physical and numerical experiments, limitations exist which preclude one from obtaining these parameters at both very low and very high frequencies. To circumvent this, Bailey et al. [21] propose a *viscous ramp* to approximate the behavior of these parameters in ranges where they cannot be computed.

For a stable linear system, the impulse response function characterizes the zero-input (decaying) system motion due to a unit impulse [59]. The system response to a continuous series of impulses is then given as the convolution of the impulse response function with the system inputs. In the case of the memory effects, $\boldsymbol{K}(t)$ characterizes the decaying radiation forces and moments due to an impulsive vehicle velocity. As a result, $\boldsymbol{K}(t)$ is often called a *retardation function* [20, 62]. The generalized forces associated with the memory effects are then given as a convolution of the retardation function and the system velocities.

Physically, the retardation functions are closely related to the memory effect potential. In the depiction of an impulsive vehicle motion (Figure 4.7), the fluid motion following the impulse was governed by a time-dependent velocity potential. Recognizing that the wave

motion only imparts appreciable forces and moments on the vehicle for a finite time, one may interpret the resulting force as an impulse response. In this case, the retardation function essentially acts as the link between the time-dependent force and the associated decaying wave motion. While there is considerable more complexity in (5.81), it is expected that similar approaches may be employed to characterize the memory effects in the nonlinear equations.

5.5 Closing Remarks

In this chapter, two nonlinear models were presented for the calm-water maneuvering of a marine craft in the presence of a free surface. By assuming two different structures for the velocity potential, the theory presented in Chapter 4 was used to derive two sets of equations of motion. The Lagrangian modeling allowed the systematic computation of the hydrodynamic forces and moments associated with specific, contributing mechanisms including free surface suction and wave resistance. The resulting models are more complicated than Kirchhoff's equations and Cummins' equations, though the added complexity is commensurate with the task of modeling a marine craft near a free surface. It is also important to note that while both models were derived with a submerged craft in mind, the approach and the results apply to surface craft as well; the Cummins equations, which are a widely used set of equations for surface craft, were shown to be a simplified model of the nonlinear maneuvering model presented here.

One application where the proposed maneuvering model might break down is when predicting whether or not a submerged craft will pierce the free surface. Determining when a vehicle will broach is largely dependent on the free surface deformations. While the model force and moment predictions may be sufficient in the presence of larger free surface deformations, the unmodeled free surface deformations could lead to broaching. Another application where the model may perform poorly is when predicting capsize, which is usually caused by significant

surface waves. In this case, the hydrodynamic forces and moments may need to be corrected to incorporate the nonlinear free surface boundary condition to sufficiently predict a vessel's response in more extreme conditions.

Perhaps the most valuable characteristic of the proposed models is that they incorporate the fluid dynamics incurred by nonlinear vehicle motions without the need to solve a set of PDEs. Prior parametric models, particularly those which are based upon Cummins' equations, are hindered by the underlying linearization assumptions. While those models are restricted to small motions from a nominal trajectory, these models are only restricted by one's ability to populate the model parameters.

Chapter 6

A Nonlinear Unified Maneuvering and Seakeeping Model

In the previous chapter, a nonlinear maneuvering model was derived for a marine vehicle operating near an otherwise calm free surface. Here, the effects due to externally generated fluid motion acting on the vehicle are incorporated by modifying the Lagrangian function developed in [63, 26]. The primary shortcoming with the Lagrangian function (and the resulting model) given in [26] is that that no consideration was given to a free surface; the model assumed that the vehicle was deeply submerged.

This chapter is broken into two parts. In the first half, The Model of Thomasson and Woolsey are reviewed, beginning with a discussion of their system Lagrangian [26]. Then, the Lagrangian function in [26] is updated to account for a free surface, and the new Lagrangian is used to derive a set of dynamic equations. The resulting model may be interpreted as a nonlinear unified maneuvering and seakeeping model.

6.1 Statement of Assumptions

Assumption 6.1.1 (Modeling assumptions)

1. *The fluid is incompressible and inviscid and the fluid velocity is irrotational (the potential flow assumptions).*
2. *The linearized free surface boundary conditions are valid.*
3. *The externally generated flow field is prescribed and the fluid motion is irrotational.*

6.2 Modeling Excitation Forces

Thomasson and Woolsey [26] characterize the exchange of energy between a deeply submerged rigid body and an infinite volume of ambient fluid with an externally generated velocity field. As compared to Kirchhoff's equations, the ambient flow field modifies the pressure field and results in additional hydrodynamic forces and moments acting on the vehicle. Using the Lagrangian function presented in [26], one may identify a *disturbance Lagrangian*, so named in anticipation that this function will characterize the disturbances acting on a vehicle operating in a natural seaway.

6.2.1 The Disturbance Lagrangian

To construct a Lagrangian function which incorporates a background flow field, Thomasson and Woolsey [26] employ the following step-by-step procedure.

1. Considering the vehicle to be initially absent from the fluid volume, establish the motion of the ambient flow field.

2. Initialize the motion of a vehicle-shaped pocket of fluid, which moves relative to the ambient flow.

3. Subtract the fluid particles contained within the vehicle-shaped pocket of fluid.

4. Add the rigid body to the fluid volume in place of the vehicle-shaped pocket of fluid.

Relating each of these steps to an addition or subtraction of system energy, one can express the combined fluid-vehicle system Lagrangian as [63, 26]

$$\begin{aligned}\mathcal{L}_{\rm b}+\mathcal{L}_{\rm f} = &\left[K+\frac{1}{2}M_{\rm f}\boldsymbol{\nu}_{\rm f}^T\boldsymbol{\nu}_{\rm f}\right] && \text{vehicle-absent fluid energy}\\ &+\left[\frac{1}{2}\boldsymbol{\nu}_{\rm r}^T\left(\boldsymbol{M}_{\mathcal{B}}+\bar{\boldsymbol{M}}\right)\boldsymbol{\nu}_{\rm r}\right] && \text{fluid-filled hullform energy}\\ &-\left[\frac{1}{2}\boldsymbol{\nu}^T\bar{\boldsymbol{M}}\boldsymbol{\nu}\right] && \text{vehicle-replaced fluid energy}\\ &+\left[\frac{1}{2}\boldsymbol{\nu}^T\boldsymbol{M}_{\rm b}\boldsymbol{\nu}\right] && \text{rigid body kinetic energy}\end{aligned} \tag{6.1}$$

In the above expression, K accounts for the energy associated with fluid vorticity and $M_{\rm f}$ defines the (infinite) mass of the ambient fluid. Also, let $\boldsymbol{V}_{\rm f}(\boldsymbol{x}_{\rm b},t)$ represent an Eulerian velocity field. Defined in the body-fixed frame, the fluid velocity is

$$\boldsymbol{\nu}_{\rm f}(\boldsymbol{q},t)=\boldsymbol{J}(\boldsymbol{\theta}_{\rm b})\begin{pmatrix}\boldsymbol{V}_{\rm f}(\boldsymbol{x}_{\rm b},t)\\ \boldsymbol{0}\end{pmatrix}=\begin{pmatrix}\boldsymbol{v}_{\rm f}(\boldsymbol{q},t)\\ \boldsymbol{0}\end{pmatrix} \tag{6.2}$$

Then, $\boldsymbol{\nu}_{\rm r}=\boldsymbol{\nu}-\boldsymbol{\nu}_{\rm f}$ represents the flow-relative velocity of the vehicle. The matrix $\boldsymbol{M}_{\mathcal{B}}$ is the deeply submerged added mass matrix (4.96) (from Kirchhoff's equations) and $\bar{\boldsymbol{M}}$ accounts for the mass $\bar{m}$ of the fluid contained within the vehicle-shaped pocket:

$$\bar{\boldsymbol{M}}=\begin{pmatrix}\bar{m}\mathbb{I}_3 & \boldsymbol{0}\\ \boldsymbol{0} & \boldsymbol{0}\end{pmatrix} \tag{6.3}$$

Note that $\bar{\boldsymbol{M}}$ doesn't have a rotational inertia component because an inviscid fluid does not resist shearing stresses.

To isolate the additional terms due to the external flow field, one may separate out the portion of the system Lagrangian which results in Kirchhoff's equations. Note that the

term $K + \frac{1}{2}M_{\mathrm{f}}\boldsymbol{\nu}_{\mathrm{f}}^T\boldsymbol{\nu}_{\mathrm{f}}$ may be neglected in the subsequent analysis since the (infinite) kinetic energy of the ambient fluid doesn't appear in the equations of motion. Rewrite the system Lagrangian as

$$\mathcal{L} = \underbrace{\frac{1}{2}\boldsymbol{\nu}^T\left(\boldsymbol{M}_{\mathrm{b}} + \boldsymbol{M}_{\mathcal{B}}\right)\boldsymbol{\nu}}_{\text{Kirchhoff's Lagrangian}} + \underbrace{\frac{1}{2}\boldsymbol{\nu}_{\mathrm{f}}^T\left(\boldsymbol{M}_{\mathcal{B}} + \bar{\boldsymbol{M}}\right)\boldsymbol{\nu}_{\mathrm{f}} - \boldsymbol{\nu}^T\left(\boldsymbol{M}_{\mathcal{B}} + \bar{\boldsymbol{M}}\right)\boldsymbol{\nu}_{\mathrm{f}}}_{\text{disturbance Lagrangian}} \tag{6.4}$$

In this form, the system Lagrangian is given as the superposition of Kirchhoff's Lagrangian $\mathcal{L}_{\mathrm{k}}$ (4.98) and a flow-modified *disturbance Lagrangian* $\mathcal{L}_{\mathrm{d}}$.

For a more physically intuitive representation of the disturbance Lagrangian, one may rewrite $\mathcal{L}_{\mathrm{d}}$ using the following identity:

$$\frac{1}{2}\boldsymbol{\nu}_{\mathrm{r}}^T\left(\boldsymbol{M}_{\mathcal{B}} + \bar{\boldsymbol{M}}\right)\boldsymbol{\nu}_{\mathrm{r}} = \frac{1}{2}\boldsymbol{\nu}^T\left(\boldsymbol{M}_{\mathcal{B}} + \bar{\boldsymbol{M}}\right)\boldsymbol{\nu} + \frac{1}{2}\boldsymbol{\nu}_{\mathrm{f}}^T\left(\boldsymbol{M}_{\mathcal{B}} + \bar{\boldsymbol{M}}\right)\boldsymbol{\nu}_{\mathrm{f}} - \boldsymbol{\nu}^T\left(\boldsymbol{M}_{\mathcal{B}} + \bar{\boldsymbol{M}}\right)\boldsymbol{\nu}_{\mathrm{r}}$$

The disturbance Lagrangian then takes the form

$$\mathcal{L}_{\mathrm{d}} = \frac{1}{2}\boldsymbol{\nu}_{\mathrm{r}}^T\left(\boldsymbol{M}_{\mathcal{B}} + \bar{\boldsymbol{M}}\right)\boldsymbol{\nu}_{\mathrm{r}} - \frac{1}{2}\boldsymbol{\nu}^T\left(\boldsymbol{M}_{\mathcal{B}} + \bar{\boldsymbol{M}}\right)\boldsymbol{\nu} \tag{6.5}$$

As before, $\bar{\boldsymbol{M}}$ is the inertia matrix for a vehicle-shaped volume of fluid. For a deeply submerged body, note that the added mass is unaffected by the "contents" of the body; whether the rigid body is hollow or filled with lead, the transfer of kinetic energy to the ambient fluid will be the same for a given body velocity. Therefore, one may interpret the matrix $\boldsymbol{M}_{\mathcal{B}} + \bar{\boldsymbol{M}}$ as the combination of mass and added mass for the vehicle-shaped pocket of fluid. Consider a function $T_{\mathrm{d}}(\cdot)$, defined by

$$T_{\mathrm{d}}(\boldsymbol{a}) = \frac{1}{2}\boldsymbol{a}^T\left(\boldsymbol{M}_{\mathcal{B}} + \bar{\boldsymbol{M}}\right)\boldsymbol{a} \tag{6.6}$$

From the discussion of Kirchhoff's equations, $T_{\mathrm{d}}(\boldsymbol{a})$ is the kinetic energy of the vehicle-shaped pocket of fluid, moving at an arbitrary velocity $\boldsymbol{a}$, combined with the fluid kinetic energy induced by the vehicle-shaped pocket. Rewritten in terms of T_{d}, the disturbance Lagrangian is simply

$$\mathcal{L}_{\mathrm{d}}(\boldsymbol{\nu}, \boldsymbol{\nu}_{\mathrm{r}}) = T_{\mathrm{d}}(\boldsymbol{\nu}_{\mathrm{r}}) - T_{\mathrm{d}}(\boldsymbol{\nu}) \tag{6.7}$$

We may thus physically interpret the disturbance Lagrangian as the difference in kinetic energies of this "pocket/fluid system" evaluated at velocity $\boldsymbol{\nu}_{\mathrm{r}}$ and at velocity $\boldsymbol{\nu}$. Finally, note that when $\boldsymbol{\nu}_{\mathrm{f}} = \mathbf{0}$, $\mathcal{L}_{\mathrm{d}} = 0$.

Remark 6.2.1 *For a neutrally buoyant vehicle ($\bar{m} = m_{\mathrm{b}}$) with coincident centers of mass and buoyancy ($\boldsymbol{r}_{\mathrm{cm}} = \mathbf{0}$), one may add the term $(\boldsymbol{\omega}^T \boldsymbol{I}_{\mathrm{b}} \boldsymbol{\omega} - \boldsymbol{\omega}^T \boldsymbol{I}_{\mathrm{b}} \boldsymbol{\omega})/2$ to (6.5) to show that the disturbance Lagrangian is equivalent to*

$$\mathcal{L}_{\mathrm{d}} = \frac{1}{2} \boldsymbol{\nu}_{\mathrm{r}}^T \left(\boldsymbol{M}_{\mathrm{b}} + \boldsymbol{M}_{\mathcal{B}} \right) \boldsymbol{\nu}_{\mathrm{r}} - \frac{1}{2} \boldsymbol{\nu}^T \left(\boldsymbol{M}_{\mathrm{b}} + \boldsymbol{M}_{\mathcal{B}} \right) \boldsymbol{\nu} \tag{6.8}$$

In this case, the system Lagrangian in [26] is simply

$$\mathcal{L} = \frac{1}{2} \boldsymbol{\nu}_{\mathrm{r}}^T \left(\boldsymbol{M}_{\mathrm{b}} + \boldsymbol{M}_{\mathcal{B}} \right) \boldsymbol{\nu}_{\mathrm{r}} \tag{6.9}$$

6.2.2 The Model of Thomasson and Woolsey

To construct the equations of motion, one can either apply the Boltzmann-Hamel equations (2.33) to the full Lagrangian (6.1), or just compute the additional contributions to Kirchhoff's Equations from the disturbance Lagrangian given in (6.5). The eqations of motion are only presented here as they are rigorously derived in [26, Eq. 13]:

$$\begin{aligned}
(\boldsymbol{M}_{\mathrm{b}} + \boldsymbol{M}_{\mathcal{B}}) \dot{\boldsymbol{\nu}}_{\mathrm{r}} = &- \begin{pmatrix} \hat{\boldsymbol{\omega}} & \mathbf{0} \\ \hat{\boldsymbol{v}}_{\mathrm{r}} & \hat{\boldsymbol{\omega}} \end{pmatrix} (\boldsymbol{M}_{\mathrm{b}} + \boldsymbol{M}_{\mathcal{B}}) \boldsymbol{\nu}_{\mathrm{r}} + \begin{pmatrix} \boldsymbol{f} \\ \boldsymbol{\tau} \end{pmatrix} \\
&- \begin{pmatrix} \hat{\boldsymbol{\omega}} & \mathbf{0} \\ \hat{\boldsymbol{v}} & \hat{\boldsymbol{\omega}} \end{pmatrix} (\boldsymbol{M}_{\mathrm{b}} - \bar{\boldsymbol{M}}) \begin{pmatrix} \boldsymbol{v}_{\mathrm{f}} \\ \mathbf{0} \end{pmatrix} - \begin{pmatrix} \mathbf{0} & \mathbf{0} \\ \hat{\boldsymbol{v}}_{\mathrm{f}} & \mathbf{0} \end{pmatrix} (\boldsymbol{M}_{\mathrm{b}} - \bar{\boldsymbol{M}}) \boldsymbol{\nu}_{\mathrm{r}} \\
&- (\boldsymbol{M}_{\mathrm{b}} - \bar{\boldsymbol{M}}) \begin{pmatrix} \hat{\boldsymbol{v}}_{\mathrm{f}} \boldsymbol{\omega} + \frac{\partial}{\partial t} \boldsymbol{v}_{\mathrm{f}} + \boldsymbol{\Phi}^T \boldsymbol{v} \\ \mathbf{0} \end{pmatrix} \\
&- \begin{pmatrix} \boldsymbol{\Phi} & \mathbf{0} \\ \mathbf{0} & \mathbf{0} \end{pmatrix} (\boldsymbol{M}_{\mathcal{B}} + \bar{\boldsymbol{M}}) \boldsymbol{\nu}_{\mathrm{r}}
\end{aligned} \tag{6.10}$$

Here, $\boldsymbol{\Phi}$ is the flow gradient matrix

$$\boldsymbol{\Phi}^T = \left(\frac{\partial \boldsymbol{v}_{\mathrm{f}}}{\partial \boldsymbol{x}_{\mathrm{b}}}\right)\boldsymbol{R} = \boldsymbol{R}^T\left(\frac{\partial \boldsymbol{V}_{\mathrm{f}}}{\partial \boldsymbol{x}_{\mathrm{b}}}\right)\boldsymbol{R}$$

For a neutrally buoyant vehicle with coincident centers of mass and buoyancy, Thomasson and Woolsey remark that the second and third lines of (6.10) would vanish [26]. If the flow were uniform, the fourth line would additionally vanish. Finally, in the absence of a background flow, only the first line would remain and the equations would reduce to Kirchhoff's equations (4.100).

Again, note that the equations (6.10) were derived without consideration for a free surface. With no free surface effects, the model will not explicitly capture any of the radiation forces associated with the free surface. The equations do, however, incorporate the forces due to a naturally occurring background flow field, for instance a natural seaway.

Comparison with an Analytical Result

To examine the accuracy of the dynamic model, the hydrodynamic forces are computed due to a plane progressive wave acting on a submerged circle of radius a at a stationary depth p in the flow; this scenario is depicted in Figure 6.1. One may compare the hydrodynamic force that acts on the circle, as predicted using equation (6.10), with the force predicted by an analytic potential flow model.

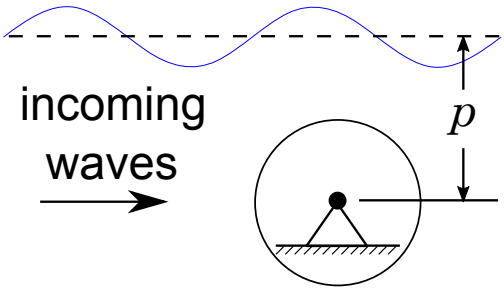

Figure 6.1: Depiction of the stationary, submerged circle subject to a plane progressive wave.

The potential flow force acting on the stationary circle can be computed by taking $\boldsymbol{v} = \boldsymbol{\omega} = \boldsymbol{0}$

and solving (6.10) for $\boldsymbol{f}$:

$$\boldsymbol{f} = -\boldsymbol{\Phi}\left(\boldsymbol{M}_{\mathrm{b}} + \boldsymbol{M}_{\mathcal{B}}\right)\boldsymbol{v}_{\mathrm{f}} - \left(\boldsymbol{M}_{\mathrm{b}} + \boldsymbol{M}_{\mathcal{B}}\right)\frac{\partial}{\partial t}\boldsymbol{v}_{\mathrm{f}} \tag{6.11}$$

The fluid velocity for a plane progressive wave was defined in (3.65). Also, from Section 4.3.1, the added mass for a deeply submerged circle was equal to the mass of the displaced fluid:

$$\boldsymbol{M}_{\mathcal{B}} = \begin{pmatrix} \pi a^2\rho & 0 \\ 0 & \pi a^2\rho \end{pmatrix} \tag{6.12}$$

Note that for a circle in potential flow, there is no hydrodynamic moment since the fluid pressure generates a force which must act through the center of the circle.

The analytical potential flow model is derived using Milne-Thompson's circle theorem [53]. Let $\boldsymbol{z} = x + iz$ identify a point in the complex plane where $i = \sqrt{-1}$. In the complex plane, the velocity potential for the plane progressive wave is defined in terms of the wave amplitude A, wave frequency ω_{w}, and wavenumber k:

$$\boldsymbol{F}(\boldsymbol{z}, t) = i\frac{gA}{\omega_{\mathrm{w}}}\left(\exp[-i(k\boldsymbol{z} - \omega_{\mathrm{w}}t)]\right)$$

Then, employing the circle theorem, the following potential gives the analytical solution for a circle in a plane progressive wave:

$$\begin{aligned}\boldsymbol{F}(\boldsymbol{z}, t) = {} & i\frac{gA}{\omega_{\mathrm{w}}}\left(\exp[-i(k\boldsymbol{z} - \omega_{\mathrm{w}}t)]\right) \\ & + i\frac{gA}{\omega_{\mathrm{w}}}\left(\exp\left[i\left(k\left(\frac{a^2}{\boldsymbol{z} - \boldsymbol{p}} - \boldsymbol{p}\right) - \omega_{\mathrm{w}}t\right)\right]\right)\end{aligned} \tag{6.13}$$

The fluid velocity in the complex plane is then obtained by differentiating (6.13) with respect to $\boldsymbol{z}$:

$$\begin{aligned}\boldsymbol{W}(\boldsymbol{z}, t) = {} & \frac{gAk}{\omega_{\mathrm{w}}}\left(\exp[-i(k\boldsymbol{z} - \omega_{\mathrm{w}}t)]\right) \\ & - \frac{gAk}{\omega_{\mathrm{w}}}\left(\frac{a^2}{(\boldsymbol{z} - \boldsymbol{p})^2}\exp\left[i\left(k\left(\frac{a^2}{\boldsymbol{z} - \boldsymbol{p}} - \boldsymbol{p}\right) - \omega_{\mathrm{w}}t\right)\right]\right)\end{aligned} \tag{6.14}$$

To verify that the body boundary condition is satisfied, a snapshot of the fluid streamlines is shown in Figure 6.2. The flow field defined by the modified velocity potential does not

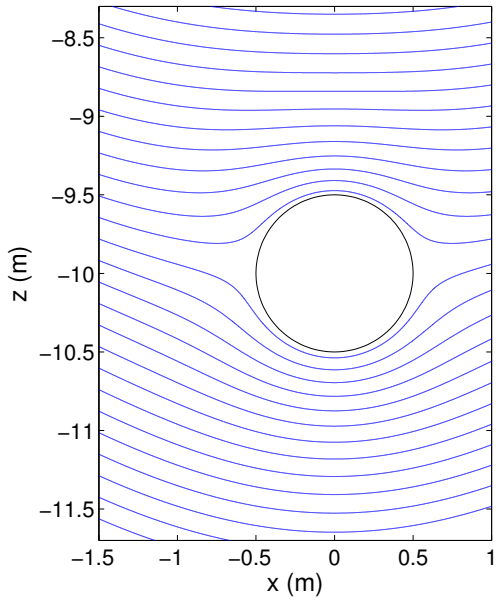

Figure 6.2: A snapshot of the streamlines plotted over the circle in a plane progressive wave.

satisfy the free-surface boundary condition, however; the presence of the circle perturbs the surface. When comparing the ODE prediction (6.11) with the potential flow solution, the only cases considered are those where the circle is deep enough that the perturbation is small. For a circle centerline depth of 10 diameters, the kinematic and dynamic free surface boundary conditions have a maximum relative error of 15% and 0.5%, respectively. It is further expected that this error will decrease for more streamlined bodies.

The pressure field along the streamlines defining the surface of the circle can be computed using the unsteady Bernoulli equation (3.29). The force on the circle is then obtained by integrating the pressure around the circumference. The force predictions for the two models show good agreement over a range of conditions. For the case depicted in Figure 6.2, and with wave characteristics $A = 1$m and $\omega_{\mathrm{w}} = 1.5$rad/s, the maximum disparity between the force coefficient magnitudes is almost zero; see Figure 6.3. Increasing the wave amplitude and placing the circle at a shallower depth, the disparity increases only marginally (on the order of a few percent). As the wavelength becomes much longer than the circle diameter,

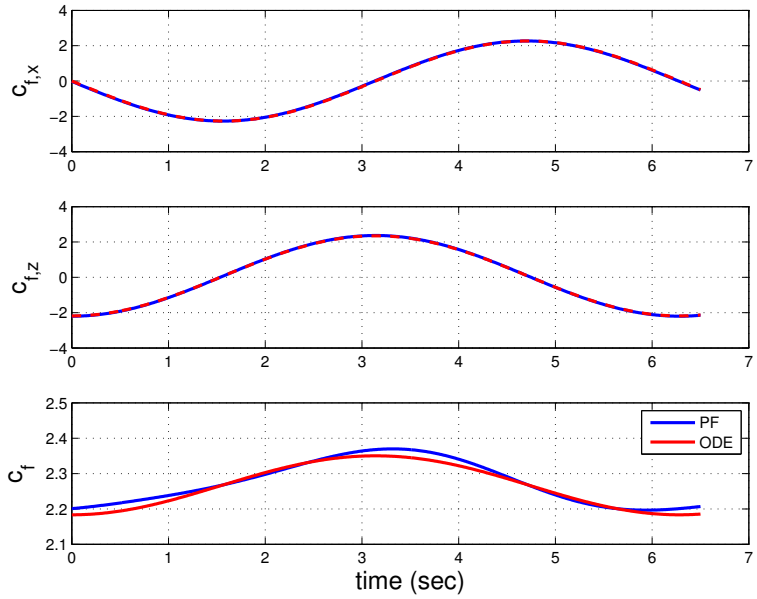

Figure 6.3: A comparison between the force coefficients and magnitude computed by the analytic potential flow solution and those predicted by the model dynamics. Force coefficients are compared in the surge direction (top), the heave direction (middle), and the magnitude is compared (bottom).

however, the disparity increases considerably. Increasing the ratio of wavelength to circle diameter by an order of magnitude, for example, gives a difference in the predicted force magnitude of 10%.

Remarks on Wave Excitation Forces

In the traditional sense, the wave excitation forces (Froude-Krylov and diffraction) are defined as hydrodynamic forces acting on a hull which is restrained from motion [8, 1, 2, 18]. In the prior example, it was appropriate to interpret the hydrodynamic forces as excitation forces since the circle was held stationary. This is *not* the case with the Thomasson and Woolsey model, however. Many of the terms in (6.10) couple the vehicle motions with the ambient fluid motion, resulting in additional forces and moments which depend on the ve-

hicle velocities. Therefore, when using (6.10) to study a maneuvering vehicle in an incident wave field waves, one cannot interpret the generalized forces due to the external fluid motion as just Froude-Krylov and diffraction forces.

This distinction between restrained and unrestrained motion suggests a natural decomposition of the disturbance Lagrangian. In the absence of vehicle motions, the disturbance Lagrangian would reduce to

$$\mathcal{L}_{\mathrm{d,e}}(\boldsymbol{\nu}_{\mathrm{f}}) = \frac{1}{2}\boldsymbol{\nu}_{\mathrm{f}}^{T}\left(\boldsymbol{M}_{\mathcal{B}} + \bar{\boldsymbol{M}}\right)\boldsymbol{\nu}_{\mathrm{f}} \tag{6.15}$$

One may consider the force and moment corresponding to $\mathcal{L}_{\mathrm{d,e}}$ to be the traditional Froude-Krylov and diffraction forces. From (6.4), the remaining contribution to the disturbance Lagrangian is

$$\mathcal{L}_{\mathrm{d},2}(\boldsymbol{\nu}, \boldsymbol{\nu}_{\mathrm{f}}) = -\boldsymbol{\nu}^{T}\left(\boldsymbol{M}_{\mathcal{B}} + \bar{\boldsymbol{M}}\right)\boldsymbol{\nu}_{\mathrm{f}} \tag{6.16}$$

Since $\mathcal{L}_{\mathrm{d},2}$ explicitly depends on the vehicle velocity, (6.16) will account for additional wave effects acting on a vehicle advancing in a seaway. Fossen [1] and Perez [2] refer to these higher-order forces which act on an advancing vessel as second-order wave drift forces.

6.3 A Nonlinear Unified Maneuvering and Seakeeping Model

If one simply added the generalized forces due to $\mathcal{L}_{\mathrm{d}}$ to the memory-affected equations of motion (5.81), the resulting equations would be

$$\begin{aligned}\boldsymbol{F}_{\mathrm{d}} = &\left(\boldsymbol{M}_{\mathrm{b}} + \boldsymbol{M}_{\mathrm{I}}(\boldsymbol{q},\boldsymbol{\nu}) + \boldsymbol{M}_{\mathrm{M}}(\boldsymbol{q},\boldsymbol{\nu},t)\right)\dot{\boldsymbol{\nu}} \\ &+ \left(\boldsymbol{C}_{\mathrm{b}}(\boldsymbol{\nu}) + \boldsymbol{C}_{\mathrm{I}}(\boldsymbol{q},\boldsymbol{\nu}) + \boldsymbol{C}_{\mathrm{M}}(\boldsymbol{q},\boldsymbol{\nu},t)\right)\boldsymbol{\nu} \\ &+ \left(\boldsymbol{D}_{\mathrm{I}}(\boldsymbol{q},\boldsymbol{\nu}) + \boldsymbol{D}_{\mathrm{M}}(\boldsymbol{q},\boldsymbol{\nu},t)\right)\boldsymbol{\nu} \\ &+ \int_{0}^{t} \boldsymbol{K}_{\mathrm{M}}(\boldsymbol{q},\boldsymbol{\nu},\boldsymbol{q}(\tau),t-\tau)\boldsymbol{\nu}(\tau)d\tau + \boldsymbol{g}(\boldsymbol{\theta}_{\mathrm{b}})\end{aligned} \tag{6.17}$$

The terms on the right-hand side are defined in Theorem 5.4.2 and $\boldsymbol{F}_{\mathrm{d}}$ is defined in [48]:

$$\boldsymbol{F}_{\mathrm{d}} = \begin{pmatrix} \boldsymbol{M}_{11}\boldsymbol{\Phi}^T - \boldsymbol{\Phi}\boldsymbol{M}_{11} & \boldsymbol{M}_{11}\widehat{\boldsymbol{v}}_{\mathrm{f}} - \widehat{\boldsymbol{M}_{11}\boldsymbol{v}_{\mathrm{f}}} \\ \widehat{\boldsymbol{v}}_{\mathrm{f}}\boldsymbol{M}_{11} - \widehat{\boldsymbol{M}_{11}\boldsymbol{v}_{\mathrm{f}}} & \boldsymbol{0} \end{pmatrix} \boldsymbol{\nu} + \begin{pmatrix} \boldsymbol{\Phi}\boldsymbol{M}_{11} + \boldsymbol{M}_{11}\frac{\partial \boldsymbol{v}_{\mathrm{f}}}{\partial t} \\ -\widehat{\boldsymbol{v}}_{\mathrm{f}}\boldsymbol{M}_{11}\boldsymbol{v}_{\mathrm{f}} \end{pmatrix} \tag{6.18}$$

In the above expression, $\boldsymbol{M}_{11}$ represents the (1,1) block of the matrix $\boldsymbol{M}_{\mathcal{B}} + \bar{\boldsymbol{M}}$. However, as remarked earlier, the external fluid forces $\boldsymbol{F}_{\mathrm{d}}$ are derived under the assumption that the vehicle is deeply submerged. From a practical point of view, one might expect that the uncertainty in the ambient fluid velocity would far exceed the modeling errors due to neglecting the free surface. In such a case, (6.17) would serve as a sufficient unified model. However, in computational experiments, one will have perfect knowledge of the ambient fluid velocity. In that case, the modeling errors in $\boldsymbol{F}_{\mathrm{d}}$ could adversely effect system identification efforts. This issue can be addressed by updating $\mathcal{L}_{\mathrm{d}}$ to account for the free surface.

6.3.1 The Unified Model System Lagrangian

In the discussion in Section 6.2.1, it was shown that the disturbance forces were effectively generated by the energy due to a deeply-submerged vehicle-shaped pocket of fluid moving relative to the ambient flow. Accounting for modifications due to the free surface is then a simple matter of updating the added mass matrix which appears in (6.5). Based on the results in Chapter 5, the deeply submerged added mass matrix was corrected with the matrices $\Delta\boldsymbol{M}_{\mathcal{B}}$ and $\boldsymbol{M}_{\mathcal{S}_0}$ to account for the free surface. Updating the disturbance Lagrangian accordingly, one finds

$$\begin{aligned} \mathcal{L}_{\mathrm{d}} = &\frac{1}{2}\boldsymbol{\nu}_{\mathrm{r}}^T \left(\boldsymbol{M}_{\mathcal{B}} + \Delta\boldsymbol{M}_{\mathcal{B}}(\boldsymbol{q}) + \boldsymbol{M}_{\mathcal{S}_0}(\boldsymbol{q},\boldsymbol{\nu}) + \bar{\boldsymbol{M}}\right)\boldsymbol{\nu}_{\mathrm{r}} \\ &- \frac{1}{2}\boldsymbol{\nu}^T \left(\boldsymbol{M}_{\mathcal{B}} + \Delta\boldsymbol{M}_{\mathcal{B}}(\boldsymbol{q}) + \boldsymbol{M}_{\mathcal{S}_0}(\boldsymbol{q},\boldsymbol{\nu}) + \bar{\boldsymbol{M}}\right)\boldsymbol{\nu} \end{aligned} \tag{6.19}$$

The question then arises whether or not it is appropriate to modify the disturbance energy to incorporate the memory effects. Since the ambient fluid motion is generated externally, there should not be any memory incurred by the vehicle-shaped pocket of fluid; the prescribed flow

field is "fixed". Moreover, any memory effects incurred by the vehicle are already accounted for in the radiation forces.

To more easily combine the disturbance Lagrangian with the memory-affected system Lagrangian (5.73), one may add the following contributions to (6.19):

$$\left(\frac{1}{2}\boldsymbol{\nu}_{\mathrm{r}}^{T}\boldsymbol{P}\boldsymbol{\nu}_{\mathrm{r}}-\frac{1}{2}\boldsymbol{\nu}^{T}\boldsymbol{P}\boldsymbol{\nu}\right)-\left(\frac{1}{2}\boldsymbol{\nu}_{\mathrm{r}}^{T}\boldsymbol{P}\boldsymbol{\nu}_{\mathrm{r}}-\frac{1}{2}\boldsymbol{\nu}^{T}\boldsymbol{P}\boldsymbol{\nu}\right) \tag{6.20}$$

where the matrix $\boldsymbol{P}$ is defined as follows

$$\boldsymbol{P}+\bar{\boldsymbol{M}}=\boldsymbol{M}_{\mathrm{b}}\quad\text{or}\quad\boldsymbol{P}=\begin{pmatrix}(m_{\mathrm{b}}-\rho\forall)\mathbb{I}_{3} & -m_{\mathrm{b}}\hat{\boldsymbol{r}}_{\mathrm{cm}}\\ m_{\mathrm{b}}\hat{\boldsymbol{r}}_{\mathrm{cm}} & \boldsymbol{I}_{\mathrm{b}}-m_{\mathrm{b}}\hat{\boldsymbol{r}}_{\mathrm{cm}}\hat{\boldsymbol{r}}_{\mathrm{cm}}\end{pmatrix} \tag{6.21}$$

Simplifying, one finds that

$$-\left(\frac{1}{2}\boldsymbol{\nu}_{\mathrm{r}}^{T}\boldsymbol{P}\boldsymbol{\nu}_{\mathrm{r}}-\frac{1}{2}\boldsymbol{\nu}^{T}\boldsymbol{P}\boldsymbol{\nu}\right)=(m_{\mathrm{b}}-\rho\forall)\left(\boldsymbol{v}^{T}\boldsymbol{v}_{\mathrm{f}}-\frac{1}{2}\boldsymbol{v}_{\mathrm{f}}^{T}\boldsymbol{v}_{\mathrm{f}}\right)+m_{\mathrm{b}}\boldsymbol{\omega}^{T}\hat{\boldsymbol{r}}_{\mathrm{cm}}\boldsymbol{v}_{\mathrm{f}}$$

This leads to the following definition of $\mathcal{L}_{\mathrm{d}}$:

$$\begin{aligned}\mathcal{L}_{\mathrm{d}}=&\frac{1}{2}\boldsymbol{\nu}_{\mathrm{r}}^{T}\left(\boldsymbol{M}_{\mathrm{b}}+\boldsymbol{M}_{\mathcal{B}}+\Delta\boldsymbol{M}_{\mathcal{B}}(\boldsymbol{q})+\boldsymbol{M}_{\mathcal{S}_{0}}(\boldsymbol{q},\boldsymbol{\nu})\right)\boldsymbol{\nu}_{\mathrm{r}}\\&-\frac{1}{2}\boldsymbol{\nu}^{T}\left(\boldsymbol{M}_{\mathrm{b}}+\boldsymbol{M}_{\mathcal{B}}+\Delta\boldsymbol{M}_{\mathcal{B}}(\boldsymbol{q})+\boldsymbol{M}_{\mathcal{S}_{0}}(\boldsymbol{q},\boldsymbol{\nu})\right)\boldsymbol{\nu}\\&+m_{\mathrm{b}}\boldsymbol{\omega}^{T}\hat{\boldsymbol{r}}_{\mathrm{cm}}\boldsymbol{v}_{\mathrm{f}}\\&+(m_{\mathrm{b}}-\rho\forall)\left(\boldsymbol{v}^{T}\boldsymbol{v}_{\mathrm{b}}-\frac{1}{2}\boldsymbol{v}_{\mathrm{f}}^{T}\boldsymbol{v}_{\mathrm{f}}\right)\end{aligned} \tag{6.22}$$

Altogether, the four system Lagrangian functions are

$$\begin{aligned}\mathcal{L}_{\mathrm{b}}=&\frac{1}{2}\boldsymbol{\nu}^{T}\boldsymbol{M}_{\mathrm{b}}\boldsymbol{\nu}+m_{\mathrm{b}}gz_{\mathrm{b}}+m_{\mathrm{b}}g\boldsymbol{x}_{\mathrm{cm}}\cdot\left(\boldsymbol{R}^{T}\boldsymbol{i}_{3}\right)\\\mathcal{L}_{\mathcal{B}}=&\frac{1}{2}\boldsymbol{\nu}^{T}\left(\boldsymbol{M}_{\mathcal{B}}+\Delta\boldsymbol{M}_{\mathcal{B}}(\boldsymbol{q})\right)\boldsymbol{\nu}+\boldsymbol{\nu}^{T}\int_{0}^{t}\boldsymbol{K}_{\mathcal{B}}(\boldsymbol{q}(\tau),t-\tau)\boldsymbol{\nu}(\tau)d\tau-\rho g\forall z_{\mathrm{b}}\\\mathcal{L}_{\mathcal{S}_{0}}=&\frac{1}{2}\boldsymbol{\nu}^{T}\boldsymbol{M}_{\mathcal{S}_{0}}(\boldsymbol{q},\boldsymbol{\nu})\boldsymbol{\nu}+\boldsymbol{\nu}^{T}\int_{0}^{t}\boldsymbol{K}_{\mathcal{S}_{0}}(\boldsymbol{q},\boldsymbol{\nu},\boldsymbol{q}(\tau),t-\tau)\boldsymbol{\nu}(\tau)d\tau\\\mathcal{L}_{\mathrm{d}}=&\frac{1}{2}\boldsymbol{\nu}_{\mathrm{r}}^{T}\left(\boldsymbol{M}_{\mathrm{b}}+\boldsymbol{M}_{\mathcal{B}}+\Delta\boldsymbol{M}_{\mathcal{B}}(\boldsymbol{q})+\boldsymbol{M}_{\mathcal{S}_{0}}(\boldsymbol{q},\boldsymbol{\nu})\right)\boldsymbol{\nu}_{\mathrm{r}}\\&-\frac{1}{2}\boldsymbol{\nu}^{T}\left(\boldsymbol{M}_{\mathrm{b}}+\boldsymbol{M}_{\mathcal{B}}+\Delta\boldsymbol{M}_{\mathcal{B}}(\boldsymbol{q})+\boldsymbol{M}_{\mathcal{S}_{0}}(\boldsymbol{q},\boldsymbol{\nu})\right)\boldsymbol{\nu}\\&+m_{\mathrm{b}}\boldsymbol{\omega}^{T}\hat{\boldsymbol{r}}_{\mathrm{cm}}\boldsymbol{v}_{\mathrm{f}}\\&+(m_{\mathrm{b}}-\rho\forall)\left(\boldsymbol{v}^{T}\boldsymbol{v}_{\mathrm{b}}-\frac{1}{2}\boldsymbol{v}_{\mathrm{f}}^{T}\boldsymbol{v}_{\mathrm{f}}\right)\end{aligned}$$

Summing $\mathcal{L}_{\rm b}$, $\mathcal{L}_{\mathcal{B}}$, $\mathcal{L}_{\mathcal{S}_0}$, and $\mathcal{L}_{\rm d}$, one finds that the complete system Lagrangian for a marine craft maneuvering in a seaway is

$$\begin{aligned}\mathcal{L} = &\frac{1}{2}\boldsymbol{\nu}_{\rm r}^T\left(\boldsymbol{M}_{\rm b} + \boldsymbol{M}_{\mathcal{B}} + \Delta\boldsymbol{M}_{\mathcal{B}}(\boldsymbol{q}) + \boldsymbol{M}_{\mathcal{S}_0}(\boldsymbol{q},\boldsymbol{\nu})\right)\boldsymbol{\nu}_{\rm r} \\ &+ \boldsymbol{\nu}^T\int_0^t\left[\boldsymbol{K}_{\rm f}(\boldsymbol{q}(\tau),t-\tau) + \boldsymbol{K}_{\rm s}(\boldsymbol{q},\boldsymbol{\nu},\boldsymbol{q}(\tau),t-\tau)\right]\boldsymbol{\nu}(\tau)d\tau \\ &+ mg\boldsymbol{r}_{\rm cm}\cdot\left(\boldsymbol{R}^T\boldsymbol{i}_3 + \frac{1}{g}\hat{\boldsymbol{v}}_{\rm f}\boldsymbol{\omega}\right) \\ &+ (\rho\forall - m_{\rm b})\left(gz_{\rm b} + \frac{1}{2}\boldsymbol{v}_{\rm f}\cdot\boldsymbol{v}_{\rm f} - \boldsymbol{v}\cdot\boldsymbol{v}_{\rm f}\right)\end{aligned} \tag{6.23}$$

For a neutrally buoyant vehicle, the last line in (6.23) will vanish; when the center of mass coincides with the center of buoyancy, the third line will vanish. If the vehicle is stationary, the memory effects on the second line will vanish, and $\boldsymbol{\nu}_{\rm r}$ would be replaced by $\boldsymbol{\nu}_{\rm f}$ on the first line.

Remark 6.3.1 (Relating radiation and excitation effects) *Consider a neutrally buoyant vehicle with coincident centers of mass and buoyancy. The system Lagrangian is then*

$$\begin{aligned}\mathcal{L} = &\frac{1}{2}\boldsymbol{\nu}_{\rm r}^T\left(\boldsymbol{M}_{\rm b} + \boldsymbol{M}_{\mathcal{B}} + \Delta\boldsymbol{M}_{\mathcal{B}}(\boldsymbol{q}) + \boldsymbol{M}_{\mathcal{S}_0}(\boldsymbol{q},\boldsymbol{\nu})\right)\boldsymbol{\nu}_{\rm r} \\ &+ \boldsymbol{\nu}^T\int_0^t\left[\boldsymbol{K}_{\rm f}(\boldsymbol{q}(\tau),t-\tau) + \boldsymbol{K}_{\rm s}(\boldsymbol{q},\boldsymbol{\nu},\boldsymbol{q}(\tau),t-\tau)\right]\boldsymbol{\nu}(\tau)d\tau\end{aligned}$$

In this form, the energy associated with the exogenous fluid motion appears as an augmentation of the calm-water system energy. Considering that the added mass matrices $\boldsymbol{M}_{\mathcal{B}}$, $\Delta\boldsymbol{M}_{\mathcal{B}}$, and $\boldsymbol{M}_{\mathcal{S}_0}$ characterize the instantaneous exchange of energy between a rigid body and a calm ambient fluid, it makes sense that they should also characterize how an external flow impacts the vehicle. This relationship suggests that the wave excitation effects are not independent from the radiation effects. Rather, the Lagrangian links these two phenomena together in a common framework.

6.3.2 The Unified Model

Noting that the contributions to the equations of motion from $\mathcal{L}_{\rm b}$, $\mathcal{L}_{\mathcal{B}}$, and $\mathcal{L}_{\mathcal{S}_0}$ are already given in (5.81), applying the Boltzmann-Hamel equations to the disturbance Lagrangian completes the unified model. The vehicle is again assumed to be neutrally buoyant. First, compute

$$\begin{aligned}\frac{\partial \mathcal{L}_{\rm d}}{\partial \boldsymbol{\nu}} &= \left(-\boldsymbol{M}_{\rm b} - \boldsymbol{M}_{\mathcal{B}} - \Delta\boldsymbol{M}_{\mathcal{B}}(\boldsymbol{q}) - \boldsymbol{M}_{\mathcal{S}_0}(\boldsymbol{q},\boldsymbol{\nu}) + \frac{1}{2}\sum_{i=1}^{6}\boldsymbol{e}_i\boldsymbol{\nu}_{\rm f}^T\frac{\partial \boldsymbol{M}_{\mathcal{S}_0}}{\partial \nu_i}\right)\boldsymbol{\nu}_{\rm f} \\ &\quad - \sum_{i=1}^{6}\left(\boldsymbol{e}_i\boldsymbol{\nu}_{\rm f}^T\frac{\partial \boldsymbol{M}_{\mathcal{S}_0}}{\partial \nu_i}\right)\boldsymbol{\nu} + \begin{pmatrix}\boldsymbol{0} & \boldsymbol{0}\\ m_{\rm b}\hat{\boldsymbol{r}}_{\rm cm} & \boldsymbol{0}\end{pmatrix}\boldsymbol{\nu}_{\rm f}\end{aligned}$$

Taking the time rate of change, one finds

$$\begin{aligned}\frac{d}{dt}\frac{\partial \mathcal{L}_{\rm d}}{\partial \boldsymbol{\nu}} &= -\sum_{i=1}^{6}\left(\boldsymbol{e}_i\boldsymbol{\nu}_{\rm f}^T\frac{\partial \boldsymbol{M}_{\mathcal{S}_0}}{\partial \nu_i} + \frac{\partial \boldsymbol{M}_{\mathcal{S}_0}}{\partial \nu_i}\boldsymbol{\nu}_{\rm f}^T\boldsymbol{e}_i\right)\dot{\boldsymbol{\nu}} \\ &\quad + \sum_{i=1}^{6}\sum_{j=1}^{6}\left(\boldsymbol{e}_i\boldsymbol{\nu}_{\rm f}^T\frac{\partial^2 \boldsymbol{M}_{\mathcal{S}_0}}{\partial \nu_i\partial \nu_j}\left(\frac{1}{2}\boldsymbol{\nu}_{\rm f} - \boldsymbol{\nu}\right)\right)\dot{\boldsymbol{\nu}} \\ &\quad + \left(-\boldsymbol{M}_{\rm b} - \boldsymbol{M}_{\mathcal{B}} - \Delta\boldsymbol{M}_{\mathcal{B}} - \boldsymbol{M}_{\mathcal{S}_0} + \frac{1}{2}\sum_{i=1}^{6}\boldsymbol{e}_i\boldsymbol{\nu}_{\rm f}^T\frac{\partial \boldsymbol{M}_{\mathcal{S}_0}}{\partial \nu_i} + \begin{pmatrix}\boldsymbol{0} & \boldsymbol{0}\\ m_{\rm b}\hat{\boldsymbol{r}}_{\rm cm} & \boldsymbol{0}\end{pmatrix}\right)\dot{\boldsymbol{\nu}}_{\rm f} \\ &\quad - \sum_{i=1}^{6}\left(\boldsymbol{e}_i\dot{\boldsymbol{\nu}}_{\rm f}^T\frac{\partial \boldsymbol{M}_{\mathcal{S}_0}}{\partial \nu_i} + \frac{\partial(\Delta\boldsymbol{M}_{\mathcal{B}} + \boldsymbol{M}_{\mathcal{S}_0})}{\partial q_i}\boldsymbol{\nu}_{\rm f}\boldsymbol{J}_i^T\right)\boldsymbol{\nu} \\ &\quad + \sum_{i=1}^{6}\sum_{j=1}^{6}\left(\boldsymbol{e}_i\boldsymbol{\nu}_{\rm f}^T\frac{\partial^2 \boldsymbol{M}_{\mathcal{S}_0}}{\partial \nu_i\partial q_j}\left(\frac{1}{2}\boldsymbol{\nu}_{\rm f} - \boldsymbol{\nu}\right)\boldsymbol{J}_j^T\right)\boldsymbol{\nu}\end{aligned}$$

Note that the time derivative of the fluid velocity is

$$\frac{d}{dt}\boldsymbol{\nu}_{\rm f} = \frac{\partial}{\partial t}\boldsymbol{\nu}_{\rm f} + \begin{pmatrix}\boldsymbol{\Phi} & \hat{\boldsymbol{v}}_{\rm f}\\ \boldsymbol{0} & \boldsymbol{0}\end{pmatrix}\boldsymbol{\nu} \tag{6.24}$$

Next, compute

$$\begin{aligned}\boldsymbol{G}\frac{\partial \mathcal{L}_{\rm d}}{\partial \boldsymbol{\nu}} &= \boldsymbol{G}\left(-\boldsymbol{M}_{\rm b} - \boldsymbol{M}_{\mathcal{B}} - \Delta\boldsymbol{M}_{\mathcal{B}} - \boldsymbol{M}_{\mathcal{S}_0} + \sum_{i=1}^{6}\boldsymbol{e}_i\boldsymbol{\nu}_{\rm f}^T\frac{\partial \boldsymbol{M}_{\mathcal{S}_0}}{\partial \nu_i} + \begin{pmatrix}\boldsymbol{0} & \boldsymbol{0}\\ m_{\rm b}\hat{\boldsymbol{r}}_{\rm cm} & \boldsymbol{0}\end{pmatrix}\right)\boldsymbol{\nu}_{\rm f} \\ &\quad - \boldsymbol{G}\sum_{i=1}^{6}\left(\boldsymbol{e}_i\boldsymbol{\nu}_{\rm f}^T\frac{\partial \boldsymbol{M}_{\mathcal{S}_0}}{\partial \nu_i}\right)\boldsymbol{\nu}\end{aligned}$$

The final contribution to the equations of motion is

$$-\boldsymbol{J}^T\frac{\partial \mathcal{L}_{\mathrm{d}}}{\partial \boldsymbol{q}} = -\boldsymbol{J}^T\left(\frac{\partial \boldsymbol{\nu}_{\mathrm{f}}^T}{\partial \boldsymbol{q}}\left(\boldsymbol{M}_{\mathrm{b}}+\boldsymbol{M}_{\mathcal{B}}+\Delta\boldsymbol{M}_{\mathcal{B}}+\boldsymbol{M}_{\mathcal{S}_0}\right)+\frac{1}{2}\sum_{i=1}^{6}\boldsymbol{e}_i\boldsymbol{\nu}_{\mathrm{f}}^T\frac{\partial(\Delta\boldsymbol{M}_{\mathcal{B}}+\boldsymbol{M}_{\mathcal{S}_0})}{\partial q_i}\right)\boldsymbol{\nu}_{\mathrm{f}}$$
$$+\boldsymbol{J}^T\left(\frac{\partial \boldsymbol{\nu}_{\mathrm{f}}^T}{\partial \boldsymbol{q}}\left(\boldsymbol{M}_{\mathrm{b}}+\boldsymbol{M}_{\mathcal{B}}+\Delta\boldsymbol{M}_{\mathcal{B}}+\boldsymbol{M}_{\mathcal{S}_0}\right)+\sum_{i=1}^{6}\boldsymbol{e}_i\boldsymbol{\nu}_{\mathrm{f}}^T\frac{\partial(\Delta\boldsymbol{M}_{\mathcal{B}}+\boldsymbol{M}_{\mathcal{S}_0})}{\partial q_i}\right)\boldsymbol{\nu}$$

Note the following expression from [26]:

$$-\boldsymbol{J}^T\frac{\partial \boldsymbol{\nu}_{\mathrm{f}}^T}{\partial \boldsymbol{q}} = \begin{pmatrix}\boldsymbol{\Phi} & \boldsymbol{0}\\ -\hat{\boldsymbol{v}}_{\mathrm{f}} & \boldsymbol{0}\end{pmatrix} \tag{6.25}$$

Anticipating the structure of the complete equations, define the "external flow perturbation matrices" $\boldsymbol{M}_{\mathrm{E}}$, $\boldsymbol{C}_{\mathrm{E}}$, and $\boldsymbol{D}_{\mathrm{E}}$:

$$\boldsymbol{M}_{\mathrm{E}}(\boldsymbol{q},\boldsymbol{\nu},t) = -\sum_{i=1}^{6}\left(\boldsymbol{e}_i\boldsymbol{\nu}_{\mathrm{f}}^T\frac{\partial \boldsymbol{M}_{\mathcal{S}_0}}{\partial \nu_i}+\frac{\partial \boldsymbol{M}_{\mathcal{S}_0}}{\partial \nu_i}\boldsymbol{\nu}_{\mathrm{f}}^T\boldsymbol{e}_i\right)$$
$$+\sum_{i=1}^{6}\sum_{j=1}^{6}\left(\boldsymbol{e}_i\boldsymbol{\nu}_{\mathrm{f}}^T\frac{\partial^2 \boldsymbol{M}_{\mathcal{S}_0}}{\partial \nu_i\partial \nu_j}\left(\frac{1}{2}\boldsymbol{\nu}_{\mathrm{f}}-\boldsymbol{\nu}\right)\right) \tag{6.26}$$

$$\boldsymbol{C}_{\mathrm{E}}(\boldsymbol{q},\boldsymbol{\nu},t) = -\boldsymbol{G}\sum_{i=1}^{6}\left(\boldsymbol{e}_i\boldsymbol{\nu}_{\mathrm{f}}^T\frac{\partial \boldsymbol{M}_{\mathcal{S}_0}}{\partial \nu_i}\right) \tag{6.27}$$

$$\boldsymbol{D}_{\mathrm{E}}(\boldsymbol{q},\boldsymbol{\nu},t) = -\begin{pmatrix}\boldsymbol{\Phi} & \boldsymbol{0}\\ -\hat{\boldsymbol{v}}_{\mathrm{f}} & \boldsymbol{0}\end{pmatrix}\left(\boldsymbol{M}_{\mathrm{b}}+\boldsymbol{M}_{\mathcal{B}}+\Delta\boldsymbol{M}_{\mathcal{B}}+\boldsymbol{M}_{\mathcal{S}_0}\right)-\sum_{i=1}^{6}\left(\boldsymbol{e}_i\dot{\boldsymbol{\nu}}_{\mathrm{f}}^T\frac{\partial \boldsymbol{M}_{\mathcal{S}_0}}{\partial \nu_i}\right)$$
$$+\sum_{i=1}^{6}\left(\boldsymbol{J}_i\boldsymbol{\nu}_{\mathrm{f}}^T\frac{\partial(\Delta\boldsymbol{M}_{\mathcal{B}}+\boldsymbol{M}_{\mathcal{S}_0})}{\partial q_i}-\frac{\partial(\Delta\boldsymbol{M}_{\mathcal{B}}+\boldsymbol{M}_{\mathcal{S}_0})}{\partial q_i}\boldsymbol{\nu}_{\mathrm{f}}\boldsymbol{J}_i^T\right)$$
$$+\sum_{i=1}^{6}\sum_{j=1}^{6}\left(\boldsymbol{e}_i\boldsymbol{\nu}_{\mathrm{f}}^T\frac{\partial^2 \boldsymbol{M}_{\mathcal{S}_0}}{\partial \nu_i\partial q_j}\left(\frac{1}{2}\boldsymbol{\nu}_{\mathrm{f}}-\boldsymbol{\nu}\right)\boldsymbol{J}_j^T\right) \tag{6.28}$$

Also, define the fluid "disturbance matrices" $\boldsymbol{M}_{\mathrm{D}}$, $\boldsymbol{C}_{\mathrm{D}}$, and $\boldsymbol{D}_{\mathrm{D}}$:

$$\begin{aligned}\boldsymbol{M}_{\mathrm{D}}(\boldsymbol{q},\boldsymbol{\nu},t) &= -\boldsymbol{M}_{\mathrm{b}} - \boldsymbol{M}_{\mathcal{B}} - \Delta\boldsymbol{M}_{\mathcal{B}} - \boldsymbol{M}_{\mathcal{S}_0} \\ &\quad + \sum_{i=1}^{6} \boldsymbol{e}_i \boldsymbol{\nu}_{\mathrm{f}}^T \frac{\partial \boldsymbol{M}_{\mathcal{S}_0}}{\partial \nu_i} + \begin{pmatrix} \boldsymbol{0} & \boldsymbol{0} \\ m_{\mathrm{b}}\hat{\boldsymbol{r}}_{\mathrm{cm}} & \boldsymbol{0} \end{pmatrix} \qquad (6.29) \\ \boldsymbol{C}_{\mathrm{D}}(\boldsymbol{q},\boldsymbol{\nu},t) &= \boldsymbol{G}\left(-\boldsymbol{M}_{\mathrm{b}} - \boldsymbol{M}_{\mathcal{B}} - \Delta\boldsymbol{M}_{\mathcal{B}} - \boldsymbol{M}_{\mathcal{S}_0}\right) \\ &\quad + \boldsymbol{G}\left(\frac{1}{2}\sum_{i=1}^{6} \boldsymbol{e}_i \boldsymbol{\nu}_{\mathrm{f}}^T \frac{\partial \boldsymbol{M}_{\mathcal{S}_0}}{\partial \nu_i} + \begin{pmatrix} \boldsymbol{0} & \boldsymbol{0} \\ m_{\mathrm{b}}\hat{\boldsymbol{r}}_{\mathrm{cm}} & \boldsymbol{0} \end{pmatrix}\right) \qquad (6.30) \\ \boldsymbol{D}_{\mathrm{D}}(\boldsymbol{q},\boldsymbol{\nu},t) &= \begin{pmatrix} \boldsymbol{\Phi} & \boldsymbol{0} \\ -\hat{\boldsymbol{v}}_{\mathrm{f}} & \boldsymbol{0} \end{pmatrix}\left(\boldsymbol{M}_{\mathrm{b}} + \boldsymbol{M}_{\mathcal{B}} + \Delta\boldsymbol{M}_{\mathcal{B}} + \boldsymbol{M}_{\mathcal{S}_0}\right) \\ &\quad - \frac{1}{2}\sum_{i=1}^{6}\left(\boldsymbol{J}_i \boldsymbol{\nu}_{\mathrm{f}}^T \frac{\partial(\Delta\boldsymbol{M}_{\mathcal{B}} + \boldsymbol{M}_{\mathcal{S}_0})}{\partial q_i}\right) \qquad (6.31)\end{aligned}$$

Theorem 6.3.2 (A Nonlinear Unified Maneuvering and Seakeeping Model) *For a neutrally buoyant vehicle operating in a fluid subject to Assumption 6.1.1, the equations of motion are*

$$\begin{aligned}\boldsymbol{F} &= \left(\boldsymbol{M}_{\mathrm{b}} + \boldsymbol{M}_{\mathrm{I}}(\boldsymbol{q},\boldsymbol{\nu}) + \boldsymbol{M}_{\mathrm{M}}(\boldsymbol{q},\boldsymbol{\nu},t) + \boldsymbol{M}_{\mathrm{E}}(\boldsymbol{q},\boldsymbol{\nu},t)\right)\dot{\boldsymbol{\nu}} \\ &\quad + \left(\boldsymbol{C}_{\mathrm{b}}(\boldsymbol{\nu}) + \boldsymbol{C}_{\mathrm{I}}(\boldsymbol{q},\boldsymbol{\nu}) + \boldsymbol{C}_{\mathrm{M}}(\boldsymbol{q},\boldsymbol{\nu},t) + \boldsymbol{C}_{\mathrm{E}}(\boldsymbol{q},\boldsymbol{\nu},t)\right)\boldsymbol{\nu} \\ &\quad + \left(\boldsymbol{D}_{\mathrm{I}}(\boldsymbol{q},\boldsymbol{\nu}) + \boldsymbol{D}_{\mathrm{M}}(\boldsymbol{q},\boldsymbol{\nu},t) + \boldsymbol{D}_{\mathrm{E}}(\boldsymbol{q},\boldsymbol{\nu},t)\right)\boldsymbol{\nu} \\ &\quad + \boldsymbol{g}(\boldsymbol{\theta}_{\mathrm{b}}) + \int_0^t \boldsymbol{K}_{\mathrm{M}}(\boldsymbol{q},\boldsymbol{\nu},\boldsymbol{q}(\tau),t-\tau)\boldsymbol{\nu}(\tau)d\tau \\ &\quad + \boldsymbol{M}_{\mathrm{D}}(\boldsymbol{q},\boldsymbol{\nu},t)\dot{\boldsymbol{\nu}}_{\mathrm{f}} + \boldsymbol{C}_{\mathrm{D}}(\boldsymbol{q},\boldsymbol{\nu},t)\boldsymbol{\nu}_{\mathrm{f}} + \boldsymbol{D}_{\mathrm{D}}(\boldsymbol{q},\boldsymbol{\nu},t)\boldsymbol{\nu}_{\mathrm{f}} \qquad (6.32)\end{aligned}$$

where the matrices $\boldsymbol{M}_{\mathrm{I}}$, $\boldsymbol{C}_{\mathrm{I}}$ and $\boldsymbol{D}_{\mathrm{I}}$ are defined in (5.35)-(5.37), the matrices $\boldsymbol{M}_{\mathrm{M}}$, $\boldsymbol{C}_{\mathrm{M}}$, $\boldsymbol{D}_{\mathrm{M}}$, and $\boldsymbol{K}_{\mathrm{M}}$ are defined in (5.77)-(5.80), the matrices $\boldsymbol{M}_{\mathrm{E}}$, $\boldsymbol{C}_{\mathrm{E}}$, and $\boldsymbol{D}_{\mathrm{E}}$ are defined in (6.26)-(6.28), the matrices $\boldsymbol{M}_{\mathrm{D}}$, $\boldsymbol{C}_{\mathrm{D}}$, and $\boldsymbol{D}_{\mathrm{D}}$ are defined in (6.29)-(6.31), and $\boldsymbol{g}$ is defined in (5.38). □

The terms in (6.32) are summarized as follows:

- $\boldsymbol{M}_{\mathrm{I}}$, $\boldsymbol{C}_{\mathrm{I}}$ and $\boldsymbol{D}_{\mathrm{I}}$ are the "instantaneous" fluid response matrices. These terms account for the energy required to generate the instantaneous fluid response to the motion of a rigid body. Some of these terms will remain for a deeply submerged vehicle.

- $\boldsymbol{M}_{\mathrm{M}}$, $\boldsymbol{C}_{\mathrm{M}}$, $\boldsymbol{D}_{\mathrm{M}}$, and $\boldsymbol{K}_{\mathrm{M}}$ are the "memory-effect" matrices. These terms account for the cumulative fluid energy which is radiated away from the body in the form of surface waves. These terms vanish for a deeply submerged vehicle.

- $\boldsymbol{M}_{\mathrm{E}}$, $\boldsymbol{C}_{\mathrm{E}}$, and $\boldsymbol{D}_{\mathrm{E}}$ are the "external" flow perturbation matrices. These terms account for the modifications to the calm water system energy due to the external flow field. This is the phenomena observed by Crook [30], who measured the changes to the calm-water free surface suction and wave resistance forces due to incident waves.

- $\boldsymbol{M}_{\mathrm{D}}$, $\boldsymbol{C}_{\mathrm{D}}$, and $\boldsymbol{D}_{\mathrm{D}}$ are the wave "disturbance" matrices. These terms would remain if the vehicle were arrested and therefore account for the energy which results in wave excitation forces.

- $\boldsymbol{g}$ is the hydrostatic vector. This term accounts for the gravitational potential energy which acts on the body and the fluid. Forces due to non-neutral buoyancy or torques due to offset centers of mass and buoyancy appear here.

- $\boldsymbol{F}$ is the vector of external generalized forces. This is where any other physical effects are incorporated which perform work on the system, such as viscous drag, vortex shedding, and control inputs.

Vehicle Motion in Waves

The equations of motion (6.32) are defined in terms of an arbitrary fluid velocity field $\boldsymbol{V}_{\mathrm{f}}$. To model the motion of a vehicle in a seaway, one may generate a flow field using the techniques outlined in Section 3.4. In the simplest case, the velocity field for a plane progressive wave is given by (3.65). Using a plane progressive wave field could enable one to derive a RAO

for a marine craft. One typically computes an RAO by combining panel method results for frequency-domain radiation and excitation forces. Using the proposed model (6.32), one would only need to solve the radiation problem for the added mass matrices. These matrices could then be used to compute the excitation forces as was done for the example in Section 6.2.2.

If one were interested in modeling a wave spectrum, a series of plane progressive waves may be used to approximate the energy density function. In this case, the fluid velocity field will be given by a superposition of plane progressive waves, each with the correct amplitude and frequency. In [64, 65, 48], the authors used the Thommasson-Woolsey equations (6.10) to model the wave disturbance forces acting on an underwater vehicle. In [48], the vehicle was tasked with tracking a desired depth and heading in a short-crested wave field; the depth and heading tracking problem is depicted in Figure 6.5. The resulting state trajectories highlight the rich dynamic behavior inherent to a marine craft operating in a wave field.

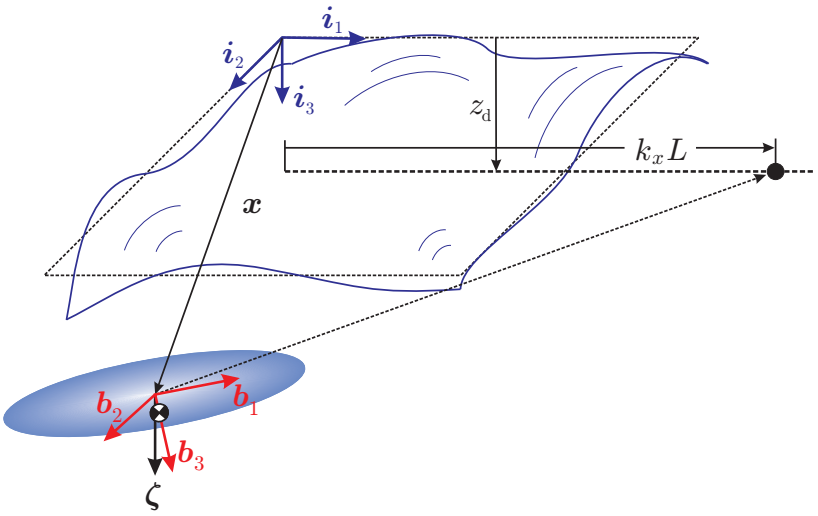

Figure 6.4: Illustration of the depth and heading tracking problem.

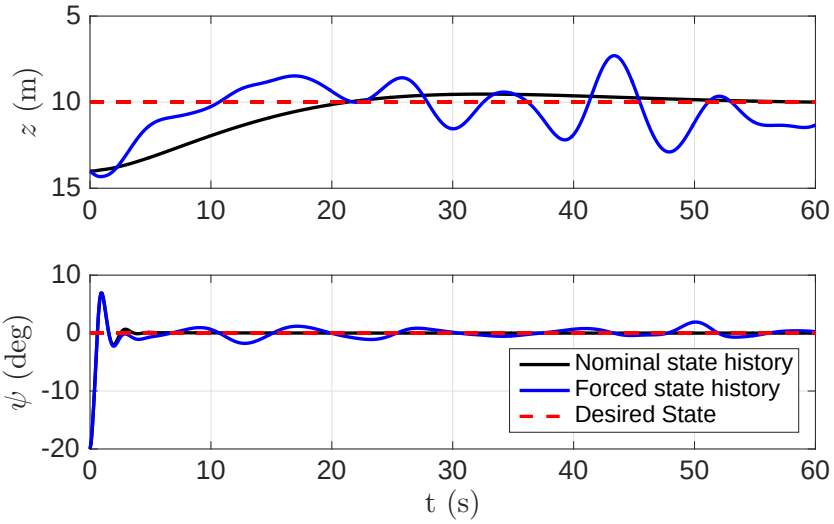

Figure 6.5: State trajectories for the depth and heading tracking problem.

6.4 Closing Remarks

In this chapter, two unified models for a marine craft maneuvering in a seaway were constructed. The first simply incorporated the generalized forces from the disturbance forces in [26] which did not account for a free surface. However, recognizing that the disturbance Lagrangian corresponds to the motion of a deeply-submerged, vehicle-shaped pocket of fluid, the disturbance Lagrangian could be augmented using the results from Chapter 5. The second unified model was derived using the disturbance Lagrangian function which was corrected for the free surface. The resulting model represents a set of nonlinear unified maneuvering and seakeeping equations.

Chapter 7

Conclusions

7.1 Summary

Parametric models for fluid-body interactions are used in a number of applications, including control design, stability analysis, real-time simulators, and low-cost design optimization. In this dissertation, a Lagrangian modeling approach was used to construct nonlinear parametric models for marine craft in several different operating conditions.

The framework for the Lagrangian modeling effort was introduced in Chapter 4, where the general system energy functions required to construct the system Lagrangian were identified. The generalized hydrodynamic forces predicted by the Lagrangian approach were also shown to be equivalent to results from Newtonian mechanics in general operating conditions and simple examples.

In Chapter 5, calm-water maneuvering for a vehicle in the presence of a free surface was addressed. Building upon the results in Chapter 4, Lagrangian functions were presented for a system with and without the fluid memory effects. The Lagrangians were then used to derive the dynamic equations of motion. Though the memory-free equations were simpler, analysis of the equations in a single degree of freedom revealed that wave resistance forces

were absent from that model. The memory-affected model, however, can account for wave resistance effects by modeling the time evolution of the free surface.

Finally, the effects due to an exogenous flow field were incorporated in Chapter 6. Beginning with a review of the Thomasson and Woolsey model [26], a disturbance Lagrangian was identified which isolates the system energy contributions from the ambient flow field. The disturbance Lagrangian was then corrected to account for the free surface using the prior results from Chapter 5. This enabled the derivation of a nonlinear set of unified maneuvering and seakeeping equations.

As noted in the conclusion of Chapter 5, one potential deficiency with the proposed models is predicting free surface elevations. While the models presented in this dissertation are valid for both fully submerged vehicles or surface craft, they employ the linearized free surface boundary conditions. Applications like predicting broaching or predicting capsize will likely require one to implement the fully nonlinear free surface boundary conditions.

7.2 Future Work

There are two primary directions for future work:

1. Devise a system identification procedure to approximate the state- and time-dependent parameters which appear in the dynamic equations.

2. Construct a model-based controller which leverages the proposed model structure for near-surface maneuvering.

Identification procedures based on CFD, including [30, 66, 12, 61], are promising for the proposed model. For a physical experiment, the fluid energy functions are generally incalculable. However, computational experiments readily compute the necessary quantities, for instance the fluid velocity everywhere within the fluid volume. Also, because the models

presented in this dissertation are derived under potential flow, it is expected that system identification from ideal flow results will yield a higher quality model. Numerical simulations can selectively disable physical phenomena, such as viscosity, so that the experimental data will better match the modeling assumptions.

Model-based control design and disturbance estimation can improve vehicle performance and expand the operating envelope for marine craft. In their current form, the memory effects which appear in the proposed model cannot be used in typical control and observer design strategies. However, in future work, one could extend the linearized realization approaches used in [22, 2, 20] to develop nonlinear state-space representations of the memory effects. Such a reduced-order model could be used for wave-disturbance estimation and ultimately feedforward disturbance rejection for a marine craft operating in rough seas. The reduced-order representation of the model could also be used in nonlinear control design to enable more aggressive maneuvering of manned submarines and underwater vehicles. One particularly promising control approach is energy-based control [44, 47, 67, 48, 68]. These strategies leverage a system Lagrangian or Hamiltonian to aid in nonlinear control design and stability analysis. The system Lagrangian functions presented in this dissertation could prove useful for developing energy-based nonlinear controllers.

Bibliography

[1] T. I. Fossen, *Guidance and Control of Ocean Vehicles*. New York: Wiley, 1994.

[2] T. Perez, *Ship Motion Control: Course keeping and roll stabilisation using rudder and fins*. Springer, 2005.

[3] S. C. Stevens and M. G. Parsons, "Effects of motion at sea on crew performance: A survey," *Marine Technology*, vol. 39, no. 1, pp. 29–47, January 2002.

[4] L. N. Virgin, "The nonlinear rolling response of a vessel including chaotic motions leading to capsize in regular seas," *Applied Ocean Research*, vol. 9, no. 2, pp. 89–95, April 1987.

[5] S. Naik and S. D. Ross, "Geometry of escaping dynamics in nonlinear ship motion," *Communications in Nonlinear Science and Numerical Simulation*, vol. 47, pp. 48–70, 2017.

[6] E. V. Lewis, *Principles of Naval Architecture Volume III: Motion in Waves and Controllability*. 601 Pavonia Avenue, Jersey City NJ: SNAME, 1989, vol. 3.

[7] M. C. Jones and E. G. Paterson, "Influence of propulsion type on the near-wake evolution of kinetic and potential energy," in *Fifth International Symposium on Marine Propulsors*. Helsinki, Finland: SMP, June 2017.

[8] J. N. Newman, *Marine Hydrodynamics*. Cambridge, MA: The MIT Press, 1977.

[9] J. H. Milgram, "Strip theory for underwater vehicles in water of finite depth," *Journal of Engineering Math*, vol. 58, pp. 31–50, 2007.

[10] L. J. Doctors and R. F. Beck, "Convergence properties of the Neumann-Kelvin problem for a submerged body," *Journal of Ship Research*, vol. 31, no. 4, pp. 227–234, December 1987.

[11] D. C. Kring, "Time domain ship motions by a three-dimensional rankine panel method," Ph.D. dissertation, Massachusettes Institute of Technology, May 1994.

[12] C. Polis, D. Ranmuthugala, J. Duffy, and M. Renilson, "Enabling the prediction of manoeuvring characteristics of a submarine operating near the free surface," in *Pacific 2013 International Maritime Conference: The commercial maritime and naval defence showcase for the Asia Pacific*. Barton, ACT: Engineers Australia, 2013, pp. 281–291.

[13] G. Berkooz, P. Holmes, and J. L. Lumley, "The proper orthogonal decomposition in the analysis of turbulent flows," *Annual Review of Fluid Mechanics*, vol. 25, pp. 539–575, 1993.

[14] I. Mezić, "Spectral properties of dynamical systems, model reduction and decompositions," *Nonlinear Dynamics*, vol. 41, pp. 309–325, 2005.

[15] P. J. Schmid, "Dynamic mode decomposition of numerical and experimental data," *Journal of Fluid Mechanics*, vol. 656, pp. 5–28, 2010.

[16] D. T. Greenwood, *Advanced Dynamics*. New York: Cambridge University Press, 2003.

[17] H. Goldstein, C. Poole, and J. Safko, *Classical Mechanics*, 3rd ed. Addison Wesley, 2000.

[18] E. M. Lewandowski, *The Dynamics of Marine Craft*, ser. Advanced Series on Ocean Engineering. River Edge, NJ, USA: World Scientific, 2004.

[19] W. E. Cummins, "The impulse response function and ship motions," David Taylor Model Basin, Hydromechanics Laboratory, Tech. Rep. 1661, 1962.

[20] T. I. Fossen, "A nonlinear unified state-space model for ship maneuvering and control in a seaway," *Journal of Bifurcation and Chaos*, vol. 15, no. 9, pp. 2717–2746, September 2005.

[21] P. A. Bailey, W. G. Price, and P. Temarel, "A unified mathematical model describing the manoeuvring of a ship travelling in a seaway," in *Trans. RINA*, vol. 140, 1998, pp. 131–149.

[22] E. Kristiansen, A. Hjulstad, and O. Egeland, "State-space representation of radiation forces in time-domain vessel models," *Ocean Engineering*, vol. 32, pp. 2195–2216, 2005.

[23] S. Gugercin and A. C. Antoulas, "A survey of model reduction by balanced truncation and some new results," *Internatial Journal of Control*, vol. 77, no. 8, pp. 748–766, May 2004.

[24] P. H. Heins, B. L. Jones, and D. J. Taunton, "Design and validation of an unmanned surface vehicle simulation model," *Elsevier Journal of Applied Mathematical Modelling*, vol. 48, pp. 749–774, 2017.

[25] H. Lamb, *Hydrodynamics*. Dover, 1932.

[26] P. G. Thomasson and C. A. Woolsey, "Vehicle motion in currents," *IEEE Journal of Oceanic Engineering*, vol. 38, no. 2, pp. 226–242, April 2013.

[27] J. Feldman, "Dtnsrdc revised standard submarine equations of motion," David Taylor Naval Ship Research and Developtment Center, Bethesda, Md., Tech. Rep., 1979.

[28] M. Gertler and G. R. Hagen, "Standard equations of motion for submarine simulation," David Taylor Naval Ship Research and Developtment Center, Bethesda, Md., Technical Report 2510, June 1967.

[29] T. F. Ogilvie, "Recent progress toward the understanding and prediction of ship motions," in *The Fifth Symposium on Naval Hydrodynamics*, Bergen, Norway, September 1964, pp. 3–80.

[30] T. P. Crook, "An initial assessment of free surface effects on submerged bodies," Master's thesis, Naval Postgraduate School, Monterey CA, September 1994.

[31] E. Licéaga-Castro and G. M. van der Molen, "Submarine H_∞ depth control under wave disturbances," *IEEE Transactions on Control Systems Technology*, vol. 3, no. 3, pp. 338–346, September 1995.

[32] S. F. Hoerner, *Fluid Dynamic Drag*, Hoerner, Ed. Midland Park, NJ: Hoerner, 1965.

[33] S. I. Sagatun and T. I. Fossen, "Lagrangian formulation of underwater vehicles' dynamics," in *Proc. IEEE International Conference on Systems, Man, and Cybernetics*. Charlottesville, Va: IEEE, October 1991, pp. 1029–1034.

[34] A. Ross, "Nonlinear manoeuvring models for ships: a Lagrangian approach," Ph.D. dissertation, Norwegian University of Science and Technology, Trondheim, Norway, 2008.

[35] A. Wolek and C. A. Woolsey, *Sensing and Control for Autonomous Vehicles*, ser. Lecture Notes in Control and Information Sciences. Springer, 2017, vol. 474, ch. Model-Based Path Planning, pp. 183–206.

[36] S. I. Newton, *Philosophiæ Naturalis Principia Mathematica*, third ed., first American ed. New York: Daniel Adee, translated by Andrew Motte, 1729.

[37] A. Ross, "A rudimentary history of dynamics," *Modeling, Identification and Control*, vol. 30, no. 4, pp. 223–235, 2009.

[38] L. N. Hand and J. D. Finch, *Analytical Mechanics*. New York, New York: Cambridge University Press, 1998.

[39] I. M. Gelfand and S. V. Fomin, *Calculus of Variations*, revised english edition ed., R. A. Silverman, Ed. Englewood Cliffs, New Jersey: Prentice-Hall, 1963.

[40] J. A. Burns, *Introduction to the Calculus of Variations and Control with Modern Applications*, ser. Applied Mathematics & Nonlinear Science. Boca Raton, Florida: CRC Press, 2013.

[41] K. Karamcheti, *Principles of Ideal-Fluid Aerodynamics*. Malabar, Florida: Krieger, 1980.

[42] H. Schaub and J. Junkins, *Analytical Mechanics of Space Systems*, 2nd ed., ser. AIAA Education Series. Reston, VA, USA: AIAA, 2003.

[43] J. E. Marsden and T. S. Ratiu, *Introduction to Mechanics and Symmetry*. Springer, 1994.

[44] N. E. Leonard, "Stability of a bottom-heavy underwater vehicle," *Automatica*, vol. 33, no. 3, pp. 331–346, 1997.

[45] K. B. Petersen and M. S. Pedersen, "The matrix cookbook," http://matrixcookbook.com, November 2012.

[46] N. E. Leonard, "Stabilization of underwater vehicle dynamics with symmetry-breaking potentials," *Systems & Control Letters*, vol. 32, pp. 35–42, 1997.

[47] C. A. Woolsey and L. Techy, "Cross-track control of a slender, underactuated AUV using potential shaping," *Ocean Engineering*, vol. 36, pp. 82–91, 2009.

[48] T. Battista, S. Jung, C. Woolsey, and E. Paterson, "An energy-Casimir approach to underwater depth and heading regulation in short-crested waves," in *Proc. 1st IEEE Conference on Control Technology and Applications*, Kohala Coast, Hawaii, August 2017.

[49] J. A. Schetz and R. D. Bowersox, *Boundary Layer Analysis*, 2nd ed., ser. AIAA Education Series, M. R. Mendenhall, Ed. Reston, VA, USA: AIAA, 2011.

[50] *A Hamiltonian formulation for nonlinear wave-body interactions*, St John's, Newfoundland, Canada, May 1993.

[51] J. C. Luke, "A variational principle for a fluid with a free surface," *Journal of Fluid Mechanics*, vol. 27, no. 2, pp. 395–397, 1967.

[52] T. Elfouhaily, B. Chapron, K. Katsaros, and D. Vandemark, "A unified directional spectrum for long and short wind-driven waves," *Journal of Geophysical Research*, vol. 102, no. C7, pp. 781–796, July 1997.

[53] L. M. Milne-Thomson, *Theoretical Hydrodynamics Fourth Edition.* St. Martin's Press Inc., 1960.

[54] P. D. Sclavounos, "Nonlinear impulse of ocean waves on floating bodies," *Journal of Fluid Mechanics*, vol. 697, pp. 316–335, 2012.

[55] L. Landweber and C. S. Yih, "Forces, moments, and added masses for Rankine bodies," *Journal of Fluid Mechanics*, vol. 1, no. 3, pp. 319–336, September 1956.

[56] L. Landweber and T. Miloh, "Unsteady Lagally theorem for multipoles and deformable bodies," *Journal of Fluid Mechanics*, 1980.

[57] D. T. Greenwood, *Principles of Dynamics.* Englewood Cliffs, New Jersey: Prentice Hall, 1988.

[58] T. Battista, F. Valentinis, and C. Woolsey, "A maneuvering model for an underwater vehicle near a free surface," *IEEE Journal of Oceanic Engineering*, 2018, (Accepted with revision.).

[59] W. J. Rugh, *Linear System Theory*, 2nd ed., ser. Information and system sciences series. Upper Saddle River, New Jersey: Prentice Hall, 1996.

[60] T. Battista, C. Woolsey, T. Perez, and F. Valentinis, "A dynamic model for underwater vehicle maneuvering near a free surface," in *Proc. 10th IFAC Conference on Control Applications in Marine Systems*, Trondheim, Norway, September 2016.

[61] S. Jung, T. Battista, E. Paterson, and C. Woolsey, "Effects of depth and added mass obtained from virtual PMM tests of a submerged prolate spheroid," in *Proc. MTS/IEEE Oceans 2017*, Anchorage, Alaska, September 2017.

[62] T. Perez and T. I. Fossen, "Time- vs. frequency-domain identification of parametric radiation force models for marine structures at zero speed," *Modeling, Identification and Control*, vol. 29, no. 1, pp. 1–19, 2008.

[63] P. G. Thomasson, "Equations of motion of a vehicle in a moving fluid," *Journal of Aircraft*, vol. 37, no. 4, pp. 630–639, August 2000.

[64] T. Battista, C. Woolsey, L. McCue-Weil, E. Paterson, and F. Valentinis, "Underwater vehicle depth and attitude regulation in plane progressive waves," in *Proc. 54th IEEE Conference on Decision and Control*, Osaka, Japan, December 2015.

[65] T. Battista and C. A. Woolsey, "Control of an underwater vehicle in irregular waves," in *Proc. MTS/IEEE Oceans 2015*, Washington D.C., October 2015.

[66] B. J. Racine and E. G. Paterson, "CFD-based method for simulation of marine-vehicle maneuvering," in *35th AIAA Fluid Dynamics Conference and Exhibit.* Toronto, Ontario Canada: AIAA, June 2015.

[67] F. Valentinis, A. Donaire, and T. Perez, "Energy-based guidance of an underactuated unmanned underwater vehicle on a helical trajectory," *Control Engineering Practice*, vol. 44, pp. 138–156, 2015.

[68] F. Valentinis and C. Woolsey, "Nonlinear control of a subscale submarine in emergency ascent," 2018.

Appendix A

A.1 Vector Calculus Identities

In the following identities, let $\boldsymbol{A}, \boldsymbol{B} \in \mathbb{R}^3$, let $a, b \in \mathbb{R}$, let $\mathcal{V}$ denote some volume contained within a surface $\mathcal{S}$, and let $\boldsymbol{n}_+$ denote the unit normal vector directed from $\mathcal{S}$ out of $\mathcal{V}$.

The Gradient Theorem [41, Ch. 2]

$$\iiint_{\mathcal{V}} \nabla a \; dV = \iint_{\mathcal{S}} a\boldsymbol{n}_+ \; dS \tag{A.1}$$

The gradient theorem relates the sum total of the gradient of a within $\mathcal{V}$ to the projection of a normal to the bounding surface $\mathcal{S}$.

The Divergence Theorem (Gauss's Theorem) [41, Ch. 2]

$$\iiint_{\mathcal{V}} \nabla \cdot \boldsymbol{A} \; dV = \iint_{\mathcal{S}} \boldsymbol{A} \cdot \boldsymbol{n}_+ \; dS \tag{A.2}$$

The divergence theorem relates the total divergence of $\boldsymbol{A}$ within $\mathcal{V}$ to the net outward flux of $\boldsymbol{A}$ through the bounding surface $\mathcal{S}$.

The Curl Theorem [41, Ch. 2]

$$\iiint_{\mathcal{V}} \nabla \times \boldsymbol{A} \; dV = \iint_{\mathcal{S}} \boldsymbol{n}_+ \times \boldsymbol{A} \; dS \tag{A.3}$$

The curl theorem relates the total vorticity of $\boldsymbol{A}$ within $\mathcal{V}$ to the sum total of the portion of $\boldsymbol{A}$ which is perpendicular to the outward unit normal vector $\boldsymbol{n}_+$ over the bounding surface $\mathcal{S}$.

The Reynolds Transport theorem [8, Ch. 3.3]

Suppose f is a scalar function of spatial coordinates $\boldsymbol{x} \in \mathbb{R}^3$ and time t ($f : \mathbb{R}^3 \times \mathbb{R} \rightarrow \mathbb{R}$). Suppose also that the volume $\mathcal{V}$ is now a function of time; let $\boldsymbol{V}_{\mathrm{s}}$ denote the velocity of the bounding surface $\mathcal{S}$ at an arbitrary point in $\mathcal{S}$. The time rate of change of the integral of $f(\boldsymbol{x}, t)$ is given by the Reynolds transport theorem:

$$\frac{d}{dt}\iiint_{\mathcal{V}(t)} f(\boldsymbol{x}, t)dV = \iiint_{\mathcal{V}} \frac{\partial f}{\partial t}dV + \iint_{\mathcal{S}} f\boldsymbol{V}_{\mathrm{s}} \cdot \boldsymbol{n}_{+}dS \tag{A.4}$$

The volume integral on the right-hand side captures the time rate of change of f due to the *unsteadiness* of f within the time-frozen volume $\mathcal{V}$. (Answers the question: how much of f are we gaining due to the explicit time dependence of f while holding the volume fixed in time.) The surface integral captures the time rate of change of f due to the instantaneous motion of the surface. (Answers the question: how much more of f are are we gaining as the volume translates, rotates, and/or dilates, holding f fixed in time.)

The Convective Derivative

$$(\boldsymbol{A} \cdot \nabla)a = \boldsymbol{A} \cdot (\nabla a) \tag{A.5}$$

$$(\boldsymbol{V}_{\mathrm{f}} \cdot \nabla)\,\boldsymbol{V}_{\mathrm{f}} = \nabla\left(\frac{1}{2}\boldsymbol{V}_{\mathrm{f}} \cdot \boldsymbol{V}_{\mathrm{f}}\right) \tag{A.6}$$

The Material Derivative

$$\frac{D}{Dt}a = \frac{\partial a}{\partial t} + (\boldsymbol{V}_{\mathrm{f}} \cdot \nabla)a \tag{A.7}$$

$$\frac{D}{Dt}\boldsymbol{V}_{\mathrm{f}} = \frac{\partial \boldsymbol{V}_{\mathrm{f}}}{\partial t} + (\boldsymbol{V}_{\mathrm{f}} \cdot \nabla)\,\boldsymbol{V}_{\mathrm{f}} \tag{A.8}$$

Additional Vector Identities

$$\nabla(ab) = a\nabla b + b\nabla a \tag{A.9}$$

$$\nabla \cdot (a\boldsymbol{A}) = a\nabla \cdot \boldsymbol{A} + \nabla a \cdot \boldsymbol{A} \tag{A.10}$$

A.2 Derivation of $\dot{\boldsymbol{R}}$ Using Euler Angles

To determine the time rate of change of the rotation matrix $\boldsymbol{R}$, we compute

$$\frac{d}{dt}\boldsymbol{R} = \dot{\boldsymbol{R}}_3(\psi_\mathrm{b})\boldsymbol{R}_2(\theta_\mathrm{b})\boldsymbol{R}_1(\phi_\mathrm{b}) + \boldsymbol{R}_3(\psi_\mathrm{b})\dot{\boldsymbol{R}}_2(\theta_\mathrm{b})\boldsymbol{R}_1(\phi_\mathrm{b}) + \boldsymbol{R}_3(\psi_\mathrm{b})\boldsymbol{R}_2(\theta_\mathrm{b})\dot{\boldsymbol{R}}_1(\phi_\mathrm{b})$$

Recall the definition, for instance, of $\boldsymbol{R}_1(\phi_\mathrm{b})$:

$$\boldsymbol{R}(\phi_\mathrm{b}) = e^{\widehat{\boldsymbol{e}_1}\phi_\mathrm{b}} = \mathbb{I} + \widehat{\boldsymbol{e}_1}\phi_\mathrm{b} + \frac{1}{2!}\widehat{\boldsymbol{e}_1}^2\phi_\mathrm{b}^2 + \frac{1}{3!}\widehat{\boldsymbol{e}_1}^3\phi_\mathrm{b}^3 + \frac{1}{4!}\widehat{\boldsymbol{e}_1}^4\phi_\mathrm{b}^4 + \dots$$

Then the time rate of change is

$$\dot{\boldsymbol{R}}_1(\phi_\mathrm{b}) = \frac{\partial \boldsymbol{R}_1(\phi_\mathrm{b})}{\partial \phi_\mathrm{b}}\dot{\phi_\mathrm{b}} = \left(\widehat{\boldsymbol{e}_1} + \widehat{\boldsymbol{e}_1}^2\phi_\mathrm{b}^1 + \frac{1}{2!}\widehat{\boldsymbol{e}_1}^3\phi_\mathrm{b}^2 + \frac{1}{3!}\widehat{\boldsymbol{e}_1}^4\phi_\mathrm{b}^3 + \dots\right)\dot{\phi_\mathrm{b}} = \boldsymbol{R}_1(\phi_\mathrm{b})\widehat{\boldsymbol{e}_1}\dot{\phi_\mathrm{b}}$$

In general, we see that $\dot{\boldsymbol{R}}_i(x) = \boldsymbol{R}_i(x)\widehat{\boldsymbol{e}_i}\dot{x}$. Then, the time rate of change of $\boldsymbol{R}$ may be written as

$$\begin{aligned}\dot{\boldsymbol{R}} &= \boldsymbol{R}_3(\psi_\mathrm{b})\left(\widehat{\boldsymbol{e}_3}\dot{\psi_\mathrm{b}}\right)\boldsymbol{R}_2(\theta_\mathrm{b})\boldsymbol{R}_1(\phi_\mathrm{b}) + \boldsymbol{R}_3(\psi_\mathrm{b})\boldsymbol{R}_2(\theta_\mathrm{b})\left(\widehat{\boldsymbol{e}_2}\dot{\theta_\mathrm{b}}\right)\boldsymbol{R}_1(\phi_\mathrm{b}) + \boldsymbol{R}_3(\psi_\mathrm{b})\boldsymbol{R}_2(\theta_\mathrm{b})\boldsymbol{R}_1(\phi_\mathrm{b})\left(\widehat{\boldsymbol{e}_1}\dot{\phi_\mathrm{b}}\right)\\ &= \boldsymbol{R}\left[\boldsymbol{R}_1^T(\phi_\mathrm{b})\boldsymbol{R}_2^T(\theta_\mathrm{b})\left(\widehat{\boldsymbol{e}_3}\dot{\psi_\mathrm{b}}\right)\boldsymbol{R}_2(\theta_\mathrm{b})\boldsymbol{R}_1(\phi_\mathrm{b}) + \boldsymbol{R}_1^T(\phi_\mathrm{b})\left(\widehat{\boldsymbol{e}_2}\dot{\theta_\mathrm{b}}\right)\boldsymbol{R}_1(\phi_\mathrm{b}) + \widehat{\boldsymbol{e}_1}\dot{\phi_\mathrm{b}}\right]\end{aligned}$$

Then, one may verify that

$$\begin{aligned}\widehat{\left(\boldsymbol{R}_1^T(\phi_\mathrm{b})\boldsymbol{R}_2^T(\theta_\mathrm{b})\boldsymbol{e}_3\dot{\psi_\mathrm{b}}\right)} &= \boldsymbol{R}_1^T(\phi_\mathrm{b})\boldsymbol{R}_2^T(\theta_\mathrm{b})\left(\widehat{\boldsymbol{e}_3}\dot{\psi_\mathrm{b}}\right)\boldsymbol{R}_2(\theta_\mathrm{b})\boldsymbol{R}_1(\phi_\mathrm{b})\\ \widehat{\left(\boldsymbol{R}_1^T(\phi_\mathrm{b})\boldsymbol{e}_2\dot{\theta_\mathrm{b}}\right)} &= \boldsymbol{R}_1^T(\phi_\mathrm{b})\left(\widehat{\boldsymbol{e}_2}\dot{\theta_\mathrm{b}}\right)\boldsymbol{R}_1(\phi_\mathrm{b})\end{aligned}$$

Substituting these expressions into $\dot{\boldsymbol{R}}$ results in

$$\dot{\boldsymbol{R}} = \boldsymbol{R}\left[\widehat{\left(\boldsymbol{R}_1^T(\phi_\mathrm{b})\boldsymbol{R}_2^T(\theta_\mathrm{b})\boldsymbol{e}_3\dot{\psi_\mathrm{b}}\right)} + \widehat{\left(\boldsymbol{R}_1^T(\phi_\mathrm{b})\boldsymbol{e}_2\dot{\theta_\mathrm{b}}\right)} + \widehat{\left(\boldsymbol{e}_1\dot{\phi_\mathrm{b}}\right)}\right] \tag{A.11}$$

Recognizing the term in brackets as $\hat{\boldsymbol{\omega}}$ from (2.9), one concludes that

$$\dot{\boldsymbol{R}} = \boldsymbol{R}\hat{\boldsymbol{\omega}} \tag{A.12}$$

A.3 Derivation of The Fluid Boundary Conditions using Hamilton's Principle

To interpret the variational operator δ, we transform the system configuration based on the transformation (2.22):

$$\phi(\boldsymbol{x}, t, \alpha) = \phi(\boldsymbol{x}, t, 0) + \alpha\ \delta\phi(\boldsymbol{x}, t)$$
$$\eta(x, y, t, \alpha) = \eta(x, y, t, 0) + \alpha\ \delta\eta(x, y, t)$$

Again, α is an arbitrary index, and $\delta\phi$ and $\delta\eta$ represent variations from the true (infinite dimensional) trajectories, $\phi(x, y, z, t, 0)$ and $\eta(x, y, t, 0)$. Assuming that ϕ and η are fixed at t_0 and t_1, we may define

$$\delta\phi(\boldsymbol{x})\Big|_{t_0} = \delta\phi(\boldsymbol{x})\Big|_{t_1} = \delta\eta(x, y)\Big|_{t_0} = \delta\eta(x, y)\Big|_{t_1} = 0 \tag{A.13}$$

Using the new definitions of ϕ and η, the first variation is evaluated as

$$\delta I(\phi, \eta) = \frac{d}{d\alpha} I(\phi(\alpha), \eta(\alpha))\Big|_{\alpha=0} = 0 \tag{A.14}$$

Substituting the given Lagrangian to the action yields

$$\frac{d}{d\alpha}\int_{t_0}^{t_1}\left\{\int_{x_1}^{x_2}\int_{y_1}^{y_2}\int_{z_1}^{\eta(x,y,t,\alpha)}\left[\frac{1}{2}(\nabla\phi)\cdot(\nabla\phi) + \frac{\partial\phi}{\partial t} + gz\right]dzdydx\right\}\Bigg|_{\alpha=0} dt = 0 \tag{A.15}$$

Recalling that η is a function of α, the Leibniz integral rule is used to move the differentiation with respect to α into the integral:

$$\begin{aligned}\frac{d}{d\alpha} I(\phi, \eta, \alpha)|_{\alpha=0} = \int_{t_0}^{t_1}\Bigg\{\int_{x_1}^{x_2}\int_{y_1}^{y_2}\Bigg[\int_{z_1}^{\eta(x,y,t,\alpha)}\frac{\partial}{\partial\alpha}\left(\frac{1}{2}(\nabla\phi)\cdot(\nabla\phi) + \frac{\partial\phi}{\partial t} + gz\right)dz \\ + \left(\frac{1}{2}(\nabla\phi)\cdot(\nabla\phi) + \frac{\partial\phi}{\partial t} + gz\right)\Big|_{z=\eta}\frac{\partial\eta(x, y, t, \alpha)}{\partial\alpha}\Bigg]dydx\Bigg\}\Bigg|_{\alpha=0} dt = 0\end{aligned} \tag{A.16}$$

Here we will just evaluate each term appearing in the above integral one at a time. First, note that

$$\begin{aligned}(\nabla\phi)\cdot(\nabla\phi) = &\left(\frac{\partial}{\partial x}[\phi(x,y,z,t,0)+\alpha\delta\phi]\right)^2 \\ &+\left(\frac{\partial}{\partial y}[\phi(x,y,z,t,0)+\alpha\delta\phi]\right)^2 \\ &+\left(\frac{\partial}{\partial z}[\phi(x,y,z,t,0)+\alpha\delta\phi]\right)^2\end{aligned}$$

Then applying the chain rule and changing the order of differentiation, we find

$$\frac{\partial}{\partial\alpha}\left[\frac{1}{2}(\nabla\phi)\cdot(\nabla\phi)\right] = \frac{\partial\phi}{\partial x}\frac{\partial\delta\phi}{\partial x}+\frac{\partial\phi}{\partial y}\frac{\partial\delta\phi}{\partial y}+\frac{\partial\phi}{\partial z}\frac{\partial\delta\phi}{\partial z} \tag{A.17}$$

Similarly, for the unsteady term,

$$\frac{\partial}{\partial\alpha}\left(\frac{\partial}{\partial t}[\phi(x,y,z,t,0)+\alpha\delta\phi]\right) = \frac{\partial\delta\phi}{\partial t} \tag{A.18}$$

Trivially,

$$\frac{\partial}{\partial\alpha}(gz) = 0 \tag{A.19}$$

Lastly,

$$\frac{\partial}{\partial\alpha}\left[\eta(x,y,t,0)+\alpha\delta\eta\right] = \delta\eta \tag{A.20}$$

Substituting these expressions into (A.16), the equation becomes

$$\begin{aligned}\int_{t_0}^{t_1}\Bigg\{\int_{x_1}^{x_2}\int_{y_1}^{y_2}\Bigg[\int_{z_1}^{\eta}&\left[\frac{\partial\phi}{\partial x}\frac{\partial\delta\phi}{\partial x}+\frac{\partial\phi}{\partial y}\frac{\partial\delta\phi}{\partial y}+\frac{\partial\phi}{\partial z}\frac{\partial\delta\phi}{\partial z}+\frac{\partial\delta\phi}{\partial t}\right]dz \\ &+\left(\frac{1}{2}(\nabla\phi)\cdot(\nabla\phi)+\frac{\partial\phi}{\partial t}+gz\right)\Big|_{z=\eta}\delta\eta\Bigg]dydx\Bigg\}dt = 0\end{aligned}$$

Next we perform integration by parts, term-by-term, on the following integral:

$$\int_{z_1}^{\eta}\left[\frac{\partial\phi}{\partial x}\frac{\partial\delta\phi}{\partial x}+\frac{\partial\phi}{\partial y}\frac{\partial\delta\phi}{\partial y}+\frac{\partial\phi}{\partial z}\frac{\partial\delta\phi}{\partial z}+\frac{\partial\delta\phi}{\partial t}\right]dz \tag{A.21}$$

Using the identity

$$\frac{\partial}{\partial z}\left(\frac{\partial z}{\partial x}\delta\phi\right) = \cancel{\frac{\partial}{\partial x}\left(\frac{\partial z}{\partial z}\right)}\delta\phi+\frac{\partial}{\partial z}(\delta\phi)\frac{\partial z}{\partial x} = \frac{\partial}{\partial x}(\delta\phi)$$

we may express the first term as

$$\begin{aligned}\int_{z_1}^{\eta}\frac{\partial\phi}{\partial x}\frac{\partial}{\partial x}(\delta\phi)dz &= \int_{z_1}^{\eta}\underbrace{\frac{\partial\phi}{\partial x}}_{u}\underbrace{\frac{\partial}{\partial z}\left(\frac{\partial z}{\partial x}\delta\phi\right)dz}_{dv}\\ &= \left[\frac{\partial\phi}{\partial x}\frac{\partial z}{\partial x}\delta\phi\right]\Big|_{z=z_1}^{z=\eta}-\int_{z_1}^{\eta}\frac{\partial z}{\partial x}\delta\phi\frac{\partial^2\phi}{\partial x^2}\frac{\partial x}{\partial z}dz\\ &= \left[\frac{\partial\phi}{\partial x}\eta_{,x}\delta\phi\right]|_{z=\eta}-\int_{z_1}^{\eta}\phi_{,xx}\delta\phi dz\end{aligned}$$

Similarly, for the second term, we find

$$\int_{z_1}^{\eta}\frac{\partial\phi}{\partial y}\frac{\partial\delta\phi}{\partial y}dz = \left[\frac{\partial\phi}{\partial y}\eta_{,y}\delta\phi\right]|_{z=\eta}-\int_{z_1}^{\eta}\phi_{,yy}\delta\phi dz$$

For the third term,

$$\begin{aligned}\int_{z_1}^{\eta}\underbrace{\frac{\partial\phi}{\partial z}}_{u}\underbrace{\frac{\partial}{\partial z}(\delta\phi)\,dz}_{dv} &= \left[\frac{\partial\phi}{\partial z}\delta\phi\right]\Big|_{z=z_1}^{z=\eta}-\int_{z_1}^{\eta}\frac{\partial^2\phi}{\partial z^2}\delta\phi dz\\ &= \left[\frac{\partial\phi}{\partial z}\delta\phi\right]|_{z=\eta}-\left[\frac{\partial\phi}{\partial z}\delta\phi\right]|_{z=z_1}-\int_{z_1}^{\eta}\phi_{,zz}\delta\phi dz\end{aligned}$$

The unsteady term can integrated similarly to the first two terms:

$$\int_{z_1}^{\eta}\left[\underbrace{1}_{u}\underbrace{\frac{\partial}{\partial z}\left(\frac{\partial z}{\partial t}\delta\phi\right)}_{dv}\right]dz = \left[\frac{\partial z}{\partial t}\delta\phi\right]\Big|_{z=z_1}^{z=\eta} = \left[\eta_{,t}\delta\phi\right]|_{z=\eta}$$

Putting together all of the integrations by parts, the critical points of J are given in terms of the following integrals:

$$\begin{aligned}\int_{t_0}^{t_1}\Bigg\{\int_{x_1}^{x_2}\int_{y_1}^{y_2}\Bigg[&\int_{z_1}^{\eta}-\left(\phi_{,xx}+\phi_{,yy}+\phi_{,zz}\right)\delta\phi dz\\ &+\left[\left(\frac{\partial\phi}{\partial x}\eta_{,x}+\frac{\partial\phi}{\partial y}\eta_{,y}+\frac{\partial\phi}{\partial z}+\eta_{,t}\right)\delta\phi\right]|_{z=\eta}\\ &+\left[\frac{1}{2}\left(\frac{\partial\phi}{\partial x}^2+\frac{\partial\phi}{\partial y}^2+\frac{\partial\phi}{\partial z}^2\right)+\frac{\partial\phi}{\partial t}+gz\right]\Big|_{z=\eta}\delta\eta\\ &+\left[-\frac{\partial\phi}{\partial z}\delta\phi\right]|_{z=z_1}\Bigg]dydx\Bigg\}dt=0\end{aligned}$$

A.4 Proof of Proposition 4.1.1

Proof. Following [8, Ch 4.12], we begin with the following identity[1]

$$\frac{d}{dt}\left[\iiint_{\mathcal{F}} \rho \boldsymbol{V}_{\mathrm{f}}\, dV\right] = \frac{d}{dt}\left[\rho \iint_{\mathcal{B}} \phi \boldsymbol{n}_{+}\, dS + \rho \iint_{\mathcal{E}} \phi \boldsymbol{n}_{+}\, dS\right] \tag{A.22}$$

Note that the expression on the left-hand side is simply the time rate of change of the fluid momentum contained within $\mathcal{E}$. Next, we employ the Reynolds Transport Theorem (A.4) to simplify the expression on the left-hand side

$$\begin{aligned}\frac{d}{dt}\iiint_{\mathcal{F}} \rho \boldsymbol{V}_{\mathrm{f}}\, dV &= \iiint_{\mathcal{F}} \rho \frac{\partial \boldsymbol{V}_{\mathrm{f}}}{\partial t}\, dV + \iint_{\mathcal{B}} \rho \boldsymbol{V}_{\mathrm{f}} \left(\boldsymbol{V}_{\mathrm{b}} \cdot \boldsymbol{n}_{+}\right)\, dS + \iint_{\mathcal{E}} \rho \boldsymbol{V}_{\mathrm{f}} \left(\boldsymbol{V}_{\mathrm{e}} \cdot \boldsymbol{n}_{+}\right)\, dS \\ &= \iint_{\mathcal{B}} \rho \left[\frac{\partial \phi}{\partial t}\boldsymbol{n}_{+} + \boldsymbol{V}_{\mathrm{f}}\left(\boldsymbol{V}_{\mathrm{b}} \cdot \boldsymbol{n}_{+}\right)\right] dS + \iint_{\mathcal{E}} \rho \left[\frac{\partial \phi}{\partial t}\boldsymbol{n}_{+} + \boldsymbol{V}_{\mathrm{f}}\left(\boldsymbol{V}_{\mathrm{e}} \cdot \boldsymbol{n}_{+}\right)\right] dS\end{aligned} \tag{A.23}$$

Here, $\boldsymbol{V}_{\mathrm{b}}$ represents the Eulerian velocity[2] of a point along $\mathcal{B}$, and $\boldsymbol{V}_{\mathrm{e}}$ similarly represents the Eulerian velocity of a point in the envelope. We assume that the bounding surface $\mathcal{E}$ is fixed, and thus $\boldsymbol{V}_{\mathrm{e}} = \boldsymbol{0}$. Substituting the results of the transport theorem into the identity (A.22), we find that

$$\iint_{\mathcal{B}} \rho \left[\frac{\partial \phi}{\partial t}\boldsymbol{n}_{+} + \boldsymbol{V}_{\mathrm{f}}\left(\boldsymbol{V}_{\mathrm{b}} \cdot \boldsymbol{n}_{+}\right)\right] dS + \rho \iint_{\mathcal{E}} \frac{\partial \phi}{\partial t}\boldsymbol{n}_{+}\, dS - \frac{d}{dt}\rho \iint_{\mathcal{B}} \phi \boldsymbol{n}_{+}\, dS - \frac{d}{dt}\rho \iint_{\mathcal{E}} \phi \boldsymbol{n}_{+}\, dS = 0 \tag{A.24}$$

Again, since $\mathcal{E}$ is not a function of time, by the Leibniz rule it is true that

$$\frac{d}{dt}\rho \iint_{\mathcal{E}} \phi \boldsymbol{n}_{+}\, dS = \rho \iint_{\mathcal{E}} \frac{\partial \phi}{\partial t}\boldsymbol{n}_{+}\, dS \tag{A.25}$$

From the kinematic body boundary condition, we know that $\boldsymbol{V}_{\mathrm{b}} \cdot \boldsymbol{n}_{+} = \boldsymbol{V}_{\mathrm{f}} \cdot \boldsymbol{n}_{+}$. With these substitutions, (A.22) becomes simply

$$\iint_{\mathcal{B}} \rho \left[\frac{\partial \phi}{\partial t}\boldsymbol{n}_{+} + \boldsymbol{V}_{\mathrm{f}}\left(\boldsymbol{V}_{\mathrm{f}} \cdot \boldsymbol{n}_{+}\right)\right] dS - \frac{d}{dt}\rho \iint_{\mathcal{B}} \phi \boldsymbol{n}_{+}\, dS = 0 \tag{A.26}$$

[1] One may verify this identity using the gradient theorem (A.1) and the fact that $\boldsymbol{V}_{\mathrm{f}} = \nabla\phi$.

[2] One may interpret the Eulerian velocity of a fluid as the velocity of the fluid at a point fixed in inertial space

Adding (A.26) to (4.4) yields

$$\boldsymbol{f} = \rho \iint_{\mathcal{B}} \left[\boldsymbol{V}_{\mathrm{f}} \left(\boldsymbol{V}_{\mathrm{f}} \cdot \boldsymbol{n}_{+} \right) - \frac{1}{2} \nabla\phi \cdot \nabla\phi \right] dS - \frac{d}{dt} \rho \iint_{\mathcal{B}} \phi \boldsymbol{n}_{+} \, dS \tag{A.27}$$

$$= -\rho \frac{d}{dt} \iint_{\mathcal{B}} \phi \boldsymbol{n}_{+} \, dS + \rho \iint_{\mathcal{B}} \left[\nabla\phi \left(\nabla\phi \cdot \boldsymbol{n}_{+} \right) - \frac{1}{2} \left(\nabla\phi \cdot \nabla\phi \right) \boldsymbol{n}_{+} \right] dS \tag{A.28}$$

Using the following identity[3] [8, Eq. (89)]

$$\rho \iint_{\mathcal{B}} \left[\nabla\phi \left(\nabla\phi \cdot \boldsymbol{n}_{+} \right) - \frac{1}{2} \left(\nabla\phi \cdot \nabla\phi \right) \boldsymbol{n}_{+} \right] dS = -\rho \iint_{\mathcal{E}} \left[\nabla\phi \left(\nabla\phi \cdot \boldsymbol{n}_{+} \right) - \frac{1}{2} \left(\nabla\phi \cdot \nabla\phi \right) \boldsymbol{n}_{+} \right] dS \tag{A.29}$$

The final form of the force equation becomes

$$\boldsymbol{f} = -\rho \frac{d}{dt} \iint_{\mathcal{B}} \phi \boldsymbol{n}_{+} \, dS - \rho \iint_{\mathcal{E}} \left[\nabla\phi \left(\nabla\phi \cdot \boldsymbol{n}_{+} \right) - \frac{1}{2} \left(\nabla\phi \cdot \nabla\phi \right) \boldsymbol{n}_{+} \right] dS \tag{A.30}$$

A similar process is taken to redefine $\boldsymbol{\tau}$, beginning with the identity

$$\frac{d}{dt} \left[\iiint_{\mathcal{F}} \nabla \times \rho \boldsymbol{V}_{\mathrm{f}} \, dV \right] = \frac{d}{dt} \left[\iint_{\mathcal{B}} \boldsymbol{n}_{+} \times \rho \nabla\phi \, dS + \iint_{\mathcal{E}} \boldsymbol{n}_{+} \times \rho \nabla\phi \, dS \right] \tag{A.31}$$

We omit the remainder of the proof ■.

[3] One may prove this identity by using the divergence and gradient theorems to relate the surface integrals over $\mathcal{B}$ and $\mathcal{E}$ to a volume integral over $\mathcal{F}$; the resulting volume integral is zero, and thus the contributions from each surface integral must be equal and opposite.